Investigating the role of RGC-32 in cell cycle disruption by EBV EBNA 3C

by

Sandra Schlick

Submitted in total fulfilment of the requirements of the degree of

Doctor of Philosophy

Department of Chemistry and Biochemistry

School of Life Sciences

University of Sussex

11 January 2010

Declaration

I hereby declare that this thesis has not been and will not be, submitted in whole or in part to another University for the award of any other degree.

UNIVERSITY OF SUSSEX

Sandra Schlick

Doctor of philosophy

Investigating the role of RGC-32 in cell cycle disruption by EBV EBNA 3C

SUMMARY

Epstein-Barr virus (EBV) immortalises resting B-lymphocyctes and is associated with a diverse range of cancers and establishes a persistent, latent infection in >90% of the world-wide population. Epstein-Barr virus nuclear antigen (EBNA) 3C is one of only six EBV latent proteins that are crucial for B-cell transformation. EBNA3C is known to disrupt cell-cycle control and to progress phase transition at G1/S and G2/M under conditions where cells should growth arrest, but the mechanism by which EBNA3C does this has not been fully determined. The cell-cycle regulator response gene to complement (RGC) 32 was found to be upregulated in EBNA3C-expressing cells in microarray experiments carried out previously. RGC-32 is involved in cell-cycle activation and also plays a role in G1/S and G2/M transition. I have shown that both EBNA3C-expressing cell-lines with upregulated RGC-32 and cell-lines overexpressing RGC-32 alone displayed disrupted G2/M checkpoint control indicating that EBNA3C may overcome cell-cycle control by upregulation of RGC-32. I also confirmed that RGC-32 increases the *in vitro* kinase activity of CDK1, the key mitotic kinase essential for G2/M transition. Surprisingly, my data showed that EBNA3C only activated RGC-32 transcription in reporter assays at a very low-level, but stabilised the RGC-32 mRNA. Further studies investigating the differential expression of RGC-32 in EBV-positive and negative cells demonstrated that RGC-32 is upregulated in LCLs and tumour (Burkitt's lymphoma) cell-lines expressing the full panel of latent genes, but intriguingly highly expressed in Burkitt's lymphoma cell-lines expressing only EBNA 1. I found that this expression pattern correlated with expression of the RUNX1 transcription factor. Reporter assays revealed that RUNX1 was able to activate the RGC-32 promoter. Together, this data indicates a new mechanism by which EBNA 3C can disrupt the G2/M checkpoint and highlights a link between RUNX1 and RGC-32 expression in B-cells.

Acknowledgements

I would like to give my biggest thank you to my supervisor Michelle West who gave me this opportunity to do my PhD. Thank you for your support in all the years I have been in this lab and for taking all the extra time to make suggestions to improve my thesis.

I would also like to thank Helen Webb for her support and for making the lab much more fun. I am not sure if I would have managed to finish my PhD so quickly without all her help and knowledge which probably saved me a lot of time doing unnecessary experiments.

A big thank you also goes to all other members of the West and Sinclair lab past and present who were always happy to help. I would also particularly like to thank Lina Chen who was very helpful and understanding, and who made my final time in the lab such a pleasure.

Ich möchte vor allem meinen Eltern danken, die immer ein offenes Ohr für meine Sorgen hatten und mir immer wieder gut zugeredet haben, auch wenn meine Laune mal wieder den absoluten Tiefpunkt erreicht hatte. Auch für die finanzielle Unterstützung genau wie den Rundum-Service, den ich in jedem Deutschlandaufenthalt genieβen durfte, möchte ich mich herzlich bedanken. Ohne Euch hätte ich es nicht geschafft.

Weiterer Dank gilt meinen Freunden, die immer Verständnis dafür hatten, dass ich mich wieder monatelang nicht gemeldet habe und die mir auch nach so langer Zeit erhalten geblieben sind.

I would also like to thank Pantelis who had to bear all my mood swings and my permanent stress level especially in the last few months. I really appreciate your constant attempts to make me feel better. Many thanks for your help with the final editing of my thesis and for teaching me all these very useful computer skills.

Many thanks also go to my examiners for taking the time and effort to read and understand my thesis.

Table of contents

Abbreviations

AIDS	Acquired immunodeficiency syndrome
aa	Amino acid
ab	Antibody
ATM	Ataxia-telangiectasia mutated
ATP	Adenosine triphosphate
ATR	Ataxia-telangiectasia-mutated and Rad3-related
BL	Burkitt's lymphoma
bZip	Basic leucine zipper
CAK	CDK-activating kinase
CDK	Cyclin-dependent kinase
CDKI	Cyclin-dependent kinase inhibtor
ChIP	Chromatin immunoprecipitation
Chk2	Checkpoint kinase 2
Cp	C promoter
CRS	Cytoplasmic retention signal
CtBP	C-terminal binding protein
DNA	Deoxyribonucleic acid
DP103	DEAD box protein of 130 kD
EBER	Epstein-Barr virus encoded RNA
EBNA	Epstein-Barr nuclear antigen
EBNA LP	Epstein-Barr nuclear antigen leader protein
EBV	Epstein-Barr Virus
etop	etoposide
HAT	Histone acetyltransferase
HD	Hodgkin's disease
HDAC	Histone deacetylase
HIV	Human immunodeficiency virus
HL	Hodgkin's lymphoma
IM	Infectious mononucleosis
IP	Immunoprecipitation
LCL	Lymphoblastoid cell line
LMP	Latent membrane protein
Oligo	Oligonucleotide
NHL	Non-Hodgkin lymphoma
NLS	Nuclear localisation signal
Plk1	Polo-like kinase 1
PTLD	Post-transplantation lymphoproliferative disorder
Qp	Q promoter

RBP-J kappa	Recombination signal-binding protein 1 for J-kappa
RGC-32	Response gene to complement 32
RINGO	Rapid inducer of G2/M progression in oocytes
RUNX	Runt box
TNF	Tumour necrosis factor
UNPC	Undifferentiated nasopharyngeal carcinoma
WCL	Whole cell lysate
Wp	W promoter

1 Introduction

1.1 The Cell Cycle

The cell cycle describes a process by which the cell grows and divides into two genetically identical daughter cells. The cell cycle is divided into four different active phases (G1, S, G2, M) and a resting phase called G0. During S (synthesis) phase the DNA in the cell is replicated from single chromatids to double (sister) chromatids. The M phase (mitosis) is subdivided into five different phases: prophase, prometaphase, metaphase, anaphase and telophase. During prophase the chromosomes become condensed, the centrioles are duplicated and position themselves at the opposite cell poles. Prometaphase describes the transition from prophase to metaphase in which the nuclear membrane is degraded and the mitotic spindles start growing. In metaphase the chromosomes move to the equatorial plate induced by the mitotic spindles. The single chromatids then move towards the cell poles in anaphase before the cell divides into two cells during telophase, when also a new nuclear membrane is formed and decondensation of the chromosomes occurs. During the gap phases G1 and G2 the cell needs to increase in mass in preparation for DNA replication or mitosis, respectively. The growth of the cell is affected by limiting growth factors, nutrients or inhibitors.

The cell cycle is highly regulated by at least four cell cycle checkpoints: G1/S, intra S, G2/M and the mitotic spindle checkpoint. The function of the G1/S checkpoint is to ensure that the cell has attained the adequate growth requirements to move forward into S phase. The S phase checkpoint is responsible for ensuring that the DNA has replicated without faults and so that the cell can proceed into G2 phase. The G2/M checkpoint then verifies whether all criteria have been met to let the cell progress into mitosis. During mitosis the spindle checkpoint ensures that the kinetochores of the sister chromatids have been attached correctly to opposite spindle poles for segregation. Cell cycle arrest is induced when any of the checkpoints become activated.

Several cyclin-dependent kinases (CDKs) are sequentially activated throughout the cell cycle and are responsible for the control of the transitions of each cell to the next phase (Pines, 1995). At least 9 CDKs are involved in the cell cycle, however, the ones essential for cell cycle progression are: CDK1, CDK2, CDK4, CDK6 and CDK7. Cell

cycle checkpoints regulate CDK activities and ensure that every phase has been completed successfully before proceeding to the next phase. Deregulation of this cell cycle control leads to uncontrolled growth and can lead to cancer if the cell cannot regain the function of the checkpoint. Therefore, these cells become immortalised.

CDKs are generally abundantly present during the cell cycle and are activated by binding their specific cyclin. The cyclins received their name as their expression fluctuates throughout the cell cycle; they are expressed only when needed and are subsequently degraded by the proteasome (Evans et al., 1983; Morgan, 1997). Cyclins contain a cyclin box which is involved in binding the CDK (Pines, 1995). The known cyclins essential for cell cycle progression are: cyclin A, cyclin B, cyclin D, cyclin E and cyclin H. Each CDK bound to a cyclin forms the holoenzyme which is essential for kinase function (Ekholm and Reed, 2000; Johnson and Walker, 1999; Obaya and Sedivy, 2002). Cyclin D needs to be upregulated to facilitate the entry of a quiescent cell in G0 into the cell cycle. Cyclin D complexes with CDK4 or CDK6 to form the active holoenzyme and the complex was found to be present until the cell enters the S phase (Blagosklonny and Pardee, 2002) (Figure 1). This complex then induces cyclin E expression which associates with CDK2 to promote the G1/S transition. During S phase cyclin A binds to CDK2 which may be required for progression through S phase. Cyclin A expression is induced by the active cyclin D/CDK4/6 and cyclin E/CDK2 complexes (Harbour et al., 1999; Zhang et al., 2000a). Cyclin A can also bind CDK1 in S and G2 phase. The actual G2/M transition is mediated by the cyclin B/CDK1 complex originally called M phase promoting factor or maturation promoting factor (MPF) (Brizuela et al., 1989; Nigg, 1995; Obaya and Sedivy, 2002; Pines, 1995).

CDK activation requires phosphorylation on a conserved threonine residue in the T-loop by the CDK-activating kinase CAK (cyclin H/CDK7/Mat1) (Fisher and Morgan, 1994; Solomon et al., 1992; Tassan et al., 1995), (reviewed in (Obaya and Sedivy, 2002)). This phosphorylation is increased when the cyclin is bound to the CDK suggesting that the activating phosphorylation occurs after the complex has formed (Morgan, 1995).

CDK activity can be negatively regulated by a family of proteins known as cyclin-dependent kinase inhibitors (CDKIs) (Peter and Herskowitz, 1994). The CDKIs are divided in 2 families: the CIP/KIP family ($p21^{WAF1/CIP1}$, $p27^{KIP1}$, $p57^{KIP2}$) and the INK4

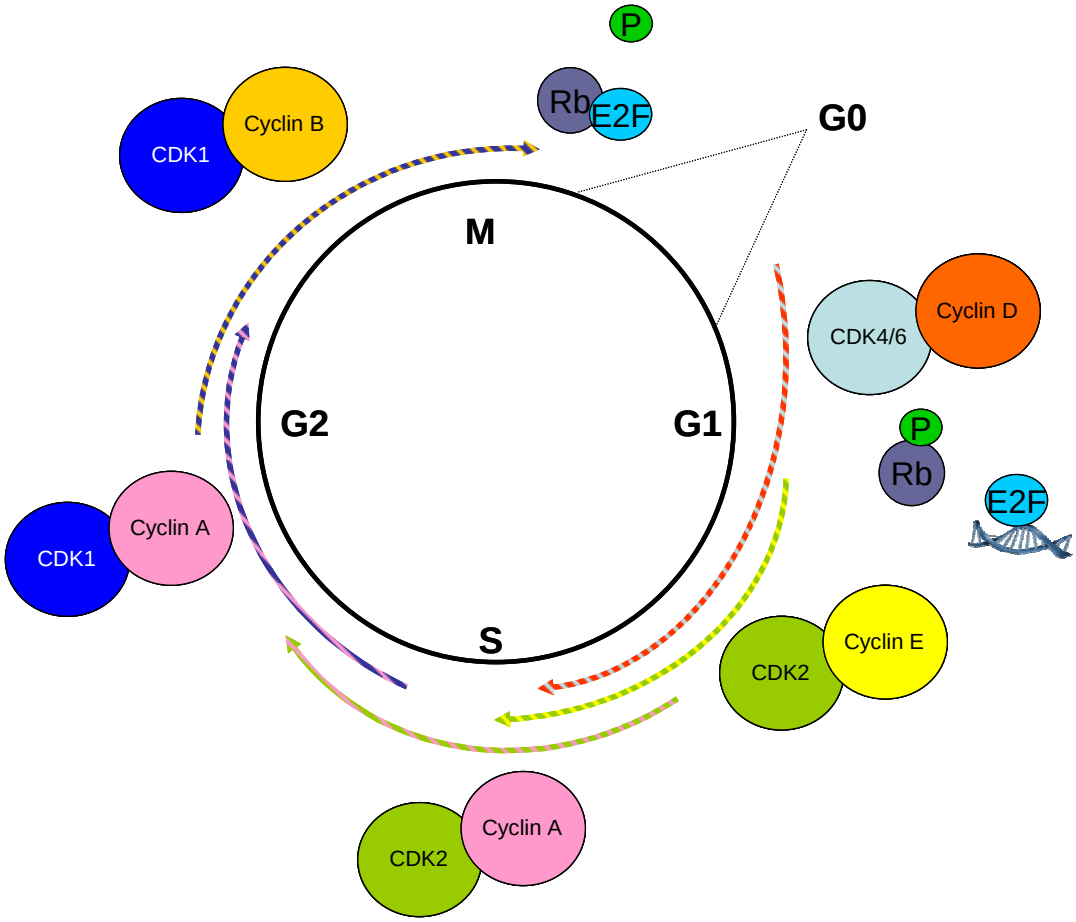

Figure 1 – Cell Cycle overview

Cyclin D expression enables the quiescent cells in G0 to enter the cell cycle. The cyclinD/CDK4/6 complex then mediates the phosphorylation of Rb during G1 phase. Phosphorylated Rb can no longer bind transcription factor E2F which results is the expression of E2F target genes required for progression into S phase, e.g. cyclin E which associates with CDK2 to promote the G1/S transition. Cyclin E/CDK2 further phosphorylate Rb which mediates transcription of cyclin A and E2F which is essential for DNA replication. The formation of the cyclin A/CDK2 complex is required for progression through S phase. Cyclin A can also bind CDK1 in S and G2 phase. The actual G2/M transition is mediated by the cyclin B/CDK1 complex. During the subsequent M phase, the Rb protein is dephosphorylated so that it can once again inhibit E2F.

(inhibitors of CDK4) family ($p16^{INK4A}$, $p15^{INK4B}$, $p18^{INK4C}$, $p19^{INK4D}$) (Morgan, 1997; Sherr and Roberts, 1999). The INK4 inhibitors bind CDK4/6 and prevent their interaction with cyclin D. The CIP/KIP inhibitors do not prevent cyclin/CDK association but inhibit their activity (Sherr and Roberts, 1999). $P27^{KIP1}$ was shown to inhibit diverse cyclin/CDK complexes, cyclin E/CDK2, cyclin A/CDK2, and cyclin D2-CDK4 (Polyak et al., 1994; Resnitzky et al., 1995).

1.1.1 Regulation of CDK1

The activity of CDK1 and CDK2 can also be inhibited by phosphorylation of Thr14 and Tyr15 at the N-terminus by the kinases wee1 and myt1 (myelin transcription factor 1) during interphase (Krek and Nigg, 1991; Lundgren et al., 1991; McGowan and Russell, 1993; Mueller et al., 1995; Parker and Piwnica-Worms, 1992). Tyr15 is located at the ATP binding site. The presence of phosphorylated Tyr15 still allows binding of ATP but inhibits the phosphorylation of a substrate, whereas phosphorylated Thr14 blocks ATP binding completely (Atherton-Fessler et al., 1993; Endicott et al., 1994). During S and G2 phase the cyclin B/CDK1 complex is kept in the inactive state through Tyr15 phosphorylation of CDK1 (Gould and Nurse, 1989; Lundgren et al., 1991; Mueller et al., 1995; Parker and Piwnica-Worms, 1992) (Figure 2, left panel). During the G2/M transition the inhibitory phosphates are removed by the cdc25 phosphatase family resulting in CDK activation (Kumagai and Dunphy, 1991; Nilsson and Hoffmann, 2000; Russell and Nurse, 1986). Cdc25 is translocated into the nucleus during G2/M transition and is activated by Polo-like kinase 1 (Plk1) and may later be phosphorylated by cyclin B1/CDK1 (Girard et al., 1992; Heald et al., 1993; Hoffmann et al., 1993; Kumagai and Dunphy, 1996).

1.1.2 Regulation of cyclin B1

Various vertebrate cyclin B isoforms have been identified: Cyclin B1, B2 and B3 and B4 and B5 were discovered in *Xenopus* (Gallant and Nigg, 1994; Hochegger et al., 2001). Cyclin B1 and B2 are known to associate with CDK1 to promote progression into mitosis. The same function was observed for cyclin B4 and B5 in *Xenopus* (Hochegger et al., 2001). Cyclin B3 was shown to bind CDK1 as well as CDK2 and the protein stays in the nucleus throughout the cell cycle (Gallant and Nigg, 1994). Cyclin B1 expression is tightly regulated by different mechanisms. Cyclin B1 protein contains

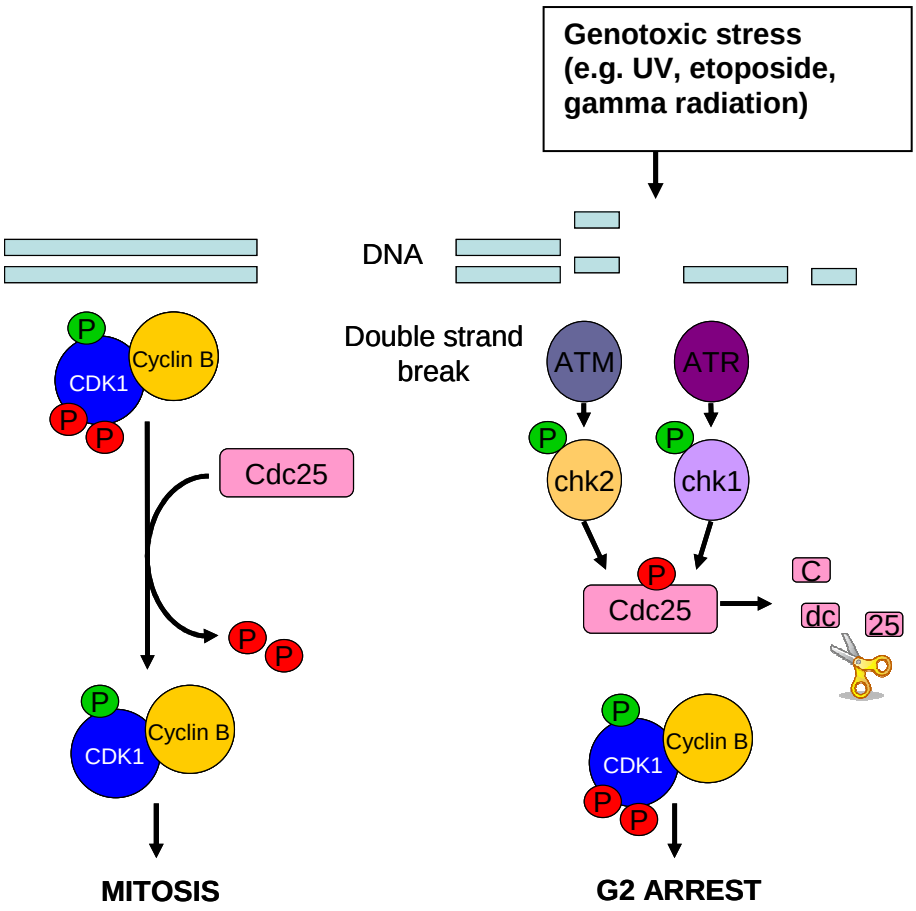

Figure 2 – G2/M checkpoint overview

In absence of cytotoxic stress the phosphatase cdc25 removes the inhibitory phosphates (red) at the Thr14- and Tyr15-residues of CDK1 which allows cell cycle progression into mitosis. In the presence of cytotoxic stress and therefore DNA damage the kinases ATM and ATR are activated which phosphorylate (green) and thus activate the kinases chk2 and chk1 respectively and phosphorylate (red) Cdc25 which is then sequestered and degraded. Therefore, Cdc25 can no longer remove the inhibitory phosphates from CDK1 which results in G2 arrest.

a cytoplasmic retention signal (CRS) which signals cyclin B1 to remain in the cytoplasm during G2 (Gallant and Nigg, 1992; Hagting et al., 1999; Pines and Hunter, 1991; Pines and Hunter, 1994). Cyclin B1 only translocates to the nucleus when phosphorylated at the CRS (Li et al., 1997). At each mitosis or meiosis, cyclin B1 is phosphorylated on 5 serine residues (Ser2, Ser94, Ser96, Ser101 and Ser113) within the CRS (Borgne et al., 1999; Izumi and Maller, 1991; Li et al., 1995; Meijer et al., 1989). All 5 sites can be autophoshorylated *in vitro* but it cannot be excluded that other kinases e.g. Plk1 could be involved *in vivo* (Izumi and Maller, 1991). Phosphorylation of cyclin B1 is required for translocation into the nucleus but is not required to activate CDK1 since unphosphorylated cyclin B was found to be able to bind and activate CDK1 to the same extent as phosphorylated cyclin B and gets normally degraded during mitosis (Hagting et al., 1999; Izumi and Maller, 1991; Li et al., 1995; Li et al., 1997). Mimicking permanent CRS phosphorylation by mutation of phosphorylation sites to glutamic acid (E) leads to accumulation of cyclin B1 in the nucleus (Hagting et al., 1999). However, it is not fully understood how phosphorylation of the CRS mediates the translocation to the nucleus. Cyclin B1 lacking its amino terminus and therefore the CRS was found to be able to directly bind importin β (Moore et al., 1999). Phosphorylation of the CRS was shown to generate a nuclear localisation signal (NLS) but its nuclear import is likely to be importin β-independent since importin β is not able to bind cyclin B1 when the CRS is present (Hagting et al., 1999). Once within the nucleus the phosphorylation of serine 113 in the CRS prevents nuclear export (Yang et al., 2001a). The CRS was found to have a nuclear export signal (NES) (Hagting et al., 1998; Toyoshima et al., 1998; Yang et al., 1998) and is likely to use an exportin1/CRM1 dependent pathway as exportin1 has been shown to bind cyclin B in *Xenopus* (Yang et al., 1998).

Synthesis of cyclin B1 occurs from late S phase and the protein is degraded at the beginning of mitosis (Piaggio et al., 1995; Pines and Hunter, 1989). Cyclin B mRNA is known to be very unstable after DNA damage and in general more stable in G2 than in G1 suggesting that the fluctuation of the protein expression is due to mRNA stability (Maity et al., 1995; Pines and Hunter, 1989).

Cyclin B1/CDK1 also has a putative role as a nuclear lamin kinase which causes nuclear envelope disassembly at the end of prophase by phosphorylation (Enoch et al., 1991; Peter et al., 1990; Ward and Kirschner, 1990). Although the role of CDK1 is thought to be only in the G2/M transition, some evidence suggests that it is also involved in the G1/S transition in higher eukaryotes (Badea et al., 2002; Hochegger et al., 2007; Kaldis and Aleem, 2005; Rus et al., 1996). It is known that CDK1 is able to associate with cyclin A as well as cyclin B. Cyclin A was shown to be able to activate CDK1 shortly before S phase begins. Furthermore, CDK1 was reported to be involved in the phosphorylation of CDK7 at Thr376 which is also known to play a role in S phase entry (Masai et al., 2000). Other reports indicated that cyclin A/CDK1 play a role in late S phase to ensure accurate completion of DNA replication rather than S phase entry (Obaya and Sedivy, 2002). CDK2 knockout experiments in mice and chicken DT40 cells revealed that CDK1 can replace the function of CDK2 by binding and activating cyclin E and therefore promoting transition from G1 into S phase (Aleem et al., 2005; Hochegger et al., 2007; Kaldis and Aleem, 2005).

1.1.3 The G2/M checkpoint

In response to DNA damage caused by e.g. ionizing radiation or DNA damaging agents, the G2/M checkpoint is activated (Figure 2, right panel). The protein kinases ATM and ATM-Rad3-related (ATR) are recruited to the break sites and act as transducers starting a cascade to recruit DNA repair proteins. ATR is activated in response to DNA damage mainly at the replication fork (single strand breaks) whereas ATM is generally activated by other DNA double strand breaks. ATM and ATR phosphorylate and activate chk2 and chk1, respectively (Matsuoka et al., 1998; Sanchez et al., 1997; Shiloh, 2003). The chk kinases phosphorylate Cdc25 at serine-216 resulting in inactivation of Cdc25 and therefore preventing the removal of the inhibitory phosphates on CDK1 and its activation (Chaturvedi et al., 1999; Matsuoka et al., 1998). Increased levels of inactive Tyr15-phosphorylated CDK1 therefore accumulate during G2-arrest following DNA damage (Barth et al., 1996; Herzinger et al., 1995; Kharbanda et al., 1994; O'Connor et al., 1994). The cell cycle is therefore halted in G2 to allow DNA repair.

1.1.4 The role of Rb and p53 in cell cycle regulation

Cell cycle progression is also regulated by the retinoblastoma protein Rb (p105). Together with p107 and p130 it belongs to the pocket protein family of the nuclear phosphoproteins. The pocket protein family is known to bind to an LXCXE motif (Dyson, 1998; Obaya and Sedivy, 2002). The general function of Rb is to prevent quiescent cells from proceeding to S phase by binding to the E2F transcription factors E2F1, E2F2 or E2F3 and inhibiting their transcriptional activity by recruiting repressing HDACs to the promoters of the E2F-responsive genes (Brehm et al., 1998; Dunaief et al., 1994; Magnaghi-Jaulin et al., 1998; Strober et al., 1996). Phosphorylated Rb can no longer bind to the E2F transcription factor, which disrupts HDAC repression and allows E2F to activate transcription of genes required for progression into S phase e.g. cyclin E (Harbour et al., 1999; Zhang et al., 2000a). Phosphorylation of Rb occurs during G1 phase and is mediated by cyclinD/CDK4/6 (Harbour et al., 1999; Mittnacht, 1998). Cyclin E/CDK2 further phosphorylates Rb which mediates transcription of cyclin A and E2F which is essential for DNA replication (Bartek and Lukas, 2001; Harbour et al., 1999; Obaya and Sedivy, 2002; Strobeck et al., 2000; Zhang et al., 2000a). During the subsequent M phase, the Rb protein is dephosphorylated so that it can once again inhibit E2F (reviewed in (Halaban, 2005)).

The tumour suppressor and transcription factor p53 which was identified in 1979 is one of the first genes to be activated following cellular stress (Lane and Crawford, 1979; Linzer and Levine, 1979; Vousden, 2002; Vousden and Lu, 2002). In its inactive state it is bound to MDM2 which tags p53 for proteasome-mediated degradation (Kamijo et al., 1997; Quelle et al., 1995; Zhang et al., 1998) (Figure 3). Its function is to induce cell cycle arrest in G1/S and G2/M after DNA damage, but the protein is also involved in DNA repair, differentiation, senescence and can initiate apoptosis (Ryan et al., 2001; Vousden, 2002; Vousden and Lu, 2002).

After DNA damage, p53 becomes active by phosphorylation and induces $p21^{WAF1/CIP1}$ transcription which then inhibits cyclin E/CDK2 and phosphorylation of Rb (el-Deiry et al., 1993; Sherr and Roberts, 1999). The stability as well as the ability to bind DNA is regulated by phosphorylation of p53 at serine 15 (Appella and Anderson, 2001; Bode and Dong, 2004; Schavolt and Pietenpol, 2007).

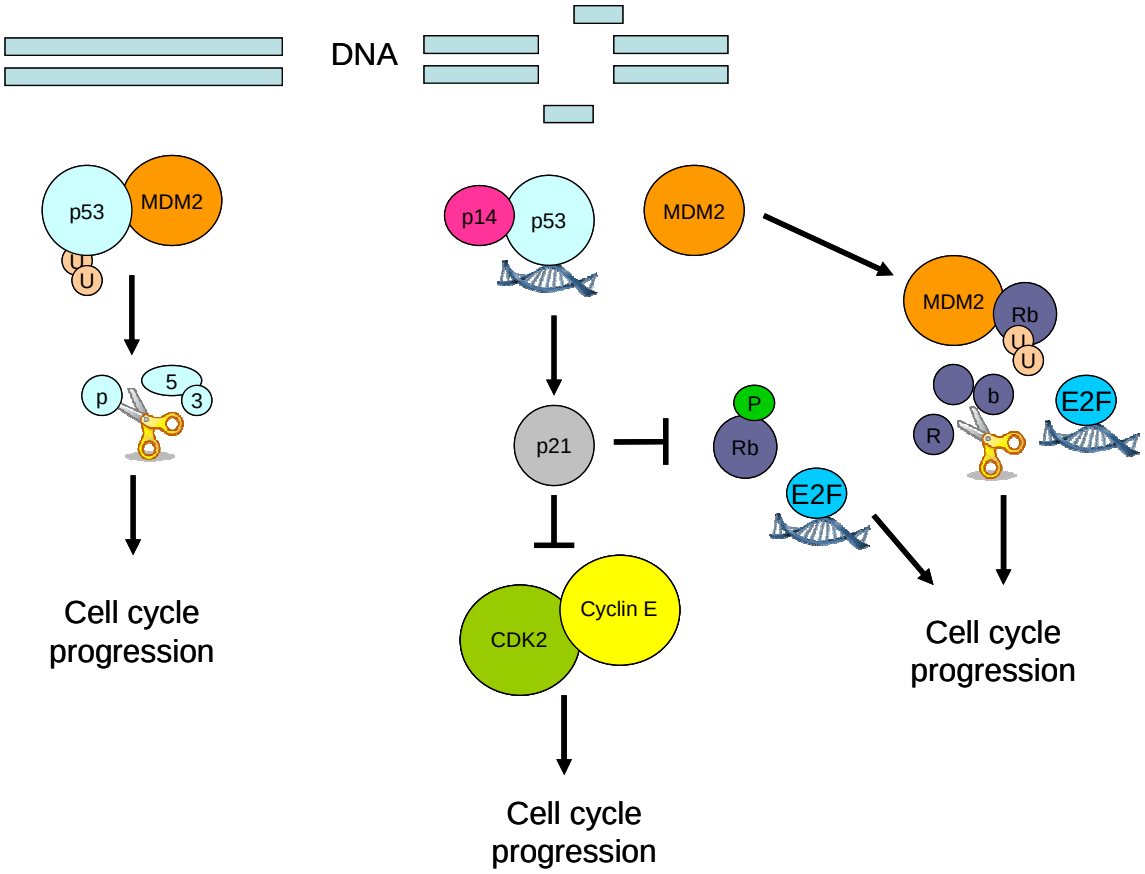

Figure 3 – p53 pathway

p53 is known to associate with MDM2 which tags the protein for ubiquitination which leads to cell cycle progression. In case of DNA damage, p53 becomes activated and no longer binds to MDM2. $P14^{ARF}$ was shown to stabilise p53 which can then induce transcription of target genes e.g. the CDK-inhibitor $p21^{WAF1/CIP1}$. $P21^{WAF1/CIP1}$ is known to inhibit the cyclin E/CDK2 complex and therefore prevents cell cycle progression. $P21^{WAF1/CIP1}$ was also shown to inhibit phosphorylation and therefore the activation of the Rb protein. The Rb protein remains associated with E2F which cannot induce transcription of its target genes to promote cell cycle progression. MDM2 was reported to bind Rb and to promote degradation of the Rb protein allowing cell cycle progression. However, it is not fully understood what triggers the association of MDM2 and Rb.

Interestingly, p53 was found to be mutated in the majority of human tumours proposing its essential role in cell cycle regulation. $P14^{ARF}$ is one known regulator of p53 which stabilises the protein by preventing MDM2 binding (Kamijo et al., 1997; Quelle et al., 1995; Sherr and Weber, 2000; Zhang et al., 1998). Further, the MDM2 gene is also transcriptionally activated by p53 and when the protein is bound to p53 it initiates the translocation of the complex from the nucleus in the cytoplasm which is associated with the ubiquitination of p53 (Kubbutat et al., 1997; Michael and Oren, 2003). Therefore, MDM2 can abolish p53-mediated arrest and apoptosis (Chen et al., 1993).

1.2 Epstein-Barr Virus (EBV)

EBV belongs to the herpesviridae family which share common virion morphology consisting of a core containing the linear, double-stranded DNA, a capsid and an envelope presenting viral glycoproteins on its surface. The herpesviridae are separated into 3 subfamilies: Alphaherpesvirinae, Betaherpesvirinae and Gammaherpesvirinae. Alpha herpes viruses can infect a wide range of hosts and have a short reproductive cycle, whereas beta herpes viruses have a restricted host range and a long reproductive cycle. Gamma herpes viruses also have a limited host range but reproduce at a more variable rate. Overall, eight different species of Herpes viruses have been isolated from humans: herpes simplex virus 1 (HSV-1), herpes simplex virus 2 (HSV-2), varicella-zoster virus (VZV), Epstein-Barr virus (EBV), human cytomegalovirus (HCMV), Roseoloviruses HHV-6 and HHV-7 and Kaposi's sarcoma-associated herpesvirus (KSHV or HHV-8).

EBV was isolated from a Burkitt's lymphoma biopsy in 1964 (Epstein et al., 1964), and was the first herpes virus to have its genome completely cloned and sequenced. EBV was the first human virus found to play a role in tumourigenesis. The virus causes a latent and persistent infection and is the only gamma herpes virus known to be associated with several cancers e.g. endemic Burkitt's lymphoma, undifferentiated nasopharyngeal carcinoma, Hodgkin's disease and AIDS-associated B-lymphoma and post-transplant lymphoproliferative disease (PTLD), reviewed in (Crawford, 2001; Kieff and Rickinson, 2001). About 90% of the entire population is infected by the virus with infection usually occurring during the early years of childhood via salivary contact (Niederman et al., 1976). Viral infection during childhood does not often show any

symptoms (De Matteo et al., 2003; Henle et al., 1969). Approximately 50% of late EBV infections lead to infectious mononucleosis (IM, see section 1.8.1), also known as Pfeiffer's disease or glandular fever, a benign disease of the leucocytes and lymph nodes (reviewed in (Kieff and Rickinson, 2001)). The variability of symptoms after primary infection with EBV is due to differences in the immune response. Proliferation of T lymphocytes followed by a release of cytokines e.g. interferon-γ and interleukin-2 has been found in patients suffering from infectious mononucleosis, whereas an asymptomatic infection does not lead to an expansion of T lymphocytes (Silins et al., 2001; Williams et al., 2004). It has been observed that in underdeveloped countries, the percentage of individuals infected with EBV during childhood is much higher than in more developed countries, where therefore a late infection followed by infectious mononucleosis is more prevalent (Henle et al., 1969).

EBV preferentially infects two different human cell types in two different ways (Figure 4). Primary infection can occur in circulating B lymphocytes or epithelial cells in the mouth and upper throat (oropharyngeal) epithelium *in vivo*. This occurs via direct binding of the viral glycoprotein gp350 to the complement receptor 2 (CD21 receptor) on the B cell. Interestingly, EBV presents mainly one glycoprotein gp350/220 on the outer surface which is different to most other herpesviruses (reviewed in (Kieff and Rickinson, 2001)). After the virus has bound to the B cell, the cell and virus membrane fuse and endocytosis of the virion occurs. The circularisation of EBV DNA was found to occur after uncoating of the virion 12-16 hours after infection when coinciding with early latent viral gene expression (Adams and Lindahl, 1975; Hurley and Thorley-Lawson, 1988).

EBV establishes a persistent latent infection in B lymphocytes and transforms resting B lymphocytes leading to uncontrolled cell proliferation. Outgrowth of these transformed cells is controlled by EBV-specific cytotoxic T lymphocytes (Pope et al., 1968b), reviewed in (Kieff and Rickinson, 2001). The purpose of the latent phase is to maintain the virus in the host and is accompanied by expression of only a small number of genes to avoid an immune response.

Infection of epithelial cells by EBV is thought to occur in a gp350-dependent or gp350-independent manner but is also able to use gp25 to bind the host cell surface

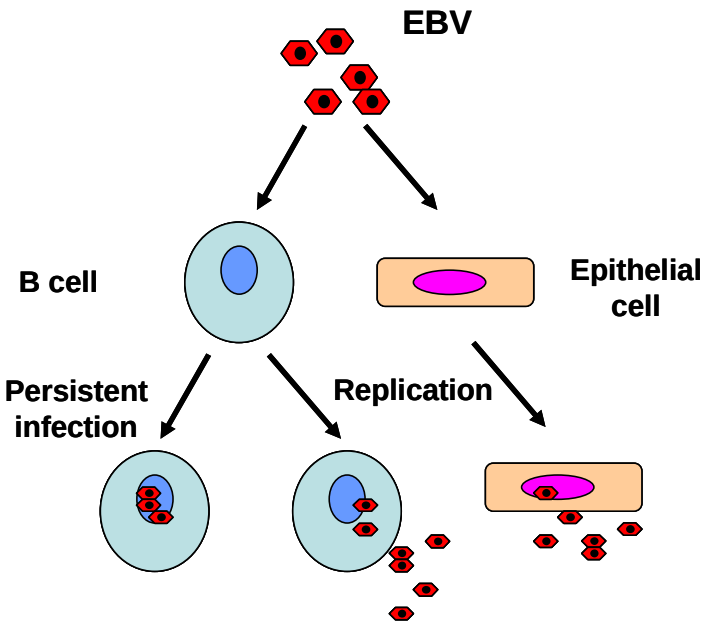

Figure 4 - Overview of the Epstein-Barr virus infection, which involves two cell types: B cells and epithelial cells. After B cells are primary infected, a latent state is established, which is controlled by EBV-specific cytotoxic T lymphocytes. Occasionally, a latently infected B cell can switch to the lytic state associated by replication of the virus by releasing it from these cells directly into the saliva whereby epithelial cells and other B cells might be infected. Epithelial cell infection results in replication of the virus followed by lysis of the cell (lytic state).

(Fingeroth et al., 1999; Maruo et al., 2001). The production and distribution of the virus occurs during the lytic phase and epethilial cell infection is usually lytic in nature (reviewed in (Schwarzmann et al., 1998)). EBV replication also occurs spontaneously in a small fraction of B cell population as the result of viral reactivation. Virions are released in the saliva during lytic cycle.

Following EBV infection, the phenotype of the cell changes; infected cells grow bigger and express several B cell activation markers e.g. CD23, CD54, CD11a and cell adhesion molecules e.g. ICAM-1 and LFA-1 leading to cell aggregation (Calender et al., 1987; Wang et al., 1988).

1.3 EBV gene expression

The EBV genome consists of a double-stranded DNA (~172 kb), which is linear in the virion and circularises post-infection forming a closed circular episome (Hurley and Thorley-Lawson, 1988; Lindahl et al., 1976). The genome contains about 90 genes, but only 11 genes are expressed when primary B cells are infected and immortalised by EBV in culture generating lymphoblastoid cell lines (LCLs). LCLs express the Epstein-Barr virus nuclear antigens (EBNAs), EBNA 1, 2, 3A, 3B, 3C and leader protein (LP) and 3 latent membrane proteins (LMPs), LMP 1, 2A und 2B. The remaining 2 genes encode the Epstein-Barr virus encoded RNAs (EBER 1 and 2) which do not contain a polyadenylated tail and remain as untranslated RNA. The expression of all 11 latent genes is defined as latency III. Five proteins (EBNA 1, 2, 3A, 3C, LMP1) have been shown to be essential for transformation of B lymphocytes whereas EBNA LP has been shown to be important but not essential for B cell immortalisation by inducing cell proliferation (Cohen et al., 1989; Kaye et al., 1993; Lee et al., 1999; Mannick et al., 1991; Tomkinson et al., 1993a). Therefore, these proteins are highlighted as proteins with oncogenic potential.

The EBV genome contains several promoters which are involved in the expression of the latent EBV proteins: the LMP promoters, Qp, Wp and Cp. The C and the W promoters are involved in the expression of all EBNAs (Figure 5): Cp, which is located within the unique region just upstream of the EBV major internal repeat (IR-1), and Wp, which is located within the IR-1 repeat and is present in multiple copies. Following

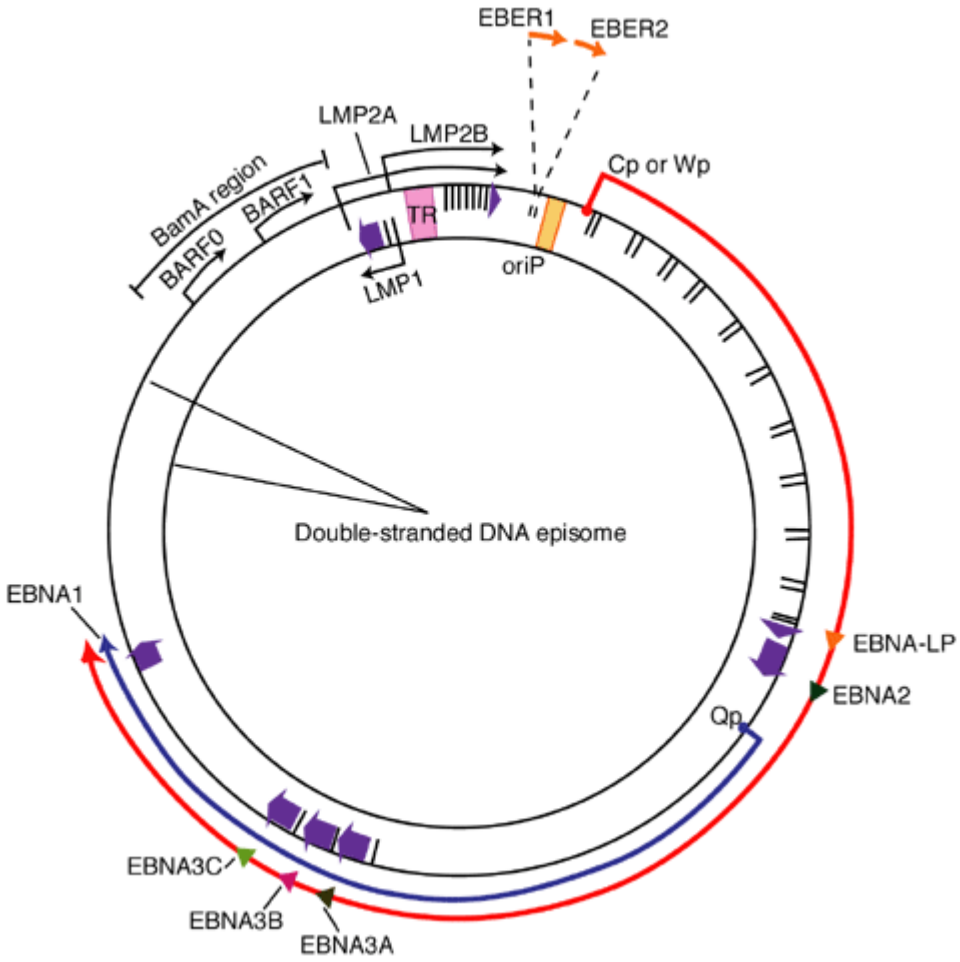

Figure 5 – EBV genome: Latent genes of the Epstein-Barr virus

Latent genes of the Epstein-Barr virus are demonstrated on the double-stranded DNA. The origin of replication (oriP) is coloured orange. The purple arrows indicate the coding exons of the proteins expressed by EBV. Figure downloaded from (Murray and Young, 2001).

infection, the W promoter is initially turned on by the binding of B cell-specific factors to 3 domains upstream of the Wp transcription start site known as UAS1, 2 and 3.

Activation of the W promoter leads to the expression of EBNA LP and EBNA 2 (Bell et al., 1998; Walls and Perricaudet, 1991).

Cp activation by EBNA 2 triggers the switch from the W to the C promoter leading to expression of all EBNA proteins within 36 h post-infection (Puglielli et al., 1996; Woisetschlaeger et al., 1990). Other cellular factors play an important role in the Wp to Cp switch, e.g. nuclear factor Y (NF-Y) as it activates the C promoter (Borestrom et al., 2003). EBV does not have its own RNA polymerase, therefore, it uses the cellular RNA polymerase II to transcribe genes from all promoters. A very long single precursor RNA molecule encoding all 6 EBNAs is generated which is processed by differential splicing to mediate protein expression of all EBNAs (Bodescot and Perricaudet, 1986). Each of the latent proteins has a specific function in the viral life cycle.

EBNA 2 also activates the expression of the bidirectional LMP1 and LMP 2B promoter. Qp drives expression of EBNA1 in the absence of Cp activity and EBNA 2 expression (Nonkwelo et al., 1996a; Schaefer et al., 1995a).

EBV possesses the ability to persist in the memory B cells of the infected host in different latent states characterised by the expression of different patterns of latent genes. Latency I, II and III pattern of gene expression are also found in different EBV-accociated tumours (Table 1).

1.4 Latent infection in healthy hosts

More than 90% of the entire human population have been infected by EBV, but it is a rare occurence that infected hosts develop an EBV-related tumour. Although EBV gene expression is highly restricted in healthy individuals, interestingly, all patterns of latency can be detected in B cells. It is therefore likely that the virus life cycle involves many different patterns of gene expression (Babcock et al., 1998; Babcock and Thorley-Lawson, 2000; Joseph et al., 2000; Miyashita et al., 1997).

	Latency 0	Latency I	Latency II	Latency III
Genes expressed		EBNA 1 EBER 1 EBER 2	EBNA 1 LMP 1 LMP 2A LMP 2B EBER 1 EBER 2	EBNA1 EBNA 2 EBNA 3A EBNA 3B EBNA 3C EBNA LP LMP 1 LMP 2A LMP 2B EBER 1 EBER 2
Diseases		BL group I	NC, HD, T-cell lymphomas	PTLD AIDS-associated lymphomas

Table 1 – EBV protein expression pattern during different latencies

In latency 0, no latent EBV proteins are expressed. EBV latency I expresses EBNA 1 and EBER1 and EBER2. This pattern of expression is found in Burkitt's lymphoma group I. EBV latency II, where EBNA 1, LMP1 and LMP2A and LMP2B are expressed, is detected in several malignant diseases, such as undifferentiated nasopharyngeal carcinoma (NC), Hodgkin's disease (HD) and T cell lymphomas. EBV latency III, where all latent EBV proteins are expressed, is detected in post-transplant lymphoproliferative disease (PTLD) and AIDS-associated lymphomas.

How EBV infects and persists in its host is not completely understood, but a model has been suggested (Thorley-Lawson, 2001; Thorley-Lawson and Gross, 2004). EBV infects resting B cells (naïve B cells) and transforms them into B blasts expressing all latent EBV proteins (latency III) (Babcock et al., 1999). B blasts differentiate into centroblasts followed by centrocytes (germinal centre cells) which display restricted expression of EBV latent genes (EBNA 1, LMP1 and LMP2a), (latency II). This may be due to the fact that EBNA 2 expression blocks differentiation of B cells into memory cells and therefore needs to be silenced (Polack et al., 1996). Centrocytes can then further differentiate into memory B cell which generally lack expression of any latent EBV genes which is described as the silent state (latency 0). Expression of EBNA 1 from the Q promoter was also observed in the rarely dividing memory B cells (latency I) to ensure that the episome is not lost during cell division (Davenport and Pagano, 1999; Hochberg et al., 2004). Occasionally, memory B cells could develop into plasma cells for viral replication expressing all lytic genes (Altmeyer et al., 1997; Crawford and Ando, 1986; Thorley-Lawson and Gross, 2004).

1.5 Immune response in EBV-infected hosts

Infection with EBV causes a massive proliferation of cytotoxic T cells which are competent to eliminate most of the infected cells (Callan et al., 1996; Callan et al., 1998). T cells mainly detect EBV-infected cells which express EBNA 2, EBNA 3A, EBNA 3B and EBNA 3C but also the LMP proteins. Since the genes expressed in latency I are not commonly recognised by T cells, these EBV-infected cells can evade the immune response and this allows the virus to persist.

1.6 Latent EBV gene expression in diseases

Unlike other herpes viruses, expression of the latent EBV proteins can induce the transformation of resting human B cells into immortalised lymphoblastoid cell lines *in vitro* indicating its tumourigenic ability (Pope et al., 1968a). Different patterns of latent EBV expression are also found in EBV-related diseases. Latency III is observed in EBV-positive tumours from post-transplant and AIDS patients and is regulated as mentioned above from the Cp/Wp promoter. In latency I and II the EBNA 1 mRNA is transcribed by the Qp promoter (Figure 5), since no other EBNAs are expressed during these latency states. The latency II phenotype is typified by the expression of only

EBNA 1, all three LMPs and the two EBERs. It was found in undifferentiated nasopharyngeal carcinoma, Hodgkin's disease Reed-Sternberg cells and T cell lymphomas (Brink et al., 2000a; Fahraeus et al., 1988; Young et al., 1988). In latency I only EBNA 1 and the two EBERs are expressed. This pattern was detected in Burkitt's lymphoma group I (Rowe et al., 1987). Lack of viral protein expression guarantees that the infected cell cannot be recognised by the immune response of the host.

1.7 Latent EBV proteins

1.7.1 EBNA 1

EBNA 1 consists of 641 amino acids and displays a size of 76 kD in denaturing polyacrylamide gels. It is known to be one of the viral proteins essential for transformation of B lymphocytes and was the first EBV protein to be identified in EBV-immortalised cells (Lee et al., 1999; Reedman and Klein, 1973).

The protein is known to be able to bind to viral and cellular DNA directly as a homodimer via its carboxy-terminus (Ambinder et al., 1990; Petti et al., 1990a). As the EBV genome only rarely integrates into the host genome, the episome needs to be replicated before mitosis which occurs by EBNA 1 binding to EBNA 1-binding motifs in the OriP (origin of replication in EBV) thereby initiating replication (Chittenden et al., 1989; Ito et al., 2002; Ito and Yanagi, 2003; Petti et al., 1990b; Rawlins et al., 1985; Yates et al., 1985). In addition to playing a role in replication, EBNA 1 also manages segregation of the episome during mitosis, maintenance of latency and transcriptional activation of latent Epstein-Barr virus genes (Marechal et al., 1999; Reisman and Sugden, 1986; Sugden and Warren, 1989). Episomal maintenance is thought to occur via tethering of the viral OriP to the host cell chromosomes which ensures that a copy of the viral episome is transferred into the daughter cell (Marechal et al., 1999). EBNA 1 also plays a role as a transcriptional activator and its interaction with OriP can transactivate the Cp and the LMP1 promoters (Reisman and Sugden, 1986; Sugden and Warren, 1989). Interestingly, the binding of multiple EBNA 1 homodimers at OriP has been shown to be required to fully transcriptionally activate Cp (Zetterberg et al., 2004). Further, EBNA 1 was found to be able to bind two sites downstream of the Q promoter (Nonkwelo et al., 1996b; Schaefer et al., 1995b). EBNA 1 expression was shown to be auto-downregulated by interaction with these two downstream sites (Sample et al.,

1992). However, work published by several authors reported that EBNA 1 binding to the Q promoter has an activating effect leading to more EBNA 1 expression. Further, the cellular transcription factor E2F1 was able to upregulate Qp by possibly binding the E2F-binding site within the EBNA 1-binding element when EBNA 1 was expressed, but can also activate Qp in the absence of EBNA 1 (Nonkwelo et al., 1997; Sung et al., 1994).

EBNA 1 is known to contain a Gly-Ala repeat domain which can inhibit its degradation by the proteasome and thus the presentation of EBNA 1 epitopes to cytotoxic T cells (Levitskaya et al., 1995; Levitskaya et al., 1997). Therefore, EBNA 1 is the only EBNA not to be detectable by cytotoxic T cells. This could explain why EBNA 1 is the only latent protein, which is consistently expressed throughout all different patterns of EBV protein expression found in EBV-associated malignancies.

This Gly-Ala repeat domain was also shown to inhibit mRNA translation of EBNA 1 both *in vitro* and *in vivo,* indicating that this domain plays a more important role in the evasion of the immune response than preventing proteasome degradation. Proteasome inhibition was therefore suggested to have its role in maintaining the EBNA 1 expression level (Yin et al., 2003).

1.7.2 EBNA 2

EBNA 2 was the first EBV latent protein to be identified as essential for B cell transformation (Cohen et al., 1989). However, it was already reported in 1974 that a specific region of DNA was deleted from the EBV strain P3HR-1 and that immortalisation of B cells could not occur using this strain for EBV infection (Miller et al., 1974). This region is now known to encode EBNA 2. When this missing region was reconstituted by cloning fragments containing the EBNA 2 gene into the EBV genome, P3HR-1 was able to transform primary B cells (Cohen et al., 1989; Hammerschmidt and Sugden, 1989). It was also demonstrated by Bettina Kempkes *et al.* that EBNA 2 is required for the ongoing proliferation on infected cells. These authors developed an EBNA 2-inducible system using a cell line containing a conditionally active estrogen receptor-EBNA 2 fusion protein and demonstrated that this cell line, ER-EB 2-5, underwent cell cycle arrest in the absence of estrogen when EBNA 2 was not functionally active (Kempkes et al., 1995b).

EBNA 2 is a transcriptional activator of cellular and viral genes and can upregulate the expression of numerous genes, including CD21, CD23, RUNX3 (AML2), *c-myc* and *c-fgr* and activate the viral Cp as well as the promoters of the LMP1 and LMP2 genes (Cohen and Kieff, 1991; Grossman et al., 1994a; Kaiser et al., 1999; Spender et al., 2001; Wang et al., 1990b). However, EBNA 2 cannot bind DNA directly but targets the promoters via the DNA-binding proteins RPB-J kappa (CBF1) and Spi-1/PU.1 (Grossman et al., 1994a; Henkel et al., 1994; Johannsen et al., 1995b; Zimber-Strobl et al., 1994). EBNA 2 then recruits proteins crucial for transcriptional activation e.g. TFIIB, TAF40 and TFIIH (Tong et al., 1995a; Tong et al., 1995b).

Further, the transcriptional activity of EBNA 2 was shown to require the activity of the RNA polymerase II CTD kinase, CDK9, and associates with the SNF-SWI complex, p300, CBP and PCAF histone acetyltransferases (HATs) (Bark-Jones et al., 2006; Wang et al., 2000; Wu et al., 1996; Wu et al., 2000).

EBNA 2 mediates the transactivation of the LMP1 promoter via binding to PU.1/Spi-1 or RBP-J kappa (CBF-1) (Grossman et al., 1994a). The C promoter is activated via RPB-J kappa in cooperation with AUF-1 and mutations in the RBP-J kappa binding site result in the loss of the transforming ability of EBV (Fuentes-Panana et al., 2000; Sung et al., 1991; Yalamanchili et al., 1994). RBP-J kappa is a downstream target in the Notch pathway. When the Notch pathway is activated by extracellular ligands bound to the Notch receptor, the intracellular domain of Notch, Notch-IC is cleaved which then interacts with RBP-J kappa bound to DNA leading to transactivation. It is thought that EBNA 2 replaces the function of Notch-IC so that the extracellular stimulation of the Notch receptor is redundant (Zimber-Strobl and Strobl, 2001).

The contribution of EBNA 2 to the B cell transformation process is thought to be due to the activation of those cellular and viral promoters which are known to have a major effect on cell cycle progression. For example, c-Myc can induce cyclin D, cyclin E and CDK4 and downregulate $p21^{WAF1/CIP1}$ and $p27^{KIP1}$. Activation of the C promoter by EBNA 2 also leads to the expression of the EBNAs LP, 2, 3A, 3B and 3C, which have been reported to play a role in cell cycle progression (Gartel et al., 2001; Kaiser et al., 1999; Santoni-Rugiu et al., 2000; Yang et al., 2001b).

1.7.3 EBNA LP

EBNA LP, also known as EBNA 5, received its name as it is expressed from mRNA generated from the leading sequence of the long EBNA transcript. It is coexpressed with EBNA 2 as early as 2 hours after transfection. It plays an important role in B cell transformation (Hammerschmidt and Sugden, 1989; Mannick et al., 1991). EBNA LP is known to activate cyclin D2 expression and can enhance EBNA2-mediated transactivation of the Cp and LMP1 promoter in primary B cells (Harada and Kieff, 1997; Nitsche et al., 1997; Sinclair et al., 1994). However, EBNA LP is not required for EBNA 2-mediated transactivation of the cyclin D2 promoter in EREB2.5 cells (Harada and Kieff, 1997; Nitsche et al., 1997; Spender et al., 2001). EBNA LP was found to be highly phosphorylated in G2/M which might be mediated by CDK1 or by the EBV encoded kinase BGLF4 (Kato et al., 2003a; Kitay and Rowe, 1996). It has been reported that LP could interact with Rb, p53 and $p14^{ARF}$ which may compromise their tumour suppressor function (Inman and Farrell, 1995; Kashuba et al., 2003b). Other suggestions were that it might target the p53/Rb pathway by inhibiting $p14^{ARF}$ which can bind MDM2 (Kashuba et al., 2003a; Kashuba et al., 2003b). However, it has not been shown that p53 function is inhibited in EBV infected cells and the p53 pathway might therefore not be affected by EBV at all (Allday et al., 1995b; O'Nions and Allday, 2003).

1.7.4 EBNA3 family

The EBNA 3 proteins EBNA 3A, 3B and 3C encode a number of similar motifs: a putative leucine zipper motif, an acidic domain, proline and glutamine rich repeats, and several arginine and lysine residues potentially important for nuclear localisation. Although their homology is relatively low, it is thought that they have duplicated from the same gene as they are tandemly arranged in the viral genome (Petti et al., 1988). Further, the three genes of the EBNA 3 family are encoded by the same structure: a short 5’ exon and a long 3’ exon. Interestingly, a binding site for RBP-J kappa is also present and highly conserved in all three genes allowing all three EBNAs to interact with this DNA-binding protein (Robertson et al., 1996; Zhao et al., 1996). Therefore, EBNA 2 enabled transcriptional activation mediated by RBP-J kappa can be regulated by EBNA 3A, 3B and 3C as RBP-J kappa binding to any of these three proteins abolishes the EBNA 2 – RBP-J kappa interaction (Johannsen et al., 1996; Waltzer et al., 1996). As EBNA 2 transactivates the C promoter and therefore EBNA 3 gene

transcription, the EBNA 3 proteins form a negative feedback loop which may result in abrogation of EBNA 2 upregulation of EBNA 3 transcription. All 3 EBNA 3 proteins can also repress EBNA 2-mediated activation of LMP1 and LMP2 (Le Roux et al., 1994; Waltzer et al., 1996). However, Jiménez-Ramírez *et al*. demonstrated that EBNA 3C expression in Raji cells does not downregulate EBNA 2 and has only little or no negative effect on EBNA 2-mediated C promoter activation (Jimenez-Ramirez et al., 2006).

In spite of their similarities, only EBNA 3A and EBNA 3C were shown to be essential for B cell transformation *in vitro*; EBNA 3B, however, is dispensable (Tomkinson et al., 1993a).

1.7.5 EBNA 3A

EBNA 3A is essential for EBV transformation of B cells and plays an important role in LCL proliferation (Kempkes et al., 1995a; Maruo et al., 2003; Tomkinson et al., 1993b). EBNA 3A plays a role in transcriptional activation as well as repression and has also been shown to regulate protein function by protein-protein interaction. Repression of the C promoter occurs via its RBP-J kappa binding site. EBNA 3A interacts with the corepressor CtBP and could play a role in repression of transcription. It was reported that RBP-J kappa recruits CtBP and mediates repression of the genes regulated by the Notch pathway and that mutated CtBP abolishes this repressing effect by RBP-J kappa (Hickabottom et al., 2002; Oswald et al., 2005). The interaction of EBNA 3A with CtBP also facilitates cooperation with (Ha)-Ras which was observed in the immortalisation and transformation of primary rodent fibroblasts (Hickabottom et al., 2002).

EBNA 3A was also shown to interact with the cell cycle protein chk2 indicating a role in disruption of cell cycle control (Chehab et al., 2000; Krauer et al., 2004b; Krauer et al., 2004c; Petti et al., 1990a). However, a deregulation of chk2 could not be observed in LCLs but G2/M checkpoint deregulation by inhibition of chk2 may still occur in tumour cell lines (Falck et al., 2001; O'Nions and Allday, 2003). Overexpression of EBNA 3A leads to a prolonged G0/G1 phase which may be due to the fact that overexpression downregulates CD21, CD23 and c-myc expression (Cooper et al., 2003). The downregulation of these genes may also occur by EBNA 3A binding to the genes

via RBP-J kappa since all 3 genes contain a RBP-J kappa binding site (Cooper et al., 2003).

EBNA 3A was shown to downregulate the proapoptotic Bcl-2-family member Bim in cooperation with EBNA 3C and can therefore mediate cell survival and tumourigenesis (Anderton et al., 2008). To support the antiapoptotic role of EBNA 3A, it was reported that EBNA 3A, not EBNA 3C, can induce expression of the chaperones Hsp70 and Hsp70B/B9 and co-chaperones Bag3 and DNAJA1/Hsp40 (Young et al., 2008). EBNA 3A was further shown to associate with Hsp70, Hsp70B9 and Hsp40 which may mediate stabilisation of the EBNA 3A protein (Young et al., 2008). This interaction of EBNA 3A with the chaperones and co-chaperones as well as the induction of their promoters did not occur via an association with CtBP (Young et al., 2008).

1.7.6 EBNA 3B

EBNA 3B is not essential for B cell transformation *in vitro* (Chen et al., 2005; Tomkinson et al., 1993a). EBNA 3B was found to localise in the nucleus signalled by nuclear localization signals (NLS) and to co-localise with EBNA 3A and 3C (Burgess et al., 2006). Lymphoblastoid cell lines infected with the B95.8 strain have been described that have lost the expression of EBNA 3B; therefore its function may not be necessary for cell proliferation (O'Nions and Allday, 2004). The loss of expression might be due to the fact that EBNA 3B is immunogenic and thus a target for cytotoxic T cells. However, EBNA 3B knockout cells were shown to grow slowly and have reduced levels of EBNA 3C indicating that EBNA 3B may be important for efficient proliferation (Chen et al., 2006). EBNA 3B was reported to have a downregulating effect on CXCR4 as a knockdown of the protein led to increased CXCR4 expression on the cell surface (Chen et al., 2006). Interestingly, CXCR4 and its only ligand CXCL12 are required for B-lymphopoiesis but downregulation of CXCR4 was also reported in herpes viruses like HHV6 and HHV7 as well as EBV (Ehlin-Henriksson et al., 2006; Ma et al., 1998; Nakayama et al., 2002; Yasukawa et al., 1999). It was suggested that EBNA 3B downregulates CXCR4 to allow EBV-infected cells to distribute to the periphery as CXCR4-expressing cells remain in the bone marrow (Chen et al., 2006; Nie et al., 2004). Further, EBNA 3B was found to downregulate the BL-associated antigen (BLA/CD77), to upregulate the cytoskeletal protein vimentin and the surface

expression of the activation antigen CD40 when overexpressed in the EBV-negative BL cell line DG75 (Silins and Sculley, 1994). EBNA 3B could also prevent serum starved DG75 cells from apoptosis probably due to increased levels of the anti-apoptotic Bcl-2 oncoprotein (Silins and Sculley, 1995).

1.7.7 EBNA 3C

EBNA 3C, also known as EBNA 6, is a protein of 992 amino acids with a molecular weight of about 155-160 kD on SDS-PAGE (Allday et al., 1988; Petti et al., 1988). EBNA 3C functions as a transcriptional activator and repressor and helps to control viral gene expression during latency. It contains a number of domains found in many transcription factors. This includes a proline-rich and a glutamine-proline-rich domain and another which shows homology to a basic leucine zipper domain (Figure 6), (Landschulz et al., 1988; Marshall and Sample, 1995). However, this domain is not capable of homodimerisation and contains atypical residues which are not normally found in zipper domains (West et al., 2004). Therefore, this domain is not likely to be functional. Several nuclear localization signals (NLS) were identified, one at the N-terminal end (aa 72–80), one in the middle (aa 412–418) and one at the C-terminal end (aa 939–945) of the EBNA 3C protein which are important for mediating translocation of EBNA 3C to the nucleus (Figure 6) (Krauer et al., 2004a). EBNA 3C is located in the nucleus throughout the cell cycle and was found to associate with the nuclear matrix (Krauer et al., 2004a; Petti et al., 1990a).

Complementation assays in LCLs showed that most amino acids of EBNA 3C are essential for continued LCL growth (Maruo et al., 2009). LCLs expressing EBNA 3C containing a mutated RBP-J kappa site could not maintain LCL proliferation indicating the importance of the EBNA 3C/RBP-J kappa interaction in LCL growth (Lee et al., 2009; Maruo et al., 2009).

1.7.7.1 Regulation of LMP1 expression by EBNA 3C

EBNA 3C was found to upregulate the expression of the EBV protein LMP1 (Allday et al., 1993). EBNA 2 was previously shown to upregulate LMP1 expression (Fahraeus et al., 1990). The EBV-positive cell line Raji which has a natural deletion in the EBNA 3C gene was observed to arrest in G1 accompanied by a reduction in LMP1 when these

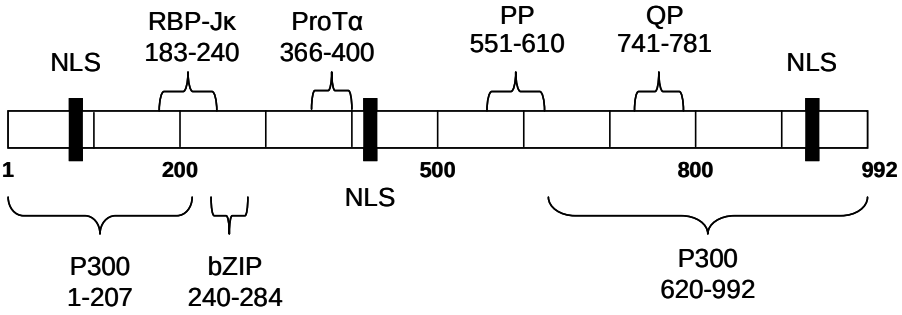

Figure 6 –Schematic of basic structure of the EBNA3C protein with the identified motifs.

This figure shows the domains for interaction with p300, RBP-Jκ and ProTα, the putative leucine zipper motif, and proline (PP) -rich and glutamine (QP) –rich domains. 3 nuclear localization signals (NLS) were identified.

cells were cultured to a high density (Allday and Farrell, 1994). This result indicates that LMP1 expression is dependent on the state of the cell cycle. Raji cells stably expressing the EBNA 3C gene did not reduce LMP1 expression in growth-arrested cells (Allday and Farrell, 1994).

Therefore, the authors suggested that EBNA 3C influences LMP1 expression either by the release of LMP1 repression or by subtle alteration of the cell cycle state of growth arrest that allows LMP1 expression (Allday and Farrell, 1994). Furthermore, EBNA 3C is able to co-activate the LMP1 promoter in reporter assays in a manner dependent on the presence of a DNA element including the Spi-1/Spi-B (PU.1) binding site in the LMP1 promoter (Zhao and Sample, 2000). The accurate regulation of LMP1 expression in EBV-transformed cells is important since high levels were found to be toxic to the cells (Wang et al., 1985). It was previously shown that EBNA 2 binds Spi-1 and EBNA 3C is also able to interact directly with the ets domain of the transcription factors Spi-1 and Spi-B *in vitro* (Johannsen et al., 1995a; Zhao and Sample, 2000). More precisely, a region of the EBNA 3C protein including the basic leucine zipper (bZIP) domain was shown to interact with this ets domain (Zhao and Sample, 2000).

1.7.7.2 Effects on cellular genes

A morphological change of the cells is also observed when EBNA 3C is expressed. ‘Spiky’ membranous projections were identified on the cell surface, which often occurred only on one side whereas the membrane at other side stayed smooth and rounded. The changes in phenotype was accompanied by an increase in the cytoskeletal protein vimentin and the B cell activation antigen CD23 (Allday et al., 1993; Allday and Farrell, 1994; Wang et al., 1990a). EBNA 3C was also shown to induce CD21 expression, which is a cell-specific receptor on mature B cells that contributes to the morphological change (Wang et al., 1990a). The mechanism by which EBNA 3C is able to increase gene expression has not been fully determined, but it has been demonstrated that the effect of EBNA 3C on CD21 occurs indirectly since no direct activation of the CD21 promoter could be detected in transient transfection assays (Radkov et al., 1997). Despite the known transcriptional regulatory functions of EBNA 3C, it has not been reported to bind directly to DNA but was shown to bind DNA via the DNA-binding protein RBP-J kappa (Marshall and Sample, 1995; Robertson et al., 1995).

1.7.7.3 Repression activity

EBNA 3C is able to interact with the transcription factor prothymosin α and together they can associate with the co-repressors human histone deacetylases HDAC1 and HDAC2 and the corepressors mSin3A and N-CoR (Knight et al., 2003a; O'Nions and Allday, 2004; Radkov et al., 1999). Binding to prothymosin α is essential to stabilise the complexes and ensures their full activity (Knight et al., 2003a). Further, the complex can also associate with the known co-activator histone acetyltransferase p300 and Histone H1 *in vitro* and *in vivo* (Cotter and Robertson, 2000). Although no reports show that these complexes actually bind to the C promoter, it is thought that these complexes may play a role in the EBNA 3C-mediated repression of the Cp via RBP-J kappa, previously demonstrated by the Allday lab (Cotter and Robertson, 2000; Haritos et al., 1984; Knight et al., 2003b; Radkov et al., 1999).

EBNA 3C was also reported to interact with the transcriptional corepressor protein C-terminal binding protein (CtBP). The mechanism of repression has not been fully determined, but it was suggested that CtBP is able to control histone modifications like deactylation and lysine methylation and can induce gene silencing (Shi et al., 2003). Further, it is known that EBNA 3C interacts with the protein through a PXDLS motif (Touitou et al., 2001). This motif is used by many transcription factors to recruit CtBP to DNA, e.g. adenovirus E1A, Marek's disease virus Meq protein and EBNA 3A as previously mentioned (Chinnadurai, 2002; Hickabottom et al., 2002).

The DEAD box protein DP103, an ATP-dependent helicase, was shown to be able to interact with the C-terminal end of EBNA 3C. DEAD box family proteins play an important role in cell development, differentiation and proliferation. For example, DP103 functions as a repressor through binding to transcription factors to repress their activities e.g. steroidogenic factor (SF-1), the early growth response factors Egr 1, 2, 3 and 4 and the spinal muscular neuron protein (SMN) (Charroux et al., 1999; Gillian and Svaren, 2004; Grundhoff et al., 1999; Yan et al., 2003). Therefore DP103 may play a role transcriptional repression mediated by EBNA 3C.

EBNA 3C was shown to repress the Notch ligand Jagged1 (Chen et al., 2006). The Notch signalling pathway was shown to be important for EBV-induced cell growth. Protein expression of Jagged1 was found upregulated when EBNA 3C was not

expressed and increased expression of Jagged1 leads to slow cell growth (Chen et al., 2006). Therefore, it was suggested that EBNA 3C represses Notch signalling (Chen et al., 2006).

1.7.7.4 Regulation of metastasis

The proline- and glutamine-rich domains of EBNA 3C were shown to be able to bind to the cellular protein Nm23-H1, a nucleoside diphosphate (NDP) kinase, which is functionally associated with the suppression of metastasis (Murakami et al., 2005; Subramanian and Robertson, 2002). Nm23-H1 was the first metastasis suppressor identified (Lacombe et al., 2000; Steeg et al., 1988). Reduction of its protein expression leads to increased metastasis in many different cancers (Tee et al., 2006). EBNA 3C was found to reverse the ability of Nm23-H1 to suppress the migration of Burkitt's lymphoma cells *in vitro* and *in vivo* (Kaul et al., 2007; Subramanian and Robertson, 2002). EBNA 3C was further shown to mediate translocation of Nm23-H1 into the nucleus which together may result in the inhibition of the kinase activity of the protein (Kaul et al., 2007; Murakami et al., 2009). Interestingly, the HPV protein E7 also appears to associate with Nm23-H1 and inhibits its function (Mileo et al., 2006). E7 expression was reported to downregulate Nm23-H1 at the transcriptional and protein level (Mileo et al., 2006).

1.7.7.5 EBNA 3C and the cell cycle

EBNA 3C expression has been shown to disrupt the G1/S, G2/M and the mitotic spindle checkpoint (Krauer et al., 2004b; Parker et al., 2000).

EBNA 3C was demonstrated to override the G1/S checkpoint induced by serum withdrawal in NIH 3T3 cells. While EBNA 3C-negative cells arrested in G1, the EBNA 3C-positive cells were still able to enter S phase and continue through G2/M. It was also observed that cell division did not necessarily lead to cytokinesis, leading to the generation of bi- and multinucleated cells (Parker et al., 2000).

Different mechanisms have been suggested for how EBNA 3C overrides the G1/S checkpoint, including disruption of the Rb and the cyclin A/CDK2 pathway. In initial studies EBNA 3C was shown to overcome this checkpoint in cooperation with activated Ras in cotransfection assays which resulted in transformation of primary rodent

fibroblasts (Parker et al., 1996). The activation of the Ras pathway leads to the production and activation of the G1 cyclin D/CDK4 or 6 complexes that catalyse the phosphorylation of Rb and promote G1/S transition (Figure 7A). The precise mechanism by which EBNA 3C and Ras can cooperate has not been identified.

It was found that EBNA 3C can relieve the $p16^{INK4A}$-mediated inhibition of cyclin D-dependent kinases (CDK4 and 6). $P16^{INK4A}$ is known to provoke growth arrest during serum-starvation by binding to the kinases CDK4 and 6 and therefore maintaining the hypophosphorylated state of Rb (Sherr and Roberts, 1995). Inhibition of the kinases CDK4 and CDK6 by $p16^{INK4A}$ suppresses cell cycle progression (Figure 7A) (Koh et al., 1995; Lukas et al., 1995; Medema et al., 1995) and (reviewed in (Sherr and Roberts, 1995)). It was suggested that EBNA 3C can target $p16^{INK4A}$ directly to inhibit its function (Parker et al., 1996). However, Rb was shown to be normally regulated by phosphorylation and dephosphorylation in LCLs which express all latent EBV proteins which implies that deregulation of cyclin/CDK activity mediated by EBNA 3C in the context of a latent infection is not evident (Allday and Farrell, 1994; Allday et al., 1995a; Allday et al., 1995b).

The cyclin D/CDK4,6 and the cyclin A/CDK2 complex can be inhibited by upregulation of the CDK inhibitor $p27^{KIP1}$ which is an important regulator of the G1/S transition and was found to be upregulated at the protein level during cell cycle arrest (Figure 8) (Polyak et al., 1994). One study showed that EBNA 3C expression decreased $p27^{KIP1}$ accumulation after serum starvation in human osteosarcoma cells (U2OS) but showed Rb hypophosphorylation despite the cells progressing through the checkpoint (Parker et al., 2000). Biochemical studies carried out in the Robertson lab then demonstrated that EBNA 3C expression was able to abolish the $p27^{KIP1}$-mediated inhibition of the cyclin A/CDK2 complex by degradation of the CDK inhibitor in human embryonic kidney (HEK) 293T cells (Knight et al., 2005a).

Experiments carried out in lymphoblastoid cell lines showed that the repression of the effects of $p27^{KIP1}$ by EBNA 3C occured by decreasing the molecular association between cyclin A and the inhibitor in the cells (Figure 8). However, EBNA 3C was shown not to be able to interact with $p27^{KIP1}$ directly. It was suggested that EBNA 3C either competes with $p27^{KIP1}$ for binding to cyclin A/CDK2 or recruitments of other

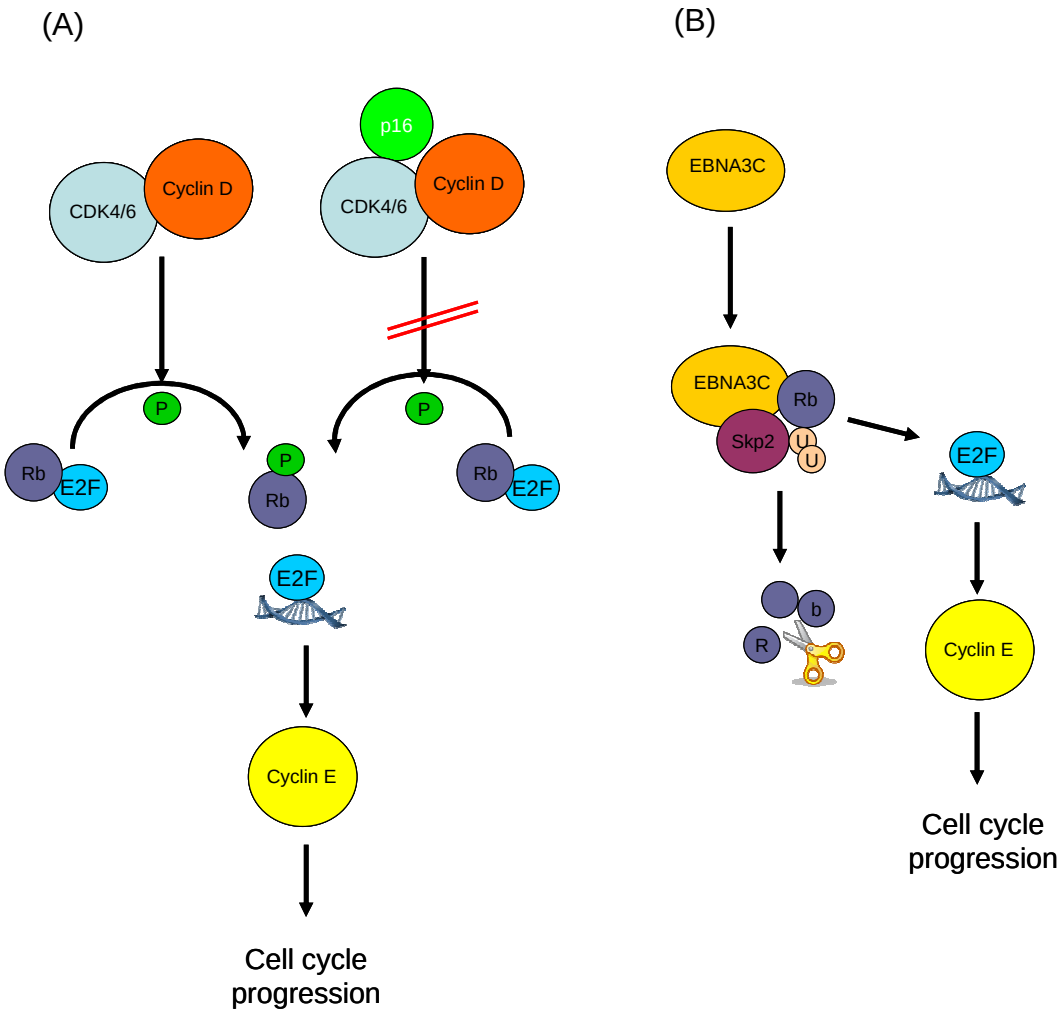

Figure 7 – (A) Cyclin D/CDK4,6 can phosphorylate Rb. Phosphorylated Rb can no longer bind E2F which then induces expression of its target genes, e.g. cyclin E which is essential for cell cycle progression. P16 is known to bind the cyclin D/CDK4,6 complex and can therefore inhibit its function which results in cell cycle arrest. **(B)** EBNA 3C was reported to be able to bind Rb and to recruit Skp2 which ubiquitinates Rb for degradation. E2F can therefore no longer bind Rb and can induce cyclin E expression leading to cell cycle progression.

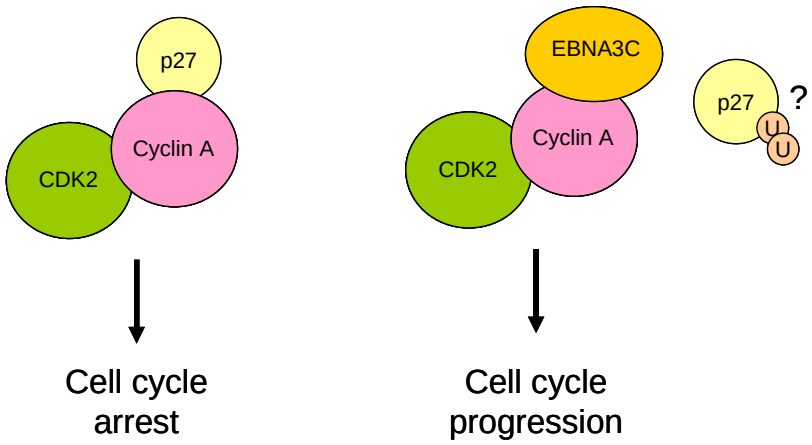

Figure 8 – The cyclin A/CDK2 complex is known to be active to promote cell cycle progression. However, p27 can bind to the complex and inhibits its function. EBNA 3C was shown to be able to bind the complex inhibiting p27 association with the complex. p27 was suggested to be degraded after the protein is not able to associate with the cyclin A/CDK2 complex any longer.

factors, which may modify $p27^{KIP1}$ by phosphorylation or may influence its stability (Knight and Robertson, 2004; Knight et al., 2004). Therefore, it was proposed that EBNA 3C disrupts the G1/S checkpoint by binding to cyclin A via its C terminus and increasing the activity of the cyclin A/CDK2 complex by inhibiting the interaction of $p27^{KIP1}$ with the complex (Knight and Robertson, 2004).

Authors from the same research group subsequently showed that EBNA 3C was also able to associate with the N-terminus of cyclin A via the cyclin box, a highly conserved sequence in cyclins. EBNA 3C is therefore also able to bind cyclin E and D1 *in vitro* even though the binding is much weaker than to cyclin A. Although it was shown that EBNA 3C is able to rescue inhibition of $p27^{KIP1}$ by binding to cyclin A with its C-terminus, this ability could not be identified for EBNA 3C binding cyclin A with its N-terminus even though the affinity of this interaction is higher. Therefore, it was suggested that the N-terminus functions to recruit cyclin A while the C-terminus plays a role in increasing the cyclin A complex kinase activity (Knight and Robertson, 2004; Knight et al., 2004).

In contradiction to previous findings, the abolishment of $p27^{KIP1}$-mediated inhibition by EBNA 3C resulted in hyperphosphorylation of Rb and no hypophosphorylated Rb could be detected in Western blotting when EBNA 3C was expressed in U2OS (Knight and Robertson, 2004). However, authors from the same research group reported one year later that no changes in Rb phosphorylation occur with EBNA 3C expression, but that EBNA 3C decreases the Rb level by augmenting the polyubiquitination of the protein (Figure 7B). These studies were carried out in HEK293T cells and the BL cell line BJAB when EBNA 3C was transiently overexpressed. The degradation of the Rb protein was demonstrated to occur via recruiting the SCF^{Skp2} to the EBNA 3C/Rb complex *in vitro* (Knight et al., 2005a).

Interestingly, an Rb interaction with EBNA 3C was first demonstrated *in vitro* and mutation of the Rb pocket domain abolished this interaction (Parker et al., 1996). The pocket domain of Rb is reported to be targeted by other viral oncoproteins like SV40 T antigen, adenovirus E1A or human papillomavirus E7 thus preventing binding to other binding partners such as E2F and inducing transcription of genes essential for cell cycle progression. The LXCXE motif through which the human papillomavirus protein E7

binds to the Rb pocket domain, resembles a motif found in EBNA 3C. Interestingly, it lies in the 10 amino acid sequence, which was identified to play a role in the regulation of Rb stability by EBNA 3C (Knight et al., 2005a).

EBNA 3C has also been shown to bind to the transcription factor c-Myc leading to c-Myc stabilisation in EBNA 3C-expressing HEK293T cells compared to a control cell line (Bajaj et al., 2008). This stabilisation then results in an increase of c-Myc-activated transcription which is known to encode many genes involved in cell cycle regulation, apoptosis and metabolism (Bajaj et al., 2008; Dang et al., 2006).

In a very recent study the Robertson lab demonstrated that EBNA 3C can interact with MDM2 *in vitro* and *in vivo* (Saha et al., 2009). MDM2 is known to associate with p53 to inhibit its function. Further, it initiates the degradation of p53. Binding of EBNA 3C to the MDM2 leads to stabilization of protein and prevents degradation of MDM2 by deubiqutination suggesting a new role for EBNA 3C as a deubiquitinating enzyme (DUB) (Saha et al., 2009). EBNA 3C was found to interact with MDM2 via an N-terminal domain (aa residues 130-190) which was also shown to interact with c-Myc, SCF^{Skp2}, Rb, Cyclin A and RBP-J kappa (Bajaj et al., 2008; Knight et al., 2004; Knight et al., 2005a; Knight et al., 2005b; Saha et al., 2009). EBNA 3C was also reported to bind p53 *in vitro* and *in vivo* via the same domain in the N-terminus and to prevent p53 from binding to DNA thus inhibiting the induction of p53-target genes paralleling the actions of adenovirus E1A and HPV E6 (Lechner et al., 1992; Steegenga et al., 1996; Yi et al., 2009). However, no p53 deregulation could be observed in lymphoblastoid cell lines (O'Nions and Allday, 2003; Wade and Allday, 2000). Therefore, EBV may not disrupt the p53 pathway to overcome cell cycle control in the context of a latent infection.

1.7.7.6 The effects of EBNA 3C on the G2/M checkpoint and mitotic checkpoints

Allday *et al.* found that EBNA 3C-expressing human osteosarcoma cells (U2OS) cells are able to override the mitotic spindle assembly checkpoint after treatment with nocodazole (Parker et al., 2000). Further, disruption of the mitotic spindle assembly checkpoint by EBNA 3C leads to nuclear division but may not always be followed by cytokinesis. As a result, bi- and multinucleated cells accumulate (Parker et al., 2000).

Investigations by Krauer *et al.* showed that EBNA 3A, 3B and 3C expressing LCLs could override G2 arrest resulting in continuous cell division and subsequent cell death induced by treatment with the histone deacetylase inhibitor azelaic bishydroxamine (ABHA) (Krauer et al., 2004b). ABHA caused G2/M arrest in cells with a functional G2/M checkpoint, e.g. normal B cells and DG75 cells but was cytotoxic in cell lines with a disrupted G2/M checkpoint e.g. many EBV-transformed LCLs (Sculley et al., 2002). The same research group further reported that the expression of the EBNA 3 gene family alone disrupts the G2/M checkpoint in response to the genotoxin etoposide, ABHA or the S phase inhibitor hydroxyurea (HU) (Krauer et al., 2004b).

EBNA 3A, 3B and 3C were also shown to reduce accumulation of the inactive form of CDK1 (p34cdc2), which is inhibited by phosphorylation at threonine 14 and tyrosine 15 during G2/M arrest (Figure 2) (Krauer et al., 2004b).

Further, the authors suggested that the EBNA 3 family can block ATM/ATR signalling since EBNA 3A is able to interact with chk2 in coimmunoprecipitation assays in LCLs which could not be observed for EBNA 3B (Krauer et al., 2004b).

However, more recent results of a microarray and real-time PCR analysis revealed that chk2 is downregulated in EBNA 3C-expressing BJAB cells (Choudhuri et al., 2007). Co-immunoprecipitation assays from the Robertson lab confirmed that EBNA 3C is able to directly interact with chk2 and that chk2 mRNA and protein expression was reduced in EBNA 3C-expressing cells. It was suggested that EBNA 3C may downregulate chk2 protein expression by destabilization of the protein or may inhibit its function (Choudhuri et al., 2007).

Further investigations into the effects of EBNA 3C on the mitotic checkpoint revealed that EBNA 3C and EBNA 3A cooperate to promote cell survival following treatment with the microtubule inhibitor nocodazole, cisplatin, which crosslinks DNA triggering apoptosis, and the CDK inhibitor roscovitine (Anderton et al., 2008). This was demonstrated to be mediated by downregulation of the proapoptotic Bcl-2 member Bim (Anderton et al., 2008).

EBNA 3C has thus been found to be involved in many pathways of cell cycle regulation which may all contribute to its ability to disrupt cell cycle control, although many suggested target pathways appear to be intact in LCLs, so the relevance and importance of many reported effects need further validation.

1.8 EBV-associated diseases

EBV was first isolated from a Burkitt's lymphoma in 1964. Since then the virus has been linked to numerous tumours found in B and T lymphocytes as well as epithelial cells as has also been shown to be involved in non-malignant diseases (reviewed in (Crawford, 2001; Kieff and Rickinson, 2001)).

1.8.1 Infectious Mononucleosis

Infectious mononucleosis (IM), also known as glandular fever, is known to develop when primary EBV infection occurs during adolescence, but only in 50% of cases (Henke et al., 1973). IM was identified as an EBV-related disease in 1968 and is characterized by symptoms including fever, pharyngitis, lymphadenopathy, splenomegaly and hepatocellular dysfunction but can also cause impending upper-airway obstruction which in rare cases can be fatal (Niederman et al., 1968). The symptoms are mediated by a strong immune response by cytotoxic T cells against EBV latent proteins expressed in EBV-infected activated B lymphocytes followed by a release of cytokines e.g. interferon-γ and interleukin-2 (Callan et al., 1996; Tierney et al., 1994; Williams et al., 2004).

1.8.2 Burkitt's lymphoma

Burkitt's lymphoma (BL) is an aggressive, monoclonal B cell tumour which can be divided in 3 categories: endemic BL (eBL) in equatorial Africa, sporadic BL (non-African non-Hodgkin lymphoma) and immunodeficiency-associated BL (HIV/AIDS-associated). eBL usually occurs in children or young adults in tropical Africa and in some other equatorial regions. Coinfection with malaria appears to play an important role alongside EBV infection (Magrath, 1990a). More than 95% of eBL tumour cells are EBV-positive whereas only 15% of sporadic BL and 30-40% of HIV-related BL are EBV-positive. Most Burkitt's lymphoma cells only express EBNA 1 which is transcribed from the alternative Q promoter. BL is thought to originate from germinal

centre (GC) B cells as BL cells express a GC B cell phenotype but may sometimes derive from memory B cells (Gregory et al., 1987; Hochberg et al., 2004). BL is characterised by translocation of the c-myc oncogene from chromosome 8 to 14, 2 or 22 (Magrath, 1990a). After translocation c-myc is constitutively active and promotes cell cycle progression (Bhatia et al., 1993; Cesarman et al., 1987; Magrath, 1990b). Malarial antigens can cause a chronic activation of B cells which is thought to increase the possibility of chromosomal translocation of c-myc (reviewed in (Lenoir and Bornkamm, 1987)). Further changes have been observed which involve the $p14^{ARF}$/MDM2/p53 pathway. Most BL cell lines and more than 30% of BL biopsies show mutations in p53. If there is no mutation in the p53 gene then a deletion of $p14^{ARF}$ or methylation or overexpression of MDM2 was found (Capoulade et al., 1998; Farrell et al., 1991; Gaidano et al., 1991; Lindstrom et al., 2001). Mutations in the p53 gene may be driven by a necessity to inhibit p53-dependent apoptosis induced by deregulated c-myc (Lindstrom and Wiman, 2002).

Interestingly, approximately 15% of BL tumours were shown to express EBNA 1 plus EBNA 3A, EBNA 3B, EBNA 3C and truncated EBNA LP as a results of transcription from the W promoter (Kelly et al., 2002a; Kelly et al., 2006). These tumours were found to have a deletion of the EBNA 2 gene and the Y1Y2 exons of EBNA LP similar to the P3HR1 strain of EBV (Kelly et al., 2002a). The lack of EBNA 2 expression is thought to account for the inactivity of the LMP and C promoters. It may be that the development of EBV-associated BL requires the downregulation of EBNA 2 rather than restricted latency I gene expression. Further, EBNA 2 and c-myc were shown to have antagonistic effects on the expression of several surface markers involved in B cell activation (Pajic et al., 2001). Therefore, the deletion of EBNA 2 in BL cells allows less limited expression of c-myc induced protein expression in addition to the expression of the EBNA 3 family involved in prevention of apoptosis and cell cycle disruption (Kelly et al., 2005).

1.8.3 Hodgkin's disease

Hodgkin's disease (HD) also known as Hodgkin's lymphoma (HL) is a tumour which can occur in the lymph nodes, spleen, liver and bone marrow (Babcock et al., 2000). 30-50% of HLs were found to be EBV-associated in developed countries (Herbst et al.,

1991; Pallesen et al., 1991). This tumour was first described in 1832 by Thomas Hodgkin and a relationship to EBV was established in 1989 after the identification of EBV DNA in the Reed-Sternberg cells isolated from Hodgkin's disease tumours (Weiss et al., 1989). Hodgkin's disease is diagnosed by the presence (usually only 1 or 2%) of Reed-Sternberg cells in the lymphoma which are large and can either be multinucleated or have a bilobed nucleus. Reed-Sternberg cells are CD30- and CD15-positive and negative for CD20 and CD45. This immunophenotype is typical of classical HD which can be EBV-positive, whereas the lymphocyte-predominant Hodgkin's lymphoma shows the opposite immunophenotype for CD30, CD15, CD20 and CD45 and is always EBV-negative. HD tumour cells are thought to have developed from post-germinal centre cells, possibly centrocytes, which express EBNA1, LMP1, LMP2A and LMP2B. EBV is found in almost all AIDS-related HD tumours (Glaser et al., 2003; Glaser et al., 1997; Uccini et al., 1990). Whether a tumour is EBV-related is also dependent on age, sex and ethnicity (reviewed in (Flavell and Murray, 2000)).

1.8.4 Post-transplant lymphoproliferative disease

Post-transplant lymphoproliferative disease (PTLD) arises in 10% of transplant recipients (Haque et al., 1996). The symptoms begin with an IM-like disease followed by tumour development mainly in the gut, brain or the transplanted organ and is fatal in more than 50% of the cases (Nalesnik, 1998). The immune system of a transplant recipient is usually weakened to reduce the risk of a rejection of the donated organ. Donated blood and organs from healthy people can contain EBV-infected B cells which can therefore lead to infection of a previously seronegative recipient (Alfieri et al., 1996; Cen et al., 1991; Gerber et al., 1969). Due to the immune system suppression of the recipient, the lower amount of EBV-specific cytotoxic T cells cannot fight the infection allowing the B cells to proliferate and the virus to express all latent proteins (latency III) (reviewed in (Holmes and Sokol, 2002)).

1.8.5 Undifferentiated nasopharyngeal carcinoma

Although the B cell appears to be the site of persistent EBV latent infection, EBV is also able to infect epithelial cells. EBV is thought to be able to transform epithelial cells which can lead to the development of undifferentiated nasopharyngeal carcinomas (UNPC); however, no evidence has been reported. UNPCs consist of undifferentiated carcinoma cells together with an infiltration of lymphocytes. UNPC is mainly found in

areas of China and south-east Asia. Interestingly, almost all UNPC tumours are linked to EBV (Pathmanathan et al., 1995; Raab-Traub and Flynn, 1986). UNPC cells are highly radiosensitive and the chances of survival are generally more than 90% when detected during early stages (Ferme et al., 2007).

1.8.6 Non-Hodgkin's lymphoma

80% of all lymphomas are classified as Non-Hodgkin's lymphomas (NHL), a broad definition covering many different types of tumours. These tumours usually occur in patients with a compromised immune response, e.g. patients with AIDS. About 20% of patients diagnosed with HIV will grow a Non-Hodgkin lymphoma. These tumours arising due to AIDS-related immune suppression are called AIDS-related lymphomas. All latent viral genes were shown to be expressed in EBV-related NHL. Lymphomas of the primary nervous system are nearly 100% EBV-associated (MacMahon et al., 1991).

1.8.7 T cell lymphomas

EBV is also thought to be involved in the development of a proportion of T cell lymphomas (Brink et al., 2000b). EBV-infected tumour cells may drive the proliferation and prevent apoptosis in T cells.

1.9 RGC-32

A cDNA microarray experiment was carried out in the West Lab to identify genes, whose expression was regulated by EBNA 3C. Besides the already known upregulation of CD21, another gene whose expression was found to be upregulated in EBNA 3C-expressing cells was RGC-32. RGC-32 (C13orf15) is a protein discovered in rat oligodendrocytes (OLG) in 1998 (Badea et al., 1998). Badea *et al.* identified new genes whose expression was altered in response to sub-lytic complement treatment with C5b-9 to mimic complement activation of the cells (Badea et al., 1998; Niculescu et al., 1997). The complement system is a part of the innate immune system. Once activated by pathogens, a cascade of protein cleavage occurs resulting in the activation of the cell killing membrane attack complex, C5b-9, which has a function in cell lysis and opsonisation which promotes phagocytosis of particular antigens.

The new genes identified to be regulated by complement were designated Response Genes to Complement (RGC) (Badea et al., 1998). Almost every RGC discovered (32 in

total) was found to encode a part of or an entire known protein. One of the unknown mRNAs identified to be upregulated by complement activation was RGC-32 which encodes a protein of 137 amino acids in rats. Human RGC-32 contains 117 amino acids and runs with an apparent molecular weight of 15 kD on SDS-PAGE (Badea et al., 2002; Badea et al., 1998). Human and mouse RGC-32 was reported to share 92% homology with rat RGC-32 (Badea et al., 2002).

RGC-32 mRNA levels were increased after treatment of oligodendrocytes with normal human serum but serum lacking the C5b-9 component C7 could not upregulate RGC-32 expression indicating that the terminal complement complex (TCC or C5b-9) assembly is essential for RGC-32 upregulation (Badea et al., 1998). C5b-9 further includes the proteins C5b, C6, C8 and C9. This complex is also known as the membrane attack complex of complement and causes cell death by forming pores (Mayer, 1972). This complex can also act as a cell cycle activator by increasing the activity of CDK1, CDK2 and CDK4 by which the complex mediates an increase in DNA synthesis and cell proliferation (Badea et al., 2002; Niculescu et al., 1999; Rus et al., 1996).

In rats, the RGC-32 transcript has a length of approximately 1000 bases and was found in several tissues like kidney, heart, brain, lung, skin, spleen and thymuses, but not in the testis or liver (Badea et al., 1998). RGC-32 mRNA expression in humans however was detected in placenta, liver, skeletal muscle, kidney and pancreas, aortic endothelial cells and in the B lymphoblastoid cell line JY25 and was weakly expressed in heart and brain and absent in lung tissue. Human RGC-32 protein expression was detected in heart, brain and liver tissue (Badea et al., 2002).

Data base analysis showed that RGC-32 has no homology with any other known proteins contains no conserved motifs, signal sequence or transmembrane domain which could provide more information about the target organelle or the function of the protein (Badea et al., 1998). The protein has been found to be localised in the cytoplasm, however, it has been shown that RGC-32 is translocated to the nucleus after sublytic complement (C5b-9) treatment of smooth muscle cells (Badea et al., 2002; Badea et al., 1998). Saigusa *et al.* have shown that RGC-32 accumulates at centrosomes during mitosis (Saigusa et al., 2007).

RGC-32 mRNA and protein levels were found to be increased in several tumour tissues e.g. kidney, colon, stomach, rectum, ovary and small intestine tumours. MRNA levels were upregulated more than 2-fold in comparison to the surrounding normal tissue indicating a role for RGC-32 in promoting tumourigenesis (Fosbrink et al., 2005).

Interestingly, the expression of RGC-32 was shown to lead to cell cycle progression into S and M phase in serum-starved cells aortic smooth muscle cells transfected with RGC-32-expressing plasmids (Badea et al., 2002). During serum-withdrawal the RGC-32-expressing cells continued cell cycle progression while 90% of the untransfected control cells arrested in G0/G1. Furthermore, a significant shifting of cells from the S to G2/M phase was observed after the RGC-32-expressing cells were exposed to complement activation.

To investigate the mechanism of the effects of RGC-32 on the cell cycle, binding studies were carried out on CDKs. RGC-32 was shown to be able to bind CDK1, but not CDK2 and CDK4 and to activate CDK1 (Badea et al., 2002; Badea et al., 1998). CDK1 is known to function in mitosis and is the major target for G2/M checkpoint control. RGC-32-induced CDK1 activity may therefore increase cell cycle progression into mitosis. CDK1 complexes with cyclin A or B during S and M phases, which results in higher activity of the kinase, but a further increase of CDK1 activity was also found during RGC-32-mediated S phase entry in aortic smooth muscle cells (Badea et al., 2002). Furthermore, the kinase activity is also increased in primary oligodendrocytes during late G1 and G1/S transition upon C5b-9 treatment. Inhibition of CDK1 activity was shown to decrease RGC-32-mediated S-phase entry introducing a new role of CDK1 besides its known function in the transition into mitosis (Badea et al., 2002; Rus et al., 1996).

RGC-32 was shown to be phosphorylated during an *in vitro* kinase assay investigating the effects of RGC-32 on CDK1 activity. Since the addition of CDK1 inhibitor $p27^{KIP1}$ abolished this phosphorylation, it appeared that RGC-32 was phosphorylated by CDK1. In the presence of $p27^{KIP1}$, RGC-32 is unable to enhance CDK1 activity (Badea et al., 2002). A CDK1 phosphorylation consensus motif, TPQK, was found in human RGC-32 and mutation of Thr-91 to alanine in this site abolished RGC-32 phosphorylation by CDK1 and reduced CDK1 kinase activity. Therefore, this RGC-32 mediated activation

is dependent on RGC-32 phosphorylation at threonine 91 by CDK1 (Badea et al., 2002; Badea et al., 1998).

RGC-32 has also been implicated as a mediator of muscle cell differentiation. Li *et al.* showed that RGC-32 expression was induced by up to 50-fold when neural crest cells were treated with TGF-β mediating vascular smooth muscle cell differentiation (Li et al., 2007). These findings suggest TGF-β as another potential regulator of RGC-32.

In contradiction to previous findings, Saigusa *et al.* reported that RGC-32 acts as a tumour suppressor gene as regions of the RGC-32 gene were found to be absent in glioma cell lines and restoration of RGC-32 expression led to suppression of glioma cell growth (Saigusa et al., 2007). Overexpression of the protein also slowed progress through mitosis in HeLa cells (Saigusa et al., 2007). Furthermore, RGC-32 expression decreased with increasing malignancy grade of primary astrocytomas and 9 of 35 primary astrocytomas tested showed a p53 mutation which also resulted in a decrease of RGC-32 mRNA expression implicating p53 as a regulator of RGC-32 and p53 is known to become activated in response to DNA damage (Saigusa et al., 2007). The same research group confirmed this result in p53 null U-373 MG cells (Saigusa et al., 2007). U-373 MG cells were infected with p53 using adenovirus-mediated transfer and showed induction of RGC-32 mRNA expression when p53 was expressed (Saigusa et al., 2007). p53 was also shown to bind to the RGC-32 gene *in vitro* which was confirmed by Chromatin immunoprecipitation (ChIP) analysis *in vivo* (Figure 9) (Saigusa et al., 2007).

1.10 RUNX proteins

During the course of the research described in this thesis, RGC-32 mRNA expression was found to be regulated by the runt-related protein RUNX1 (Jo and Curry, 2006). Knock-down of RUNX1 expression in rat ovulating follicles resulted in a decrease of RGC-32 mRNA levels (Jo and Curry, 2006). The same research group found 3 RUNX1 binding sites on the RGC-32 gene and a further 3 potential binding sites with 89% homology to the known consensus sequence. RUNX1 was shown to bind directly to the RGC-32 promoter in ChIP assays using rat periovulatory granulosa cells (Park et al., 2008). Mutation of one RUNX1-binding site resulted in reduced RGC-32 promoter

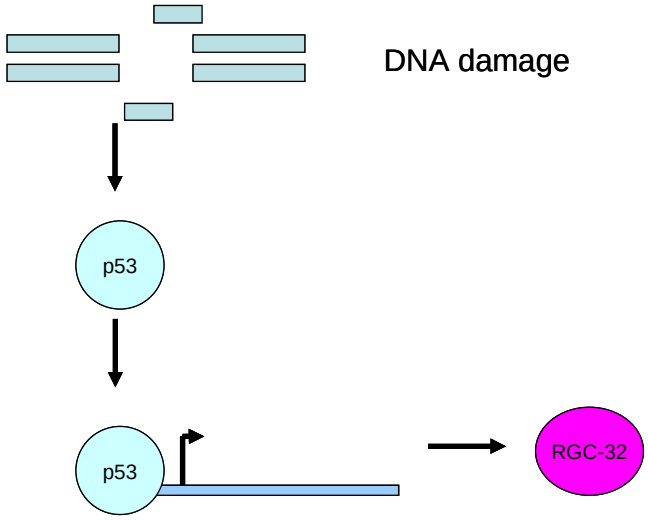

Figure 9 – In response to DNA damage, p53 becomes activated. p53 induces RGC-32 gene expression by binding to the RGC-32 promoter resulting in RGC-32 expression.

activity in rat periovulatory follicles (Park et al., 2008). The RUNX proteins RUNX1 (AML-1, CBF-α2), RUNX2 (AML-3, CBF-α1) and RUNX3 (AML-2, CBF-α3) belong to the family of Runt-related transcription factors, (reviewed in (van Wijnen et al., 2004)). Runt is a gene expressed in *Drosophila melanogaster* and is essential for segmentation, sex determination and neurogenesis (Daga et al., 1992; Duffy and Gergen, 1991; Duffy et al., 1991; Erickson et al., 1992; Gergen and Wieschaus, 1986; Kania et al., 1990). All RUNX proteins are known to associate with the core-binding factor CBF-β which is not able to bind DNA itself but increases the affinity of RUNX proteins for DNA (Ogawa et al., 1993a; Wang et al., 1996b; Wang et al., 1993). The Runt domain is involved in association with CBF-β in addition to DNA-binding and nuclear localisation (Lenny et al., 1995; Lu et al., 1995; Meyers et al., 1993; Meyers et al., 1995; Ogawa et al., 1993b). The RUNX/CBF-β complex is able to bind DNA containing a RUNX-binding site identified as the 7 bp consensus sequence 5'-PyGPyGGTPy-3' (Melnikova et al., 1993). This sequence is found in a number of enhancers and promoters, and can either activate or repress transcription. Repression and activation by RUNX family members is cell type-specific and appears to depend on associated cofactors.

Activation of genes by the RUNX family occurs via recruitment of cofactors and other DNA-binding transcription factors like C/EBPα, ETS family members, c-Myb, SMADs and histone acetyltransferases including p300/CBP (Britos-Bray and Friedman, 1997; Hanai et al., 1999; Kim et al., 1999; Kitabayashi et al., 1998; Mao et al., 1999; Pelletier et al., 2002; Petrovick et al., 1998; Westendorf et al., 1998; Zhang et al., 1996). The recruitment of HDACs appears to be required for RUNX-mediated repression but which HDAC is recruited is distinct for each RUNX protein (see below). RUNX proteins have been shown to associate with the corepressors TLE1 and TLE2, mSin3A, N-CoR and SMRT (Aronson et al., 1997; Imai et al., 1998; Javed et al., 2000; Lutterbach et al., 2000). A VWRPY motif in the RUNX proteins interacts with TLE1 and TLE2 in yeast 2-hybrid systems and *in vitro* assays (Aronson et al., 1997; Imai et al., 1998; Levanon et al., 1998). TLE-independent repression has also been described suggesting that corepression by TLE may be promoter-specific (Javed et al., 2000).

A connection between EBV latent gene expression and RUNX expression was first demonstrated by Spender *et al.* investigating EBNA 2-induced genes in a microarray study (Spender et al., 2002b). The authors reported that RUNX3 mRNA and protein expression was induced by EBNA 2 (Spender et al., 2002b). RUNX3 expression was found to inversely correlate with RUNX1 expression in B cell lines and the same authors demonstrated that RUNX3 downregulates RUNX1 transcription via RUNX3-binding sites in the RUNX1 promoter (Spender et al., 2005a). Therefore, RUNX1 and RUNX3 expression correlate with the EBV latency type dependent on EBNA2 expression (Figure 10).

1.10.1 RUNX1

Three transcript variants encoding different isoforms of RUNX1 have been described: RUNX1a, 1b and 1c. RUNX 1c is transcribed from the P1 promoter and RUNX1 1a and 1b from the P2 promoter which is located adjacent to the P1 promoter. Alternative splicing of the transcripts results in the 3 isoforms of RUNX1 (Figure 11), (reviewed in (Whiteman and Farrell, 2006)). Only RUNX1c was found to be expressed in B cells (Spender et al., 2005a).

RUNX1 was found to be involved in the development of definitive haematopoiesis (adult) as well as B and T lymphocyte differentiation (Ichikawa et al., 2004; Lacaud et al., 2002; Okuda et al., 1996). Further, RUNX1 was found to interact with the B cell-specific tyrosine kinase (Blk) promoter to activate transcription. Blk is known to bind to the B cell receptor (BCR) following B cell activation (Libermann et al., 1999).

Mouse embryos carrying a mutated RUNX1 gene did not survive beyond 12.5 days. Death was found to occur due to lack of fetal liver haematopoiesis and hemorrhaging in the central nervous system (CNS) indicating the essential role played by the RUNX1 gene in development (Okuda et al., 1996; Wang et al., 1996a).

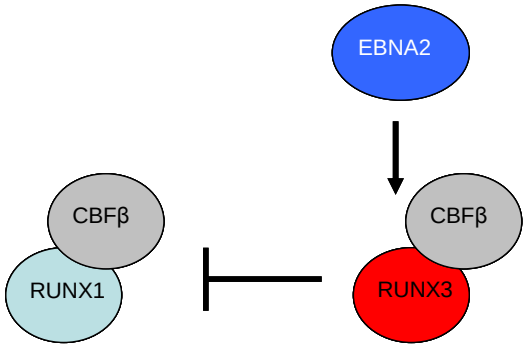

Figure 10 - All RUNX proteins form a complex with the same subunit CBFbeta which allows DNA binding. EBNA 2 was shown to induce RUNX3 expression which inhibits RUNX1 expression.

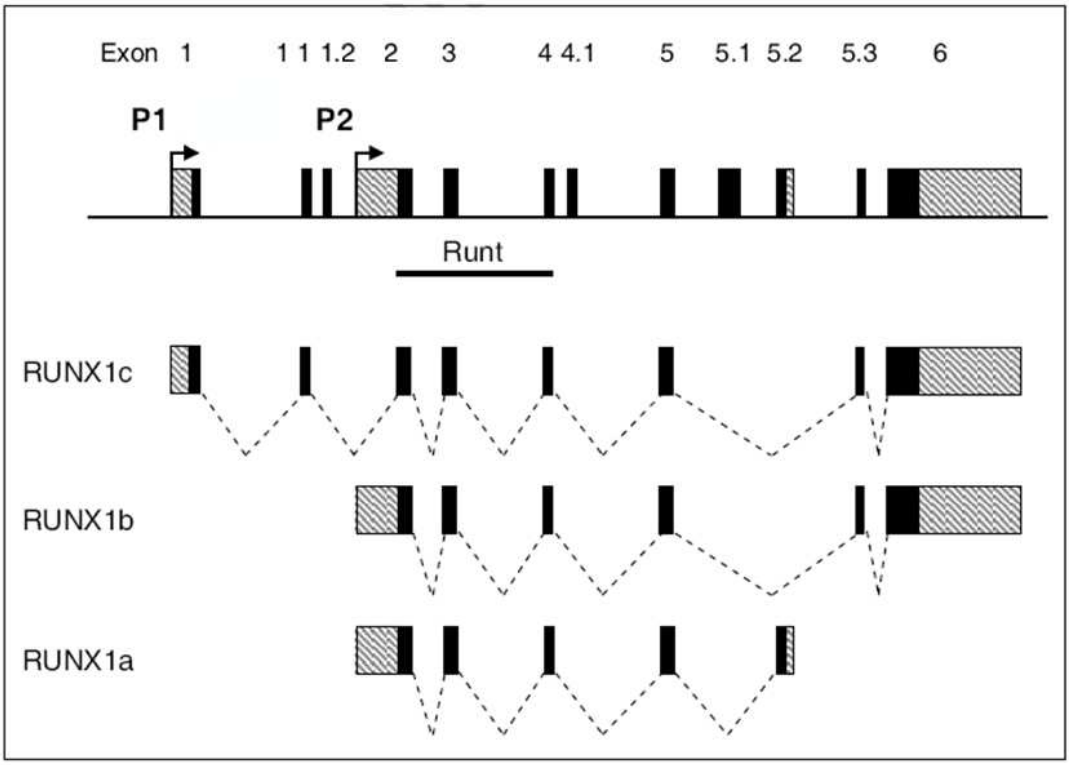

Figure 11 – RUNX1 gene overview showing the different exons and promoters. Alternativley spliced transcripts results in the 3 isoforms: RUNX1a, 1b and 1c. Figure adapted from (Whiteman and Farrell, 2006).

1.10.2 Mutations and translocations of the RUNX1 gene

Interestingly, the RUNX1 gene is often translocated in acute myeloid leukemia (AML), especially the M2 subtype of AML but also in autoimmune diseases and in 20% of acute lymphocytic leukemia (ALL) (Golub et al., 1995; Look, 1997; Romana et al., 1995a; Romana et al., 1995b). Common translocation include t(8:21) which fuses the N-terminus and Runt domain of RUNX1 to the corepressor ETO and t(12;21) that fuses the N-terminus of TEL to the Runt and transcription domains of RUNX1 (Erickson et al., 1992; Golub et al., 1995; Miyoshi et al., 1991). The fusion proteins RUNX1-ETO and RUNX1-TEL recruit corepressors like mSIN3A and HDACs to generate permanent repression complexes at the promoters of RUNX1 target genes which is thought to contribute to leukemogenesis (Amann et al., 2001; Fenrick et al., 1999; Lutterbach et al., 1998; Wang et al., 1998; Wang and Hiebert, 2001). Overexpression of TEL-RUNX1 could only induce ALL in mice when $p16^{INK4A}$/$p19^{ARF}$ expression is lost implicating further genetic in leukemogenesis (Bernardin et al., 2002).

1.10.3 RUNX1 as a transcriptional regulator

RUNX1 can inhibit $p21^{WAF1/CIP1}$ transcription by binding to its promoter and recruiting mSin3A and HDACs (Laherty et al., 1997; Lutterbach et al., 2000). RUNX1 was also found to directly and strongly associate with HDACs 1, 3 and 9 and weakly with HDACs 2, 5, and 6 (Durst et al., 2003). RUNX1 has been shown to interact with TLE1, oncoproteins C-jun and C-Fos, the calcitriol receptor, involved in mineral metabolism, and the Histone-lysine N-methyltransferase SUV39H1 (Chakraborty et al., 2003; D'Alonzo et al., 2002; Hess et al., 2001; Levanon et al., 1998; Puccetti et al., 2002). Association with SUV39H1 was also found to be required for the RUNX1-mediated repression of $p21^{WAF1/CIP1}$ (Reed-Inderbitzin et al., 2006).

RUNX1c expression was shown to be upregulated in BL group I cell lines compared to BL group III and LCLs but varied in EBV-negative B cell lines (Spender et al., 2002b). However, no or only low level of RUNX1c could be detected in cell lines expressing EBNA 2 which was later reported to be due to transcriptional crossregulation of RUNX1c by RUNX3 (Spender et al., 2002b; Spender et al., 2005a). RUNX3 was found to bind to the RUNX1c promoter near the transcription start site to repress transcription (Spender et al., 2005a). RUNX1c is highly expressed in quiescent B cells but rapidly

downregulated after RUNX3 expression induced by EBV infection, PMA or TGF-β (Shi and Stavnezer, 1998; Spender et al., 2005a).

1.10.4 RUNX2

RUNX2 was found to be required for osteoblastic differentiation and skeletal morphogenesis (Fujita et al., 2004; Komori et al., 1997; Yoshida et al., 2004). Mutations in RUNX2 are associated with the disease Cleidocranial dysostosis which results in the abnormal development of bones in the skull and collar.

RUNX2 was shown to be able to interact with STUB1, MYST4, C-jun, Mothers against decapentaplegic homolog 3 (SMAD3), (SMAD1) and C-Fos, HDAC3 and HDAC6 but not HDAC2, 4 and 5 (D'Alonzo et al., 2002; Hanai et al., 1999; Hess et al., 2001; Li et al., 2008; Pelletier et al., 2002; Schroeder et al., 2004; Westendorf et al., 2002; Zhang et al., 2000b). HDAC6 was found to be required for RUNX2-mediated repression of $p21^{WAF1/CIP1}$ (Westendorf et al., 2002).

There is also an indication that RUNX2 can downregulate RUNX1 since RUNX2 null mice expressed increased levels of RUNX1 (Yamashiro et al., 2004).

1.10.5 RUNX3

RUNX3 was found to play an important role in neurogenesis as well as growth regulation of gastric epithelial cells (Inoue et al., 2002; Levanon et al., 2002; Li et al., 2002). Deletions of the RUNX3 gene have been found in hepatocellular carcinoma, testicular yolk sac tumours, pancreatic, gastric cancers and lead to hyperplasia in mouse gastric mucosa (Guo et al., 2002; Kato et al., 2003b; Li et al., 2002; Wada et al., 2004; Xiao and Liu, 2004).

RUNX3 is a tumour suppressor as it is involved in the TGF-β apoptotic signalling pathways but also plays a role in TGF-β-induced B cell antibody class switching to IgA in common with RUNX1 (Fainaru et al., 2004; Shi and Stavnezer, 1998). A TGF-β response element in the mouse germline (GL) alpha gene, involved in antibody class switching, was found to contain 2 RUNX-binding sites required for TGF-β-induced promoter activation (Lin and Stavnezer, 1992; Shi and Stavnezer, 1998). TGF-β is able to induce expression of CDKIs p15 and $p21^{WAF1/CIP1}$ and can therefore block

progression into S phase and can suppress expression of c-myc, (reviewed in (Hanahan and Weinberg, 2000)). Changes in TGF-β expression can therefore induce uncontrolled cell cycle progression.

1.11 Aims of my project

Microarray studies previously carried out in the West lab demonstrated that RGC-32 was upregulated in EBNA 3C-expressing BJAB cells. Since RGC-32 was demonstrated to activate the cyclin B/CDK1 complex and play a role in cell cycle regulation. This project set out to investigate whether some of the effects of EBNA 3C on the G2/M checkpoint may be mediated by RGC-32. During the course of these studies, RGC-32 was shown to be induced by RUNX1 in rat cells so the contribution of RUNX1 to RGC-32 regulation in EBV-immortalised cells was also examined.

2 Materials and Methods

2.1 Tissue Culture

Dulbecco Modified Eagles medium (DMEM): with 4.5 g/L glucose, 110 mg/L sodium pyruvate and non-essential amino acids and without L-Glutamine (Invitrogen).

Fetal Bovine Serum (FBS): pre-screened for Mycoplasma and viruses, performance tested (Invitrogen). Heat inactivated at 56°C for 1 hour and stored at -20°C in 50 ml aliquots.

Freezing mix: 70% medium (DMEM (for adherent cells) or RPMI (for suspension cells)), 20% FBS, 10% DMSO (Dimethyl sulphoxide**:** Hybri-Max®, sterile filtered (Sigma)) and 0.7% Penicillin-Streptomycin-Glutamine.

Dulbecco's Phosphate Buffered Saline (PBS): without $CaCl_2$ and $MgCl_2$ (Invitrogen).

100 x Penicillin-Streptomycin-Glutamine (PSG): containing 10,000 units/ml penicillin G sodium, 10 mg/ml streptomycin sulfate, 29.2 mg/ml L-glutamine and 10 mM sodium citrate in 0.14% NaCl (Invitrogen). It was stored in 5 ml aliquots at -20°C.

Propidium Iodide Stain: 25 mg of PI powder (Sigma) in 250 ml PBS (100µg/ml) containing 0.1% Triton X-100.

RNase A: 20 mg RNase A/ml in 50 mM Tris-HCl pH 8.0, 10 mM EDTA (Invitrogen)

RPMI 1640 medium (RPMI): without L-Glutamine (Invitrogen).

Trypsin: Trypsin-EDTA (1x) in Hanks' Balanced Salt Solution (HBSS), without calcium and magnesium (Invitrogen).

2.1.1 Adherent cell lines

2.1.1.1 HeLa

HeLa cells were derived from a human cervical carcinoma from a 31-year old woman in 1951. These cells are epithelial cells which were transformed by human papillomavirus 8 (Scherer et al., 1953). HeLas were grown in DMEM containing 10% FBS and 1% PSG at 37°C with 5% CO_2 and were passaged by trypsinization 1 in 10 twice weekly.

2.1.1.2 Suspension cell lines

All suspension cell lines were cultured in RPMI + 10% FBS + 1% PSG at 37°C with 5% CO_2 and were passaged twice weekly.

2.1.1.3 BJAB

The BJAB cell line was originally thought to have derived from an EBV-negative African's Burkitt's lymphoma in 1975 (Klein et al., 1974; Menezes et al., 1975). However, this cell line does not have a c-myc translocation characteristic of Burkitt's lymphoma cell lines, so is likely to be of B cell lymphoma origin.

2.1.1.3.1 BJAB stable cell lines

The BJAB cell lines E3C-3, E3C-4, E3C-7, pZ1, pZ2 and pZ3, kindly provided by Professor Alan Rickinson, were originally transfected with the expression vector pZipNEOSV(X) containing the open reading frames for EBNA 3C (E3C-3, E3C-4, E3C-7) or the empty vector (pZ1, pZ2, pZ3) and stable cell lines were selected using 2 mg/ml G-418 (Wang et al., 1990a).

The cell lines BJAB FRT and BJAB FRT pFLAG RGC-32 were generated by Helen Webb using the Flp-In™ System from Invitrogen. Normal BJAB cells were transfected with 10 µg linearised pFRT/lacZeo (Invitrogen) via electroporation at 260 V and 950 µF to create a stable Flp-In™ host cell line. After 48 hours Zeocin was added to a final concentration of 400 µg/ml and cells were aliquoted into 96-well plates (200 µl/well). Genomic DNA was isolated from Zeocin resistant clones and Southern blot analysis was performed to determine the number of integrated FRT sites in each of these clones. Cell lines containing single integrants were then screened for beta-galactosidase activity and those with the highest expression levels were stably transfected with 1.8 µg pOG44 (Invitrogen) and 0.2 µg FRT RGC-32 plasmid using the Amaxa kit T (programme T-

016). 48 hours after transfection cells were diluted in media containing hygromycin (200 µg/ml) and hygromycin resistant clones were tested for Zeocin sensitivity, lack of beta-galactosidase activity and pFLAG-RGC-32 expression.

2.1.1.4 DG75

The B cell line DG75 (gift from M. Rowe) was derived from a human EBV-negative Burkitt's lymphoma from the pleural effusion of a 10-year-old boy with Burkitt's lymphoma in 1975 (Ben-Bassat et al., 1977).

The cell lines DG75 FRT and DG75 FRT pFLAG RGC-32 were generated by Helen Webb using the method described above (see section 2.1.1.3).

2.1.1.5 Raji

Raji cells are EBV-positive B lymphocytes and were isolated from the left maxilla of a 12-year-old African boy who suffered from Burkitt's lymphoma. The cell line was established in 1963 and was therefore the first human lymphoma cell line (Pulvertaft, 1964). Raji cells carry a virus with a deletion encompassing the EBNA 3C gene (Hatfull et al., 1988). The EBNA 3C coding region is known to run from bp 86083 to 86442 (ORF: BERF3) and from bp 86517 to 89135 (ORF: BERF4) of the EBV genome (Petti et al., 1988). The deletion of more than 75% of the EBNA 3C gene in Raji cells runs from 86838 to 89830 bp of the EBV genome.

The Raji cell lines 13.6, 11.2.1, 11.5.8 as well as the cell lines 13.6.4 and 11.2.5 were kindly provided by Martin Allday (Allday et al., 1993). The cell lines 11.2.1 and 11.5.8 were made by stable transfection with an EBNA 3C-expressing plasmid (pSV2E3/4) which contains the coding region for EBNA 3C under the control of an SV40 promoter as well as the selectable vector pSV2Hyg. The cell lines 13.6 and 13.6.4 were created by transfection using only the selectable vector pSV2Hyg and were used as an EBNA 3C-negative control. The cell line 11.2.5 was also made by transfection with the pSV2E3/4 plasmid but does not express EBNA 3C and was therefore also used as an EBNA 3C-negative control (Allday et al., 1993).

2.1.2 Freezing cells

A 175 cm^2 flask was harvested and pelleted at 1300 rpm in a Sorvall Legend RT centrifuge using a Sorvall Legend rotor 75006445 for 10 minutes at 4°C. The pellet was then resuspended in 5 ml of freezing mix, aliquoted in 5x 1ml in freezing vials (Nunc) and frozen at -80°C in a freezing container (Nalgene). The vials were transferred to liquid nitrogen after at least 24 hours at -80°C.

2.1.3 Thawing cells

To defrost cells, a freezing vial from liquid nitrogen was thawed rapidly in a 37°C water bath. The cells were then transferred to a 25 ml flask containing 10 ml of prewarmed 37°C supplemented media and then incubated at 37°C with 5% CO_2.

2.1.4 Cell counting

Cell counting was performed using a Neubauer haemocytometer. The 16 squares of each corner were counted separately and then averaged. The average number of cells counted provides the number of cells x 10^4 per ml of the sample.

2.1.5 Cell harvesting

Cells were transferred to a centrifuge tube and pelleted at 1300 rpm in a Sorvall Legend RT centrifuge for 10 minutes at 4°C. Cell pellets were resuspended in an appropriate amount of PBS and counted (see section 2.1.4).

2.1.6 Whole cell lysate preparation

For protein analysis, cells were washed in PBS, counted using the Neubauer cytometer (see section 2.1.4), then pelleted by centrifugation at 2000 rpm for 5 minutes and lysed in 100 µl 1x GSB per 10^6 cells. Each sample was sonicated 5x for 10 sec with 30% amplitude using the Vibra-Cell™ VC 750 (Sonics & Materials, inc.), then heated at 95°C for 10 minutes, vortexed and briefly spun down before analysing by SDS-PAGE (see section 2.2.15).

2.1.7 Hygromycin kill curve

IB4 cells were diluted to 5x10^5/ml and 5 ml aliquots placed in a 6-well plate. Different concentrations of hygromycin (0-500 µg/ml) were added the. Samples of cells (200 µl)

were taken on day 0 and after 2, 4 and 7 days, pelleted at 2000 rpm in an Eppendorf 5415 C centrifuge for 5 minutes and resuspended in 200 µl PBS. 10 µl of cells were mixed with 10 µl of Trypan blue (Sigma) and counted for cell viability (see Appendix 8.6).

2.1.8 Transient Transfection

2.1.8.1 Electroporation

DG75 cells were diluted 1:3 24 hours before electroporation. Cells were pelleted at 1300 rpm in a Sorvall Legend RT centrifuge and the supernatant kept as conditioned media. Differences in DNA content were compensated with pFLAG, pSG5 or pCEP4 empty vector dependent on the experiment. The DNA was prepared in electroporation cuvettes (Bio-Rad) in a total volume of 32 – 40 µl. The DNA was then incubated on ice for 10 minutes. The cells were resuspended in serum-free media, counted, re-pelleted and resuspended at 2x 10^7/ml in serum-free media. 0.5 ml of cells were added to each cuvette and mixed with the DNA. Samples were cooled on ice for 10 minutes and then electroporated at 230 V and 950 µF using a BioRad Gene Pulser II. Following incubation at 37°C with 5% CO_2 for 30 minutes, the cells were transferred into 25 ml flasks containing 10 ml warm conditioned media and incubated at 37°C for 24 - 48 hours. Cells were pelleted, resuspended in PBS and counted. They were then re-pelleted and resuspended in 1 ml PBS for transfer into a 1.5 ml tube. The cells were then pelleted at 2000 rpm in an Eppendorf 5415 C centrifuge for 5 minutes and the supernatant was removed. The cells were either lysed in lysis buffer (Jin et al., 2005) for kinase assays (see section 2.2.23), in EBC buffer for immunoprecipitation (see section 2.2.20 or in 1x Passive Lysis Buffer (Promega) for luciferase assays (see section 2.1.13).

2.1.8.2 Amaxa Nucleofection

BJAB E3C-3 cells were transiently transfected with 2 µg of scrambled control or pSilencer 3.0HI plasmids expressing RGC-32 siRNA1-siRNA5 using program O-017 with an Amaxa nucleofector and the Nucleofector® solution T following the manufacturer's protocol. IB4 cells were stably transfected with 3 µg of RUNX3 siRNA30, siRNA118 or control plasmid using program A-023 with an Amaxa nucleofector and the Nucleofector® solution T following the manufacturer's protocol.

2.1.8.2.1 Silencing of RUNX3 expression

IB4 cells were transfected as previously described (see section 2.1.8.2) and transferred into a total volume of 6 ml complete RPMI media. Hygromycin was added to a final concentration of 300 µg/ml 24 hours after transfection. 3 ml of cells were harvested 6, 9 and 14 days after transfection and 3 ml complete RPMI media containing 300 µg/ml hygromycin was added. Cell pellets were used for protein analysis (see sections 2.1.6, 2.2.15 and 2.2.16) or RNA analysis (see sections 2.2.11, 2.2.13 and 2.2.14).

2.1.8.3 Fugene

HeLa cells were counted and plated at a final concentration of $5x10^4$ cells/ml in a 10 cm plate (Fisher) 24 hours prior to transfection. 12 µl FuGENE (Roche) was mixed with 180 µl of unsupplemented DMEM and left at room temperature for 5 minutes. A total of 4 µg of plasmid was then added, the sample gently mixed and then incubated for 30 minutes at room temperature. Just before adding the sample dropwise to the plate, the cells were washed in PBS which was then replaced with fresh DMEM. The cells were incubated at 37°C for 48 hours before harvesting.

2.1.9 Gamma irradiation

Exponentially growing cells were pelleted and resuspended in fresh media at a final concentration of $4x\ 10^5$/ml the previous day. The cells were treated with 10 Gy using a ^{137}Cs source to irradiate the cells and then incubated at 37°C with 5% CO_2 for 4, 8 and 24 hours. The cells were then washed and counted in PBS and divided between 2 tubes. One half of the cells was used for FACS analysis and the other half for protein analysis. For FACS analysis the cells were pelleted, resuspended in 1 ml of 70% ethanol per 10^6 cells, incubated for at least 30 minutes at 4°C and then stained with propidium iodide (see section 2.1.10).

2.1.10 Propidium Iodide staining

1 ml ethanol containing the fixed cells ($1x\ 10^6$ cells) was transferred to a FACS tube (BD Biosciences) and pelleted at 1000 rpm for 5 minutes at 4°C using the Sorvall Legend RT centrifuge. The pellet was resuspended and washed in 1 ml PBS. After the cells were pelleted again, 500 µl of PI stain (Sigma) and containing 50 µg/ml RNase A (Sigma) and the samples incubated at room temperature for 30 minutes. The cell cycle distribution was analysed with the BD FACSCanto Flow Cytometer (BD Biosciences).

2.1.11 Etoposide treatment

The cells were set up at a final concentration of 4x 10^5/ml the previous day as described for gamma irradiation (see section 0). The cells were treated with 50, 100, 300 or 500 nM etoposide using dilutions of a 1 M stock dissolved in DMSO and incubated at 37°C with 5% CO_2 for 24 or 48 hours. The cells were then washed and counted in PBS. Cells were pelleted and one half of the pellet was fixed in 1 ml of 70% ethanol per 10^6 cells for at least 30 minutes at 4°C and then stained with propidium iodide (see section 2.1.10). The other half was used for whole cell lysate preparation for protein analysis (see section 2.1.6 and 2.2.15).

2.1.12 DNA damage and BrdU incorporation

The BJAB cell lines pZ1, pZ3, E3C-3 and E3C-4 were diluted to 4x 10^5/ml 24 hours prior treatment. For etoposide treatment, the pZ and E3C lines were treated with 10 µM BrdU (Sigma), incubated for 1 hour, washed and resuspended in fresh media containing 0, 300 or 500 nM etoposide for 24 hours. For FACS analysis, unlabelled control cells were fixed cells, stained with PI for 30 minutes (see section 2.1.10) and analysed using the BD FACSCanto Flow Cytometer (BD Biosciences) for cell cycle distribution. Cells of all other samples were stained with PI for 1 hour, pelleted and resuspended in 0.1% PBS-Tween. The appropriate primary antibody was then added (either 40 µl of 1:15-diluted anti-BrdU antibody (c=0.5mg/ml, Upstate) or 40 µl 1:1.5-diluted anti-IgG2a antibody (c=0.05 mg/ml, BD)) (see Table 2).

Sample	BrdU	Mouse-anti-BrdU (1° ab)	Mouse-anti-IgG2 (1° ab)	Anti-mouse-FITC (2° ab)	PI
unlabelled control	×	×	×	×	×
IgG2 antibody control	✓	×	✓	✓	✓
DMSO control	✓	✓	×	✓	✓
300 nM	✓	✓	×	✓	✓
500 nM	✓	✓	×	✓	✓

Table 2 – showing an overview of what each sample contained.

Cells were incubated at room temperature for 1 hour, pelleted and resuspended in a 1:20 dilution of a FITC-conjugated, polyclonal rabbit anti-mouse antibody (Dako). Following incubation at room temperature for 30 minutes, the cells were washed, resuspended in PBS and analysed by FACS.

2.1.13 Luciferase assay

48 hours after transfection using the Bio-Rad Gene Pulser® II or FuGENE transfection techniques, cells were pelleted at 1300 rpm for 10 minutes at 4°C in a Sorvall Legend RT centrifuge and resuspended in 1 ml PBS. Cells were then transferred to an 1.5 ml tube and pelleted in an Eppendorf 5415C centrifuge at 2000 rpm in an Eppendorf 5415 C centrifuge for 5 minutes. The cells were lysed in 100 µl 1x passive lysis buffer (Promega) at room temperature for 30 minutes followed by another 30 minute incubation on ice. The cell debris was then pelleted at 13000 rpm in a Heraeus Biofuge Pico for 5 minutes. The supernatant was transferred to a new 1.5 ml tube. For the luciferase assay 2x 10 µl of each sample was added to a 96-well plate. With the sequential injection system on a Lucy 2 luminometer (LabTech) 50 µl of LarII followed by 50 µl of Stop and Glo solutions (Promega luciferase dual assay kit) were added to the samples and the signals from the reporter genes were measured after each step. The pCp-1425-GL2 and the RGC-32pLuc plasmids used contain the firefly luciferase gene, controlled by the C or RGC-32 promoters respectively. The pRL-CMV plasmid contains the *Renilla* luciferase gene controlled by the CMV promoter and was used as a control for transfection efficiency. The values for firefly luciferase activity were therefore corrected by dividing them by the values for the *Renilla* luciferase activity.

2.1.14 Proteasome inhibition

The cells were diluted 1:3 24 hours before the experiment. The proteasome inhibitor MG132 was added to a final concentration of 50, 100 or 200 µM. Cells were pelleted after 1, 2, 8 or 24 hours, washed and counted in PBS. The cells were then pelleted and whole cell lysates prepared for SDS-PAGE analysis (see section 2.1.6 and 2.2.15).

2.1.15 Transcription inhibition

The BJAB cell lines pZ1, pZ3, E3C-3 and E3C-7 were set up at $2x10^5$/ml in a 6-well plate 72 hours prior to treatment. 2 µM of actinomycin D (Sigma) was added to all cell

lines and a 0 hour control was harvested at the same time. Further samples were taken 2, 4, 6 and 8 hours after addition of actinomycin D. Cells were then lysed and RNA extracted for real-time PCR (see section 2.2.11, 2.2.14)

2.1.16 Centrifugal elutriation

BJAB pZ3 and E3C-3 cells were fractionated using centrifugal elutriation which was kindly performed by Aloys Schepers (University of Munich).

2.2 Molecular Biology

ADBI buffer: 20 mM MOPS pH 7.2, 25 mM sodium glycerophosphate, 5mM EGTA, 1 nM Sodium orthovanadate, 1 mM dithiothreitol (DTT).

Agar: 5 g agar (Oxoid) in 400 ml L broth before autoclaving.

Ampicillin: (Sigma): 100 mg/ml in filter-sterilised H_2O using a 0.2 μm filter (Nalgene) and stored at -20°C in 1 ml aliquots.

Blotting Buffer: 4 litre dH_2O, 1 litre methanol (Fisher), 75 g Glycine (Fisher), 15 g Tris(hydroxymethyl)-methylamine (Fisher).

Buffer A: 300 mM NaCl, 40 mM PO_4 buffer pH 7.5, 20 mM Imidazole, 3.5 mM β-mercaptoethanol, 2 mM benzamidine and protease inhibitor cocktail tablet (Roche).

Buffer B: 300 mM NaCl, 40 mM PO_4 buffer pH 7.5, 20 mM Imidazole, 3.5 mM β-mercaptoethanol, 2 mM benzamidine, 1% NP40 and protease inhibitor cocktail tablet (Roche).

Buffer C: 1 M NaCl, 40 mM PO_4 buffer pH 7.5, 20 mM Imidazole, 3.5 mM β-mercaptoethanol, 2 mM benzamidine, 1% NP40, protease inhibitor cocktail tablet (Roche).

Buffer X: 50 mM HEPES (KOH) pH 7.5, 10% glycerol, 2 mM benzamidine, 1 M GuHCl.

Buffer Y: 50 mM HEPES (KOH) pH 7.5, 10% glycerol, 2 mM benzamidine, 6 M GuHCl.

CsCl prep solution I: 50 mM glucose, 25 mM Tris-HCl pH 8.0, 10 mM EDTA (Sigma).

CsCl prep solution II: 200 mM NaOH, 1% SDS.

CsCl prep solution III: 300 ml 5 M KAC, 57.5 ml glacial acetic acid, 142.5 ml H_2O.

CsCl-saturated butanol: 100 g Caesium chloride (Invitrogen) in 200 ml H_2O and 200 ml butanol.

EBC buffer: 50 mM Tris pH 8, 120 mM NaCl, 0.5% nonidet P40 (NP40) and 5 mM Dithiothreitol (DTT, Sigma).

ECL: Solution I: 2.5 mM luminol, 400 µM coumaric acid, 100 mM Tris pH 8.5 in 20 ml dH_2O. Solution II: 0.15% Hydrogen Peroxide (H_2O_2) and 100 mM Tris pH 8.5 in 20 ml dH_2O.

Elution Buffer E: 300 mM NaCl , 100 mM EDTA, 40 mM PO_4 buffer pH 7.5.

Fixing buffer (kinase assay): 40% methanol, 10% glacial acetic acid.

Fixing buffer (gel shift): 20% methanol, 10% glacial acetic acid.

1x gel sample buffer (GSB): 50 mM Tris, 4% SDS, 5% 2-mercaptoethanol (Sigma), 10% glycerol, 1 mM EDTA, 0.01% bromophenol blue.

L broth: 10 g tryptone (Oxoid), 5 g yeast extract (Oxoid), 10 g NaCl, made up to 1 litre in distilled H_2O followed by autoclaving.

Lysis buffer (Jin et al., 2005): 100 mM NaCl, 50 mM NaF, 50 mM Tris pH 7.5, 40 mM Sodium β-glycerophosphate (Fisher), 5 mM EDTA, 1 mM Sodium orthovanadate (Fisher), 1% Triton X-100, protease inhibitor tablet.

Lysis buffer B (Topisirovic et al., 2002): 10 mM Tris pH 8.4, 140 mM NaCl, 1.5 mM $MgCl_2$, 0.5% NP40, 1 mM DTT and 200U/ml RNasin (Promega).

Protease inhibitor: 2 mM phenylmethylsulfonyl fluoride (PMSF) in ethanol.

Stripping buffer: 100 mM 2-mercaptoethanol (Sigma), 2% SDS, 62.5 mM Tris-HCl pH 6.7.

10 x TBE: 540 g Tris, 275 g Boric acid and 46.5 g EDTA dissolved in 5 litre H_2O.

4 x TBE loading dye: 5 ml glycerol, 0.1 ml 10% bromophenol blue, 1 ml 1% xylene cyanol and 3.9 ml 10 x TBE.

TE: 10 mM Tris-HCl pH 8.0, 1 mM EDTA in ultra pure H_2O.

Washing Buffer (PBS-T): 10 litre dH_2O, 100 PBS tablets (Fisher) and 10 ml Tween 20 (Fisher).

2.2.1 Agar plates

Agar was melted in the microwave and left to cool. Antibiotics were added to the following final concentrations: Ampicillin (100 µg/ml), Kanamycin (25 µg/ml), Chloramphenicol (42 µg/ml). When the agar was mixed with the antibiotics, the plates were poured, left to set and stored at 4°C.

2.2.2 Plasmids and siRNA-expressing plasmids

To create the **pFLAG RGC-32** plasmid, RGC-32 was amplified from BJAB E3C-4 cell cDNA using the RGC-32 primer set (see Appendix 8.3) and cloned into pFLAG-CMV-2 (Sigma) as an Xba1/BamH1 fragment (Helen Webb).

FLAG-RGC-32 was cut out of the plasmid as a Sac1/Sma1 fragment and the Sac1 overhang was blunt-ended using mung bean nuclease and the fragment cloned into pcDNA5/FRT (Invitrogen) cut with EcoRV to create **pFLAG RGC-32/FRT** (Helen Webb).

To create the **pET RGC-32** plasmid RGC-32 was cut out of pFLAG-RGC-32 (see above) as a Sal I/BamHI fragment and cloned into pET16b (Sigma) digested with Xho I/ BamHI (Helen Webb).

RGC-32-expressing *E.coli* BL21 *plysS* (Sigma) were generated by Helen Webb by transforming this E. coli strain with pET RGC-32.

SiRNA oligonucleotides were designed by Helen Webb using *pSilencer* Expression Vectors Insert Design Tool (Ambion) against the 3' UTR region of RGC-32 (Table 3). These were phosphorylated, annealed and cloned into pSilencer 3.0HI digested with BamH1/HindIII. The negative control (Scrambled siRNA) encoding vector was obtained from Ambion.

siRNA	Sequence
siRNA 1	GAT CCG TTT GAA CTG AAC CTC GTG CTT CAA GAG AGC ACG AGG TTC AGT TCA AAT TTT TTG GAA A AGC TTT TCC AAA AAA TTT GAA CTG AAC CTC GTG CTC TCT TGA AGC ACG AGG TTC AGT TCA AAC G
siRNA 2	GAT CCG CAG ACG ATC CAT GCT AAT ATT CAA GAG ATA TTA GCA TGG ATC GTC TGT TTT TTG GAA A AGC TTT TCC AAA AAA CAG ACG ATC CAT GCT AAT ATC TCT TGA ATA TTA GCA TGG ATC GTC TGC G
siRNA 3	GAT CCG TCA GCC CTT GAT CCC ATT TCT CAA GAG AAA ATG GGA TCA AGG GCT GAT TTT TTG GAA A AGC TTT TCC AAA AAA TCA GCC CTT GAT CCC ATT TTC TCT TGA GAA ATG GGA TCA AGG GCT GAC G
siRNA 4	GAT CCA GAC GTG CAC TCA ACC TTC TTC AAG AGA GAA GGT TGA GTG CAC GTC TTT TTT TGG AAA AGC TTT TCC AAA AAA AGA CGT GCA CTC AAC CTT CTC TCT TGA AGA AGG TTG AGT GCA CGT CTG
siRNA 5	GAT CCG CTT CAG AAA GTT CCG AGG TTC AAG AGA CCT CGG AAC TTT CTG AAG CTT TTT TGG AAA AGC TTT TCC AAA AAA GCT TCA GAA AGT TCC GAG GTC TCT TGA ACC TCG GAA CTT TCT GAA GCG

Table 3- Overview of RGC-32 siRNA sequences.

To create the **RGC-32pLuc** vector a 1.2 kb fragment (approximately –1150 to +62 relative to predicted transcription start site) of the RGC32 promoter was amplified from genomic DNA and cloned into pGL2-Basic (Promega) cut with HindIII/Kpn1 (Helen Webb). For some experiments a newer version of the RGC-32pLuc plasmid was used in the pGL3-Basic vector background instead of the pGL2-Basic vector background. The RGC-32 promoter fragment was cut with HindIII/KpnI and cloned into a pGL3-Basic vector (Promega).

To mutate the RUNX1-binding site in the **RGC-32pLuc** plasmid the RGC-32 promoter of pGL2 was amplified with primers containing a 3 bp mutation at the RUNX1-binding site. The mutated promoter sequence was cut with NheI/KpnI and inserted into the pGL3 basic vector together with a NheI/HindIII fragment from the wildtype RGC-32pLuc plasmid, **RGC-32pLuc mut** (see section 2.2.3).

RGC-32pLuc up was created by cutting the original RGC-32pluc (pGL2) was cut with KpnI and NdeI. A 1.1 kb upstream RGC-32 promoter region was amplified from HEK293 genomic DNA using RGC-32-specific primers containing KpnI and NdeI sites and cloned into pRGC-32pLuc (Felicity Poulter).

The **pRL-CMV** vector (Promega) contains the CMV promoter region, which provides constitutive expression of *Renilla* luciferase from the R*luc* gene.

pCp-1425-GL2 contains the EBV C promoter (-1425 to +3) inserted into the the BglII site of vector **pGL2 basic** (Promega) which has a Firefly luciferase reporter gene (gift from A. Bell and F. Nitsche) (West et al., 2004).

The plasmid **pSG5 2A** contains full length EBNA 2 (EBV type 1) under the control of the simian virus 40 (SV40) early promoter within the vector **pSG5** (Stratagene) (gift from M. Rowe) (Tsang et al., 1991).

The plasmid **pSG5 3C** expresses full length EBNA3C which was also inserted in the pSG5 vector (Stratagene) (West et al., 2004).

The **pBK-CMV-RUNX1c** plasmid expresses the RUNX1 isoform 1c. The plasmid was kindly provided by Paul Farrell.

The **pCEP4-RUNX1c** and **pCEP4-RUNX3** plasmids express RUNX isoform 1c and RUNX3 respectively (Spender et al., 2005a). The plasmids were kindly provided by Paul Farrell.

The siRNA plasmids for RUNX3 (**RUNX3 siRNA-30** and **-118**) and the empty vector were made using the pHEBoSUPER plasmid. pHEBoSUPER was created by cutting out

the pSUPER BamHI to XhoI fragment containing the H1 promoter which was cloned into the pHEBo vector between BamHI and SalI sites. The siRNA oligonucleotides were cloned in between the HindIII and BglII sites (Spender et al., 2005a). These plasmids were kindly provided by Paul Farrell.

2.2.3 Site-directed mutagenesis

2.2.3.1 Primer design

Two 39 bp primers (see Appendix 8.3) were designed to bind the original RGC-32pLuc plasmid at the RUNX1-binding site but incorporated a 3 bp mutation which would be amplified in the PCR reaction. The primers were designed following the Primer Design Guidelines of the QuikChange® Site-Directed Mutagenesis Kit recommended by Stratagene® and were ordered from Invitrogen.

2.2.3.2 PCR-based site-directed mutagenesis

To mutate the RUNX1-binding site in the RGC-32 promoter 50 ng of DNA template (RGC-32pLuc plasmid) was mixed with 125 ng of forward and reverse primer (see Appendix 8.3), 300 µM dNTP mix, 1 mM $MgSO_4$, 3x PCR enhancer (Invitrogen), 5 µl 10x Pfx amplification buffer (Invitrogen) and 1 µl (2.5 U) Platinum *Pfx* (Invitrogen). The reactions were made up to a final volume of 50 µl using sterile-filtered water.

The PCR programme was set up as follows. The extension time was calculated using 1 min/kb of plasmid length as recommended by Stratagene®:

Segment	Cycles	Temperature	time
1	1	95°C	30 sec
2	16	95°C	30 sec
		48°C	1 min
		55°C	6 min 50 sec

Table 4 – Overview of PCR program used for site-directed mutagenesis.

After completed mutagenesis the samples was placed on ice for 2 minutes, 1 µl DpnI (10U/µl) was added, mixed and the sample incubated at 37°C for 1 hour. DNA was

visualised in an agarose gel (see section 2.2.4), subsequently transformed (see section 2.2.5), the DNA purified (see section 2.2.6) and sequenced (see section 2.2.7).

2.2.4 Agarose gel electrophoresis

A 1% agarose gel was used to visualise DNA. 50 mg of agarose powder (Helena BioSciences) was dissolved in 50 ml of 1 x TBE buffer by heating in the microwave. 0.5 µl of Gel Red (Biotium) was added and the agarose was poured into a BioRad Mini sub cell GT tank including a comb to form the wells. After the gel had set, it was covered with 1x TBE buffer and the comb was removed. 5 µl of DNA sample were mixed with 1.5 µl 4x TBE loading buffer. 6 µl of each plasmid sample and 5 µl of the DNA marker (100 base pair ladder (Invitrogen) or Hyperladder II (Bioline)) were loaded onto the gel. The gel was run at 75 V for 60 min and DNA bands were then visualised with UV light.

For DNA gel purification 2 teeth of the comb were taped together so that 2 wells formed 1 large well in the agarose gel and 50 µl of sample were loaded and run as described above.

2.2.5 Transformation of bacterial cells

0.5 µg of plasmid DNA or 10 µl of mutated or ligated DNA was mixed with 100 µl of competent E. coli $DH5_{\alpha}$ cells and incubated on ice for 40 min. The cells were then heat-shocked at 42°C for 45 seconds and left on ice for 2 minutes. Transformed cells were pipetted onto agar plates containing the respective antibiotics and spread using a sterile glass spreader. Colonies were grown overnight at 37°C.

2.2.6 Miniprep

Several colonies were picked with a sterile toothpick and each was grown in 2 ml LB containing 100 µg/ml ampicillin. The transformed bacteria were incubated at 37°C overnight with shaking. 1.5 ml of each culture was pelleted by centrifugation at 13000 rpm for 1 minute. Plasmid DNA was extracted using a QIAprep Spin Miniprep kit (Qiagen) according to the manufacturer's instructions.

2.2.7 Sequencing of DNA

10 µl of miniprep DNA was dried in a Savant DNA110 Speedvac Concentrator vacuum centrifuge at medium drying rate for 20 minutes. The dried DNA was sent to Eurofins MWG for sequencing (see Appendix 8.7).

2.2.8 Cloning

2.2.8.1 Enzyme digest

In general, 5 µg of plasmid were digested in a 20 µl reaction with 2 µl enzyme (NEB) and the appropriate buffer +/- BSA (NEB). The samples were incubated at 37°C for at least 1 hour. The linearised DNA fragments were separated on an agarose gel (see section 2.2.4) and the DNA purified as required (see section 2.2.8.2).

2.2.8.2 DNA gel purification

The DNA of interest was cut out of the gel using a razor blade. DNA was then purified using the gel purification kit (Qiagen) following the manufacturer's instructions. The DNA was eluted in 30 µl EB buffer (Qiagen).

2.2.8.3 Alkaline phosphatase treatment of vector DNA

To prevent single cut linearised vector from re-ligating, the samples were treated with alkaline phosphatase (Roche) to remove the 5' phosphate group from the cut ends. 20 µl of DNA was mixed with 4.3 µl alkaline phosphatase and 2.7 µl of 10x alkaline phosphatase buffer in a total volume of 27 µl. The samples were incubated at 37°C for 30 minutes.

2.2.8.4 Ligation

The KpnI/NheI fragment containing the mutated RUNX-binding site sequence was then cloned into a pGL3 vector (Promega). To achieve ligation approximately 100 ng of vector was mixed with the inserts in molar ratios of 1:1, 1:3, 1:5 and 3:1 in the presence of 2 µl of T4 ligase buffer, 1 µl of T4 ligase (Invitrogen) and filter-sterilised water in a final volume of 10 µl. The samples were incubated on ice for 1 hour followed by 1 hour at room temperature and 1 hour at 37°C. The samples were then used for transformation of DH5$_\alpha$ (see section 2.2.5).

2.2.9 Glycerol stocks

$DH5_{\alpha}$ cells were transformed with plasmid DNA (see section 2.2.2) and streaked onto agar plates containing the appropriate antibiotics. A single colony was restreaked twice to ensure the colony contained the desired plasmid. After an overnight incubation at 37°C, 4 ml of L broth was added to the plate, and the colonies were scraped off the agar. The bacteria were transferred into two cryogenic vials and 15% glycerol added. The cryogenic vials were then stored at -80°C. These glycerol stocks could be used for long-term storage and the bacteria can be restreaked to grow colonies containing the desired plasmid.

2.2.10 Caesium chloride (CsCl) DNA preparation

A colony of $DH5_{\alpha}$ transformed with the plasmid of interest was picked and spread onto a new agar plate containing the appropriate antibiotics. The cells were cultured overnight at 37°C. A colony was picked on the following day with a sterile toothpick and mixed with 2 ml L broth containing the appropriate antibiotics. Cultures were incubated at 37°C for 6 hours with shaking. The 1 ml culture was then transferred to 250 ml L broth, antibiotics added and the culture incubated at 37°C overnight with shaking.

Cells were pelleted by centrifugation at 6000 rpm for 10 minutes at 4°C a JA-10 rotor (Beckman) in a Beckman Coulter Avanti J-20 XP centrifuge. The cell pellet was resuspended in 7 ml of solution I. To lyse the cells, 14 ml of solution II was added to the cell suspension and mixed well. 11 ml of solution III were then added followed by thorough mixing and incubation on ice for 5 minutes. The cell debris was pelleted by centrifugation at 7000 rpm for 10 minutes at 4°C and the supernatant filtered through a tissue. 0.6 volumes of isopropanol was added and the sample incubated at room temperature for 10 minutes to precipitate the DNA. The samples were centrifuged at 4000 rpm for 10 minutes at 4°C in a Sorvall Legend RT centrifuge. The pellets were resuspended in 3 ml TE and 2 ml of 5M NH_4 acetate was added to precipitate the RNA.

After 1 hour incubation on ice, the precipitated RNA was pelleted by centrifugation at 4000 rpm for 10 minutes at 4°C and the supernatant was mixed with 2 volumes of 100% ethanol to precipitate DNA. After 10 minutes incubation at room temperature the DNA

was pelleted by spinning at 4000 rpm for 10 minutes at 4°C. The DNA was resuspended in 4 ml TE and 4.3 g CsCl and 1 mg Ethidium Bromide was added to each sample. The solution was transferred to optiseal tubes (Beckman) and placed in Beckman VTi 65.2 rotor with a spacer and torqued screw seal. The CsCl gradient was used to separate plasmid DNA and chromosomal DNA by centrifugation of the samples at 50000 rpm overnight at 20°C in a Beckman Optima LE-80K ultracentrifuge.

A 23G needle was used to extract the plasmid DNA. Ethidium bromide was removed by several extractions using an equal volume of CsCl saturated butanol. 4 volumes of TE were added and the DNA was precipitated with 3 volumes of ethanol. After a 10 minute incubation at room temperature, the DNA was pelleted by centrifugation at 4000 rpm for 10 minutes at 4°C, resuspended in 5 ml TE and precipitated with 10 ml ethanol and 0.1 volumes of 3 M NaAc pH 5.2. After a 10 minute incubation at room temperature, the DNA was again pelleted by centrifugation at 4000 rpm for 10 minutes at 4°C, air dried for 10 minutes and resuspended in 0.5 ml TE. The concentration of plasmid DNA was then determined by spectrophotometry (see section 2.2.12).

2.2.11 RNA Extraction

RNA was isolated from cells using TRI Reagent® (Sigma) according to the manufacturer's instructions (1 ml/10x 10^6 cells).

The RNA was then purified using the RNeasy Mini Kit from Qiagen according to the manufacturer's instructions and stored at -80°C.

2.2.12 Spectrophotometric Determination of DNA and RNA Concentration

Plasmid DNA samples were diluted 1:200 (5 µl of DNA in 995 µl TE) in a UV-cuvette micro from Plastibrand® and mixed. The amount of DNA was then measured in the Eppendorf Biophotometer at 260 nm. The ratio of optical density readings at 260 nm and 280 nm provided the purity of the nucleic acid (1.8 for pure double stranded DNA).

RNA samples were diluted 1:100 (1 µl of RNA in 99 µl distilled H_2O) in an UVette from Eppendorf and mixed. The absorbance was read using the Eppendorf

Biophotometer. The ratio of optical density readings at 260 nm and 280 nm provided the purity of the nucleic acid (2.0 for pure RNA).

The concentration of DNA was calculated using the following formula: DNA concentration (µg /ml) = A_{260} x 50 µg /ml x 200 (dilution factor). The concentration of RNA was calculated using the following formula: RNA concentration (µg / ml) = A_{260} x 40 µg / ml x 100 (dilution factor).

2.2.13 cDNA Synthesis

RNA extraction was followed by cDNA synthesis using the ImProm-II™ Reverse Transcription System Kit from Promega. Based on the manufacturer's instructions 1 µg of each RNA was mixed with 1 µl Random Primer and water added to a final volume of 5 µl. The samples were then incubated at 70ºC for 5 minutes and then placed on ice for 5 minutes. 15 µl of the Mastermix (containing 4.5 µl nuclease-free H_2O, 4.0 µl ImProm™ 5x Reaction Buffer, 4.0 µl $MgCl_2$, 1.0 µl dNTP Mix, 0.5 µl ribonuclease inhibitor and 1.0 µl reverse transcriptase) was added to the RNA. The samples were then incubated for 5 minutes at 25°C, 60 minutes at 42°C and 15 minutes at 70°C and finally stored at -80°C.

2.2.14 Real-Time Polymerase Chain Reaction

The QuantiTect® SYBR® Green PCR Kit (Qiagen) was used for real-time PCR (polymerase chain reaction) reactions. The cDNA samples were diluted either 1:10 or 1:20 with sterile filtered water. A final volume of 25 µl was added to each well (containing 1x QuantiTect® SYBR® Green Mix, 0.15 mmol forward and 0.15 mmol reverse primers (see Appendix 8.3) and 5µl diluted cDNA following the instructions provided by Qiagen.

The thermal cycler 7500 Real Time PCR system from Applied Biosystems was used with the following cycling conditions: initial denaturation step at 95°C for 10 minutes, amplification step of 40 cycles of 15 sec at 95°C and 1 minute at 60°C. A dissociation curve was then generated by one cycle of 15 sec at 95°C, 1 minute at 60°C and 15 sec at 95°C (Figure 12).

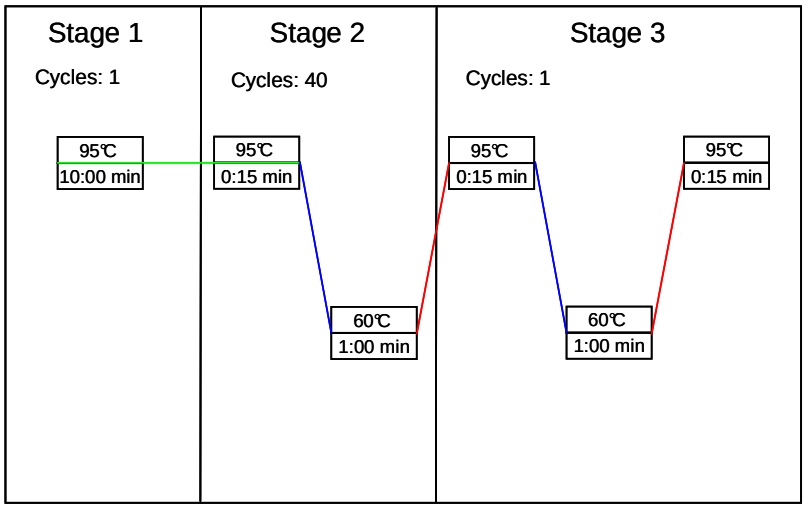

Figure 12 – Thermal profile of cycling conditions for Real-time PCR.

CDNA from an appropriate cell line was used to generate standard curves for each primer set. A 1:10, 1:50, 1:250, 1:1000 and 1:5000 dilution of cDNA corresponded to 25, 5, 1, 0.25 and 0.05 ng of input RNA. These standard curves were used to convert the crossing threshold (C_t) values obtained for all samples into arbitrary RNA quantity values. This allows comparison between different cell lines. The results are displayed relative to GAPDH to correct for differences in the efficiency of the reverse transcriptase reaction and validation between samples.

2.2.15 SDS – PAGE

15 µl of lysate were resolved using 12 well 10%, 12% or 4-12% Bis-Tris gels (Invitrogen). The gels were run in 1x MES or 1x MOPS running buffer (Invitrogen) depending on the separation required. The gels were run at 200V for 35 minutes in MES or 50 minutes in MOPS buffer. 5 µl of a marker (SeeBlue® Plus2 pre-stained standard, Invitrogen) was used to allow the determination of the molecular weights of the proteins.

2.2.16 Western Blotting

After separation of the proteins by SDS-PAGE, the proteins were transferred to Protran nitrocellulose membranes (Schleicher & Schuell) or Immobilon™ P (Millipore) by Western blotting at 85 V for 90 minutes in blotting buffer using a Transblot apparatus (Biorad). The blots were then blocked by shaking with 5% milk powder (Marvel) in PBS-T for 1-2 hours. The appropriate primary antibody (see Appendices 8.4 and 8.5) diluted in 10 ml PBS-T containing 5% milk was added and the blot incubated overnight at 4°C on a rocking platform. The following day the blots were washed 3x 10 minutes

with PBS-T and then incubated with secondary antibody (see Appendices 8.4 and 8.5) conjugated to horseradish peroxidase diluted in PBS-T supplemented with 5% milk on a rocking platform for 1 hour. The blots were then washed 3x for 10 minutes with PBS-T. Each membrane was briefly incubated with 2 ml ECL (enzymatic chemiluminescence) solution (1:1 mixture of solution 1 and 2). The blots were then exposed to Fuji medical X-ray film (Fisher) for varying times depending on intensity of the signal. The films were developed using a Konica SRX-101A film processor.

2.2.17 Anti-RGC-32 antibody

Several blood samples before and after immunisation were taken from two rabbits to obtain sera containing anti-RGC-32 antibodies (performed by Eurogentec) (see Table 5).

Sample	Week	Bleeding/Immunisation
1st bleed	1	Pre-immune bleeding/ 1st Immunisation
-	3	2nd Immunisation
-	5	3rd Immunisation
2nd bleed	6	Small bleeding
-	9	4th Immunisation
3rd bleed	10	Large bleeding
4th bleed	13	Additional large bleed
-	14	5th Immunisation
5th bleed	15	Final bleed

Table 5 – Bleeding timetable of rabbit 2817 and 2818.

2.2.18 Stripping blots

Western blot membranes were probed as required after removing the antibodies bound to the membrane. This procedure was performed by washing 2x with PBS-Tween for 5 minutes, incubating with stripping buffer at 50°C for 15 minutes and washing again 2x with PBS-Tween for 5 minutes. The blots were then blocked with 5% milk in PBS-Tween for 1 hour and probed for a second time with a different primary antibody.

2.2.19 Coomassie staining

After completion of SDS-PAGE, the gel was washed in deionised water 3x for 5 minutes. 10 ml of Bio-Safe™ Coomassie stain (Biorad) was applied to the gel and incubated for 1 hour on the shaker. The gel was then washed with deionised water 3x for 5 minutes followed by an incubation of 1 hour with deionised water to remove the background staining. The gel was then dried onto filter paper using a vacuum gel dryer set at 80°C for 45 minutes.

2.2.20 Immunoprecipitation

For immunoprecipitation the cells were pelleted at 1300 rpm in a Sorvall Legend RT centrifuge. 2 x 10^7 cells were lysed in 1 ml of EBC buffer and incubated on ice for 30 minutes. Each sample was sonicated 5x for 10 sec. The lysates were then spun down at 13000 rpm in a Fisher Scientific accuSpin™ MicroR centrifuge at 4°C for 5 minutes. The supernatant was transferred to a new 1.5 ml tube. 40 µl lysate of each sample was kept for analysis and mixed with 10 µl 5x GSB for SDS-PAGE. To preclear the lysate, it was transferred to a tube containing 40 µl of a 1:1 protein A-sepharose beads/PBS slurry. The samples were incubated with rotation for 90 minutes at 4°C. The precleared lysates were then spun briefly and transferred to a new 1.5 ml tube. 4 µg of either rabbit IgG (negative control), anti-FLAG antibody (positive control) or 10 µl of rabbit 2818 pre-immune serum or rabbit 2818 serum from 3rd bleed containing the anti-RGC-32 antibodies was added to the lysates and incubated for 2.5 hours at 4°C with rotation. All lysates except the anti-FLAG antibody IP samples were then added to 1.5 ml tubes containing 40µl of a 1:1 protein A-sepharose beads/PBS slurry. The lysates incubating with the anti-FLAG antibody were added to a slurry of protein G-sepharose beads and incubated with rotation at 4°C overnight.

The following day the beads were washed 3x in 0.5 ml EBC containing 0.03% SDS. After each wash step the samples was spun briefly and the supernatant removed. The beads were then washed in PBS, spun briefly and the supernatant removed. 15 µl of 2x GSB was added and the sample incubated at 95°C for 10 minutes, vortexed briefly, spun briefly and loaded onto a SDS-PAGE gel (see section 2.2.15).

2.2.21 Cellular fractionation

$3x10^7$ cells were washed twice in ice cold PBS and pelleted at 1300 rpm for 5 minutes. The pellet was resuspended with slow pipetting in 1 ml of lysis buffer B so that no clumps were visible. The sample was centrifuged at 2500 rpm for 3 minutes at 4°C using a Sorvall Legend RT centrifuge. The supernatant was kept as the cytoplasmic fraction. The pellet containing the nuclei was resuspended in 1 ml lysis buffer B containing 1/10 volume (100 µl) of detergent (3.3% [wt/vol] sodium deoxycholate and 6.6% [vol/vol] Tween 40) was added under slow vortexing to prevent clumping and the sample incubated on ice for 5 minutes. The sample was centrifuged at 2500 rpm for 3 minutes at 4°C. The nuclear fraction was rinsed with 1 ml of lysis buffer B and centrifuged at 2500 rpm for 3 minutes at 4°C. The supernatant was discarded. 1 ml of TRI Reagent was added to both nuclear and cytoplasmic fractions for RNA isolation (see section 2.2.11). For SDS-PAGE 1 ml of 1x GSB was added to the nuclear fraction and 20 µl of the cytoplasmic fraction was mixed with 5 µl 5x GSB. 20 µl of each fraction was used for SDS-PAGE.

2.2.22 Kinase Assay (*in vitro*)

2 units of recombinant CDK1/Cyclin B1 (NEB) in a 1:10 dilution of ADBI (Upstate) were mixed with different concentrations (0 µM control, 0.6 µM, 1.2 µM, 2.4 µM and 3.6 µM) of RGC-32 protein in phosphate buffer pH 7.5 (see section 2.2.25 and 2.2.23) (Table 6). A kinase assay was performed using the CDK1/cdc2 kinase assay kit from Upstate. After a 10 minute incubation at 30°C, 12.5 µl of 5x GSB was added and the sample incubated at 95°C for 10 minutes, vortexed, spun briefly, loaded to a 10% Bis-Tris gel (Invitrogen) and run in 1x MOPS buffer (see section 2.2.15). Following SDS-PAGE, the gel was fixed by rocking for at least 1 hour in fixing solution (40% methanol, 10% glacial acid (acetic acid)) and then dried onto filter paper (Whatman) for 45 minutes. The dried gel was then exposed to a phosphor screen for various times depending on the intensity of the radioactivity to visualise phosphorylated Histone H1. The phosphor screen was scanned by a Storm 860 scanner and analysed using ImageQuant 5.1 software (Amersham Biosciences). The remaining sample was analysed by SDS-PAGE and the amount of CDK1 immunoprecipitated was determined by immunoblotting (see section 2.2.15 and 2.2.16).

Sample	Recombinant CyclinB1/ CDK1	Histone H1	RGC-32	Phosphate Buffer (20 mM)	ATP/ ^{32}P Mg	ADBI	Inhibitor
no CDK1 control	-	10 µl	-	5 µl	10 µl	5 µl (1:10) +10µl	10 µl
no protein control	5 µl (2 units)	10 µl	-	5 µl	10 µl	10 µl	10 µl
0.8 µM	5 µl (2 units)	10 µl	5 µl	-	10 µl	10 µl	10 µl
1.7 µM	5 µl (2 units)	10 µl	5 µl	-	10 µl	10 µl	10 µl
3.3 µM	5 µl (2 units)	10 µl	5 µl	-	10 µl	10 µl	10 µl
5.0 µM	5 µl (2 units)	10 µl	5 µl	-	10 µl	10 µl	10 µl

Table 6 – showing an overview of what each sample contained.

2.2.23 Kinase Assay (*in vivo*)

Immunoprecipitation prior to the kinase assay was carried out following the protocol previously described (see section 2.2.20). Cell pellets were lysed in 1 ml lysis buffer (Jin et al., 2005) per 2x10^7 cells instead of EBC buffer and 2 µg rabbit anti-cyclin B1 or rabbit-IgG antibody were used. The following day the beads were washed 3x in 0.5 ml lysis buffer (Jin et al., 2005) containing 0.03% SDS. After each wash step the samples was spun briefly and the supernatant removed. Then the beads were washed 2x with ADBI buffer, spun briefly and the supernatant removed. The CDK1 Kinase Assay was performed following the manufacturer's instructions (Upstate). The beads were then incubated at 30°C in a waterbath for 10 minutes. 10 µl of 5x GSB was added and samples analysed as described above (see section 2.2.22).

2.2.24 Gelshift assays

2.2.24.1 Preparing labelled double-strand DNA probes

Oligonucleotides (Invitrogen) were labelled by mixing 1 µl of sense oligonucleotide (100ng/µl; forward) with 5 µl 5x forward reaction PNK buffer (Invitrogen), 4 µl ^{32}P γ-ATP (Perkin-Elmer) and 1 µl T4 Polynucleotide Kinase (PNK) (Invitrogen) in a total

volume of 25 µl. The samples were then incubated at 37°C for 30 minutes. The kinase was then inactivated by heating the samples to 65°C for 20 minutes. After this incubation 2 µl (200 ng) of complementary oligonucleotide (anti-sense) (100 ng/ µl) was added to create a double-stranded probe. The samples were heated to 95°C for 3 minutes to denature the DNA and slowly annealed by moving the heat block containing the samples to room temperature. This slow cooling ensures in accurate hybridisation of the oligonucleotides. 80 µl of TE pH 7.5 was added to dilute the sample and unincorporated ^{32}P γ-ATP was removed by spinning through a SPIN-X® column (Costar) containing 500 µl of a 50% PBS/Sephadex® G-50 (Sigma) slurry.

Name	Number	Sequence (5'-3')
Cp RBP-J kappa	MW 54	AAA CAC GCC **GTG GGA AA**A AAT
Cp RBP-J kappa mut	MW 115	AAA CAC GCC **GTG GCT AA**A AAT
RGC32p RBP-J kappa	MW 123	CCC AGC ACT **TTG GGA G**GC TGA
RGC32p RBP-J kappa mut	MW 121	CCC AGC ACT **TTG GCT G**GC TGA

Table 7 – Oligonucleotides used gel shift. Only the forward oligonucleotides are shown. RBP-J kappa sites are shown in bold, mutations of the sequence is highlighted in red.

2.2.24.2 Preparation of double-strand unlabelled competitor DNA

12.5 µl (1 µg/µl) of each of the complementary oligonucleotides were mixed with 25 µl TE, heated at 95°C for 3 minutes and then left to cool to room temperature in the heating block (see above). 200 µl of TE pH 7.5 was added to dilute the sample.

2.2.24.3 Preparation of the gel shift sample

For each sample 0.5 µl water, 1 µl probe (2 ng), 5 µl of gel binding buffer, 0.5 µl DTT was mixed with TE (negative control) or 3 µl GST-RBP-J kappa protein in the presence or absence of 3 µl competitor. The samples were left at room temperature for 30 minutes. 2.5 µl 4x TBE loading buffer was then added and the entire sample was loaded onto a 6% TBE gel. The gel was run at 100 V for 55 minutes in 0.5x TBE buffer, then fixed in fixing solution for 1 hour, dried onto filter paper for 45 minutes and then exposed to a phosphor screen.

2.2.25 RGC-32 protein preparation

The E. coli strain BL21 pLYS was transformed with pET-RGC-32 (by Helen Webb). The bacteria were streaked out on a plate containing 100 µg/ml ampicilin and 42 µg/ml chloramphenicol and grown overnight at 37°C. 50 ml of LB containing both antibiotics were inoculated with a single colony and grown overnight at 37°C. 4 ml of the growing culture were added to 5x flasks containing 400 ml LB. When the OD at 600 nm reached 0.5, RGC-32 expression was induced by adding 1 mM of IPTG for 4 hours at 37°C. The cells were then pelleted at 8000 rpm at 4°C for 10 minutes. The pellets were resuspended in a total volume of 80 ml cold Buffer A. To lyse the cells, the bacteria were frozen in dry ice and defrosted 3 times. 10 µg/ml DNase I was added, swirled at room temperature for 15 minutes and cooled on ice for 15 minutes. The lysates were then sonicated 6x 10 sec with 10 sec gaps using the Sonics Vibra Cell. Cell lysates were centrifuged at 9800 rpm at 4°C for 20 minutes using a JA-20 rotor (Beckman) in a Beckman Coulter Avanti J-20 XP centrifuge and resuspended in 20 ml buffer X. After repeating this step, the cells were resuspended in 20 ml buffer Y. A 1:1 slurry of HIS-Select® Nickel Affinity Gel (Sigma) was added to the supernatant and samples rotated for 90 minutes at 4°C. Beads were washed twice with 25 ml buffer A, twice with 25 ml buffer B, twice with 25 ml buffer C and twice with 25 ml buffer A. One sample was kept for anti-RGC-32 antibody purification. For all other samples the protein was eluted by adding 3x 1 ml elution buffer.

2.2.26 Dialysis

RGC-32 protein from the RGC-32 protein preparation (see section 2.2.25) was dialysed against 20 mM PO_4 buffer using a Slide-A-Lyzer® Dialysis Cassette (Thermo Scientific) and following manufacturer's instructions.

2.2.27 Antibody purification

2.2.27.1 HIS-Select® Nickel Affinity Gel

500 µl of HIS-Select® Nickel Affinity Gel (Sigma) containing RGC-32 protein from RGC-32 protein preparation (see section 2.2.25) was transferred into a 1.5 ml tube, centrifuged at 4000 rpm for 1 minute at 4°C and the supernatant discarded. The beads were washed twice by adding 500 µl PBS. The beads were gently mixed, spun down and the supernatant removed and again 500 µl of PBS added. 80 µl of DMSO was

added to an ampoule of disuccinimidyl suberate (DSS, Piercenet) and the sample vortexed for 5-10 minutes to dissolve the powder. 75 µl of DSS/DMSO was added to beads containing the RGC-32 protein and incubated at room temperature for 1 hour at 4°C with rotation. The beads were briefly centrifuged and washed 4x with 500 µl of 10 mM glycine pH1. A Bradford assay was carried out to ensure that no protein was eluted with the glycine. The beads were washed twice with 500 µl of PBS, and then 3 ml of rabbit 2818 serum (final bleed) were added and incubated for 1 hour at 4°C with rotation. Following the incubation the beads were washed 4x with 10 ml PBS followed by one wash in 1:10 diluted PBS. A sample of the supernatant was taken before the first wash and kept as flow-through. To elute the antibody, the beads were washed 4x with 500 µl of 10 mM glycine pH1 by rotating for 5 minutes and keeping the supernatant. For each sample the pH and the protein content was measured. 100 µl of 1 M Tris pH 8.5 was added to increase the pH to 7.5 and to stabilise the antibody.

2.2.27.2 CH sepharose column

300 mg CH sepharose was swollen in 25 ml of 1 mM ice cold HCl to activate the resin. After a 15 minutes incubation on ice, the beads were spun down and washed twice in 25 ml 0.1 M $NaHCO_3$ pH 8 mixed with 0.5 M NaCl, vortexed, centrifuged and the supernatant discarded. The supernatant was then adjusted to obtain a 1:1 resin. 3 mg of RGC-32 protein was added to the beads and incubated at room temperature for 1 hour with rotation. After the incubation the beads were centrifuged and a 10 µl aliquot was taken to compare the protein content to the original concentration. 200 µl of 50 mM glycine pH 8 was added to the beads and incubated at room temperature for 1 hour with rotation. The beads were then washed with 25 ml of 20 mM glycine pH 8 mixed with 0.5 M NaCl and washed twice with 25 ml 10 mM glycine pH1 mixed with 0.5 M NaCl. A Bradford assay was carried out to ensure that no protein was eluted.

2 ml of rabbit 2818 serum (final bleed) was added to the resin and incubated at 4°C for 1 hour with rotation. The beads were washed 4x with 25 ml of PBS and once with 1:10 diluted PBS. An aliquot was taken before the first wash and used as flow-through. To elute the antibody, the beads were washed 4x with 500 µl of 10 mM glycine pH 1 by rotating for 5 minutes and keeping the supernatant. For each sample the pH and the protein content was measured. 100 µl of 1 M Tris pH 8.5 was added to increase the pH to 7.5 and to stabilise the antibody.

2.2.27.3 Montage® Prosep-A® Kit

10 ml of rabbit serum 2818 (final bleed) was applied to a Montage® Kit Prosep-A® column (Millipore). The anti-RGC-32 serum was purified according to manufacturer's instructions.

2.2.28 Bradford Assay

10 µl of all 0.5 ml samples obtained from the RGC-32 protein or anti-RGC-32 antibody purification were added to 200 µl of a 1:5 dilution of Bradford reagent (Fisher). The colour change of the assay reagent was monitored by measuring the absorbance at 595 nm using an Anthos reader 2001 plate reader.

3 The effects of RGC-32 upregulation on the cell cycle

3.1 Introduction

The EBV protein EBNA 3C is essential for B cell transformation and disrupts numerous cell cycle checkpoints (reviewed in (West, 2006)). Many cell cycle pathways have been suggested as EBNA 3C targets, but the entire mechanism by which EBNA 3C deregulates the cell cycle has not been fully elucidated. Previous microarray studies in the West lab revealed that the expression of the novel cell cycle regulator RGC-32 is upregulated in the EBNA 3C-positive BJAB cell line E3C-3 compared to the EBNA 3C-negative cell line pZ2 (for cell lines see (Wang et al., 1990a)). Real-time PCR follow-up studies detected RGC-32 mRNA upregulation of up to 14-fold in additional EBNA 3C-expressing BJAB cell lines implicating RGC-32 as a downstream target of EBNA 3C (Figure 13A, Helen Webb). Additional experiments also detected RGC-32 upregulation on stable expression of EBNA 3C in the EBV-positive Burkitt's lymphoma cell line, Akata (Figure 13B, Helen Webb) (for cell lines see review (West, 2006)). Response Gene to Complement 32 (RGC-32) was originally identified as a gene activated by the sublytic complement complex C5b-9 (Badea et al., 1998). RGC-32 protein was shown to play a role in cell cycle progression into S and M phase and was demonstrated to bind and activate the key mitotic kinase, CDK1 (Badea et al., 2002). The activation of CDK1 is essential to promote transition into mitosis and its activation is prevented when the G2/M checkpoint is triggered. The upregulation of RGC-32 in EBNA 3C-expressing cells may therefore contribute to cell cycle checkpoint disruption by EBNA 3C by promoting activation of CDK1. This chapter aims to investigate the effects of RGC-32 on the cell cycle and its potential role as a downstream target of EBNA 3C.

3.2 EBNA 3C-expressing BJAB cell lines overcome the G2/M checkpoint

EBNA 3C has been shown to disrupt the G2/M checkpoint in response to a variety of agents when expressed in the EBV-negative Burkitt's lymphoma cell line DG75 (Krauer et al., 2004b). To confirm that EBNA 3C also disrupted this checkpoint in the BJAB cells stably expressing EBNA 3C and increased levels of RGC-32, EBNA 3C-negative BJAB cells were exposed to different concentrations of etoposide. Etoposide is

(A)

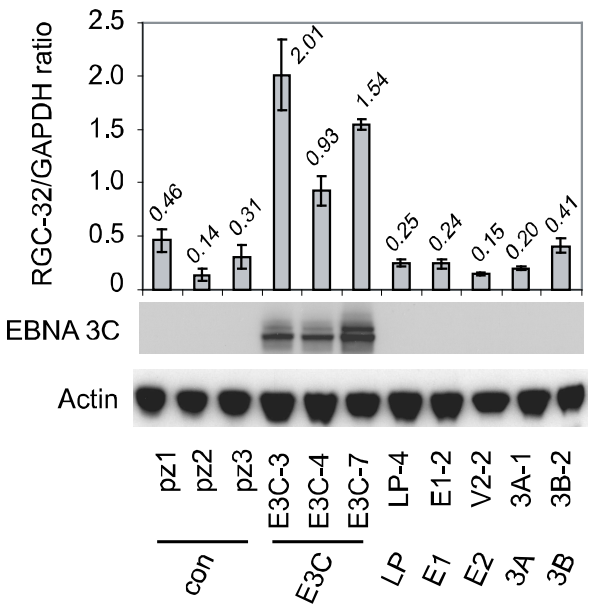

(B)

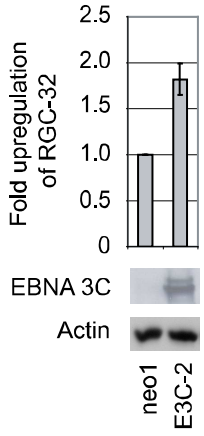

Figure 13 - (A) Real-time PCR of BJAB cells stably expressing the EBNAs showing the ratio of RGC-32/GAPDH mRNA levels. EBNA 3C expression was detected by western blotting (lower panel). **(B)** Real-time PCR of the control Akata stable cell-line, neo1, and the Akata E3C-2 cell-line stably expressing EBNA 3C showing the ratio of RGC-32/GAPDH mRNA levels relative to neo1. Results represent the mean +/- standard deviation for 3 independent dilutions of cDNA. Experiments were carried out by Helen Webb and Michelle West.

a topoisomerase II inhibitor which activates the G2/M checkpoint by causing DNA double strand breaks resulting in G2 arrest. PI staining and FACS analysis was carried out to visualise the cell cycle distribution of the EBNA 3C-positive BJAB cell line E3C-3 and the EBNA 3C-negative cell line pZ3 after treatment with 100 and 300 nM of etoposide for 24 hours. The representative FACS profile in Figure 14A shows that pZ3 cells clearly accumulate in G2/M after treatment with 300 nM etoposide indicative of G2 arrest. A reduction was found in the G2/M population of E3C-3 cells relative to pZ3 cells indicating that cell cycle arrest is reduced in the EBNA 3C-expressing cell line despite DNA damage. Significantly, a 4.6-fold increase in the percentage of cells in G0/G1 was also observed following treatment with 300 nM etoposide indicating that a significant proportion of cells overcome the G2/M checkpoint and continue progression through the cell cycle into G1 (Figure 14A).

To further confirm this observation, two more BJAB cell lines, the EBNA 3C-negative cell line pZ1 and the EBNA 3C-positive cell line E3C-7, were treated with 300 nM and 500 nM etoposide. Consistent with the previous observation, FACS analysis revealed that the G2/M population of E3C-7 cells was reduced by approximately 11% compared to pZ1 cells and the G0/G1 population of the E3C-7 cells was increased by more than 2-fold in the presence of etoposide (Figure 14B). These data indicate that a significant proportion of E3C-7 cells are able to overcome cell cycle arrest.

Results of three independent experiments demonstrated that the cell population in G0/G1 increased by an average of 3.5-fold and 2.3-fold in E3C-3 cells treated with 300 nM and 500 nM etoposide respectively, compared to control pZ3 cells (Figure 15A+B). A similar observation can be made for E3C-7 cells which showed an increase of the G0/G1 population of more than 2-fold relative to pZ3 cells (Figure 15A+B).

To determine whether the increase in the number of cells in G0/G1 in E3C-3 cells compared to pZ3 cells after DNA damage was due to transit through the checkpoint rather than slower growth of these cells, S phase cells were pulse-labelled with BrdU prior to etoposide treatment. Only 2.6% BrdU-positive pZ3 cells were observed in G0/G1 after etoposide treatment for 24 h (Figure 16A). However, 12.3% of the EBNA

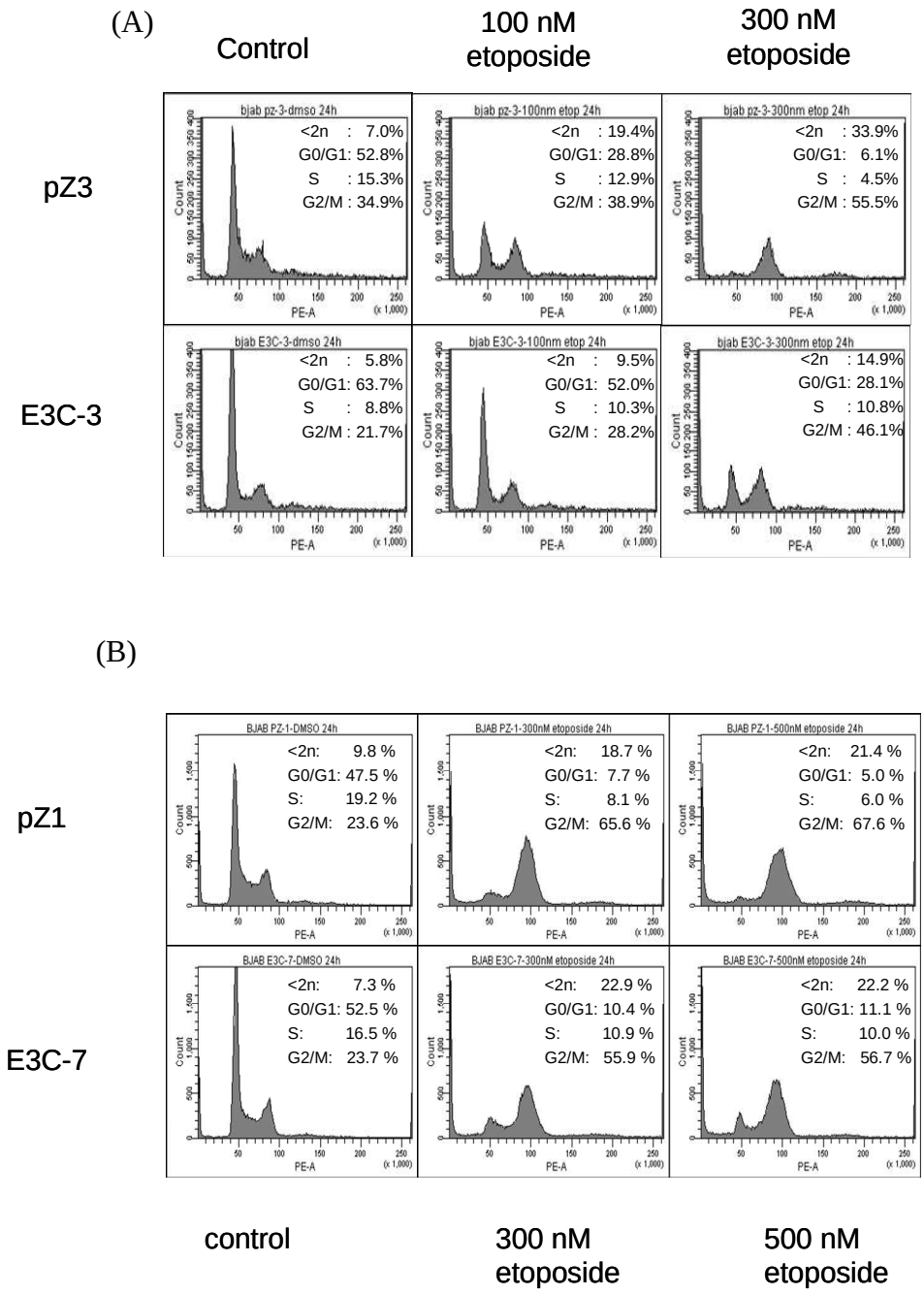

Figure 14 – Representative FACS profiles after DNA damage showing untreated (Control) and cells exposed to etoposide harvested after 24 h. Cells were stained with propidium iodide to visualise cell cycle distribution and gated into the cell cycle populations by their DNA content (PE-A). Numbers represent the percentage cell population in <2n (apoptotic cells), G0/G1, S or G2/M phase. **(A)** shows BJAB cell lines pZ3 and E3C-3 after exposure to 100 nM & 300 nM etoposide. **(B)** shows BJAB cell lines pZ1 and E3C-7 after exposure to 300 nM and 500 nM etoposide.

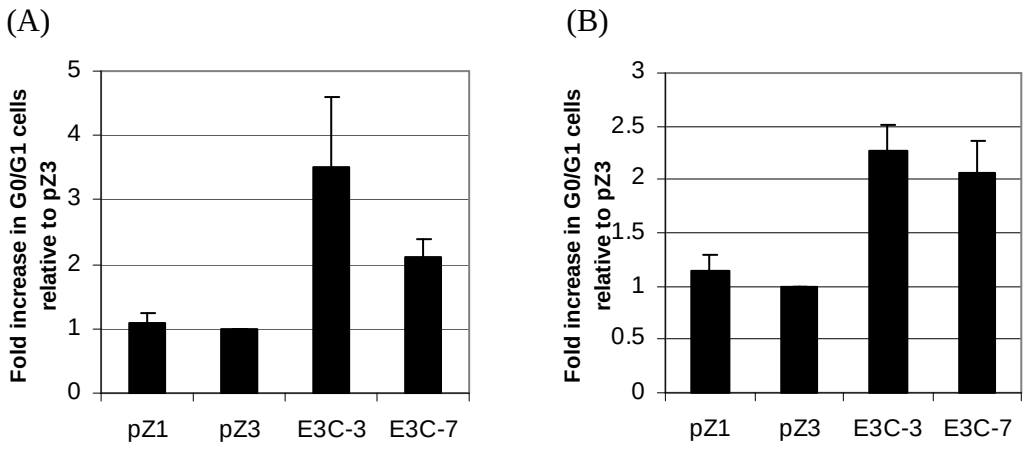

Figure 15 - Fold increase of BJAB control and EBNA 3C-positive cells in G1 phase relative to BJAB pZ3 control cells **(A)** after 24 h exposure to 300 nM etoposide and **(B)** after 24 h exposure to 500 nM etoposide. Results represent the mean of 3 independent experiments +/- standard deviation.

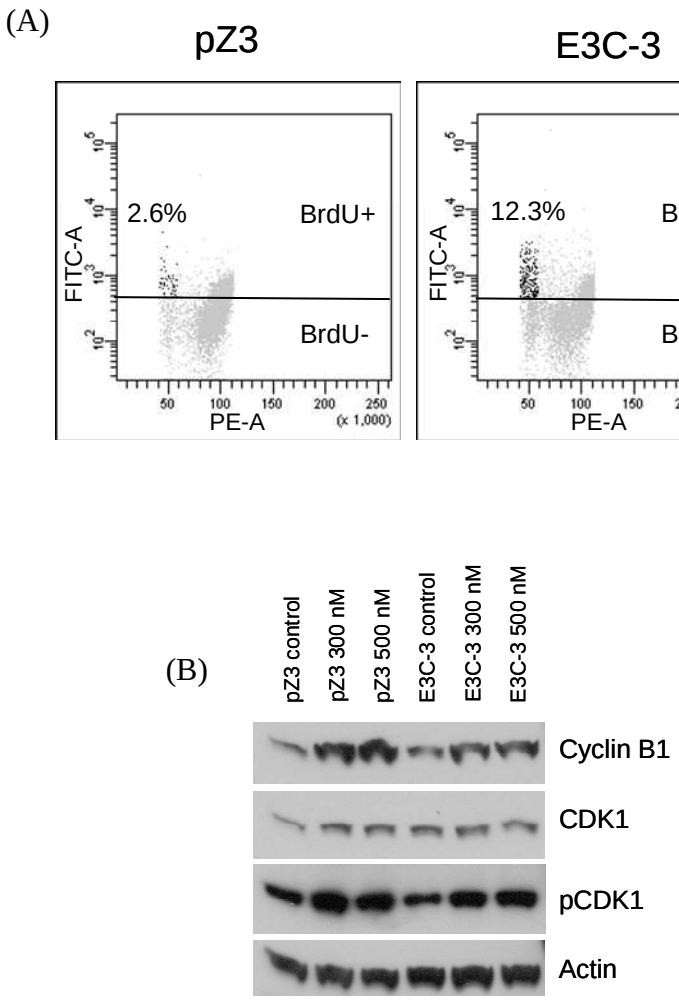

Figure 16 - (A) Representative FACS profile showing the cell cycle distribution of BrdU-positive pZ3 and E3C-3 cells following treatment with 500 nM etoposide for 24 hours. Numbers indicate the percentage of gated BrdU-positive cells in G0/G1. The PE-A channel was used to visualise PI-stained DNA content and the FITC-A channel was used to gate for FITC-positive (BrdU-positive) cells. **(B)** Western blot analysis of EBNA 3C-negative pZ3 and EBNA 3C-positive E3C-3 cell lysates following etoposide treatment for 24 hours. Whole cell lysates were separated using 10% NuPAGE Novex Bis-Tris gels in MOPS running buffer (Invitrogen). Nitrocellulose membranes containing the transferred proteins were probed with anti-Cyclin B1 (1:2000, Santa Cruz), anti-CDK1 antibody (1:1000, Invitrogen), anti-pCDK1 antibody (1:1000, Santa Cruz) which detects Tyrosine 15-phosphorylated CDK1 or anti-Actin antibody (1:5000, Sigma) as an internal control. Bands were visualised with ECL.

3C-positive E3C-3 cells in G0/G1 had incorporated BrdU which verifies the previous result that more EBNA 3C-positive BJAB cells were able to progress through the G2/M checkpoint despite DNA damage. Western blot analysis was carried out to investigate G2/M checkpoint regulation in EBNA 3C-expressing and control BJAB cells. Cyclin B1 is known to be highly expressed during G2 phase where it binds and activates CDK1 to promote cell cycle progression into mitosis. Soon after the transition into mitosis has occurred cyclin B1 is degraded. As expected, cyclin B1 levels are higher in the EBNA 3C-negative control cell line after etoposide treatment which indicates G2 arrest (Figure 16B). An accumulation of cyclin B1 can also be observed in the EBNA 3C-positive E3C-3 cells but the expression is reduced compared to the control cell line indicating reduced G2 arrest.

DNA double strand breaks lead to phosphorylation and degradation of the cdc25 phosphatases which activate CDK1 by dephosphorylation of threonine 14 and tyrosine 15 residues (Krek and Nigg, 1991). This dephosphorylation is required for mitotic progression. Tyrosine 15-phosporylated CDK1 levels were found to be increased in both BJAB cell lines but the accumulation is slightly reduced in EBNA 3C-expressing BJAB E3C-3 cells compared to the EBNA 3C-negative control cell line pZ3 after treatment with etoposide (Figure 16B). This experiment has been repeated twice with the same outcome. This result further indicates that a proportion of EBNA 3C-expressing BJAB cells continue to progress through the cell cycle after treatment with etoposide.

To confirm that EBNA 3C-positive BJAB cells showed disrupted G2/M checkpoint regulation in response to other treatments the cell lines pZ1, pZ3, E3C-3 and E3C-7 were exposed to gamma radiation. Consistent with the results obtained using etoposide, E3C-3 and E3C-7 cells showed a significant decrease in the number of cells in G2/M and an increase in the G0/G1 population. FACS analysis reported that only 5.3% of pZ3 cells could be found in G0/G1 24 h after treatment whereas E3C-3 cells showed 15.4% in G0/G1 (Figure 17A). Therefore, an average of a 2.2-fold higher population could be observed in G0/G1 phase in the EBNA 3C-positive cell line E3C-3 compared to the EBNA 3C-negative cell line pZ3 (Figure 17B). This result further verifies that EBNA 3C-expressing BJAB cells overcome the G2/M checkpoint despite DNA damage.

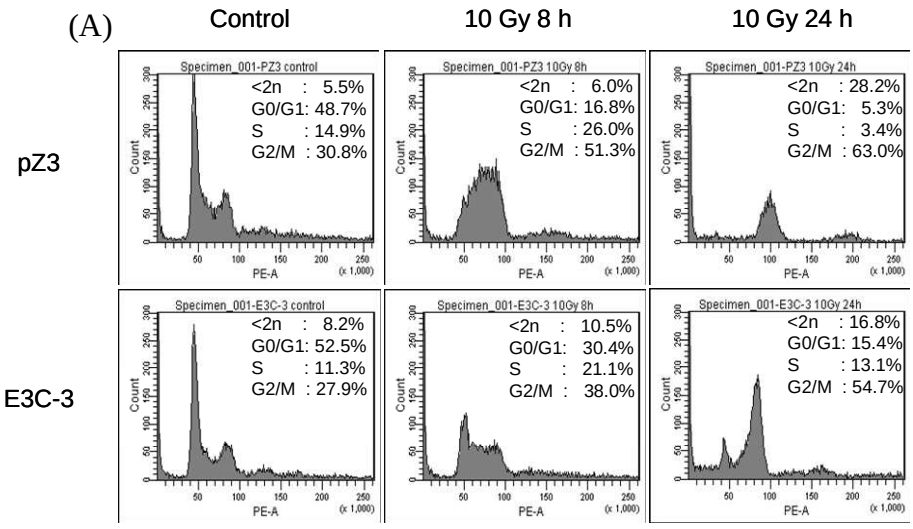

(B)

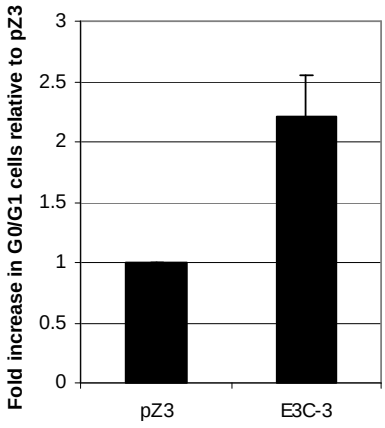

Figure 17 - (A) Representative FACS profiles of pZ3 and E3C-3 cells after DNA damage showing untreated (Control) and gamma irradiated cells (10 Gy) harvested after 8 and 24 h. Cells were stained with propidium iodide to visualise cell cycle distribution. **(B)** Fold increase of control and EBNA 3C-positive cells in G0/G1 phase relative to pZ3 cells 24 h after exposure to 10 Gy. This Figure shows the mean of 3 independent experiments +/- standard deviation.

Similar results could be observed in the BJAB cell lines pZ1 and E3C-7 after exposure to gamma radiation (Figure 18). pZ1 cells show a clear arrest in G2/M of 74.1% whereas only 33.3% of the E3C-7 cells arrested in G2/M. Interestingly, the G0/G1 population in the EBNA 3C-positive cell line is increased approximately 3-fold compared to the EBNA 3C-negative cell line indicating that more cells are able to overcome cell cycle control. It can also be observed that the apoptotic cell population is strongly increased in E3C-7 cells after gamma irradiation. This may further indicate that gamma irradiated cells were able to overcome the G2/M checkpoint but died after or during mitosis due to excessive DNA damage.

These results clearly demonstrate that EBNA 3C-positive BJAB cells can overcome the G2/M checkpoint in response to DNA damage. Since the EBNA 3C-positive cell lines E3C-3 and E3C-7 express higher RGC-32 mRNA levels than the EBNA 3C-negative cell lines pZ1 and pZ3 and RGC-32 is known to support cell cycle progression into mitosis, the higher RGC-32 expression might play an important role in the G2/M checkpoint disruption.

3.3 Investigating the effects of exogenous RGC-32-overexpression on the G2/M checkpoint

3.3.1 Introduction

To determine whether the observed disruption of cell cycle regulation in BJAB cells overexpressing EBNA 3C was due to higher RGC-32 expression, stable cell lines overexpressing FLAG-tagged RGC-32 were generated in the lab by Helen Webb. These cell lines were made using the Flp-in system (Invitrogen) by first generating FRT host cell lines in 2 different cell backgrounds: the EBV-negative cell lines, BJAB and DG75.

Exogenous expression of RGC-32 in both cell backgrounds led to G2/M checkpoint disruption in response to etoposide (Figure 19A+B, Helen Webb). BJAB FRT RGC-32 cells show a reduced proportion of cells in G2/M and an increased cell population in G0/G1 in response to etoposide. A representative experiment demonstrated that the cell population in G0/G1 increases by 31.3% and 54.1% in BJAB cells stably expressing FLAG RGC-32 compared to the control cell line after treatment with 150 and 200 nM etoposide respectively (Figure 19A).

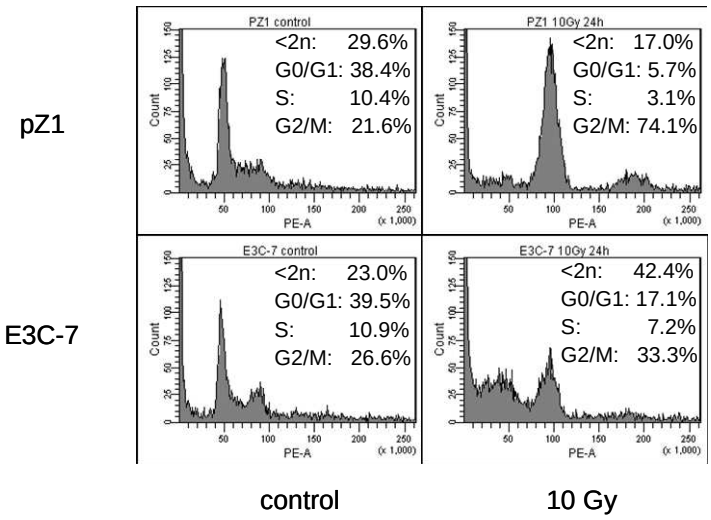

Figure 18 - Representative FACS profiles of pZ1 and E3C-7 cells after DNA damage showing untreated (Control) and gamma irradiated cells (10 Gy) harvested after 8 and 24 h. Cells were stained with propidium iodide to visualise cell cycle distribution.

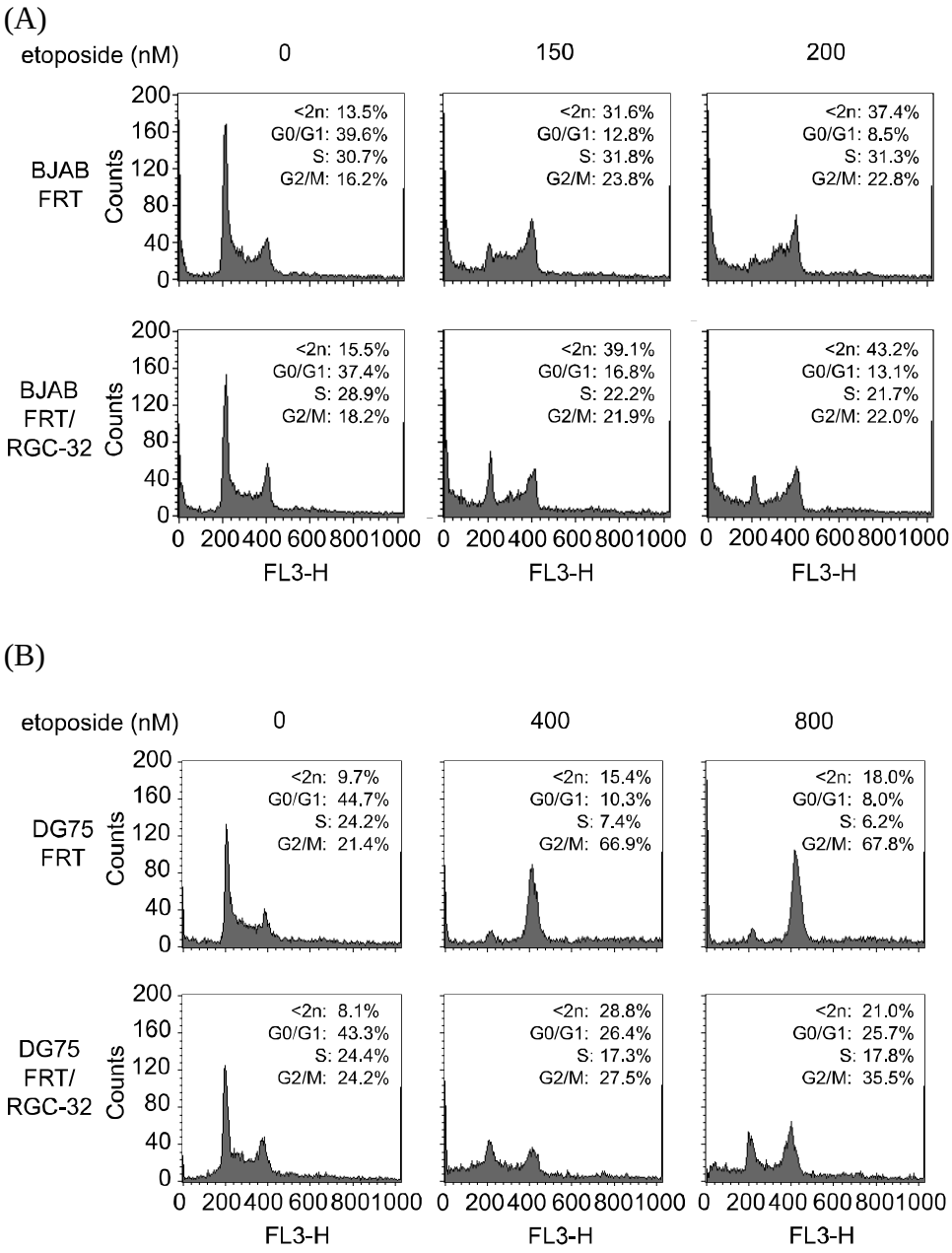

Figure 19 - Stable expression of FLAG-RGC-32 is sufficient to disrupt the G2/M checkpoint. **(A)** Representative cell cycle profile analysis of DG75 FRT control cells and DG75 FRT/FLAG RGC-32 cells treated for 24 hours with etoposide. Control cells (0) were harvested prior to etoposide treatment. **(B)** Representative cell cycle profile analysis of BJAB FRT control cells and BJAB FRT/FLAG-RGC-32 cells treated for 48 hours with etoposide.

DG75 cells stably overexpressing RGC-32 also showed an increase of cells in G0/G1 and reduced levels of cells in G2/M consistent with transition of cells through the checkpoint whereas DG75 FRT control cells accumulated in G2/M displaying G2 arrest (Figure 19B). A 2.6 and 3.2-fold increase in the proportion of cells in G0/G1 was observed in DG75 FRT/RGC-32 cells compared to control cells in the presence of 400 nM and 800 nM etoposide, respectively. RGC-32 expressing DG75 cells also displayed a decrease of 60% and 52% in the G2/M population at 400 and 800 nM etoposide respectively.

Clear differences were observed in the cell-cycle distribution of BJAB FRT/RGC-32 and DG75 FRT/RGC-32 cells compared to control FRT cells in response to etoposide, with increased numbers of cells in G0/G1 indicating increased passage of cells through the G2/M checkpoint.

3.3.2 Characterisation of stable RGC-32 expressing cell lines

When follow-up experiments were initiated using the previously established FRT cell lines it became apparent that the cell cycle disruption phenotype was reduced (Figure 20A). Results of three independent experiments demonstrated that the mean cell population in G0/G1 increases by 12, 13 and 14% in BJAB cells stably expressing FLAG RGC-32 compared to the control cell line after treatment with 50, 100 and 200 nM etoposide respectively (Figure 20B). This increase in the G0/G1 population was consistently observed throughout multiple etoposide experiments. The change in the phenotype could have resulted from continued passage in culture allowing the cells to compensate for RGC-32 overexpression by alteration of other cell cycle regulatory pathways. This hampered further experiments using these cell lines.

Attempts were made to make additional new stable cell lines overexpressing RGC-32 by transfecting the previously established BJAB FRT host cell line with the FRT FLAG-RGC-32 vector and pOG44 which mediates integration of the FRT vector expressing RGC-32 into the genome via Flp Recombination Target (FRT) site. The attempts to make new stable BJAB cell lines overexpressing RGC-32 were unsuccessful possibly due to overdilution during the early stages of selection.

(A)

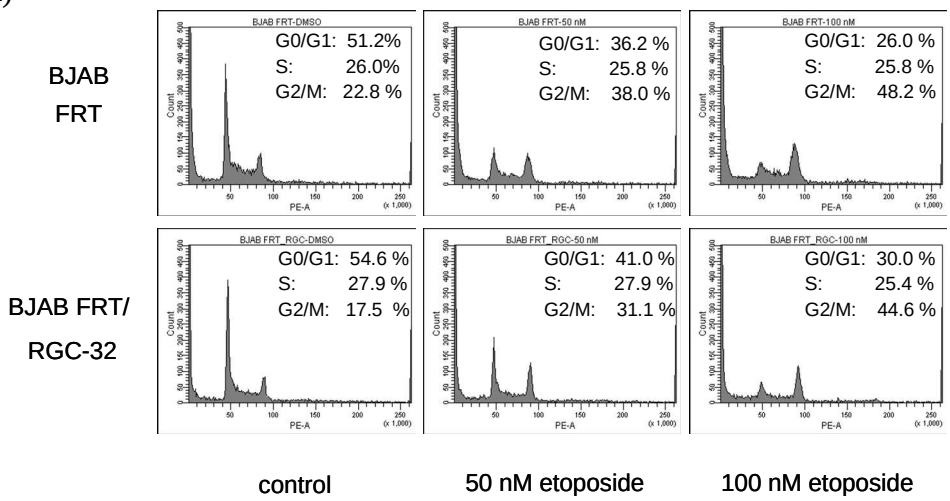

(B)

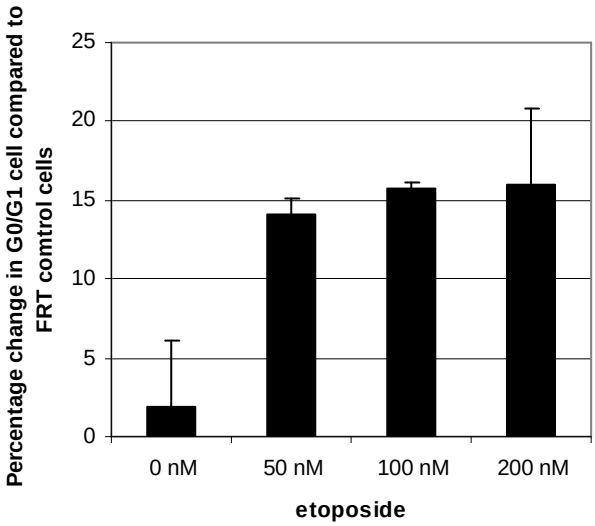

Figure 20 - (A) Representative FACS profiles of BJAB FRT and FRT/RGC-32 cells after DNA damage showing untreated (Control) and cells treated with 50 and 100 nM etoposide. Cells were harvested before and after 48 h of etoposide treatment. Cells were stained with propidium iodide to visualise cell cycle distribution. **(B)** Percentage change of G0/G1 cell population of BJAB FRT RGC-32 compared to the control cell line after 48 h of etoposide addition. This Figure shows the mean of 3 independent experiments +/- standard deviation.

3.3.3 The effects of transient RGC-32 overexpression

Experiments were carried out to investigate whether the effects of RGC-32 on the cell cycle could be assayed in transient transfection assays in B cells. Transient expression of RGC-32 has previously been shown to override serum-induced G1 arrest in aortic smooth muscle cells (Badea et al., 2002).

DG75 cells were transiently transfected with a FLAG-RGC-32-expressing construct using electroporation techniques (Figure 21A). Under the conditions used a transfection efficiency of approximately 33% was achieved (Figure 21B). Western blot analysis confirmed the overexpression of RGC-32 (Figure 21A). When transiently transfected cells were treated with etoposide to induce G2 arrest, we observed no detectable difference between control and RGC-32-expressing cells (Figure 22).

This result may indicate that transient RGC-32 overexpression might not be sufficient to disrupt the G2/M checkpoint since a transfection efficiency of only 33% was achieved (Figure 21B).

3.4 RGC-32 knockdown may cause partial G0/G1 arrest

To determine whether RGC-32 knock-down could resolve the G2/M checkpoint defect in BJAB cells overexpressing RGC-32, RNA interference experiments were carried out using small interfering RNA (siRNA)-expressing plasmids. BJAB E3C-3 cells were transiently transfected with 4 RGC-32-specific siRNA-expressing plasmids (siRNA1, 2, 4 or 5) or control scrambled siRNA-expressing plasmid. Transfection efficiencies of approximately 60% were achieved in these experiments using Amaxa nucleofection. The initial experiment showed that siRNA4 reduced RGC-32 mRNA by 5%, siRNA1 by 24%, siRNA5 by 50% and siRNA2 by 78% (Figure 23A). Since the best RGC-32 mRNA reduction was achieved by transfection with siRNA2, all further experiments were carried out using this siRNA. To investigate the effects of RGC-32 on cell cycle disruption, the cells were treated with 300 nM etoposide 24 hours after transfection with either the plasmid expressing siRNA2 or the scrambled (control) and harvested after a further 24 hours. To confirm that RGC-32 mRNA knockdown was successful, a sample of each experiment was analysed using real-time PCR (Figure 23B). The results showed

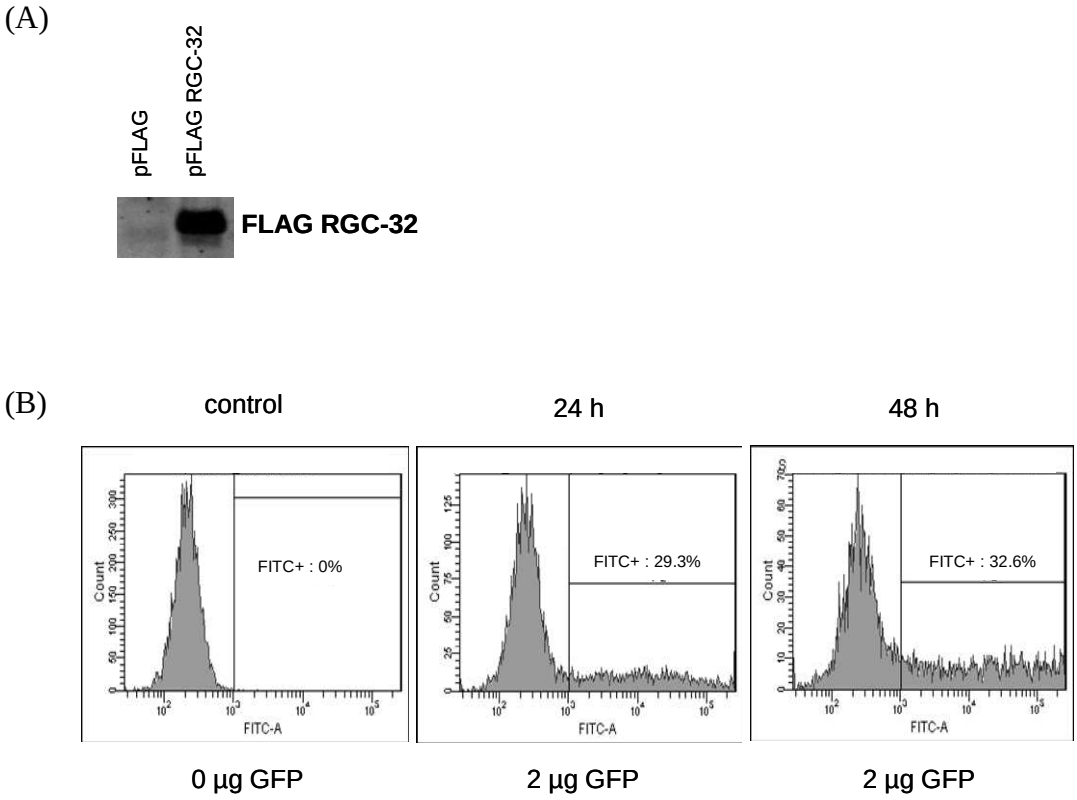

Figure 21 – DG75 cells were transiently transfected with 40 µg of pFLAG empty vector or pFLAG RGC-32. **(A)** DG75 cells were harvested 48 hours post transfection and whole cell lysates were separated using 10% NuPAGE Novex Bis-Tris gels in MES running buffer (Invitrogen). Nitrocellulose membranes containing the transferred proteins were probed with anti-RGC-32 serum 2818 (1:500). Bands were visualised with ECL. **(B)** Transfection efficiencies were determined in DG75 cells transiently transfected with 2 µg of empty FLAG vector (0 µg GFP control) or with 2 µg pmaxGFP® were harvested after 24 and 48 hours and the percentage GFP-positive cells determined by flow cytometry.

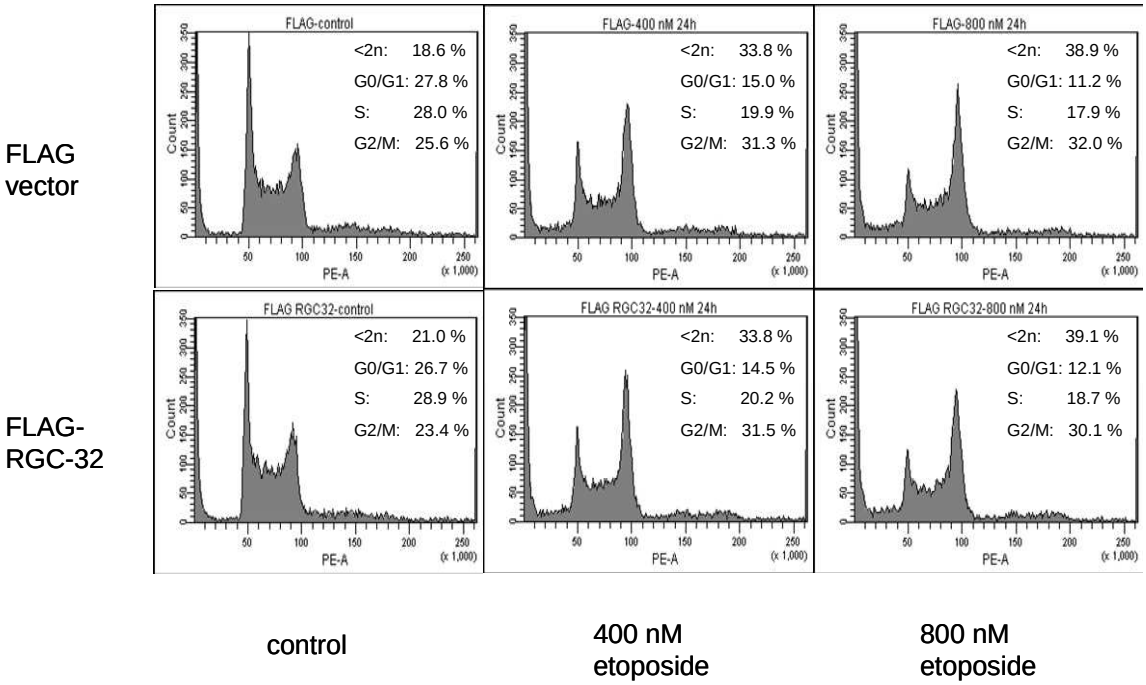

Figure 22 - DG75 cells were transiently transfected with 40 µg of pFLAG empty vector or pFLAG RGC-32. 24 hours post transfection DMSO, 400 or 800 nM etoposide were added. The cells were harvested 48 hours post transfection and cells were stained with propidium iodide to visualise cell cycle distribution.

(A)

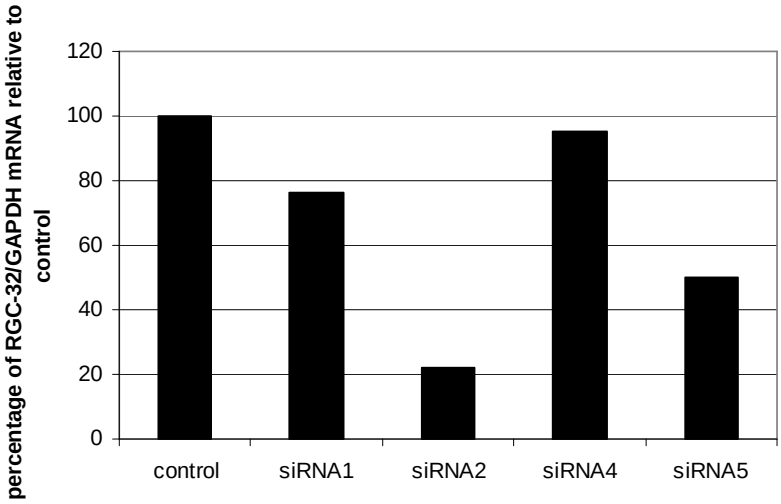

(B)

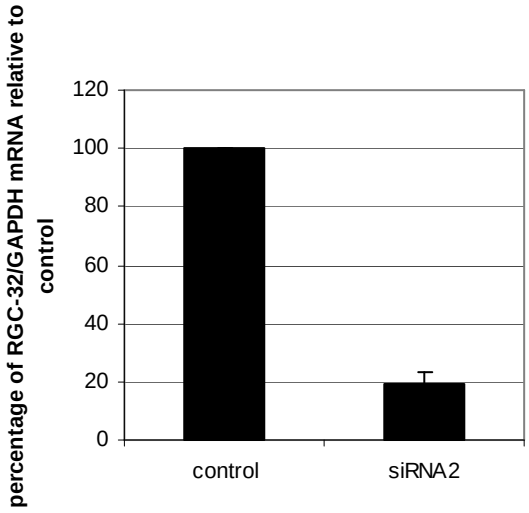

Figure 23 – Real-time PCR analysis of RGC-32 mRNA levels normalised to GAPDH expression in BJAB E3C-3 cells transfected with 2 µg plasmids expressing indicated siRNAs using Amaxa nucleofection. (A) Results show one representative experiment to determine the most efficient siRNA. (B) Results show mean expression ratios of 5 independent experiments +/- standard deviation.

that siRNA2 knocks RGC-32 down consistently by approximately 80% relative to the control.

Surprisingly, FACS analysis revealed that RGC-32 knock-down resulted in an increased cell population in G0/G1 (Figure 24A). The representative FACS profile showed that the G0/G1 population of the untreated E3C-3 cells transfected with plasmid expressing RGC-32 siRNA2 was increased (57%) compared to the scrambled control (51.3%). After treatment with etoposide the G0/G1 population of the E3C-3 cells transfected with plasmid expressing RGC-32 siRNA2 increased even more (27.7%) relative to the scrambled control (21%). Results from 3 independent experiments demonstrated that the G0/G1 population was increased and a corresponding decrease in the proportion of cells was found in S and G2/M. The G0/G1 population increased by an average of 10% when RGC-32 expression was silenced in the untreated cells and by 30% when RGC-32 expression was silenced and cells were treated with 300 nM etoposide (Figure 24B). These results indicated that knock-down of RGC-32 may cause a delay in progress through G1 or G1/S transition.

The FACS analysis of E3C-3 cells transfected with the plasmid expressing siRNA5 which only achieved a 50% knockdown of RGC-32 also showed an increased G0/G1 cell population. Interestingly, cells expressing siRNA5 show an intermediate increase in the G0/G1 population relative to cells transfected with the scrambled control or siRNA2 (Figure 25). However, a similar phenotype to siRNA2 can be seen in siRNA5-expressing cells after treatment with etoposide suggesting that the 50% RGC-32 knock down was sufficient to partly cause a G1 or G1/S delay (Figure 25).

Asynchronous B cell populations usually show a large percentage in G0/G1 when analysed by FACS. Since RGC-32 overexpression was shown to override the G1/S checkpoint as well as the G2/M checkpoint to promote S and M phase entry (Badea et al., 2002), it is possible that the RGC-32 knockdown causes G1 arrest or delayed progress into S phase. It was therefore impossible to study the function of RGC-32 at the G2/M checkpoint using this method. However, these results further support the model that RGC-32 expression promotes progression through the cell cycle.

(A)

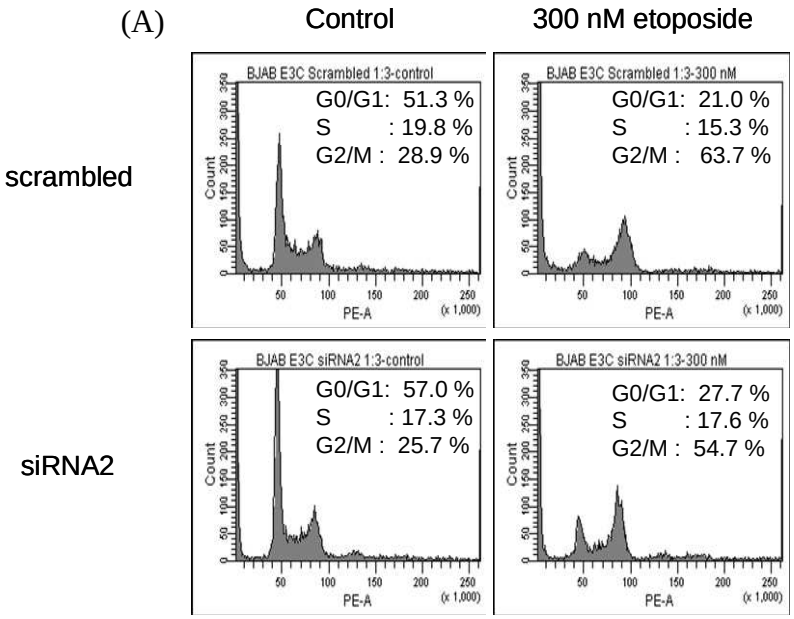

(B)

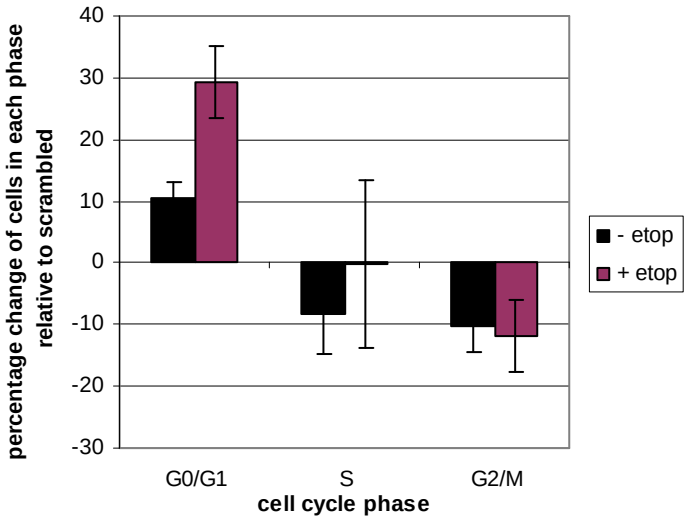

Figure 24 – (A) Representative FACS profiles of EBNA 3C-positive E3C-3 cells transfected with 2 µg of either the control siRNA scrambled or siRNA2-expressing plasmid. Cells were treated with DMSO (Control) or 300 nM etoposide and harvested after 24 h. Cells were stained with propidium iodide to visualise cell cycle distribution. **(B)** Percentage change of BJAB E3C-3 cells in each cell cycle phase relative to scrambled control cells after 24 h DMSO and after 24 h exposure to 300 nM etoposide. This Figure shows the mean of 3 independent experiments +/- standard deviation.

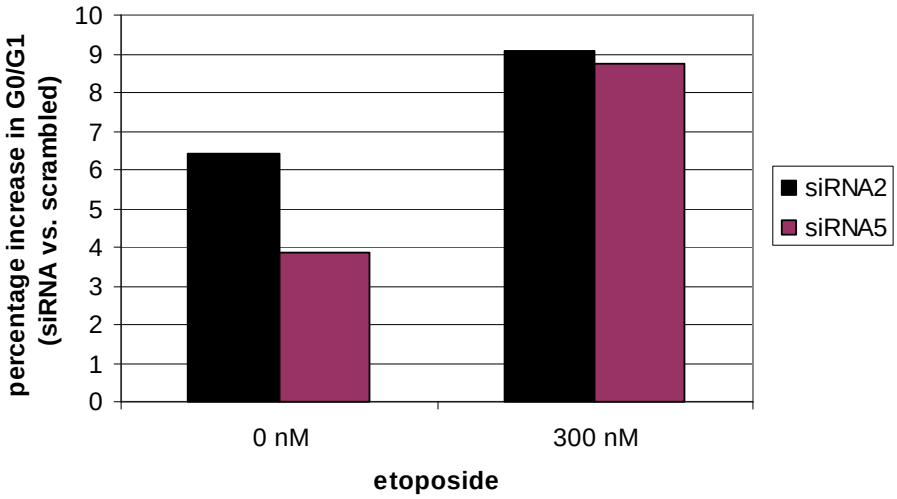

Figure 25 – G0/G1 population before and after treatment with 300 nM etoposide. Results from a representative experiment showing the percentage increase in the G0/G1 population of BJAB E3C-3 cells transiently transfected with plasmids expressing siRNA2 and 5 compared to the cells transfected with the scrambled control.

3.5 The effects of EBNA 3C-expressing Raji cells on the G2/M checkpoint

Raji cells are EBV-positive B lymphocytes expressing a latency III pattern. However, these cells have a natural deletion of more than 75% of the EBNA 3C gene (Hatfull et al., 1988). Raji cell lines stably expressing EBNA 3C were previously shown to upregulate LMP1 expression and to cause phenotypic changes of the cell membrane including expression of the cytoskeletal protein vimentin and CD23 (Allday et al., 1993). In initial real-time PCR experiments RGC-32 expression was found to be upregulated in the EBNA 3C-expressing Raji cell lines 11.2.1 (30-fold) and 11.5.8 (50-fold) compared to the control cell line 13.6 transfected with empty vector (gift from Prof Martin Allday) (Figure 26A). EBNA 3C expression was confirmed by Western blotting (Figure 26B).

When the Raji cell lines were exposed to 1 µM etoposide to activate the G2/M checkpoint, FACS analysis revealed that the EBNA 3C-negative Raji 13.6 cells arrested in G2/M whereas the EBNA 3C-expressing Raji cell lines show a reduction of cell cycle arrest (Figure 27A). To further confirm this result, the Raji cell lines were exposed to gamma radiation. Raji 13.6 cells arrested in G2/M after gamma irradiation but a reduced population of G2-arrested cells could be observed for the EBNA 3C-expressing Raji cell lines (Figure 27B).

However, different patterns of non-specific background bands observed in Western blots carried out on Raji 13.6 cells led us to investigate their origin. When the protein expression of EBNA 1 and EBNA 2 expression was examined, we found that the 13.6 cell lines did not express either protein unlike all other Raji clones used in these experiments (Figure 28). These results indicated that the Raji 13.6 cell line we received was likely not to be EBV- positive and was therefore not a Raji cell-derived line. A further control cell line 13.6.4 was obtained described as a subclone of 13.6. The Raji cell line 11.2.5 also served as a EBNA 3C-negative control although the cells were transfected with the EBNA 3C-expressing plasmid like 11.2.1 and 11.5.8 they were subsequently found to be EBNA 3C-negative (Allday et al., 1993). These additional cell lines were found to express EBNA 1 and EBNA 2, but not EBNA 3C, in line with their Raji origin (Figure 29A). Surprisingly, these cell lines did not arrest at similar

(A)

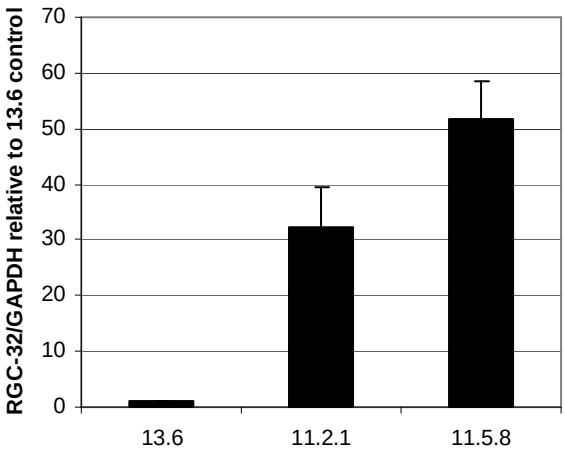

(B)

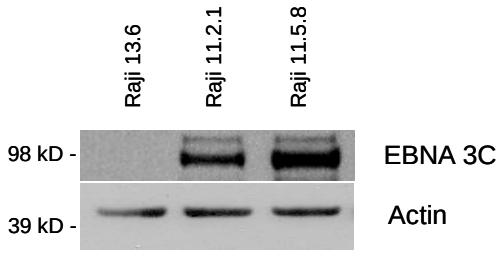

Figure 26 - (A) Real-time PCR analysis of Raji cell lines 13.6, 11.2.1 and 11.5.8. The graph shows RGC-32 mRNA levels divided by GAPDH mRNA levels relative to the EBNA 3C-negative control Raji 13.6. Error bars represent the results of 3 independent experiments. **(B)** Western blot analysis. Cell lysates of Raji cell lines 13.6, 11.2.1 and 11.5.8 were separated in a 10% NuPAGE Novex Bis-Tris gel in MES running buffer (Invitrogen). Nitrocellulose membranes containing the transferred proteins were probed with anti-EBNA 3C antibody (1:300) or anti-Actin antibody (1:5000, Sigma) as an internal control. Bands were visualised with ECL.

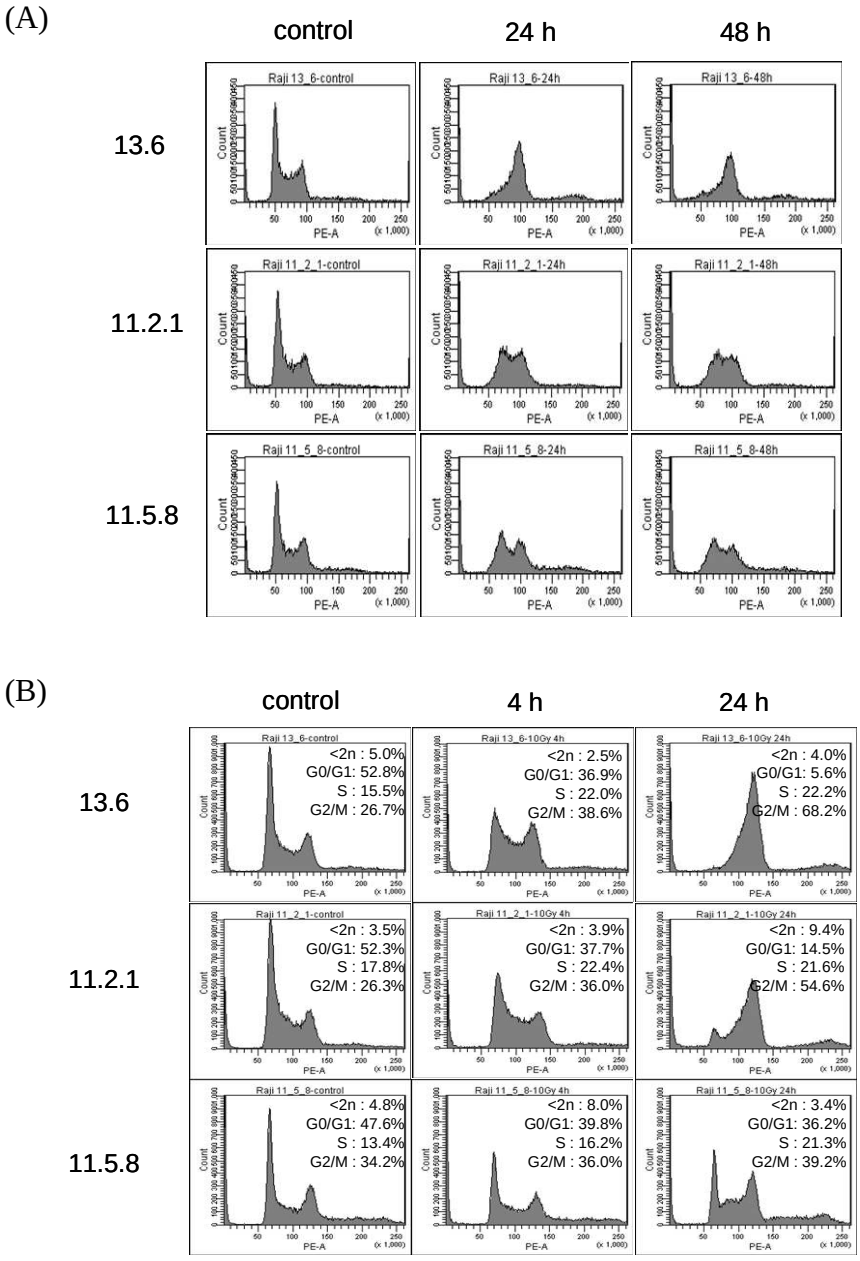

Figure 27 – FACS profile of Raji cell lines. Raji cell lines stably expressing EBNA 3C (11.2.1 and 11.5.8) and control Raji cell line (13.6) were exposed to **(A)** 1 µM etoposide for 24 and 48 hours or **(B)** 10 Gy and harvested after 4 and 24 hours. Cells were stained with propidium iodide to visualise cell cycle distribution.

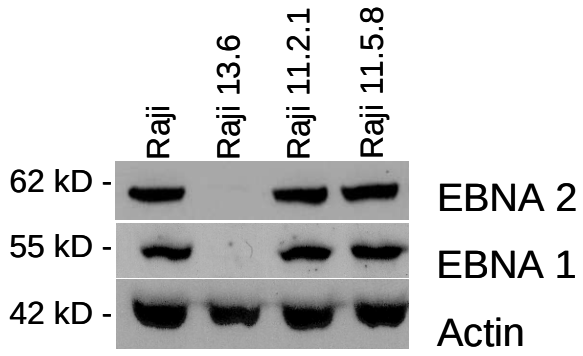

Figure 28 – Western blot analysis. Proteins of cell lysates of all Raji cell lines were separated in a 12% NuPAGE Novex Bis-Tris gel in MOPS running buffer (Invitrogen). Nitrocellulose membranes containing the transferred proteins were probed with M. Stacey serum (1:200), anti-EBNA2 antibody (1:300) or anti-actin antibody (1:5000, Sigma) as an internal control. Bands were visualised with ECL.

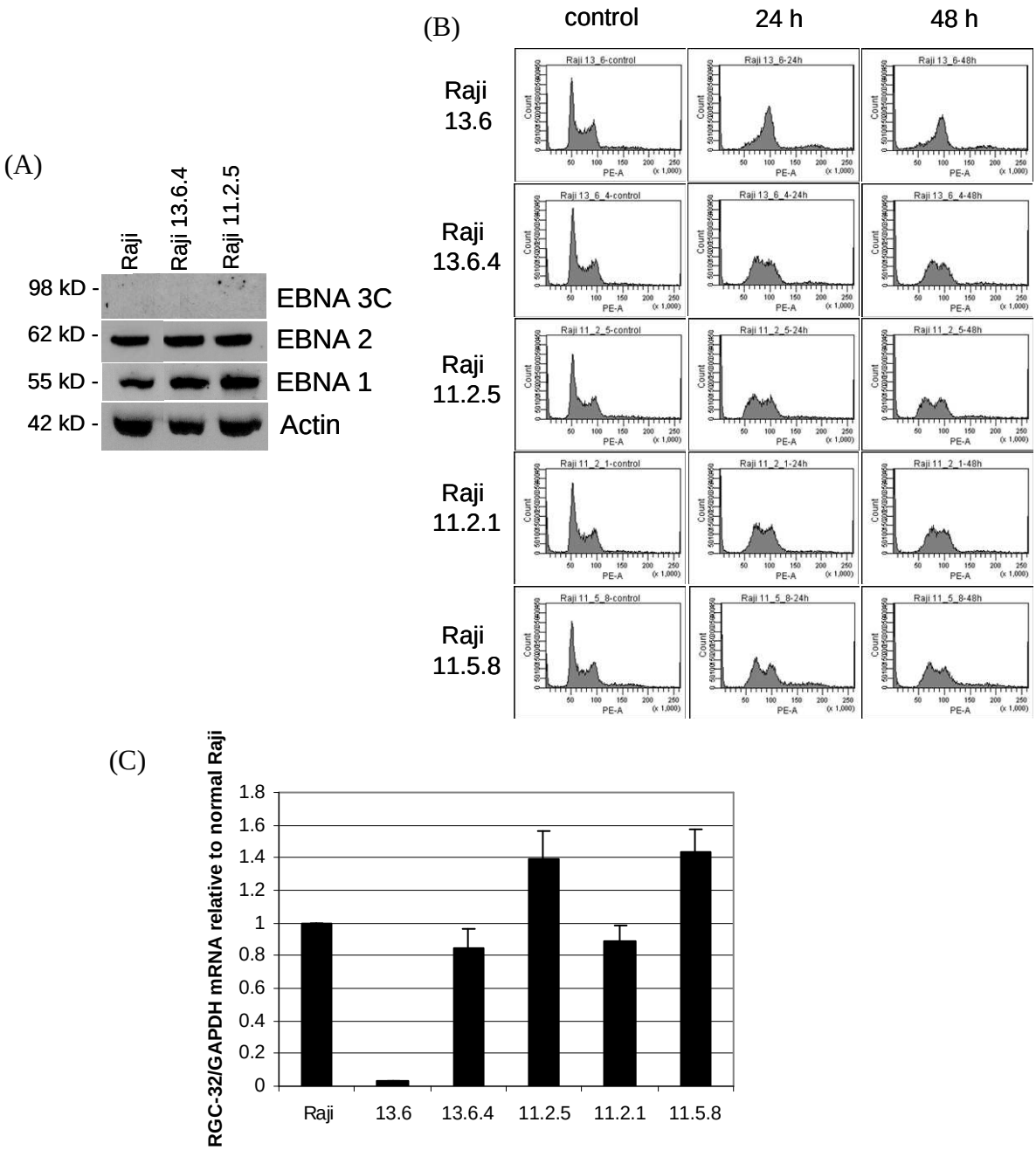

Figure 29 – (A) Western blot analysis. Proteins of cell lysates of all Raji cell lines were separated in a 12% NuPAGE Novex Bis-Tris gel in MOPS running buffer (Invitrogen). Nitrocellulose membranes containing the transferred proteins were probed with M. Stacey serum (1:200), anti-EBNA2 antibody (1:300) or anti-actin antibody (1:5000, Sigma) as an internal control. Bands were visualised with ECL. **(B)** FACS profile of Raji cell lines. Raji cell lines stably expressing EBNA 3C (11.2.1 and 11.5.8) and control Raji cell lines (13.6, 13.6.4 and 11.2.5) were exposed to 1 µM etoposide for 24 and 48 hours. Cells were stained with propidium iodide to visualise cell cycle distribution. **(C)** Real-time PCR analysis of Raji cell lines. The graph shows RGC-32 mRNA levels divided by GAPDH mRNA levels relative to normal Raji mRNA. Error bars represent the results of 3 independent experiments.

concentrations of etoposide used previously and displayed similar cell cycle arrest levels to EBNA 3C-expressing cells (Figure 29B). Moreover, RGC-32 levels were similar in this line to the EBNA 3C-expressing Raji cell lines (Figure 29C).

Taken together, the results indicate that EBNA 3C expression does not contribute to higher endogenous RGC-32 levels in Raji cells. This may be due to the fact that this cell line has adapted to immortalised cell growth without EBNA 3C expression due to deregulation of other genes involved in cell cycle control. Since the expression of EBNA 3C in Raji cells cannot overcome cell cycle regulation in response to DNA damaging agents, RGC-32 may be required for EBNA 3C-mediated disruption of cell cycle control.

3.6 RGC-32 can increase CDK1 activity *in vitro*

EBNA 3C-positive BJAB cells express higher RGC-32 mRNA levels and can disrupt cell cycle control of the G2/M checkpoint. RGC-32 was demonstrated to play a role in G2/M transition via binding to the cyclin B/CDK1 complex *in vitro* and increasing CDK1 activity in a manner dependent on the phosphorylation of threonine 91 in RGC-32 by CDK1 (Badea et al., 2002). RGC-32 also coimmunoprecipitates with CDK1 in smooth muscle cells. However, Saigusa *et al*. showed that transiently overexpressed Flag or Myc-tagged RGC-32 did not co-precipitate with exogenously expressed cyclin B1 in HEK 293-T cells and stated that RGC-32 was not phosphorylated by CDK1 in preliminary experiments (Saigusa et al., 2007). To verify whether RGC-32 can increase CDK1 activity, *in vitro* kinase assays were carried out using purified recombinant His-tagged-RGC-32 protein and recombinant CDK1/cyclin B1. CDK1 activity was determined by measuring the phosphorylation of Histone H1 by CDK1 using ^{32}P-labelled ATP. The result clearly showed that RCG-32 was able to increase CDK1 activity *in vitro* (Figure 30A, top panel). Western blot analysis confirmed the different levels of RGC-32 protein induced in the kinase assay (Figure 30A, bottom panel). Results of 3 independent experiments showed that CDK1 activity was enhanced by up to 11.6-fold with the highest RGC-32 protein concentration used (5 µM) (Figure 30B). These results confirm that CDK1 activation by RGC-32 could be a potential mechanism for the disruption of G2/M checkpoint regulation.

(A)

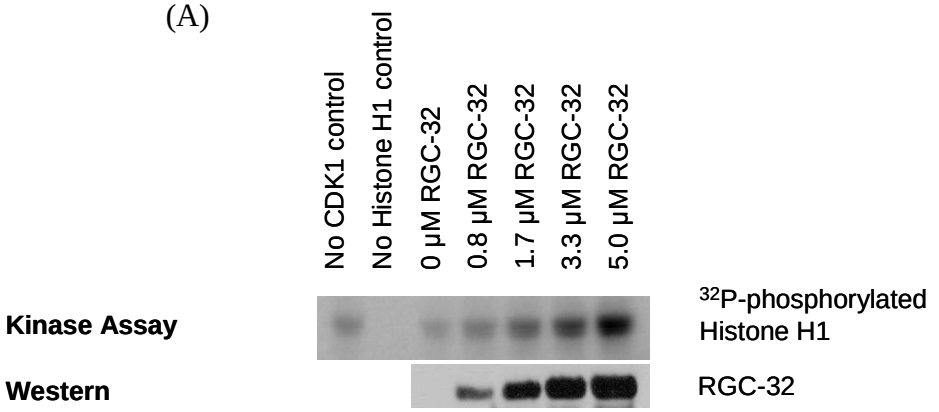

(B)

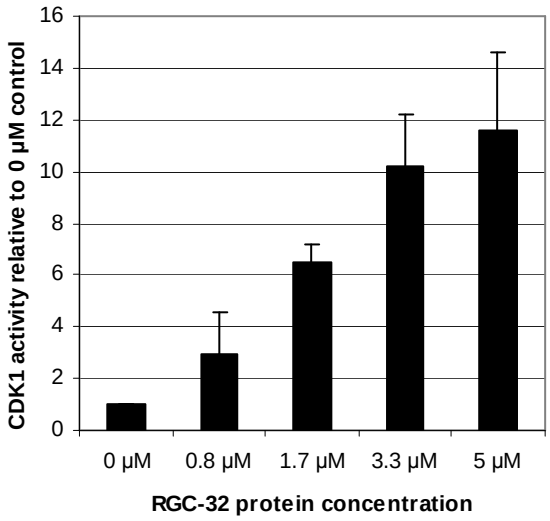

Figure 30 – Recombinant CDK1/Cyclin B1 was mixed with His-RGC-32 to a final concentration of 0.8, 1.7, 3.3 and 5 µM in the presence of γ-^{32}P ATP and histone H1. **(A)** Samples were separated in a 10% NuPAGE Novex Bis-Tris gel in MES running buffer (Invitrogen). The gel was fixed in fixing solution and dried onto filter paper. Radioactively phosphorylated histone H1 was measured using a phosphorimager. Protein levels were confirmed by Western blotting using the anti-RGC-32 serum 2818 (1:500). **(B)** CDK1 activity relative to control (0 µM RGC-32). This Figure shows the mean of 3 independent experiments +/- standard deviation.

3.7 The effects of RGC-32 on CDK1 activity in EBV-negative B cells

To determine whether RGC-32 is able to increase CDK1 activity in B lymphocytes, asynchronous EBV-negative DG75 cells were transiently transfected with different amounts of pFLAG RGC-32. The CDK1/cyclin B1 complex was immunoprecipitated with an anti-cyclin B1 antibody. The phosphorylation of Histone H1 and therefore CDK1 activity was then measured by performing a kinase assay. A significant increase in CDK1 activity could not be observed (Figure 31A+B, top panel). Increasing RGC-32 protein levels were confirmed by Western blotting but RGC-32 did not appear to affect CDK1 activity (Figure 31B). Tyrosine15-phosphorylated CDK1 (pCDK1) and CDK1 levels remained constant (Figure 31B), but a slight increase in cyclin B1 protein levels was observed (Figure 31B). CDK1 activity appeared to correlate with the amount of cyclin B1 and CDK1 in the immunoprecipitation (Figure 31B, top panel). In addition, we had been unable to demonstrate effects of RGC-32 on the G2/M checkpoint in transient transfections, possibly because of low transfection efficiency (Figure 22).

To investigate the CDK1 activating effect further, the kinase assay was repeated using BJAB and DG75 cells stably overexpressing RGC-32. An RGC-32-induced increase in CDK1 activity could not be confirmed in asynchronous cultures of these EBV-negative cell lines. In fact, RGC-32 expression appeared to suppress CDK1 activity (Figure 32A and B). However, protein analysis by SDS-PAGE and Western blotting revealed that cyclin B1 levels were lower in the RGC-32 overexpressing BJAB and DG75 cell lysates and immunoprecipitates (Figure 32C). The decreased CDK1 activity of RGC-32-overexpressing cells may therefore be due to lower cyclin B1 expression. CDK1 levels appear to be constant in BJAB cell lines, although a difference in the immunoprecipitate from the DG75 FRT cells can be observed. CDK1 activity changes could therefore be caused by differences in the amounts of immunoprecipitated proteins.

Further investigations are needed to verify the result that long-term expressed RGC-32 may downregulate cyclin B1 levels but no such effects of RGC-32 on cyclin B1 levels have been reported yet.

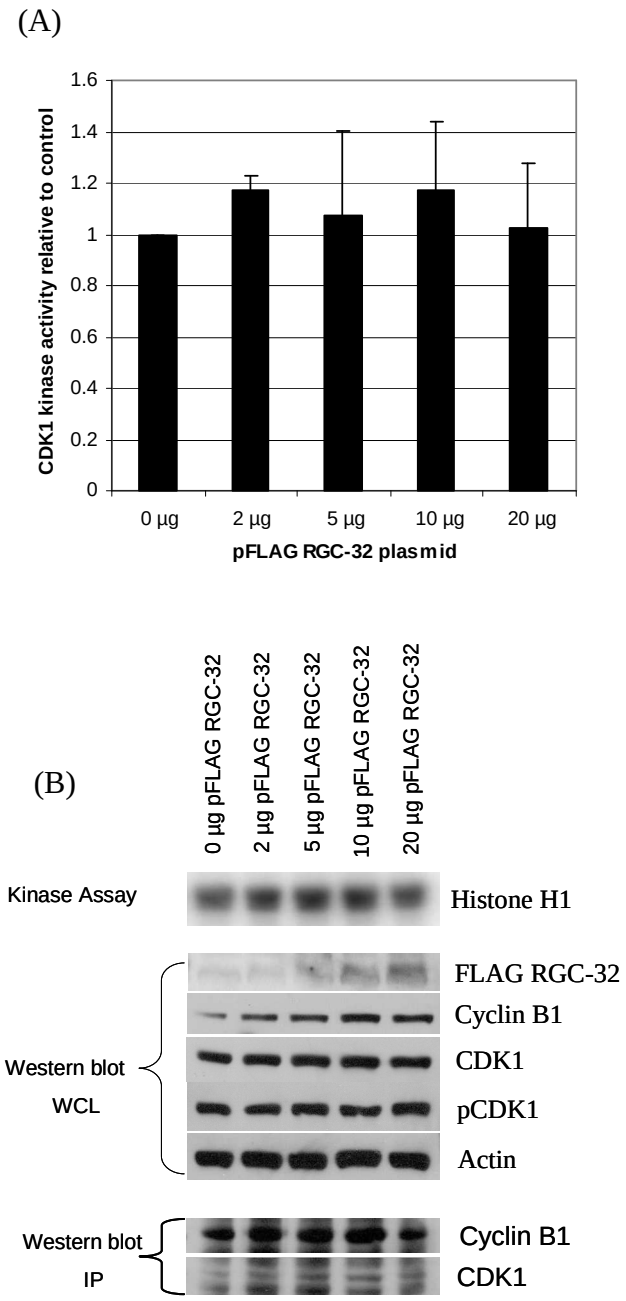

Figure 31 - DG75 cells were transiently transfected with increasing amounts of a FLAG-RGC-32-expressing plasmid. CDK1/Cyclin B1 complexes were immunoprecipitated with an anti-cyclin B1 antibody and γ-^{32}P ATP was used to phosphorylate histone H1 in a kinase assay. **(A)** CDK1 activity relative to control cells not expressing FLAG-RGC-32. This Figure shows the mean of 3 independent experiments +/- standard deviation. **(B)** Radioactively phosphorylated histone H1 was measured using a phosphorimager. Protein expression in whole cell lysates and immunoprecipitates was determined by Western blotting using antibodies against RGC-32, cyclin B1, CDK1, Actin and pCDK1.

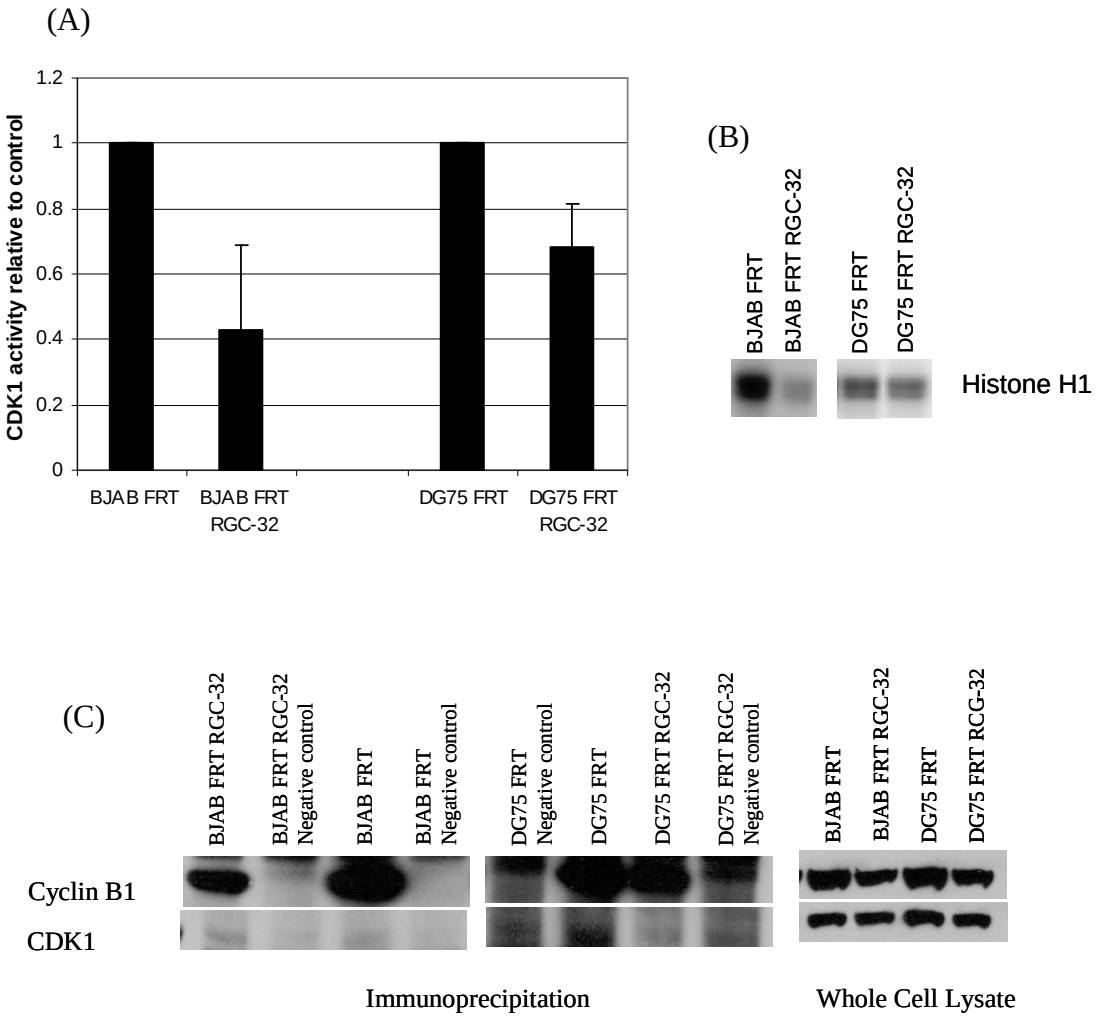

Figure 32 – CDK1/Cyclin B1 complexes were immunoprecipitated with an anti-Cyclin B1 antibody or IgG antibody as a negative control in BJAB and DG75 cells stably over-expressing RGC-32. A kinase assay was performed measuring γ-^{32}P ATP phosphorylated histone H1. **(A)** CDK1 activity is shown here relative to the FRT host cell lines. This Figure demonstrates the result of 3 independent experiments +/- standard deviation. **(B)** Radioactively phosphorylated histone H1 was measured using a phosphorimager. **(C)** Protein expression in whole cell lysates (WCL) and immunoprecipitates (IP) were determined using antibodies against Cyclin B1 and CDK1.

Further investigations into whether RGC-32 expression upregulates CDK1 activity *in vivo* were carried out using the EBNA 3C-negative cell line BJAB pZ1 and pZ3 and the EBNA 3C-positive cell lines E3C-3 and E3C-7. Although in some experiments E3C-3 and E3C-7 cells showed higher CDK1 activity, the results of those experiments were highly variable and no conclusions could be drawn from them (Figure 33).

To investigate whether CDK1 activity was increased in the EBNA 3C-positive BJAB cell line E3C-3 compared to the control cell line pZ3 after DNA damage, asynchronous cultures of BJAB cells exposed to 0, 300 and 500 nM etoposide were analysed in a kinase assay. Results of the kinase assay showed no significant difference between both BJAB cell lines after treatment with etoposide (Figure 34A). Both cell lines show an unexpected increase of CDK1 activity of approximately 2-fold after exposure to 300 nM etoposide and an increase of 1.8-fold after 500 nM etoposide compared to the untreated control. G2 arrest should lead to a decrease in CDK1 activity as a result of the degradation of the cdc25 phosphatase that normally dephosphorylates Threonine-14 and Tyrosine-15 to activate CDK1. Since etoposide causes G2 arrest and cyclin B1 is highly expressed during this phase, the higher CDK1 activity might be due to higher cyclin B1 expression during G2 arrest resulting in the precipitation of more cyclin B1/CDK1. The reduction of CDK1 activity with the higher concentration of etoposide compared to the lower concentration is probably due to cell death due to more DNA damage. Western blot analysis showed that cyclin B1 expression as well as the level of Tyrosine-15-phosphorylated (pCDK1) expression increased after etoposide treatment in both cell lines although pZ3 cells showed higher cyclin B1 and pCDK1 levels compared to E3C-3 cells as previously seen (Figure 34B). Accumulation of cyclin B1 is reduced in EBNA 3C-expressing cells indicating less G2 arrest. Again, increased cyclin B1 levels resulted in increased CDK1 activity although the accumulation of cyclin B1 and pCDK1 suggest cell cycle arrest indicating that CDK1 should be inactive. In fact, inactive pCDK1 was efficiently precipitated by the anti-cyclin B1 antibody making it surprising that CDK1 activity was still detectable. CDK1 levels in the whole cell lysates varied and appeared to follow the pattern of CDK1 activity. The only activity difference detected therefore appeared to be due to the variation of CDK1/cyclin B1 protein levels.

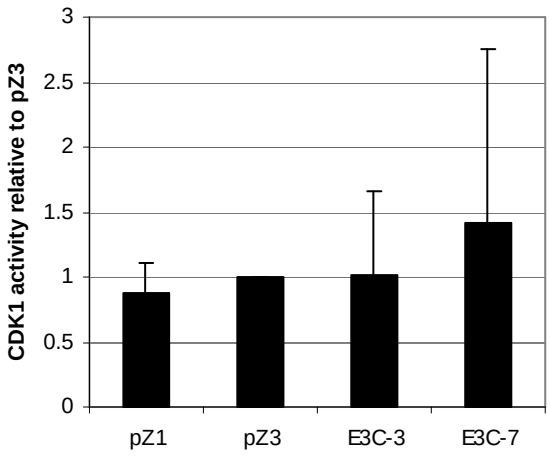

Figure 33 – CDK1/Cyclin B1 complexes of BJAB cells stably expressing EBNA 3C and control cell lines were immunoprecipitated with an anti-cyclin B1 antibody and γ-^{32}P ATP was used to phosphorylate histone H1 in a kinase assay. CDK1 activity is shown relative to control cell line pZ3. This Figure shows the mean of 2 independent experiments +/- standard deviation.

(A)

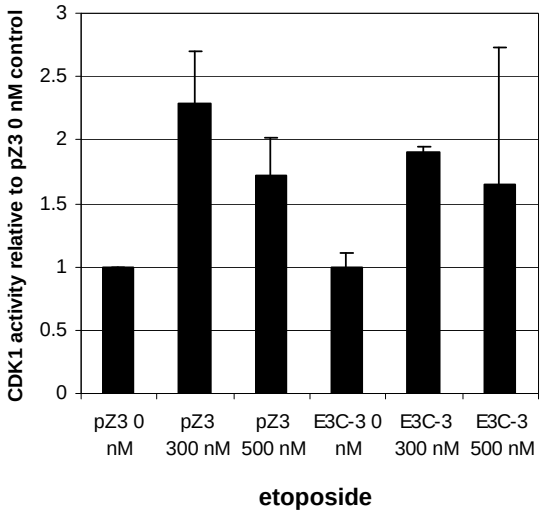

(B)

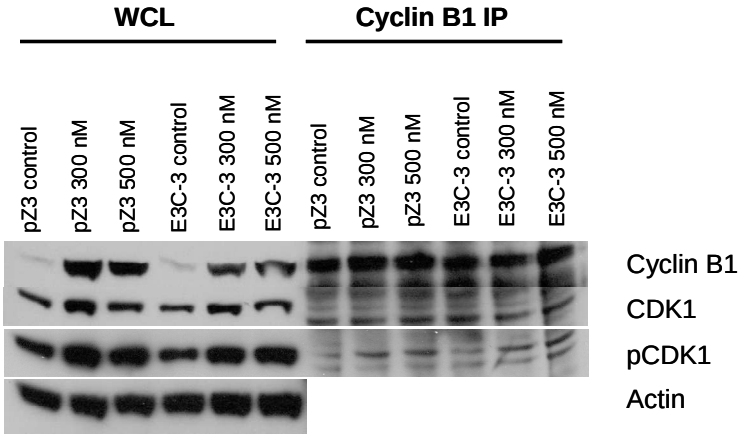

Figure 34 - CDK1/cyclin B1 complexes of BJAB cells stably expressing EBNA 3C and control cell lines were immunoprecipitated with an anti-cyclin B1 antibody. **(A)** γ-32P ATP was used to phosphorylate histone H1 in a kinase assay. CDK1 activity is shown relative to control cell line pZ3. This Figure shows the mean of 2 independent experiments +/- standard deviation. **(B)** Western blot analysis of whole cell lysates (WCL) and immunoprecipitates (IP). Proteins were separated in a 10% NuPAGE Novex Bis-Tris gel in MOPS running buffer (Invitrogen). Nitrocellulose membranes containing the transferred proteins were probed with anti-cyclin B1 (1:2000, Santa Cruz), anti-CDK1 (1:1000, Zymed), anti-pCDK1 (Tyr15-phosphorylated CDK1, Santa Cruz) or anti-actin antibody (1:5000, Sigma) as an internal control. Bands were visualised with ECL.

CDK1 was also immunoprecipitated using an anti-CDK1 antibody instead of an anti-cyclin B1 antibody. Kinase assay results of the BJAB cell lines pZ3 and E3C-3 exposed to 300 and 500 nM etoposide showed that no significant difference in CDK1 kinase activity can be observed between the two cell lines (Figure 35). Further, immunoprecipitation with CDK1 leads to the same profile observed when CDK1 was immunoprecipitated using an anti-cyclin B1 antibody (Figure 34A).

3.8 Discussion

RGC-32 expression was shown to be upregulated in EBNA 3C-expressing Akata and BJAB cell lines. Since RGC-32 is known to promote S and M phase entry, investigations aimed to determine whether EBNA 3C may upregulate RGC-32 to overcome cell cycle control.

EBNA 3C has been shown to disrupt the G2/M checkpoint after DNA damage when overexpressed in DG75 cells (Krauer et al., 2004b). Exposure of EBNA 3C-expressing BJAB cells to gamma radiation or etoposide confirmed that those cell lines also displayed this phenotype. The cell cycle disruption phenotype correlated with RGC-32 upregulation.

We also confirmed that RGC-32 overexpression alone could overcome the G2/M checkpoint in BJAB and DG75 FRT RGC-32 cell lines. To generate these cell lines the Flp-In™ System from Invitrogen was used. Host cell lines were generated to aid the generation of stable cell lines in a rapid and directed manner. However, the use of these cell lines proved problematic. Although in BJAB cells, the RGC-32 expression cassette integrated into the FRT sites incorporated into the host BJAB cell line. This was not the case for the DG75 cell lines generated. In DG75 FRT RGC-32 cell lines, integration occurred at a random site on two separate occasions. For both BJAB and DG75 cells stable cell line generation proved to be just as inefficient as conventional strategies and the host cell lines showed high levels of apoptosis indicating that the FRT cassette or selection was not well tolerated.

Moreover, these stable cell lines appeared to adapt to RGC-32 overexpression with time since the BJAB FRT RGC-32 cells showed a less convincing phenotype in follow-up experiments I carried out.

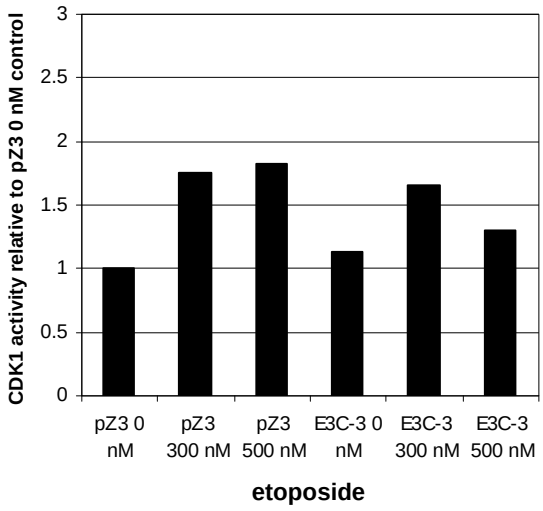

Figure 35 - CDK1/cyclin B1 complexes of BJAB cells stably expressing EBNA 3C and control cell lines were immunoprecipitated with an anti-CDK1 antibody and γ-32P ATP was used to phosphorylate histone H1 in a kinase assay. A representative experiment is shown where CDK1 activity is expressed relative to control cell line pZ3.

Therefore, we examined whether transient RGC-32 overexpression could be used to examine the effects of RGC-32 on the cell cycle. Although transient transfection of DG75 cells could dramatically increase FLAG-RGC-32 protein expression, the phenotype observed after etoposide treatment did not show any significant difference to the control cell line. This could be due to the relatively low transfection efficiency of approximately 33% suggesting that it was not sufficient enough to change the phenotype of the cell cycle distribution after exposure to etoposide. However, treatment with up to 800 nM etoposide did not fully arrest the cells. It may be that RGC-32 overexpressing cells exposed to higher doses which could sufficiently arrest the cells would show a difference in the cell cycle distribution of RGC-32-overexpressing cells compared to the control cell line.

Knock-down of RGC-32 expression in BJAB E3C-3 cells increased the G0/G1 cell population after etoposide treatment but also in untreated cells. RGC-32 was shown to induce serum-starved aortic smooth muscle cells to enter S phase and to significantly increase DNA synthesis (Badea et al., 2002; Badea et al., 1998). Since RGC-32 is known to promote S phase entry as well as M phase entry, knock-down of RGC-32 expression may therefore result in G0/G1 arrest.

Surprisingly, despite misleading early analyses due to the receipt of an incorrect cell line, EBV-positive Raji cells which have a natural deletion of the EBNA 3C gene, did not express upregulated levels of RGC-32 when EBNA 3C was stably expressed. This could be due to the fact that all the other latent EBV proteins are expressed which might abolish the effect of EBNA 3C on RGC-32 expression. However, it is also possible that EBNA 3C has no effect on RGC-32 in Raji cells since this cell line has adapted to their EBV expression pattern and does not need EBNA 3C for proliferation. Therefore, Raji cells may not be the ideal model to investigate the function of EBNA 3C.

Although RGC-32 was able to activate CDK1 *in vitro*, the activation of CDK1 by RGC-32 could not be confirmed *in vivo* using EBV-negative B cell lines BJAB and DG75 overexpressing RGC-32. In addition, EBNA 3C-expressing BJAB cells which have high RGC-32 levels compared to control cell lines did not show a significant difference in CDK1 activation before or after DNA damage. However, CDK1 is inactive throughout interphase and becomes active shortly prior mitosis. Since asynchronous

cells were used in all experiments, only a very small percentage of cells would have active CDK1 leading to a relatively low activity and high background noise. This may have been reflected in the variability observed in these assays and our inability to detect a downregulation of CDK1 activity during G2 arrest. Alternatively, it is possible that these cell lines arrest in G2 without an accompanying decrease in CDK1 activity, despite the increase in Tyrosine-15 phosphorylation. Kinase assays could be repeated using mitotic cells obtained by arresting the cells with the spindle poison nocodazole, for example.

4 Mechanism of RGC-32 upregulation by EBNA 3C

4.1 Introduction

Since microarray studies and real-time PCR follow-up experiments had detected increased RGC-32 mRNA levels in EBV-negative BJAB cells stably expressing EBNA 3C, we next investigated the mechanism of this upregulation. EBNA 3C contains a region that can mediate transactivation in Gal-4 fusion assays and has been shown to upregulate CD21 and LMP1 expression (Marshall and Sample, 1995). We therefore initiated these studies by examining the effect of EBNA 3C on RGC-32 transcription.

4.2 RGC-32 promoter activation by EBNA 3C

Reporter assays were carried out in EBV-negative DG75 and HeLa cells to investigate the effects of EBNA 3C expression on an RGC-32 promoter-reporter construct containing the –1150 to +62 region of the RGC-32 promoter relative to predicted transcription start site. Our results detected RGC-32 promoter activation with increased levels of EBNA 3C expression reaching a maximum of approximately 2-fold in DG75 cells (Figure 36A). A maximum upregulation of approximately 1.3-fold could be detected in HeLa cells (Figure 36B). Western blotting confirmed EBNA 3C protein expression (Figure 36A+C, bottom panels). Control experiments were carried out with C promoter-reporter constructs and EBNA 2-expressing constructs which confirmed that both cell types were competent for gene activation.

An additional control experiment was carried out using the RGC-32 promoter-reporter construct and an EBNA 2-expressing plasmid since EBNA 2 did not affect RGC-32 expression when stably expressed in BJAB cells (Figure 13A). Surprisingly, the control experiment showed that EBNA 2 was able to activate the RGC-32 by more than 6-fold in HeLa cells (Figure 37A). To confirm this result the experiment was repeated in DG75 cells. RGC-32 promoter activation in DG75 cells was highly variable and did not support the observation in HeLa cells (Figure 37B).

The luciferase assay was repeated with EBV-negative BJAB and EBV-positive Raji cells. Transfection of BJAB and Raji cells with up to 10 µg of an EBNA 3C-expressing plasmid did not show any significant changes in RGC-32 promoter activation

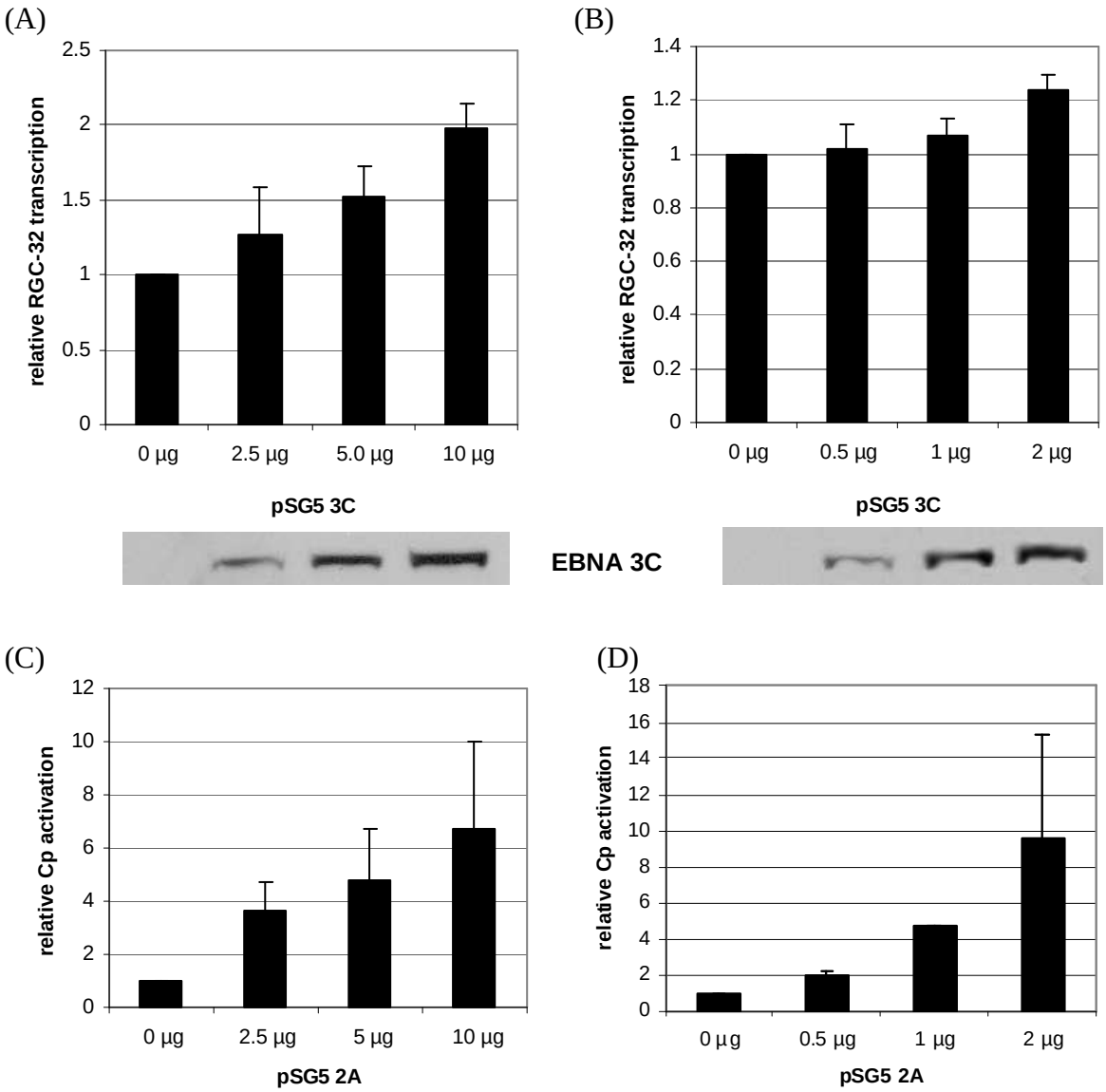

Figure 36 – **(A+C)** DG75 cells were transiently transfected with different amounts of (A) the EBNA 3C-expressing plasmid pSG5 3C or (C) the EBNA 2-expressing plasmid pSG5 2A (2.5, 5 and 10 µg), 2 µg of a Renilla luciferase plasmid to determine the transfection efficiency and 4 µg of a firefly luciferase reporter plasmid containing (A) the RGC-32 promoter or (C) the C promoter. **(B+D)** HeLa cells were transiently transfected with different amounts of (B) the EBNA 3C-expressing plasmid pSG5 3C or (D) the EBNA 2-expressing plasmid pSG5 2A (0.5, 1 and 2 µg), 1 µg of a *Renilla* luciferase plasmid to determine the transfection efficiency and 2 µg of a firefly luciferase reporter plasmid containing (B) the RGC-32 promoter or (D) the C promoter. These graphs show the results of 3 independent experiments +/- standard deviation in which RGC-32 promoter activation was measured and are displayed relative to the EBNA 3C-negative control. The values for firefly luciferase activity (RGC-32 or C promoter reporter) were corrected by dividing them by the values for the *Renilla* luciferase activity (pRL-CMV transfection control). Luciferase assay samples were analysed by Western blotting for EBNA 3C expression using an anti-EBNA 3C antibody (1:300).

(A)

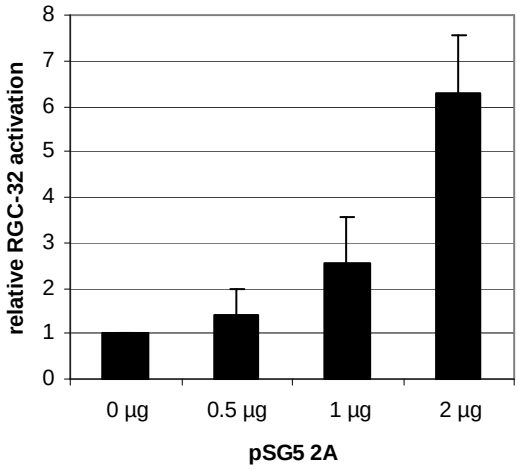

(B)

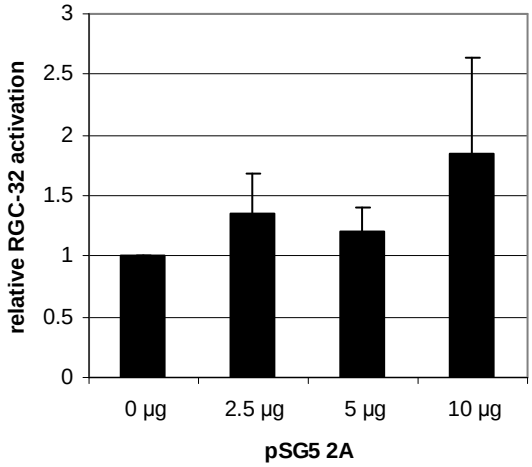

Figure 37 – (A) HeLa cells were transiently transfected with different amounts of the EBNA 2-expressing plasmid pSG5 2A (0.5, 1 and 2 µg), 1 µg of a *Renilla* luciferase plasmid to determine the transfection efficiency and 2 µg a firefly luciferase reporter plasmid containing the RGC-32 promoter. **(B)** DG75 cells were transiently transfected with different amounts of the EBNA 2-expressing plasmid pSG5 2A (2.5, 5 and 10 µg), 2 µg of a *Renilla* luciferase plasmid to determine the transfection efficiency and 4 µg of a firefly luciferase reporter plasmid containing the RGC-32 promoter. These graphs show the results of 3 independent experiments +/- standard deviation in which RGC-32 promoter activation was measured and displayed relative to the EBNA 2-negative control. The values for firefly luciferase activity (RGC-32 promoter reporter) were corrected by dividing them by the values for the *Renilla* luciferase activity (pRL-CMV transfection control).

(Figure 38A+B). Further, the EBNA 3C-negative BJAB cell lines pZ1 and pZ3 were compared to the EBNA 3C-positive cell lines E3C-3 and E3C-7 by transfecting these cell lines with RGC-32pluc and pRL-CMV. Luciferase assay results revealed no difference between the EBNA 3C-positive and -negative cell lines (Figure 39). Together, these data suggest that the RGC-32 promoter activity may not be upregulated by EBNA 3C although a 2-fold increase in activation could be observed in DG75 cells.

4.3 RBP-J kappa is not able to bind a predicted site in the RGC-32 promoter

EBNA 3C does not bind DNA directly but interacts with the cellular DNA-binding proteins RBP-J kappa and PU.1 (Marshall and Sample, 1995; Zhao and Sample, 2000). RBP-J kappa also targets EBNA 2 to DNA (Grossman et al., 1994b; Henkel et al., 1994).

The transcription factor prediction programme MatInspector identified a potential RBP J-kappa site in the RGC-32 promoter at (-941 to -935) (Table 8). To investigate whether RBP-J kappa can bind the RGC-32 promoter, gel shift experiments were carried out using recombinant RBP-J kappa. Although RBP-J kappa was able to bind an oligonucleotide encompassing the C promoter RBP-J kappa site, the protein did not bind to the predicted RBP-J kappa site in the RGC-32 promoter (Figure 40). These results were confirmed by another member of the lab (Lara Boyd, Master's dissertation, data not shown). It is therefore unlikely that EBNA 3C or EBNA 2 bind to the RGC-32 promoter via this RBP-J kappa binding site. The variation in the RBP-J kappa site compared to bona fide RBP-J kappa sites in Cp and LMP1 for example is likely to be sufficient to prevent efficient RBP-J kappa binding (Table 8). Interestingly, further database searches using Alggen Promo revealed that the RGC-32 promoter contained another RBP-J kappa binding site in a region upstream from the promoter region (-1649 to -1643). This site showed 100% identity with the core consensus sequence known to bind RBP-J kappa (Table 8 and Figure 41).

(A)

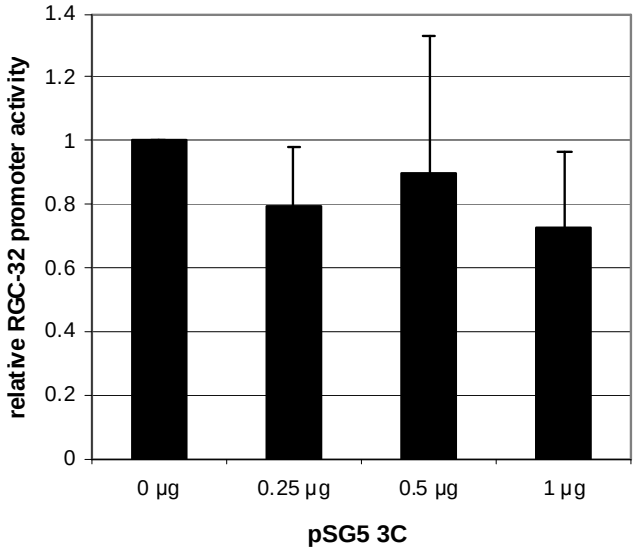

(B)

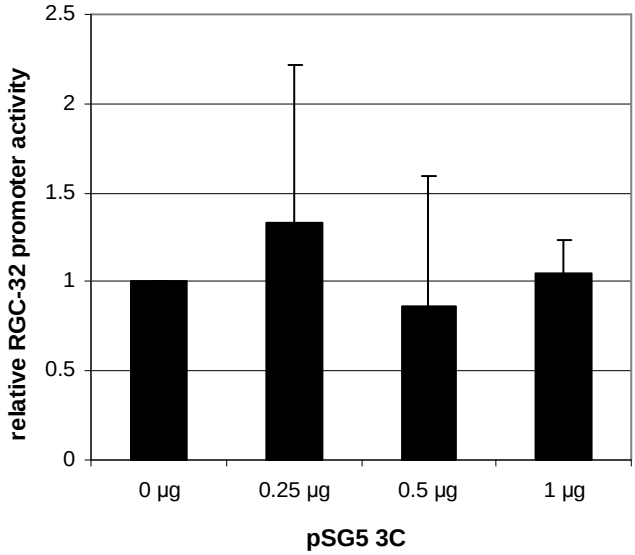

Figure 38 – (A) Raji cells and **(B)** BJAB cells were transiently transfected with different amounts of the EBNA 3C-expressing plasmid pSG5 3C (0.25, 0.5 and 1 µg), 1 µg of a *Renilla* luciferase plasmid to determine the transfection efficiency and 2 µg of a firefly luciferase reporter plasmid containing the RGC-32 promoter. These graphs show the results of 3 independent experiments +/- standard deviation in which RGC-32 promoter activation was measured and are displayed relative to the EBNA 3C-negative control. The values for firefly luciferase activity (RGC-32 promoter reporter) were corrected by dividing them by the values for the *Renilla* luciferase activity (pRL-CMV transfection control)

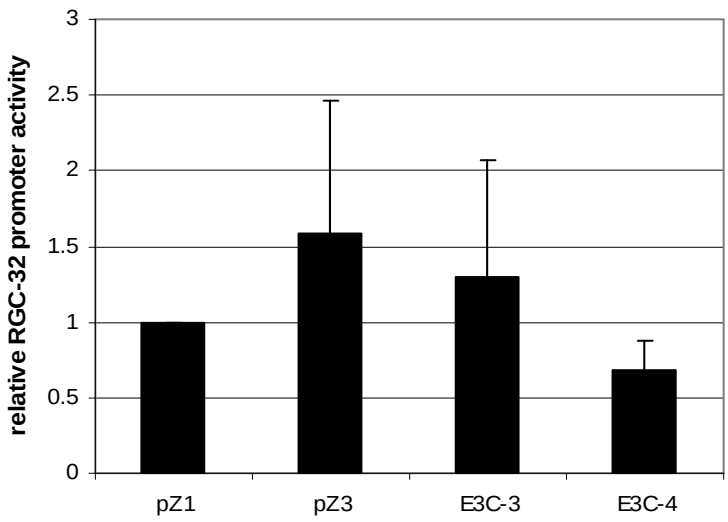

Figure 39 - BJAB cell lines stably expressing EBNA 3C (E3C-3 and E3C-4) and control cell lines (pZ1 and pZ3) were transiently transfected with 1 µg of the EBNA 3C-expressing plasmid pSG5 3C, 2 µg of a *Renilla* luciferase plasmid to determine the transfection efficiency and 4 µg a firefly luciferase reporter plasmid containing the RGC-32 promoter. These graphs show the results of 3 independent experiments +/- standard deviation in which RGC-32 promoter activation was measured and are displayed relative to the EBNA 3C-negative control pZ1. The values for firefly luciferase activity (RGC-32 promoter reporter) were corrected by dividing them by the values for the *Renilla* luciferase activity (pRL-CMV transfection control)

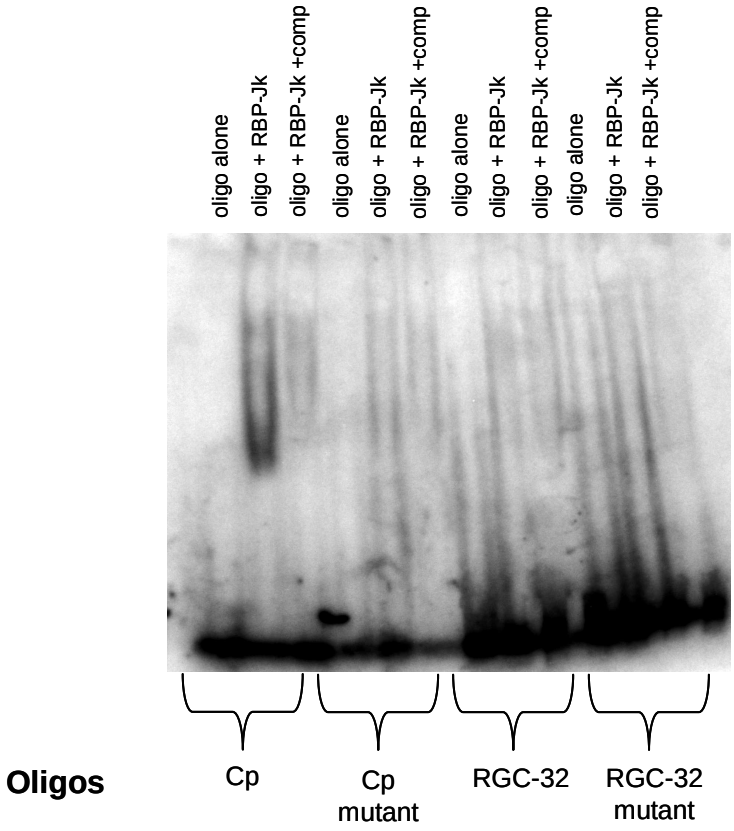

Figure 40 – Gel shift assays were performed using 2 ng radiolabelled oligonucleotides (probe) from the RGC-32 or C promoter containing the RBP-J kappa site or a mutated RBP-J kappa site. The probe was either incubated alone (oligo alone) or was mixed with 0.5 μg GST-RBP-J kappa protein in the absence or presence of 60x excess of competitor cold oligonucleotide. Samples were resolved using a 6% TBE gel.

-2247			GAGAGTC	ATATCATCCT	CTTTCGCTCT
-2220	GGATATTAGG	AACAATATCA	CAGGGTTGTG	TACTCCCCCT	GCGATATTGG
-2170	GAGTAATATC	ATTCTCTCTC	CCTGTGGATT	TTAGGAAGAG	TATTACAGGG
-2120	CTGTGTACAC	CCCCTGCGCT	ATTGGGAGTA	ATATCATCCT	CTCTCCCTCT
-2070	GGATAGTAGG	AAGAGTTTCA	TAGGGGTGTG	TACACCCCCT	GTGATATTGG
-2020	GAGTAATATC	ATCCTGTCGC	CCTGAGGAGA	GAAGCCATTT	CGCTACTGTC
-1970	TCCTGTCTCT	GAAGAGGAGG	AGGAAGTAAA	AGTTGGAAAA	CAACAGGAAT
-1920	GAAGTCAGTG	TCAAGACCAG	CCGGTGGCAA	TGAGGAGCCG	GCCTGAGGTG
-1870	AAACAATCAA	CCCCCGTGAC	TCTAAGTACA	TGTGCTCTCA	ATCCATCAAG
-1820	ACCCTTTCAC	GTGGAACCCC	TTAAAGCTGT	AAGCCCTTAA	ACGGGCCAGG
-1770	AACTCTGTCT	TCCTTCCGGG	AGCTCGGCTC	TTACGCGAGT	CTGCCGAAGC
-1720	TCCCAGCGGA	ATAAAAAAAA	CTCTTCCTTC	TTTAATCCGC	TGTCTGAGGG
-1670	GTTTTGTCCG	CTGCTCATCC	ATGCTCCATT	TCTTTGTTCC	CTGACCGGGA
-1620	ATCGAACGCA	GGCAGCAGCG	GTGAGAGCAC	CGAATCCTAA	GCACTAGACC
-1570	ACCAGGGGAA	CTTAGAACCT	TGTGGGAAAT	AGATTGCGCA	CCATTAGAAG
-1520	TGGGTTGGCC	ATCAGAAGGA	AGCCTGGACA	GGTCCCTTGT	TTCTAAGGCG
-1470	TGGCACAAGG	TAACTGGTAA	AGATACCTAG	ACCAGTTCCC	ATACATAGAC
-1420	ACTTGGTGAC	AGCTGGTGCT	AGAACCCCCA	CAGTGGCTGA	GGGCATGCAG
-1370	CAGCAATACT	AGTAGCAAAG	GGACAGATAG	CTAAGGAAGG	ATCCCGCTCC
-1320	ACTCACCCAG	GGAAATCAAC	TCCTGAAGTT	CTGTTCGACC	CCACATCAGA
-1270	GGATCCATTG	CAGGAGATGG	CACCAGAGAT	CCCAGTGGTG	TCCTCCCCTT
-1220	AACAGGGAAA	GAGGCTCCCC	ACTCTTGAGC	CCACAGTGCT	TGTGCCTCCA
-1170	CAAGACAAGC	ATATCCCTAG	GCCACCCAGA	GTAGACAAGA	GAGGAGGACT
-1120	ATTCATATGA	TTAGTGGTCA	TTAACATATA	CTCCTTTGTG	AGGTGTATGT
-1070	TTCAATGTTT	TGCTCATTTT	TAATTTTTAC	CAGGTTGTCT	ATTTGTGATT
-1020	ACTTTGTAGA	TGGGTCTTTC	TATATTCTGA	AAACAAATCC	TGGCTGGGTG
-970	CGGTGGCTCA	CGCCTGTAAT	CCCAGCACTT	TGGGAGGCTG	AGGTGGGCAG
-920	ATCACCTGAG	GTCGGGAGTT	CGAGACCAGC	CTGGCCAACA	TGGACAAACC
-870	CCGTCTCTGC	TAAAAATACA	AAAACTAGCT	GGGAGTGGAG	GCTGAATGTT
-820	TCACTCCGTT	ACATGTTAAT	TGCTCTACAT	TTAATTAGCC	GTCTGTGGTG
-770	AGAGGCGAGA	GGCTAGCGCC	TAGCTCAGCG	CACAGTCCAG	GGCGTTCGCC
-720	CCCGCAGGCC	GCGGGGCAGG	GTGGCTCGTT	ACTCCGTGGA	CACTGCAAGG
-670	CGCCCTGTTC	GCGCTGCGTC	GACGCAGTAG	TTTCTTCCCA	TAATAAACCC
-620	CTTCTAGATA	AAGTCAGGCT	GGCGGGAGCG	CCCTGGACCG	TAGTTCAGGC
-570	CCCCGCGCTC	CGCGGTGGGA	ACAGTTCAGG	ACTCCCCCAA	CTCCTGCCCC
-520	TCTCGCCCCG	ACCCTCTCCA	CTCCGCCCGC	CCACCATCTC	GGAAGTCCCC
-470	TTGGGACAAT	GCGTAGGGGA	CCTCCGCGTC	CCCGACACCC	GACTGGGACA
-420	CGGCCGCGGG	CTCCTTCGTC	CCTCACCGCC	AGCCAGGGAG	GCTCTGCATG
-370	CCCACGTCCA	CTTCACAGCC	GAGGAAGCTG	CGGCTCGCGG	AGGTGCCTGG
-320	CACGCGGCGG	GAAGCAGCAG	AGCTCGCGCC	CAGCAGTCAG	CTCTGGTGAC
-270	GCCGAGGACA	CCGCGTGGGC	CGGGTTGTCA	GGGCGCGGGG	GCGAGAGGCG
-220	GGTAAATATT	TGGGGCTGTA	ACCGGGGCTT	CGGCGACTCC	TCGTCACCGC
-170	GGTTCCAGGG	CGGGCGCGTG	GCGAGGGCGG	TGCCTGGGGG	CAGGGGCCTC
-120	CTCGGAGGGC	GGCGGGGACA	GACCCGTCGC	CCCGGCTCCG	CAGCCCCGCC
-70	CCGGCCCCGC	CTCCGCTCCG	GCCGCCGAAG	GCTATAAGAT	CTAGGAACCC
-20	GAGCCGGTGG	TAGGGCGGGC	GCGGACCGTG	CTGGGAGCGG	CGCGGCTGGA
-31	GCGCAGCGCC	GAAGGGACTG	GCAGGGCTGA	AGTGTGCGGG	ACAGCAAGCA
+81	AGCTTGGCAT	TCCGGTACTG	TTGGTAAAAT	GGAAGACGCC	AAAAACATAA
+131	AGAAAGGCCC	GGCGCCATTC	TATCCTCTAG	AGGATGGAAC	CGCTGGAGAG
+181	CAACTGCATA	AGGCTATGAA	GA		

Figure 41 – Sequence of the RGC-32 promoter construct pGL2 RGC-32pluc-up. Bases in red and blue letters together represent the previously used RGC-32 promoter construct pGL2 RGC-32pluc. The blue letters show a part of the sequence which is transcribed into mRNA. The black letters represent the additional upstream sequence cloned into the pGL2 RGC-32pluc vector. The yellow highlighted sequences indicate the potential binding sites for RBP-J kappa.

Therefore, the upstream sequences were cloned into the original pGL2-RGC-32pluc vector by another lab member (Felicity Poulter, undergraduate project year 2008/09).

promoter	sequence	location
Cp	5'-GTGGGAA-3'	
LMP1	5'-GTGGGAA-3'	
RGC-32	5'-GTGGGAA-3'	-1649 to -1643
RGC-32	5'-TTGGGAG-3'	-941 to -935
RGC-32	5'-GTGGGAA-3'	-556 to -550

Table 8 – Overview of RBP-J kappa sites of different gene promoters

To investigate whether EBNA 3C could increase the RGC-32 promoter activity when the additional upstream RBP-J kappa site was present, DG75 cells were transiently transfected with an EBNA 3C-expressing plasmid and the RGC-32 promoter construct containing the additional upstream sequences. Luciferase assays revealed that the activity of the RGC-32 promoter does not significantly increase with the additional RBP-J kappa binding site (Figure 42).

Towards the end of this study, another RBP-J kappa binding site was identified (-556 to -550) by manual searching for the known core binding sequence GTGGGAA that was not predicted by MatInspector or Alggen Promo as a potential RBP-J kappa binding site. Lack of time meant that further investigations into the functionality of this site were not possible.

Together, the data indicate that EBNA 3C does not reproducibly activate the RGC-32 promoter in reporter assays suggesting that there may be another mechanism by which EBNA 3C upregulates RGC-32.

4.4 RGC-32 mRNA stability is increased in EBNA 3C-expressing BJAB cells

Other pathways were considered to further investigate the mechanism of the RGC-32 mRNA upregulation. To determine whether EBNA 3C could upregulate RGC-32 by stabilisation of the RGC-32 mRNA, the EBNA 3C- negative cell lines BJAB pZ1 and

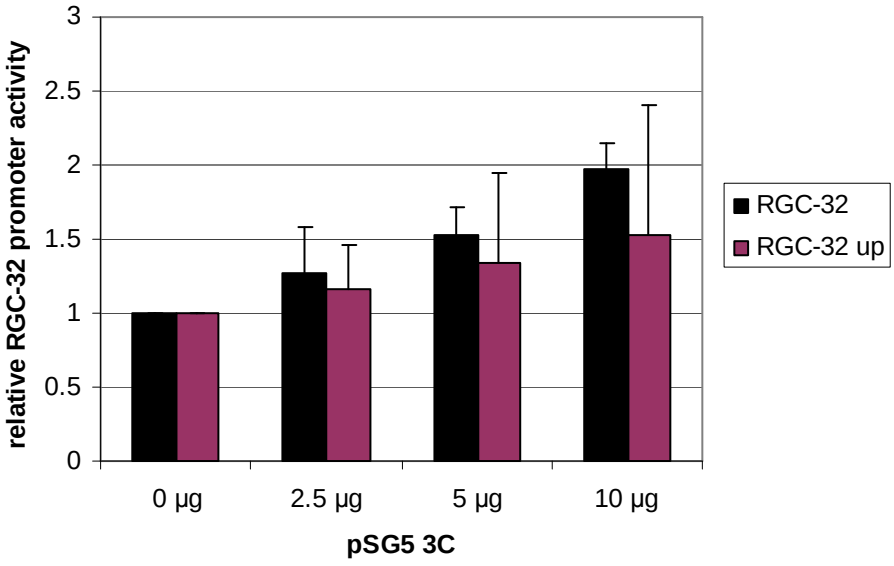

Figure 42 - DG75 cells were transiently transfected with different amounts of the EBNA 3C-expressing plasmid pSG5 3C (2.5, 5 and 10 µg), 4 µg of a Renilla luciferase plasmid to determine the transfection efficiency and 8 µg a firefly luciferase reporter plasmid containing the RGC-32 promoter (RGC-32, black) or containing the RGC-32 promoter including upstream sequences (RGC-32 up, purple). This graph shows the mean of 3 independent experiments +/- standard deviation in which RGC-32 promoter activation was measured and displayed relative to the EBNA 3C-negative control. The values for firefly luciferase activity (RGC-32 promoter reporter) were corrected by dividing them by the values for the *Renilla* luciferase activity (pRL-CMV transfection control).

pZ3 and the EBNA 3C-positive cell lines BJAB E3C-3 and E3C-7 were treated with 2 µM actinomycin D to halt transcription and RGC-32 mRNA levels measured at time intervals up to 8 hours. Initial experiments established that 2 µM actinomycin was not significantly toxic for 8 hours or more. RGC-32 mRNA levels were analysed by real-time PCR. As shown in Figure 43A and B RGC-32 mRNA levels decreased faster in pZ3 cells compared to E3C-3 cells. Non-linear regression estimated an RGC-32 half life of about 1 h for the EBNA 3C-negative cell line pZ3 and a half life of more than 10 h for the EBNA 3C-positive cell line E3C-3. Similar results were determined for pZ1 an E3C-7 for which RGC-32 half lives of 0.3 and 4 h respectively were estimated (data not shown).

These results indicate that stabilisation of RGC-32 mRNA in the BJAB E3C-3 and E3C-7 cell lines is likely to mediate the RGC-32 upregulation seen in EBNA 3C-expressing cells and in fact may be the only mechanism through which the upregulation is achieved. These results provide the first demonstration of EBNA 3C-driven RNA stabilisation.

4.5 Discussion

RGC-32 mRNA is upregulated up to 14-fold in BJAB cells stably expressing EBNA 3C compared to control cell lines. We investigated whether the viral protein EBNA 3C was able to upregulate the cellular RGC-32 by activating the promoter in a direct or indirect manner. Transient transfection using an EBNA 3C-expressing plasmid resulted in a 2-fold upregulation of the RGC-32 promoter observed in DG75 cells and a 1.3-fold upregulation in HeLa cells. However, this activation of the RGC-32 promoter could not be confirmed in EBV-negative BJAB cells. Furthermore, transient transfection of EBV-positive Raji cells and EBV-negative BJAB cells both stably expressing EBNA 3C did not result in activation of the RGC-32 promoter indicating that initiation of RGC-32 gene transcription may not be the mechanism by which EBNA 3C upregulates RGC-32 mRNA. The DG75 results could be an artefact resulting from non-specific effects of EBNA 3C in the cell.

Surprisingly, a 6-fold induction of the RGC-32 promoter by EBNA 2 could be observed in HeLa cells. This was unexpected as real-time PCR experiments showed that BJAB

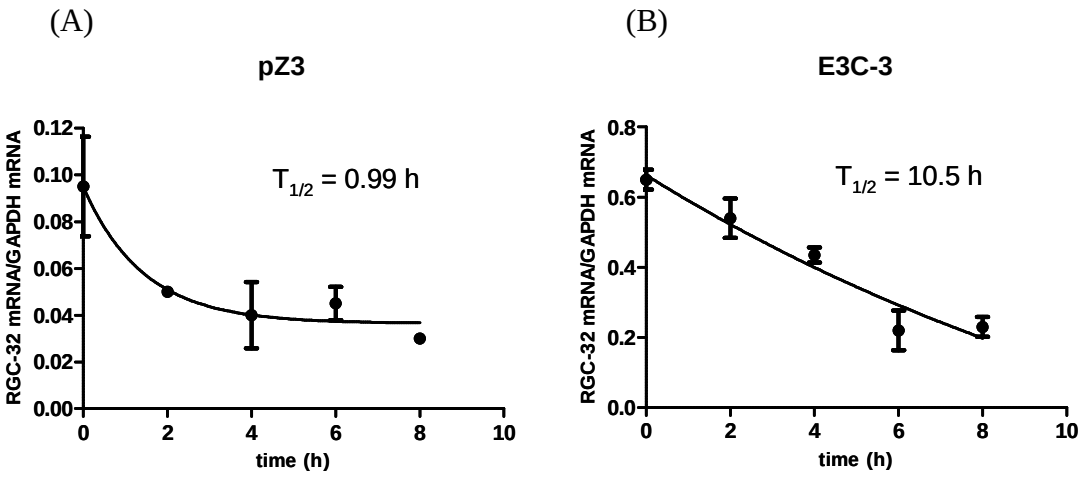

Figure 43 – RGC-32 mRNA half life

BJAB pZ3 **(A)** and E3C-3 **(B)** cells were treated with the transcription inhibitor actinomycin D (2 μM) for 2, 4, 6 and 8 hours. RGC-32 mRNA levels were measured in duplicate by real-time PCR and divided by GAPDH mRNA levels. Calculated half lives using SigmaPlot are displayed on the graphs which show the mean of three independent experiments +/- standard deviation.

cells overexpressing EBNA 2 did not increase RGC-32 mRNA levels (Figure 13A). The observation made in the cervical carcinoma cell line HeLa could not be confirmed in the B cell line DG75 and might therefore be cell type-specific and may result from interaction with HeLa cell-specific proteins.

EBNA 3C does not bind DNA directly but may be targeted by the DNA-binding protein RBP-J kappa, in a similar manner to EBNA 2. Interestingly, the RGC-32 promoter contains a predicted RBP-J kappa-binding site that could potentially mediate the effects of EBNA 3C or EBNA 2. However, gel shift assays revealed that RBP-J kappa does not bind to the predicted binding site suggesting that RBP-J kappa does not mediate the effects of EBNA 3C and EBNA 2. However, this predicted RBP-J kappa site only shows approximately 71% identity of the core sequence. Used RBP-J kappa sites seen in the LMP1 and C promoter showed 100% identity of the core sequence suggesting that the predicted RBP-J kappa site might not be functional. Another RBP-J kappa site with 100% identity of the core was found further upstream of the promoter which was not part of the original RGC-32pluc plasmid. Transfection with a plasmid containing the additional upstream region did not result in increased RGC-32 promoter activation by EBNA 3C suggesting that RBP-J kappa does not target EBNA 3C to the RGC-32 promoter.

Chromatin immunoprecipitation (ChIP) experiments carried out by Helen Webb and Richard Palermo examined RNA polymerase II association with the RGC-32 promoter and gene. Chromatin was purified from EBNA 3C-negative BJAB cell lines pZ1 and pZ3 as well as from the EBNA 3C-positive cell lines E3C-3 and E3C-7. The EBNA 3C-expressing BJAB cell lines E3C-3 and E3C-7 did not show increased RNA polymerase II association at the transcription start site of the RGC-32 gene as well as upstream regions of up to -1000 base pairs and downstream regions of down to +500 base pairs compared to the EBNA 3C-negative cell lines pZ1 and pZ3 (data not shown). These results further confirm that RGC-32 upregulation in EBNA 3C-expressing cells does not result from increased RGC-32 transcription in BJAB cell lines. Taken together, results from luciferase assay, gel shift and ChIP analysis indicate that EBNA 3C is not able to transactivate the RGC-32 promoter.

Investigations into other mechanisms by which EBNA 3C could upregulate RGC-32 mRNA levels revealed that stabilisation of the RGC-32 mRNA occurred in EBNA 3C-expressing BJAB cell lines. To examine potential mechanisms for these effects other genes differentially regulated by EBNA 3C in the original microarray study were screened for involvement in mRNA stability processes when EBNA 3C is expressed. Interestingly, expression of the CUG-binding protein 2 (CUGBP2) was found to be regulated by EBNA 3C. CUGBP2 is known to regulate pre-mRNA alternative splicing and was found to play a role in mRNA editing (Anant et al., 2001; Philips et al., 1998). Furthermore, it was shown to be involved in RNA stabilisation and inhibition of translation (Mukhopadhyay et al., 2003; Subramaniam et al., 2008). However, CUGBP2 gene expression was downregulated in EBNA 3C-expressing BJAB cells and can therefore not account for the increase in RGC-32 mRNA stabilisation.

Expression of the RNA binding protein RBM9 (RNA binding motif 9, Fox-2) was also found to be upregulated by EBNA 3C. This protein was shown to be involved in alternative exon splicing via binding a conserved UGCAUG element found downstream of many alternatively spliced exons and promotes inclusion of the alternative exon in mature transcripts (Ponthier et al., 2006). RNASE4 was also shown to be regulated by EBNA 3C which is another protein involved in alternative splicing (Shapiro et al., 1986). However, alternative splicing does not necessarily correlate with RNA stabilisation.

Therefore, the mechanism by which EBNA 3C stabilises RGC-32 mRNA could not be identified at this stage.

5 Detecting the RGC-32 protein

5.1 Introduction

RGC-32 protein was shown to play a role in cell cycle progression into S and M phase by increasing the activity of CDK1. Further, RGC-32 was shown to bind CDK1 which mediates transition into mitosis (Badea et al., 2002; Badea et al., 1998; Niculescu et al., 1999; Rus et al., 1996). Interestingly, RGC-32 mRNA and protein expression is increased in many tumour tissues indicating a role for RGC-32 in cancer development (Fosbrink et al., 2005). All of the studies performed in this thesis this far have relied on detection of endogenous RGC-32 mRNA. The next series of experiments described in this chapter set out to determine whether RGC-32 was also upregulated at the protein level in EBNA 3C-expressing cell lines.

5.2 Characterisation of an RGC-32 antibody

To determine whether RGC-32 is upregulated at the protein level in the cell lines previously examined, it was necessary to obtain an anti-RGC-32 antibody. After the failure of an anti-RGC-32 peptide antibody generated by the West lab to detect endogenous RGC-32 protein, polyclonal anti-RGC-32 antibodies were raised against a His-tagged full length RGC-32 recombinant protein purified from bacteria by Helen Webb. Sera were received from two rabbits (2817 and 2818) following a series of 5 immunisations. The first experiments carried out using the polyclonal sera aimed to determine whether the antibodies were able to detect RGC-32 on Western blots and also to identify which serum contained more specific antibodies. Whole cell lysates of EBV-negative DG75 cells were used which were transiently transfected with either empty pFLAG vector or pFLAG RGC-32.

Figure 44A shows that DG75 cells had been transfected successfully and expressed FLAG-RGC-32 which could be detected with the expected molecular weight of 17 kD using an anti-FLAG antibody (top panel). The antibodies obtained from rabbit 2817 (middle panel) could not detect overexpressed RGC-32 protein; however, serum 2818 antibodies (bottom panel) were able to bind the RGC-32 protein overexpressed in DG75 cells. However, endogenous RGC-32 protein (predicted molecular weight of approximately 14 kD) was not detected in the EBV-negative DG75 cells. For further experiments, I then focussed on the serum from rabbit 2818.

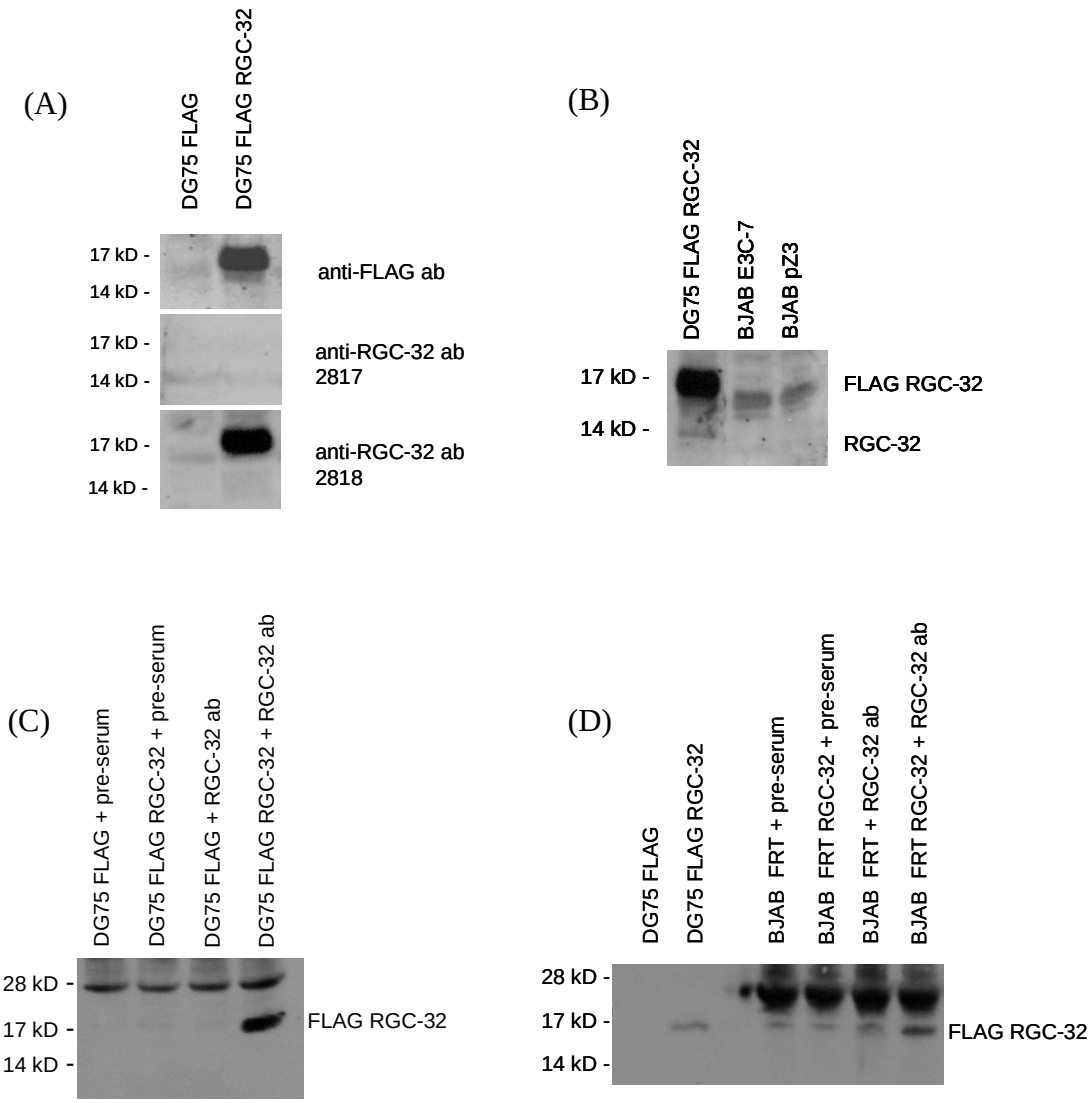

Figure 44 – Anti-RGC-32 antibody testing - Western blot analysis. Proteins of all cell lysates or immunoprecipitations were separated in a 10% NuPAGE Novex Bis-Tris gel in MES running buffer (Invitrogen). **(A)** Lysates of transiently transfected DG75 cells (40 μg of pFLAG-RGC-32 or empty pFLAG vector) were probed with an anti-FLAG antibody (1:500) or rabbit serum 2817 or 2818 (1:500 of 4th bleed). **(B)** Western blot analysis of DG75 cells transiently transfected with 40 μg of pFLAG-RGC-32 as positive control and BJAB pZ3 and E3C-7. Proteins were detected using rabbit serum 2818 (1:500 final bleed). **(C)** Lysates of DG75 cells transiently transfected with 40 μg of pFLAG-RGC-32 or empty pFLAG were immunoprecipitated with either the pre-immune serum or the serum from the 3rd bleed from rabbit 2818. Immunoprecipitated RGC-32 was detected with a purified anti-FLAG antibody (1:200, Sigma). **(D)** Lysates of DG75 cells transiently transfected with 40 μg of pFLAG-RGC-32 or empty pFLAG were used as a positive and negative control. Lysates of BJAB cells stably expressing FLAG RGC-32 and negative control cells were immunoprecipitated with either the pre-immune serum or the serum from the 3rd bleed from rabbit 2818. Immunoprecipitated RGC-32 was detected with 3rd bleed rabbit 2818 serum (1:500). Bands were visualised with ECL.

Additional experiments showed that endogenous RGC-32 protein could not be detected in the EBV-negative BJAB cell line pZ3 (Figure 44B). Unexpectedly, endogenous RGC-32 could not be detected in the BJAB cell line E3C-7 which stably expresses EBNA 3C and showed a 6.5-fold upregulation of RGC-32 mRNA compared to pZ3 (Figure 13A). RGC-32 protein expression was detected reproducibly in DG75 transiently expressing RGC-32 as previously shown (Figure 44B). To further test and to increase the detection level of the anti-RGC-32 serum, immunoprecipitations were carried out using lysates of DG75 cells transiently expressing FLAG-RGC-32 and BJAB cells stably expressing FLAG-RGC-32 with either preimmune-serum or rabbit serum obtained after the 4^{th} immunisation (3^{rd} bleed). Western blot analysis using an anti-FLAG antibody revealed that RGC-32 was detectable in DG75 cells transiently transfected with pFLAG RGC-32 and immunoprecipitated with anti-RGC-32 serum (Figure 44C) indicating that the sera could be used for immunoprecipitations.

Although FLAG RGC-32 could also be detected in DG75 or BJAB FRT-RGC-32 cells which stably overexpress RGC-32 in immunoprecipitations using the anti-RGC-32 serum (Figure 44D), a non-specific band ran in the same place which restricted a clear identification of the RGC-32 band. Further, endogenous RGC-32 protein was not detectable in BJAB cells using immunoprecipitation. Since the Western blot showed a sizeable amount of non-specific binding and detection of endogenous protein appeared to be difficult, the anti-RGC-32 serum 2818 was purified.

5.3 Anti-RGC-32 antibody purification

5.3.1 RGC-32 protein preparation

To purify the anti-RGC-32 serum, recombinant RGC-32 protein was purified from the *E. coli* strain BL21 *plysS* containing the pET RGC-32 vector. This vector expresses His-tagged RGC-32 in inclusion bodies upon IPTG induction at 37°C and His-RGC-32 was purified using denaturation and renaturation techniques. The purity of the protein (elutions 1 to 6) was determined by SDS-PAGE followed by Coomassie staining. Figure 45 shows that RGC-32 was obtained with a high degree of purity in pooled elutions 1-3 and that the concentration expectedly decreased in later elutions. The His-tagged RGC-32 protein has a molecular weight of 16 kD. The band of smaller size is probably a degradation product of RGC-32. His- RGC-32 was eluted in 40 mM PO_4, 300 mM

NaCl and 100 mM EDTA and was then dialysed against 20 mM PO_4 buffer (pH 7.5) to make the buffer compatible for the following anti-RGC-32 antibody purification. A RGC-32 protein concentration of 0.8 mg/ml (60 μM) was obtained.

5.3.2 Antibody purification and antibody testing

To increase the specificity of the anti-RGC-32 antibody serum, the antibodies of the final bleed of rabbit 2818 were purified using various techniques. In the first attempt His-tagged-RGC-32 protein was bound to HIS-Select® Nickel Affinity Gel (Sigma) and crosslinked with DSS (Disuccinimidyl suberate). After several washing steps the rabbit serum 2818 was added to the resin. A sample of starting material was kept for later analysis as well as a sample of the flow through before the first wash. After several washing steps the antibody was eluted with 10 mM glycine pH1. Coomassie staining of the elutions revealed that a major amount of the antibody came off the resin with the first elution but surprisingly RGC-32 was also eluted (Figure 46A). It appears that the crosslinking between protein and resin was not very stable. The two elutions with the highest protein concentration were pooled and tested for RGC-32 specificity by Western blot analysis.

The unpurified antibody (starting material) was able to detect the transiently overexpressed FLAG-RGC-32 protein as expected. The flow-through, which was obtained after the serum was first loaded to the column, could not detect the protein suggesting that the antibody had bound successfully to the resin. However, none of the different dilutions (1:100 - 1:1000) of the purified antibody was able to detect overexpressed FLAG-RGC-32 protein (Figure 46B).

In a second attempt RGC-32 was coupled to a CH sepharose resin (Sigma). 3 mg of RGC-32 protein were added to the swollen and washed beads. The input protein was compared to the flow-through in a Bradford assay which revealed that 75% of the input RGC-32 protein had bound to the beads (data not shown). 1 M Tris pH 8.5 was used to wash the resin after the protein was bound which resulted in precipitation of the protein. An additional experiment carried out by Helen Webb confirmed that RGC-32 was insoluble in Tris buffer. In a repeat of the experiment the beads were washed with 20 mM glycine pH 8 and 0.5 M NaCl instead of 1 M Tris pH 8.5. Using glycine and NaCl

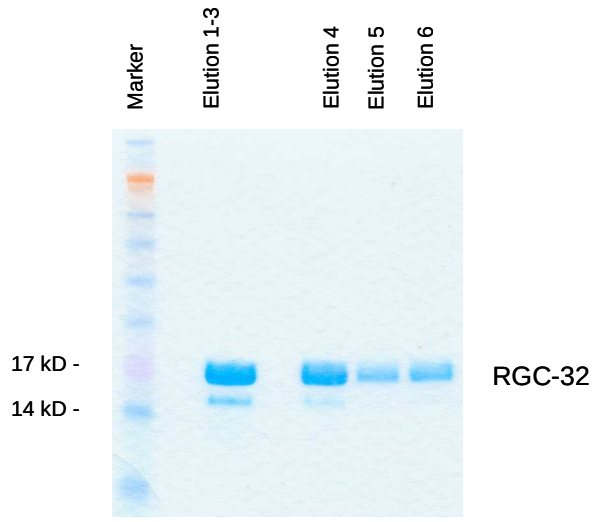

Figure 45 - Different elutions of purified His-RGC-32 protein were loaded to a 10% NuPAGE Novex Bis-Tris gel and run in MES running buffer (Invitrogen). After completion the gel was washed 3x 5 minutes with filter-sterilised water followed by 1 hour of Coomassie staining (Bio-Rad). The gel was dried onto filter paper.

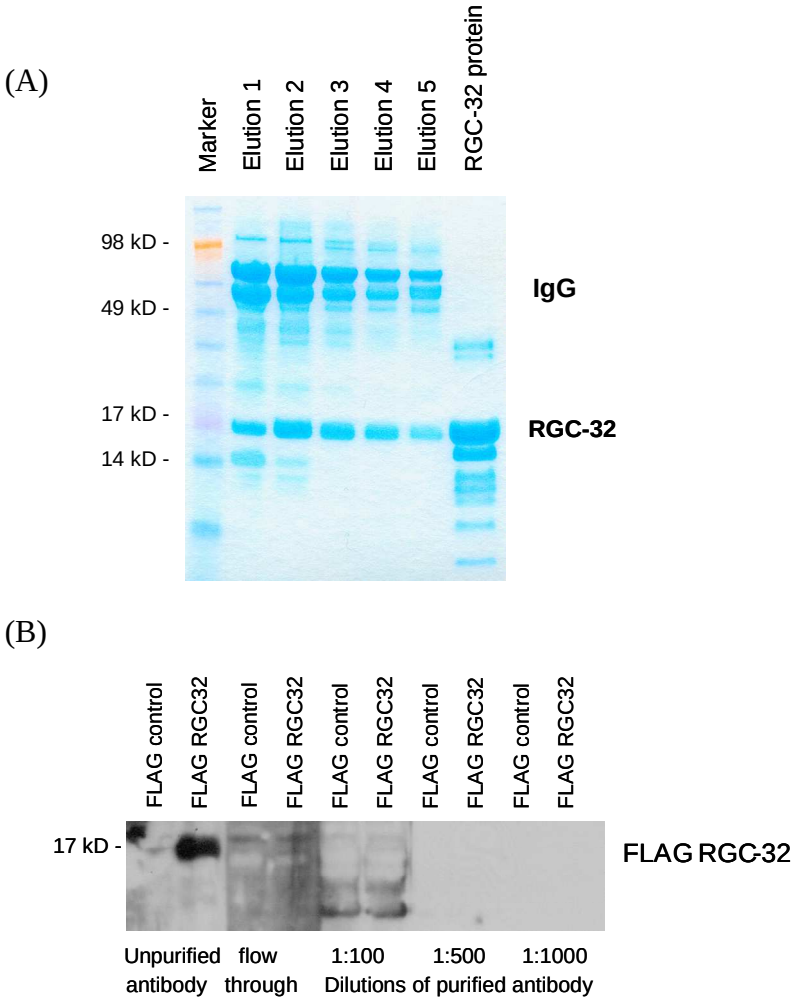

Figure 46 – Cell lysates were loaded to a 10% NuPAGE Novex Bis-Tris gel and run in MES buffer (Invitrogen). **(A)** Different elutions of purified antibody samples as well as purified His-RGC-32 protein were loaded to a 10% NuPAGE Novex Bis-Tris gel and run in MES running buffer (Invitrogen). After completion the gel was washed 3x 5 minutes with filter-sterilised water followed by 1 hour of Coomassie staining (Bio-Rad). The gel was dried onto filter paper. **(B)** Cell lysates of DG75 cells transfected with 40 µg pFLAG empty vector or pFLAG-RGC-32 were separated in a 10% NuPAGE Novex Bis-Tris gel in MES running buffer (Invitrogen). Original rabbit serum 2818 (1:500), flow-through of antibodies after binding to column (1:500) and different dilutions of anti-RGC-32 antibodies (1:100, 1:500, 1:1000) purified using Nickel agarose beads were used to detect FLAG RGC-32. Bands were visualised with ECL.

to wash the resin, the RGC-32 protein remained bound to the beads. The rabbit serum was added to allow the antibodies to bind to the protein. After several washing steps the antibody was eluted with 10 mM glycine pH 1. The purified antibody was then tested for RGC-32 specificity by Western blot analysis. Again, the purified anti-RGC-32 antibodies could not detect the protein (Figure 47). Bradford Assay results showed a very low protein concentration in the eluates which indicated that the antibody might not have bound well to the resin or has eluted during washing steps.

In a third attempt, the rabbit serum was purified using the Prosep-A® Montage® Antibody Purification Kit from Millipore. 10 ml of rabbit 2818 final bleed serum was added to the Montage spin column. Bradford assay analysis of the applied sample compared to the flow through confirmed that 37% of the serum protein content had bound to the column. The relatively low binding efficiency was probably due to overloading of the column as no maximum binding capacity was recommended by the supplier. The column was then washed twice with Binding buffer A (Millipore). However, the first wash contained 64% of the protein which was thought to have been bound to the column. With the second wash another 7% of the protein came off the column. When the remaining protein was finally eluted with Elution Buffer B2 (Millipore), the eluate only contained 2% of the originally bound protein and only 0.8% of the entire protein applied to the column. Coomassie staining showed that protein was only visible in the starting material, the flow through and after the first wash (Figure 48A). Although the protein content was very low, the antibody was tested in a Western blot using a dilution of 1:40. The purified antibody could not detect the RGC-32 protein (Figure 48B, bottom panel) in cell lines which previously showed detectable levels of RGC-32 (Figure 48B, top panel).

The eluted antibody was then concentrated using an Amicon® Ultra-15 Centrifugal filter (30,000 NMWL Ultracel®). Using this filter the volume of the elution containing the antibodies could be reduced from 10 ml to 500 µl. Therefore, the antibody concentration could be increased by up to 20-fold.

The concentrated antibody was tested using a titration of 1:100 – 1:5000. Western blot analysis revealed that FLAG RGC-32 could be detected in the dilutions 1:100, 1:200,

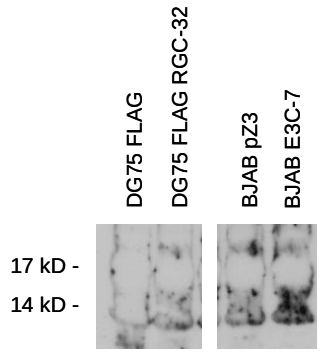

Figure 47 –Transiently transfected DG75 cells as well as BJAB pZ3 and E3C-7 were tested for RGC-32 specificity of the anti-RGC-32 antibodies which were purified using a CH sepharose column. Cell lysates were loaded to a 10% NuPAGE Novex Bis-Tris gel and run in MES buffer (Invitrogen). The purified serum was used at 1:100 dilution. Bands were visualised with ECL.

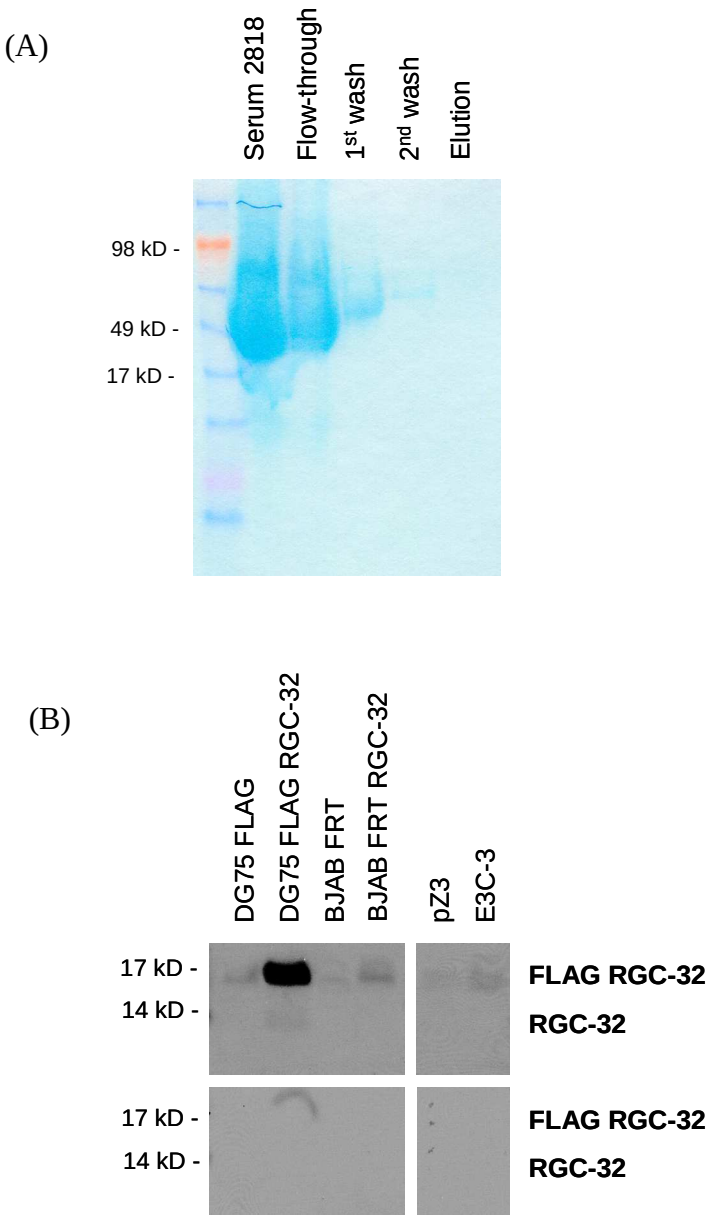

Figure 48 – Coomassie and Western blot analysis using purified anti-RGC-32 antibodies. **(A)** Samples taken at different stages of the antibody purification were loaded to a 10% NuPAGE Novex Bis-Tris gel and run in MES running buffer (Invitrogen). After completion the gel was washed 3x 5 minutes with filter-sterilised water followed by 1 hour of Coomassie staining (Bio-Rad). The gel was dried onto filter paper. **(B)** Transiently tranfected DG75 cells as well as BJAB pZ3 and E3C-3 were tested for RGC-32 specificity of the anti-RGC-32 antibodies which were purified using the Prosep-A® Montage® antibody purification kit. The top panel shows the Western blot probed with the original serum 2818 (1:750) and the bottom panel with the purified serum (1:40). Bands were visualised with ECL.

1:300 and 1:500 and weakly in 1:1000 (Figure 49A). The purified antibody appeared to be much cleaner and background detection was clearly reduced. Therefore, BJAB FRT, EBNA 3C-postive BJAB and DG75 cells transiently overexpressing RGC-32 were tested for RGC-32 protein expression using a 1:200 dilution of the purified anti-RGC-32 serum. Western blot analysis demonstrated that the purified antibody was able to detect FLAG-RGC-32 overexpressed in DG75 but not in BJAB cells and could not visualise endogenous RGC-32 protein of any cell line including E3C-3 cells in which RGC-32 mRNA is overexpressed (Figure 49B).

This result indicated that the antibody appeared to give cleaner detection of RGC-32, but it also seemed to be weaker. Therefore, it can be concluded that the purified anti-RGC-32 gives a cleaner result but can only detect protein which is expressed at a relatively high level.

The original anti-RGC-32 serum 2818 was able to detect overexpressing RGC-32 protein but endogenous RGC-32 could not be detected in EBNA 3C-positive BJAB cell lines with either the original or the purified antibody. Therefore, we decided to use the original serum for further experiments and investigated the reasons for the difficulties of RGC-32 protein detection in BJAB cells.

5.4 RGC-32 is not actively degraded by the proteasome

The anti-RGC-32 serum 2818 was able to detect RGC-32 protein in DG75 and BJAB cells overexpressing FLAG-RGC-32. However, endogenous RGC-32 could not be detected in BJAB E3C-3 showing a 6.5-fold mRNA upregulation compared to EBNA 3C-negative BJAB pZ3 cells. Therefore, it could be possible that the protein is actively degraded by the proteasome in BJAB cells which could occur directly after or during protein synthesis, so the protein is only active for a short time in the cell which is known to occur with cell cycle regulators such as cyclins. To prevent protein degradation by the proteasome, the cells were treated with 50 µM MG132, a proteasome inhibitor, for 1, 2, 8 or 24 hours then harvested and lysed. However, Western blotting did not confirm the suggestion that RGC-32 was actively degraded in BJAB cells as protein levels remained undetectable in the presence of MG132 (Figure 50). In addition,

(A)

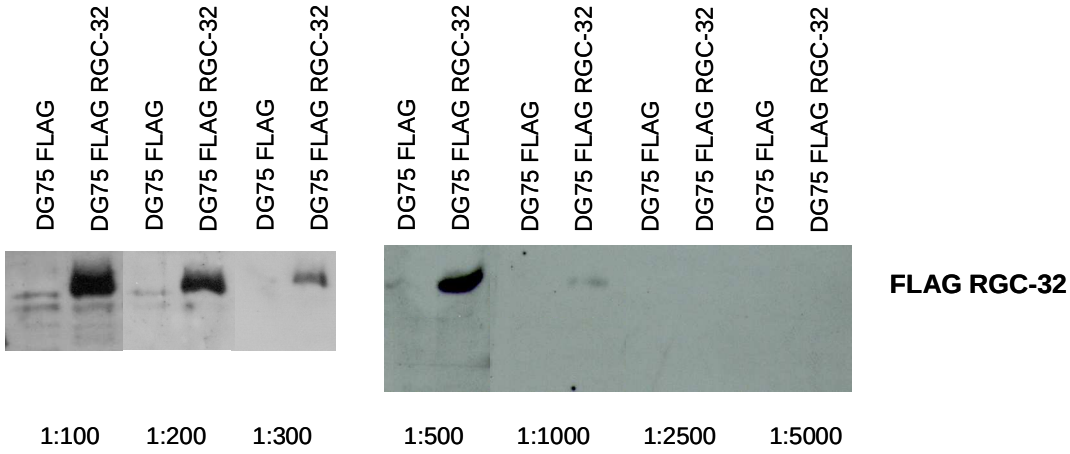

(B)

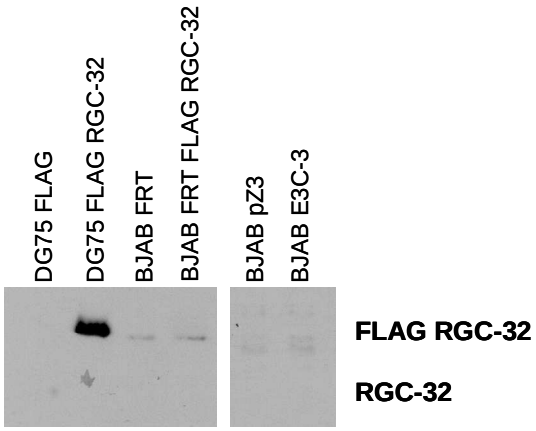

Figure 49 – Western blot analysis of whole cell lysates using the purified anti-RGC-32 serum. **(A)** Lysates of DG75 cells transiently transfected with either empty FLAG vector or FLAG RGC-32 were loaded to a 10% NuPAGE Novex Bis-Tris gel and run in MES running buffer (Invitrogen). The different blots were incubated with several titrations (1:100 – 1:5000) of the Prosep-A® Montage®-purified anti-RGC-32 serum. **(B)** Transiently transfected DG75 cells as well as BJAB pZ3 and E3C-3 were tested for RGC-32 specificity of the anti-RGC-32 serum 2818 which was purified using the Prosep-A® Montage® antibody purification kit. The Western blot was probed with the purified serum (1:200). Bands were visualised with ECL.

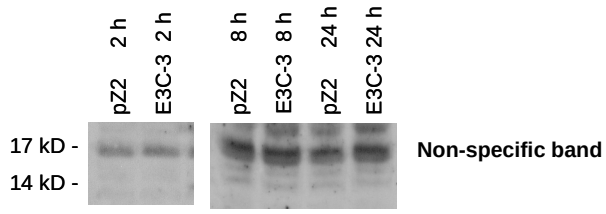

Figure 50 – Western blot analysis of BJAB cells pZ2 and E3C-3 after treatment with 50 μM MG132 harvested after 2, 8 and 24 h. The blots were probed with rabbit serum 2818 (1:500, final bleed). Bands were visualised with ECL.

higher concentrations (100 or 200 µM) of MG132 did not increase RGC-32 protein levels in BJAB cells (data not shown). Therefore, it does not appear that failure to detect RGC-32 protein results from rapid degradation of the protein.

5.5 RGC-32 expression in BJAB cells is not dependent on the cell cycle phase

Since RGC-32 was not found to be degraded in BJAB cells and purified anti-RGC-32 serum 2818 could not detect endogenous RGC-32 in BJAB cells, other approaches were considered as to why endogenous RGC-32 protein was undetectable in BJAB E3C-3. To investigate whether the protein is expressed in a cell cycle phase-specific manner and therefore undetectable in asynchronous cell cultures, BJAB pZ3 and E3C-3 cells were fractionated using centrifugal elutriation (kindly performed by Aloys Schepers, University of Munich). Cell cycle fractions were analysed by Western blotting and probed with rabbit serum 2818 (final bleed). However, no RGC-32 protein band was found at the expected endogenous size of approximately 14 kD in any cell cycle phase (Figure 51). EBNA 3C protein expression was confirmed using an anti-EBNA 3C antibody. The EBNA 3C protein levels appeared to be increasing towards mitosis but this might be due to unequal gel loading since the actin control shows an increased signal in the E3C-3 G2/M sample.

Further experiments were carried out to investigate the possibility that RGC-32 was degrading or precipitating during sample preparation. However, RGC-32 could not be detected in fresh BJAB cell lysates (data not shown). Another attempt was to change the ingredients of the lysis buffer (1x GSB, see section 2.2) which was used to lyse cells for whole cell lysates. The Tris was replaced by 40 mM phosphate buffer since RGC-32 precipitated in Tris which was discovered during the RGC-32 antibody purification. Western blot analysis of cell samples lysed in 1xGSB without Tris showed that the RGC-32 was still undetectable (data not shown). RIPA buffer was also used for initial cell lysis followed by addition GSB buffer but with no improvement of RGC-32 protein detection (data not shown).

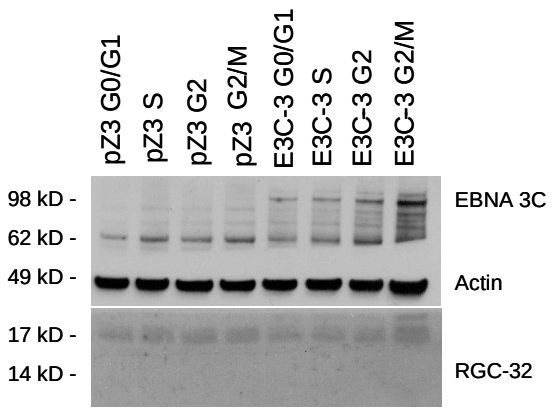

Figure 51 – Western blot analysis. Proteins of BJAB cell lysates of cell cycle fractions were separated in a 10% NuPAGE Novex Bis-Tris gel in MES running buffer (Invitrogen). Proteins were detected using anti-EBNA 3C A10 (1:300), anti-Actin antibody (Sigma) or rabbit serum 2818 against RGC-32 protein (1:500, final bleed). Bands were visualised with ECL.

5.6 Discussion

To detect the RGC-32 protein a specific antibody needed to be generated. Sera from two rabbits (2817 and 2818) were obtained after immunisation with RGC-32 protein since no commercial antibody is available to detect the protein. Sera from rabbit 2818 were able to detect the RGC-32 protein when it was overexpressed after transient transfection of EBV-negative DG75 cells. Sera from rabbit 2817 failed to detect the protein. Endogenous RGC-32 protein, however, has not been detectable in BJAB cells with upregulated RGC-32 mRNA to date.

Other approaches carried out to attempt to visualise endogenous RGC-32 protein in BJAB cells included analysis of fresh lysates, changes to the lysis buffer and immunoprecipitation using the anti-RGC-32 serum. However, all these attempts did not result in endogenous RGC-32 detection. Further, analysis of cell cycle fractions did not reveal that RGC-32 was expressed in a cell cycle phase-dependent way in BJAB cells.

Since endogenous RGC-32 protein could not be detected and the anti-RGC-32 serum bound many non-specific proteins, the anti-RGC-32 serum 2818 was purified to increase the specificity for RGC-32. The recombinant His-tagged RGC-32 protein was able to bind to the HIS-Select® Nickel Affinity Gel (Sigma). The binding was increased by crosslinking with DSS (disuccinimidyl suberate) which is a bifunctional crosslinker and contains two N-hydroxysuccinimide esters. These esters are able to interact with primary amines which are present at the N-terminus of each polypeptide chain and in the side chain of lysine residues. Therefore, the binding of the His-tag on the N-terminus of the recombinant RGC-32 to the Nickel beads should be increased by the crosslinker. However, as the Coomassie staining showed some of the RGC-32 protein was eluted as well as the antibody. Further, in the first elution the pH was not low enough to allow the antibody to be eluted through disruption of antibody-protein interactions but protein was lost from the column. Increases in pH did not increase the protein content in the eluates. The loss of the protein from the column may have resulted from overloading or aggregation since protein characterisation for crystalisation studies has revealed that RGC-32 forms aggregates of very high molecular weight. Therefore, the low binding efficiency could be caused by aggregation of the RGC-32 protein, thus not all protein molecules could bind to the column and may have been

eluted during washing steps. Since Western blot analysis revealed that the purified antibodies did not display increased specificity for RGC-32, an alternative purification method was attempted. CH sepharose is also known to react with primary amines and therefore with the amino terminus of a protein. 90% of the input protein was able to bind the resin which confirms the efficiency of the binding. However, the precipitation of RGC-32 in Tris buffers may have led to elution of the protein during the washing steps. In a repeat of the experiment Tris was replaced with 20 mM glycine and 0.5 M NaCl. 75% of the input protein bound to the resin in the second attempt, but 50% of the originally bound protein eluted during washing steps probably due to the aggregation problem. The loss of protein was most likely crucial, since Western blot analysis revealed again that the purification of the RGC-32-specific antibodies failed. Protein assays revealed only low protein content could be measured in the final eluate which contained the antibodies.

Since the purification techniques did not improve the result, we decided in a last attempt to use an alternative to purify the Ig molecules from the serum rather than RGC-32-specific antibodies using the Montage® Antibody Purification Kit (Millipore). 37% of the protein applied to the column was able to bind, possibly due to overloading of the column as the supplier did not specify a maximum loading capacity for serum. Another possibility could be that lipids in the serum could have affected the binding efficiency. During several washing steps more antibody was unexpectedly eluted which might have been again due to the aggregation of the RGC-32 protein resulting in elution of RGC-32 protein/antibody complexes. Although 2% of the originally bound protein (0.8% of the entire protein applied to the column) was finally eluted it could not detect the RGC-32 protein. Subsequent concentration of the sample produced an antibody preparation that was able to detect RGC-32 in overexpressing DG75 cells but not in BJAB. Therefore, it can be concluded that the purified anti-RGC-32 gives a cleaner result but can only detect protein which is expressed at a relatively high level and may not be efficient enough to detect endogenous RGC-32. For all my further experiments, I therefore used the original anti-RGC-32 unpurified serum.

Surprisingly, the EBNA 3C-expressing BJAB cell line E3C-3 which showed a 14-fold higher expression of RGC-32 mRNA compared to BJAB pZ2 did not express detectable

protein. This observation led to the suggestion that the RGC-32 protein was degraded either during or after translation thus hampering detection. However, treatment of the BJAB cell lines pZ2 and E3C-3 with the proteasome inhibitor MG132 did not increase the RGC-32 protein expression making this possibility unlikely.

6 Regulation in B cells - interplay between RUNX and RGC-32

6.1 Introduction

During the course of this study it was reported that knockdown of the transcription factor RUNX1 resulted in reduced RGC-32 mRNA expression in rat periovulatory cells (Jo and Curry, 2006). Subsequent studies indentified RUNX binding sites in the rat RGC-32 promoter (Park et al., 2008). RUNX family proteins play key roles in B lymphogenesis and have been shown to be differentially expressed in different forms of EBV latency (Spender et al., 2002a; Spender et al., 2005a). This differential regulation results from the upregulation of RUNX3 transcription by EBNA 2 in EBV-positive cells exhibiting the latency III phenotype (Spender et al., 2005a). RUNX3 directly represses transcription of RUNX1 leading to RUNX1 downregulation in latency III (Spender et al., 2005a).

6.2 RGC-32 and RUNX1 mRNA expression is upregulated in latency I compared to latency III

Initial experiments were carried out to verify differential RUNX1 and RUNX3 expression in a panel of EBV-negative and EBV-positive B cell lines. Real-time PCR results revealed that RUNX1 mRNA expression was variable in EBV-negative cell lines but generally expression was increased in Burkitt's lymphoma group I cell lines and cell lines which have a deletion of the EBNA 2 gene compared to cell lines displaying a latency III pattern of gene expression (Figure 52A). These results are consistent with previously published data and western blot analysis confirmed that RUNX1 protein expression was similar to mRNA expression in the cell panel (Figure 52B), (Spender et al., 2002a).

RUNX3 mRNA expression was also found to broadly follow the reported pattern of higher expression in latency III cell lines compared to latency I cell lines and was expressed in EBV-negative cell lines at a similar level to latency III lines (Figure 53A). The RUNX3 mRNA levels for EBNA 2-deleted cell lines varied with Daudi and OKU showing expected lower levels but Sal and P3HR1 displaying higher mRNA levels. It is important to note

(A)

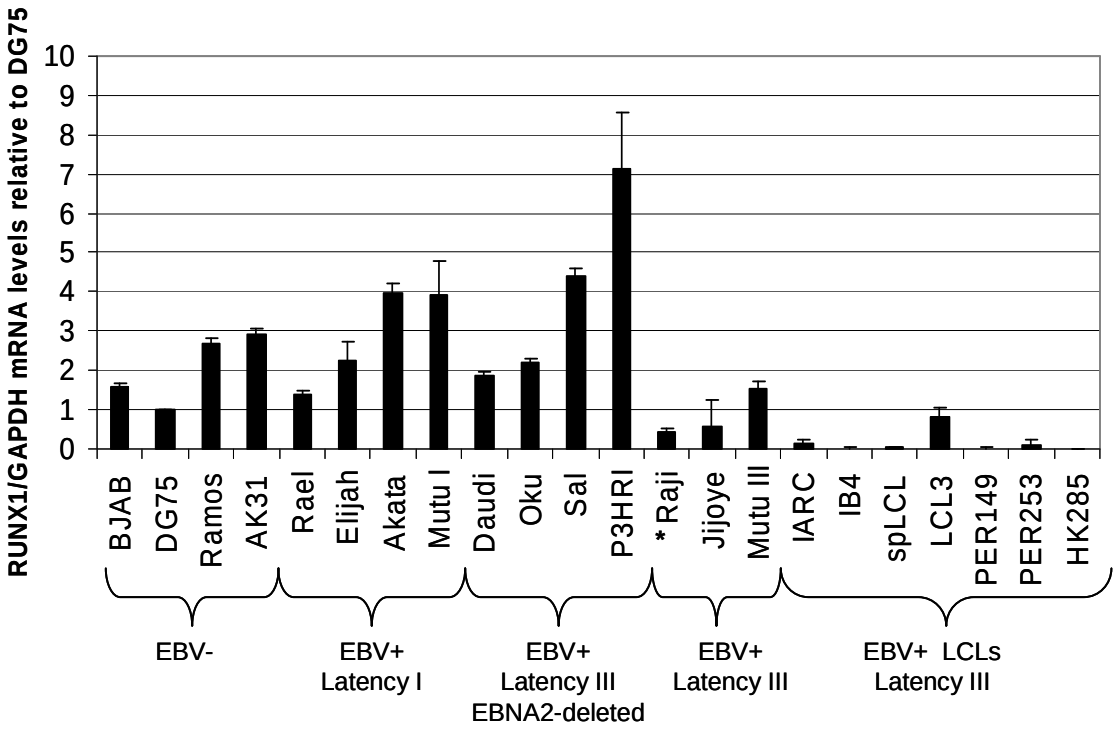

(B)

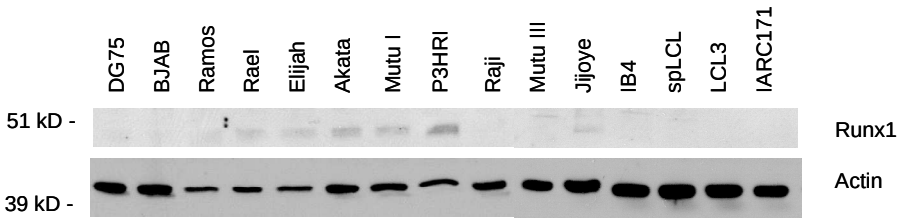

Figure 52 – RUNX1 mRNA and protein expression. (A) Real-time PCR analysis of cell panel cDNA was carried out in duplicate and normalised to GAPDH expression. The graph shows the mean of 3 independent experiments +/- standard deviation. *Raji cells have a deletion of the EBNA 3C gene. **(B)** Western blot analysis. Cell lysates were separated using a 10% NuPAGE Novex Bis-Tris gel in MOPS running buffer (Invitrogen). Proteins were detected using anti-RUNX1 (1:40, Calbiochem, ab-2) and anti-Actin antibody (1:5000, Sigma). Bands were visualised with ECL.

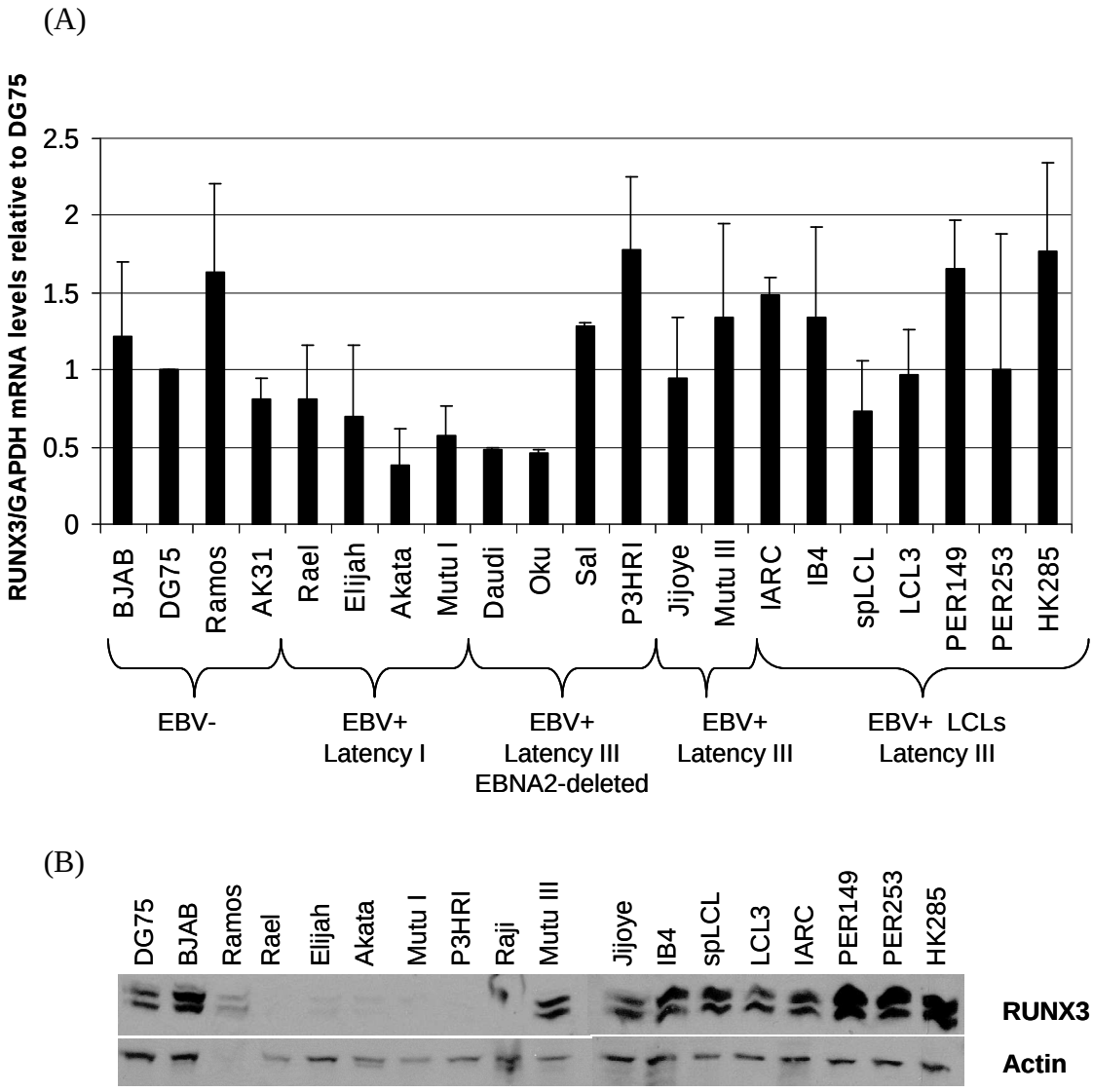

Figure 53 – RUNX3 mRNA and protein expression. (A) Real-time PCR analysis of cell panel cDNA was carried out in duplicate and normalised to GAPDH expression. The graph shows the mean of 3 independent experiments +/- standard deviation. **(B)** Western blot analysis. Proteins of cell lysates were separated using a 10% NuPAGE Novex Bis-Tris gel in MOPS running buffer (Invitrogen). Proteins were detected using anti-RUNX3 (1:500, Calbiochem) and anti-Actin antibody (1:5000, Sigma). Bands were visualised with ECL.

however that RUNX3 real-time results were quite variable reflected in the larger error bars for the some cell lines. Western blot analysis showed a much clearer upregulation of RUNX3 protein in latency III-expressing cell lines and reduced protein levels in latency I-expressing cell lines (Figure 53B). RUNX3 protein expression in EBV-negative cell lines was similar to latency III-expressing cell lines.

Significantly when real-time PCR analysis of RGC-32 mRNA expression levels was carried out, the results showed that they correlated well with RUNX1 expression levels in the cell panel. Thus, RGC-32 was expressed at highest levels in EBV-positive group I Burkitt's lymphoma cell lines and at lowest levels in EBV-negative, latency III-expressing Burkitt's lymphoma cells lines and LCLs (Figure 54A). RGC-32 mRNA expression for EBNA 2-deleted latency III-expressing cells varied. These results indicated that RGC-32 could be regulated by RUNX1 in human B cells.

6.3 RUNX1 activates the RGC-32 promoter

Luciferase reporter assays were carried out to investigate the effects of RUNX1c on the RGC-32 promoter. DG75 cells were transfected by electroporation with increasing amounts of the RUNX1c-expressing plasmid pBK-CMV-RUNX1c, the B cell isoform of RUNX1 (Spender et al., 2005b). Figure 55 shows that the RGC-32 promoter is activated by up to 2.2-fold with increasing expression of RUNX1c indicating that RUNX1c is able to increase RGC-32 transcription in human B cells.

6.4 Investigations of the RUNX-binding sites of the RGC-32 promoter

Since RUNX1 was able to activate RGC-32 transcription, the promoter region used in the reporter construct (RGC-32pLuc) was examined for RUNX1-binding sites. RUNX family proteins all recognize the consensus sequence TGTGGT. A potential RUNX binding site (-777 to -772) was identified which was present in the RGC-32pluc promoter construct used for luciferase assays (Figure 56). Using the transcription factor binding prediction program MatInspector (http://www.genomatix.de/online_help/help_matinspector/matinspector_help) another RUNX-binding site was found in further upstream sequences of the RGC-32 promoter which were not included in the pGL2-RGC-32pluc construct. Therefore, a plasmid containing the previously cloned sequence

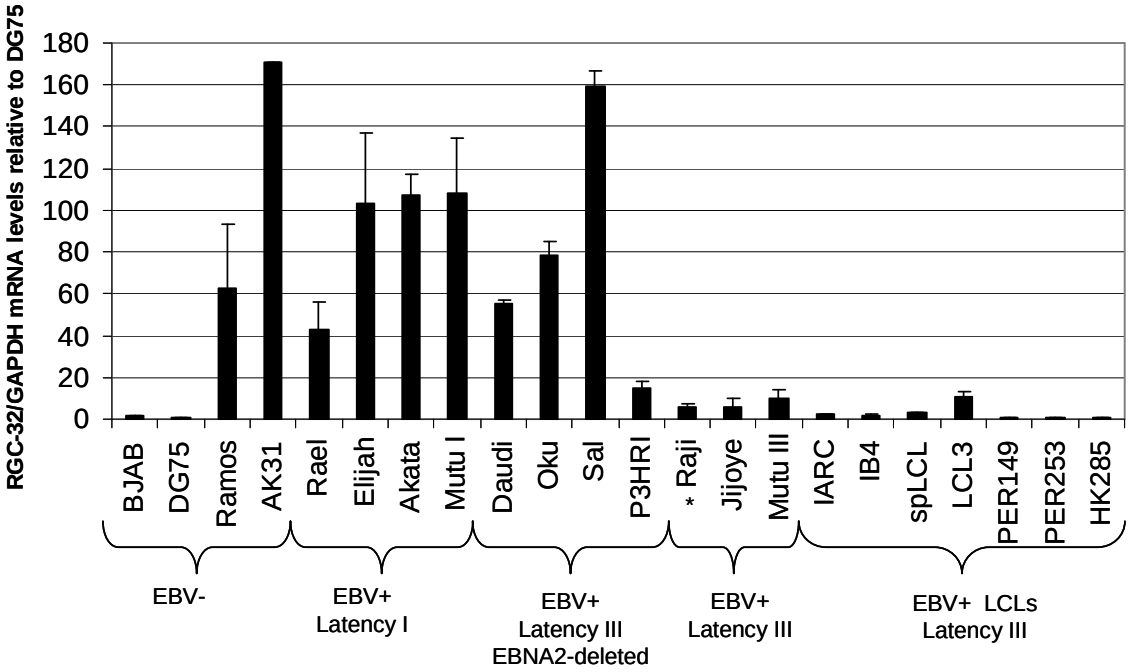

Figure 54 – RGC-32 mRNA expression. Real-time PCR analysis of cell panel cDNA was carried out in duplicate and normalised to GAPDH expression. The graph shows the mean of 3 independent experiments +/- standard deviation.

(A)

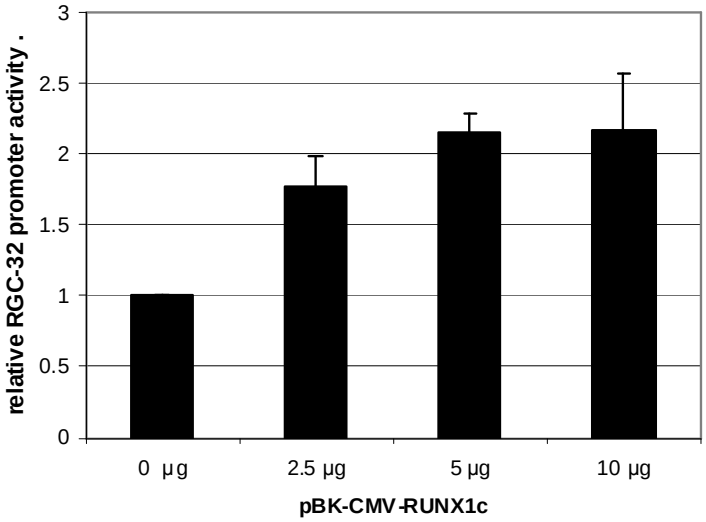

(B)

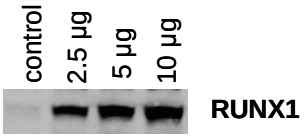

Figure 55 – Luciferase assay. DG75 cells were transiently transfected with different amounts of RUNX1c-expressing plasmid (pBK-CMV-RUNX1c), (2.5, 5 and 10 µg), 2 µg of a *Renilla* luciferase plasmid to determine the transfection efficiency and 4 µg of a firefly luciferase reporter plasmid containing the RGC-32 promoter. **(A)** This graph shows the results of 3 independent experiments +/- standard deviation. The values for firefly luciferase activity (RGC-32 promoter activation) were corrected by dividing them by the values for the *Renilla* luciferase activity. RGC-32 promoter activation is displayed relative to the RUNX1-negative control. **(B)** Western blot analysis for RUNX1c (1:40, Calbiochem) expression.

```
- 1178 -  CGGGAGGT ACCGACAAGC ATATCCCTAG GCCACCCAGA GTAGACAAGA
- 1130 - GAGGAGGACT ATTCATATGA TTAGTGGTCA TTAACATATA CTCCTTTGTG
- 1080 - AGGTGTATGT TTCAATGTTT TGCTCATTTT TAATTTTTAC CAGGTTGTCT
- 1030 - ATTTGTGATT ACTTTGTAGA TGGGTCTTTC TATATTCTGA AAACAAATCC
 - 980 - TGGCTGGGTG CGGTGGCTCA CGCCTGTAAT CCCAGCACTT TGGGAGGCTG
 - 930 - AGGTGGGCAG ATCACCTGAG GTCGGGAGTT CGAGACCAGC CTGGCCAACA
 - 880 - TGGACAAACC CCGTCTCTGC TAAAAATACA AAAACTAGCT GGGAGTGGAG
 - 830 - GCTGAATGTT TCACTCCGTT ACATGTTAAT TGCTCTACAT TTAATTAGCC
 - 780 - GTCTGTGGTG AGAGGCGAGA GGCTAGCGCC TAGCTCAGCG CACAGTCCAG
 - 730 - GGCGTTCGCC CCCGCAGGCC GCGGGGCAGG GTGGCTCGTT ACTCCGTGGA
 - 680 - CACTGCAAGG CGCCCTGTTC GCGCTGCGTC GACGCAGTAG TTTCTTCCCA
 - 630 - TAATAAACCC CTTCTAGATA AAGTCAGGCT GGCGGGAGCG CCCTGGACCG
 - 580 - TAGTTCAGGC CCCCGCGCTC CGCGGTGGGA ACAGTTCAGG ACTCCCCCAA
 - 530 - CTCCTGCCCC TCTCGCCCCG ACCCTCTCCA CTCCGCCCGC CCACCATCTC
 - 480 - GGAAGTCCCC TTGGGACAAT GCGTAGGGGA CCTCCGCGTC CCCGACACCC
 - 430 - GACTGGGACA CGGCCGCGGG CTCCTTCGTC CCTCACCGCC AGCCAGGGAG
 - 380 - GCTCTGCATG CCCACGTCCA CTTCACAGCC GAGGAAGCTG CGGCTCGCGG
 - 330 - AGGTGCCTGG CACGCGGCGG GAAGCAGCAG AGCTCGCGCC CAGCAGTCAG
 - 280 - CTCTGGTGAC GCCGAGGACA CCGCGTGGGC CGGGTTGTCA GGGCGCGGGG
 - 230 - GCGAGAGGCG GGTAAATATT TGGGGCTGTA ACCGGGGCTT CGGCGACTCC
 - 180 - TCGTCACCGC GGTTCCAGGG CGGGCGCGTG GCGAGGGCGG TGCCTGGGGG
 - 130 - CAGGGGCCTC CTCGGAGGGC GGCGGGGACA GACCCGTCGC CCCGGCTCCG
  - 80 - CAGCCCCGCC CCGGCCCCGC CTCCGCTCCG GCCGCCGAAG GCTATAAGAT
  - 30 - CTAGGAACCC GAGCCGGTGG TAGGGCGGGC GCGGACCGTG CTGGGAGCGG
 + 21 - CGCGGCTGGA GCGCAGCGCC GAAGGGACTG GCAGGGCTGA AGTGTGCGGG
 + 71 - ACAGCAAGCA AGCTTGGCAT TCCGGTACTG TTGGTAAAAT GGAAGACGCC
+ 121 - AAAAACATAA AGAAAGGCCC GGCGCCATTC TATCCTCTAG AGGATGGAAC
+ 171 - CGCTGGAGAG CAACTGCATA AGGCTATGAA GA
```

Figure 56 – RGC-32 promoter sequences within the RGC-32pluc plasmid. The enzyme restriction sites are highlighted in different colours: KpnI (red), HindIII (turquoise), XbaI (light gray), NheI (yellow). The RUNX-binding site used for mutation is highlighted in pink, additional RUNX-binding sites are highlighted in dark red. The transcription start site is highlighted in dark yellow. The point mutation from C to T is highlighted in dark grey.

as well as an additional upstream sequence (pGL2-RGC-32pluc-up) was created in the lab by Felicity Poulter. Luciferase assay results revealed that the additional RUNX-binding site did not have an augmenting effect on the RGC-32 promoter activity indicating that it may be non-functional (Figure 57A).

To verify whether RUNX1c binds and activates the RGC-32 promoter via the RUNX-binding site in the original promoter construct, site-directed mutagenesis was performed to mutate the RUNX binding site from TGTGGT to TGCTTT which has been previously shown to abrogate RUNX1-binding (Bristow and Shore, 2003). Sequencing analysis of the plasmid confirmed the 3 bp mutation of the RUNX-binding site, however, a random point mutation further downstream from the RUNX-binding site was also detected. An RGC-32 promoter fragment from -1160 to -750 (KpnI/NheI fragment) excluding the mutation was therefore subcloned. To update the luciferase reporter plasmid from the pGL2 to the pGL3 background, subcloning of this fragment was carried out, in conjunction with the downstream promoter region from the original RGC-32pLuc plasmid into pGL3 basic. Sequencing results revealed that the subcloning was successful, but despite the attempt to revert to the original promoter sequence to avoid the point mutation from C to T, this base was again mutated. Since sequencing of the original RGC-32pLuc plasmid did not contain this point mutation, the mutation of the wild-type plasmid may have occurred during repeated plasmid preparations.

The pGL3-RGC-32pluc construct containing the RGC-32 promoter was then tested for activation by RUNX1c. Luciferase assay results revealed a similar activation of the RGC-32 promoter of approximately up to 2.3-fold with increasing RUNX1c expression (Figure 57B). Surprisingly, the RGC-32 plasmid containing the mutated RUNX-binding site was also activated to the same extent by RUNX1c indicating that RUNX1c may activate RGC-32 through an alternative site.

Together these results suggest that RUNX1 does not bind the RGC-32 promoter directly via two of the identified RUNX-binding sites. Three more potential RUNX-binding sites present in the original RGC-32pLuc promoter construct need further investigation to identify whether RUNX1c targets the RGC-32 promoter via these sites. Another possibility may be that RUNX1 activates the RGC-32 promoter in an indirect manner

(A)

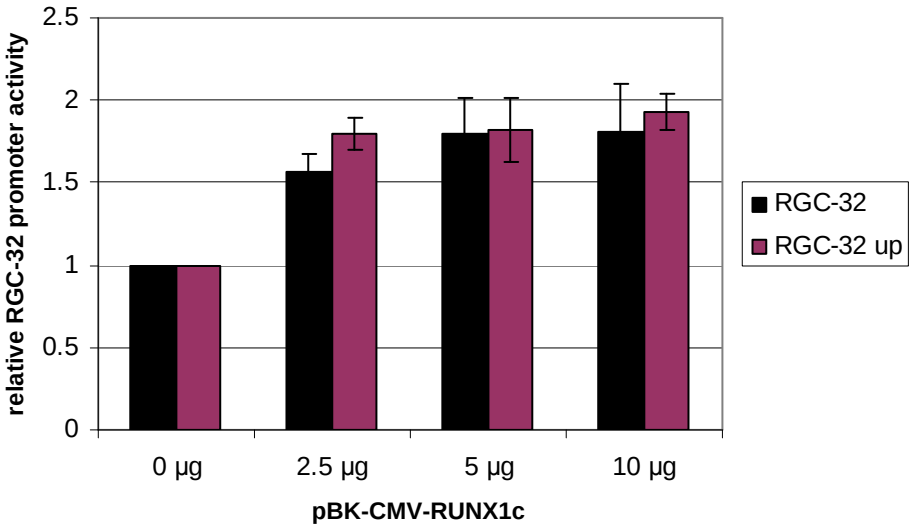

(B)

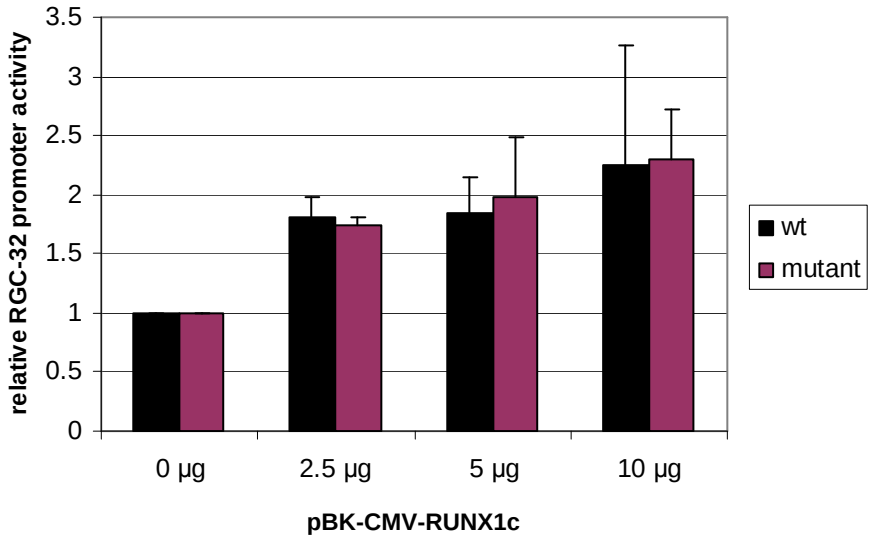

Figure 57 – DG75 cells were transiently transfected with increasing amounts of the RUNX1c-expressing plasmid (pBK-CMV-RUNX1c), (2.5, 5 and 10 µg), 2 µg of a *Renilla* luciferase plasmid to determine the transfection efficiency and 4 µg a firefly luciferase reporter plasmid containing **(A)** the RGC-32 promoter or the RGC-32 promoter with additional upstream sequences (RGC-32 up) containing an additional RUNX-binding site or **(B)** the RGC-32 promoter or the RGC-32 promoter with a mutated RUNX-binding site. The graph shows the results of 3 independent experiments +/- standard deviation. The values for firefly luciferase activity (RGC-32 promoter activation) were corrected by dividing them by the values for the *Renilla* luciferase activity. RGC-32 promoter activation is displayed relative to the RUNX1-negative control.

by upregulation of another transcriptional activator which may be able to bind the RGC-32 promoter and promote transcription.

6.5 Investigations of the role of RUNX3 in RGC-32 upregulation

Since RUNX family proteins recognise a common site, the other RUNX family member expressed in B cells, RUNX3, was examined for its effects on the RGC-32 promoter. Surprisingly, luciferase assay results showed that RUNX3 was able to activate the RGC-32 promoter to a similar extent as RUNX1c (2.3-fold) (Figure 58A). These results indicate that RUNX1c and RUNX3 are individually able to activate the RGC-32 promoter in transient reporter assays in DG75 cells. Western blotting confirmed the increasing amounts of RUNX proteins expressed (Figure 58A).

6.6 Investigating the effects of RUNX1 upregulation on RGC-32 *in vivo*

RUNX1 expression was shown to be downregulated when RUNX3 is expressed (Spender et al., 2005a). In turn, when RUNX3 is knocked down in LCLs, RUNX1c mRNA expression increases (Spender et al., 2005a). Interestingly, expression of RUNX1c in LCLs results in B cell death. Since RUNX1c was able to activate the RGC-32 promoter in reporter assays, the effects of increased endogenous RUNX1c expression were examined in LCLs. RUNX3 expression was reduced using siRNA-expressing plasmids (gift from Paul Farrell). The IB4 LCLs were transfected with the control empty vector or two different plasmids expressing RUNX3 siRNA (siRNA 30 and 118) which are hygromycin resistant. 24 hours after transfection hygromycin was added to the cells and samples taken after 6, 9 and 14 days. Real-time PCR analysis confirmed that the RUNX3 siRNA 30 decreased RUNX3 expression after 6 days and both plasmids efficiently reduced RGC-32 expression at 10 and 14 days post-transfection (Figure 59A). Western blot analysis also confirmed this at the protein level (Figure 59B).

(A)

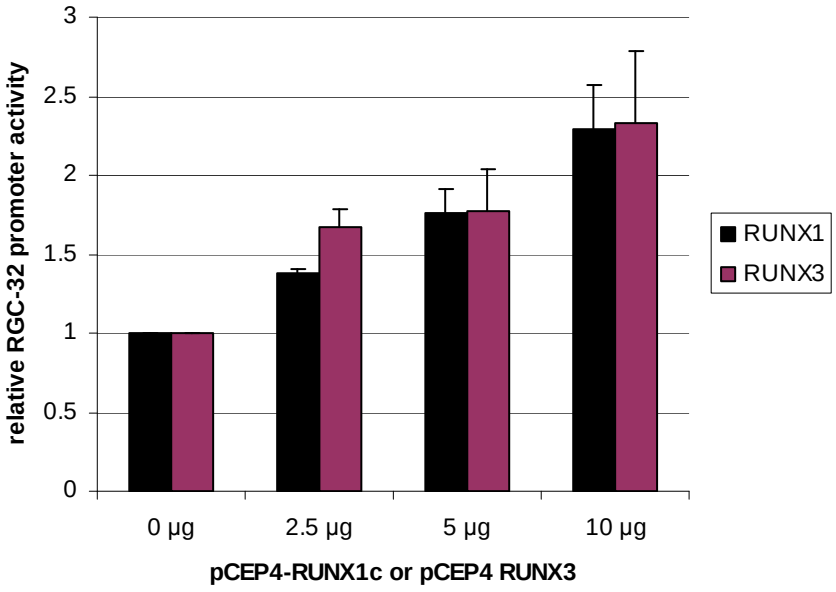

(B)

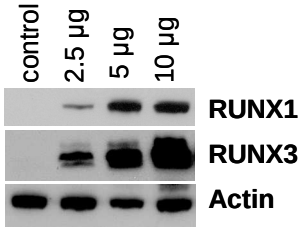

Figure 58 – DG75 cells were transiently transfected with increasing amounts of a RUNX1c-expressing plasmid (pCEP4-RUNX1c) or a RUNX3-expressing plasmid (pCEP4-RUNX3), (2.5, 5, 10 µg). All samples were also transfected with 2 µg of a *Renilla* luciferase plasmid to determine the transfection efficiency and 4 µg a firefly luciferase reporter plasmid containing the RGC-32 promoter (pGL2-RGC-32pluc). **(A)** This graph shows the mean of 2 independent experiments +/- standard deviation. The values for firefly luciferase activity (RGC-32 promoter activation) were corrected by dividing them by the values for the *Renilla* luciferase activity. RGC-32 promoter activity is displayed relative to the RUNX1/RUNX3-negative control. **(B)** Western blot analysis for RUNX1c (1:40, Calbiochem), RUNX3 (1:300, Calbiochem) and actin (1:5000, Sigma) expression.

(A)

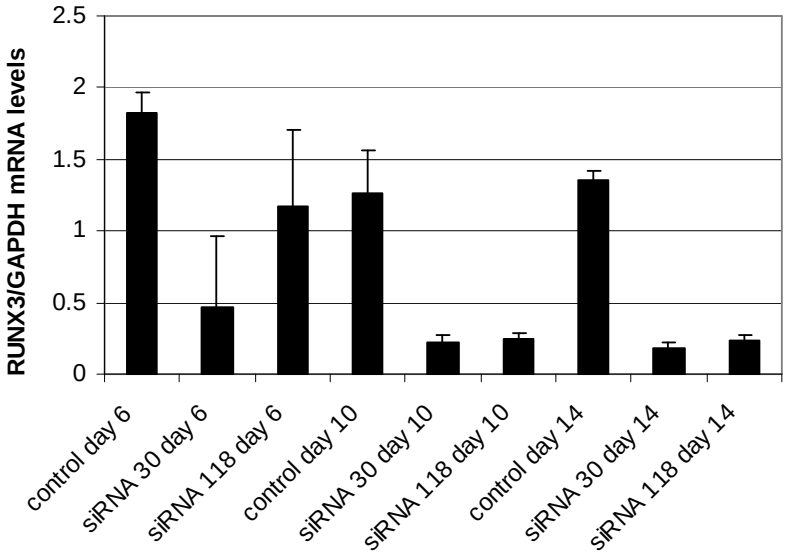

(B)

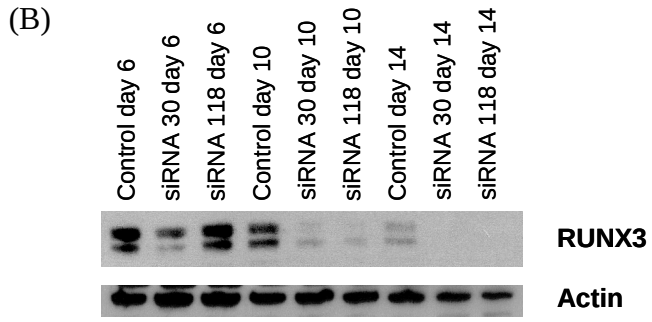

Figure 59 – IB4 cells were transfected with 3 μg of the control vector (pHEBoSUPER), the RUNX3 siRNA-expressing plasmid 30 or the RUNX3 siRNA 118 and grown for 14 days in the presence of 300 μg/ml hygromycin. **(A)** Real-time PCR analysis of samples harvested after 6, 10 or 14 days was carried out in duplicate. RUNX3 mRNA levels were normalised to GAPDH levels. The graph shows the mean of duplicates +/- standard deviation of a representative result from 3 similar experiments. **(B)** Protein samples were separated in a 10% NuPAGE Novex Bis-Tris gel in MOPS running buffer (Invitrogen) for Western blot analysis. Proteins were detected using anti-RUNX3 (1:500, Calbiochem) and anti-Actin antibody (1:5000, Sigma). Bands were visualised with ECL.

Consistent with previous findings, RUNX1c mRNA expression increased with time when RUNX3 was knocked down (Figure 60). However, RUNX1c protein expression could not be detected in IB4 cells (data not shown).

Interestingly, RGC-32 mRNA expression increased in a similar way to RUNX1c mRNA expression suggesting that RGC-32 expression correlates with RUNX1 expression and that RUNX1c may act as a transcriptional activator of the RGC-32 promoter (Figure 61A).

For completeness, attempts were also made to detect RGC-32 expression at the protein level using Western blotting with the crude RGC-32 rabbit serum. Surprisingly, the RGC-32 serum produced much less background in these later experiments and clearly detected a band of the expected molecular weight (14 kD) that was upregulated in line with RUNX1 upregulation in these cells (Figure 61B). Importantly, RGC-32 was also detected in day 6 control IB4 samples. RGC-32 expression in control samples appeared to be reduced to undetectable levels in later samples possibly due to the negative effects of RUNX1 on cell growth and may therefore correlate with increased cell death with time.

6.7 RGC-32 protein is differentially expressed in EBV latency

As a result of the detection of RGC-32 protein by Western blotting in IB4 cells, a panel of cell lysates was tested for RGC-32 protein expression. Western blot analysis revealed that RGC-32 protein was undetectable in EBV-negative B cell lines (consistent with our previous results) and in Burkitt's lymphoma group I lines and was only expressed in EBV-positive latency III cell lines (Figure 54 and Figure 62). This result was particularly surprising given that RGC-32 mRNA expression is lowest in EBV-negative and latency III cells and higher in latency I cells (Figure 54 and Figure 62).

Interestingly, two EBNA 2-deleted cell lines do not express RGC-32 protein (P3HR1 and Daudi). Taken together, these results suggest that high levels of RGC-32 mRNA do not drive protein expression in group I latency cell lines. It is possible that RGC-32 protein expression is blocked in these cell lines leading to mRNA accumulation and that efficient RGC-32 translation in group III latency cell lines results in mRNA degradation.

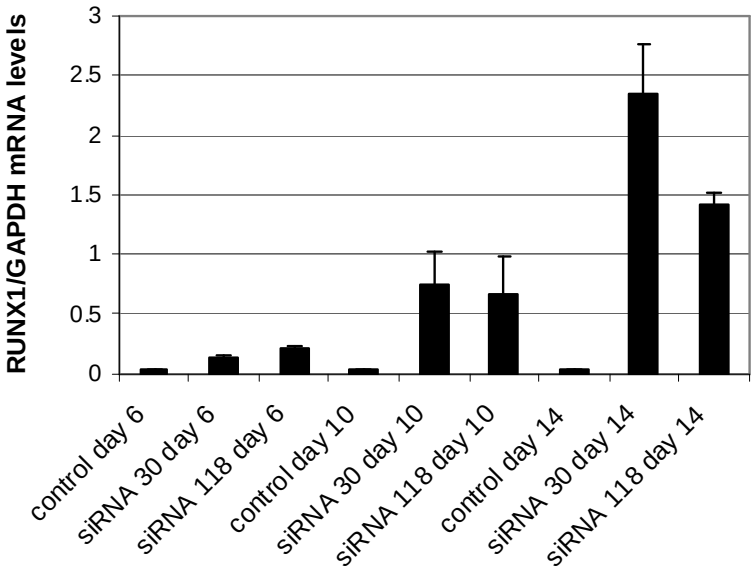

Figure 60 – IB4 cells were transfected with 3 μg of the control vector (pHEBoSUPER), the RUNX3 siRNA-expressing plasmid 30 or the RUNX3 siRNA 118 and grown for 14 days in the presence of 300 μg/ml hygromycin. Real-time PCR analysis of samples harvested after 6, 10 or 14 days was carried out in duplicate. RUNX3 mRNA levels were normalised to GAPDH levels. The graph shows the mean of duplicates +/- standard deviation of a representative result from 3 similar experiments.

(A)

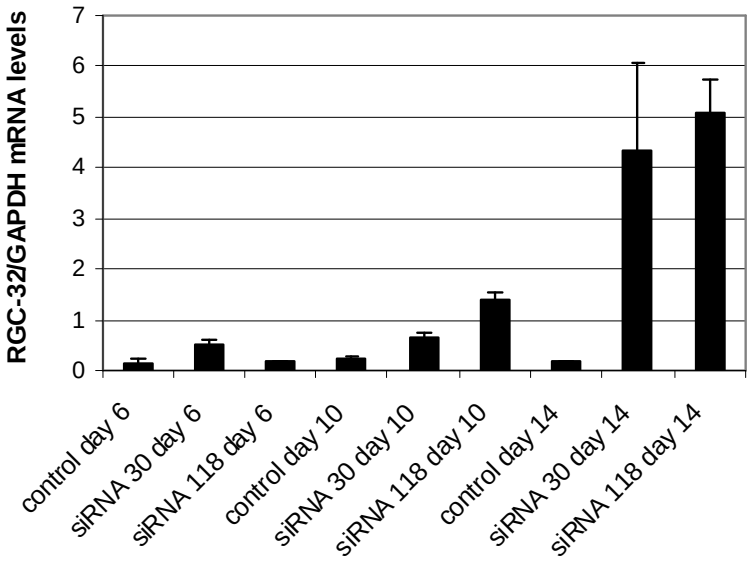

(B)

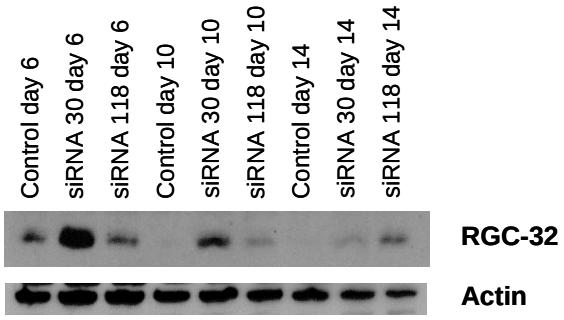

Figure 61 – IB4 cells were transfected with 3 μg of the control vector (pHEBoSUPER), the RUNX3 siRNA-expressing plasmid 30 or the RUNX3 siRNA 118 and grown for 14 days in the presence of 300 μg/ml hygromycin. **(A)** Real-time PCR analysis of samples harvested after 6, 10 or 14 days was carried out in duplicate. RUNX3 mRNA levels were normalised to GAPDH levels. The graph shows the mean of duplicates +/- standard deviation of a representative result from 3 similar experiments. **(B)** Protein samples were separated in a 10% NuPAGE Novex Bis-Tris gel in MES running buffer (Invitrogen) for Western blot analysis. Proteins were detected using anti-RGC-32 serum 2818 (1:750, final bleed) and anti-actin antibody (1:5000, Sigma). Bands were visualised with ECL.

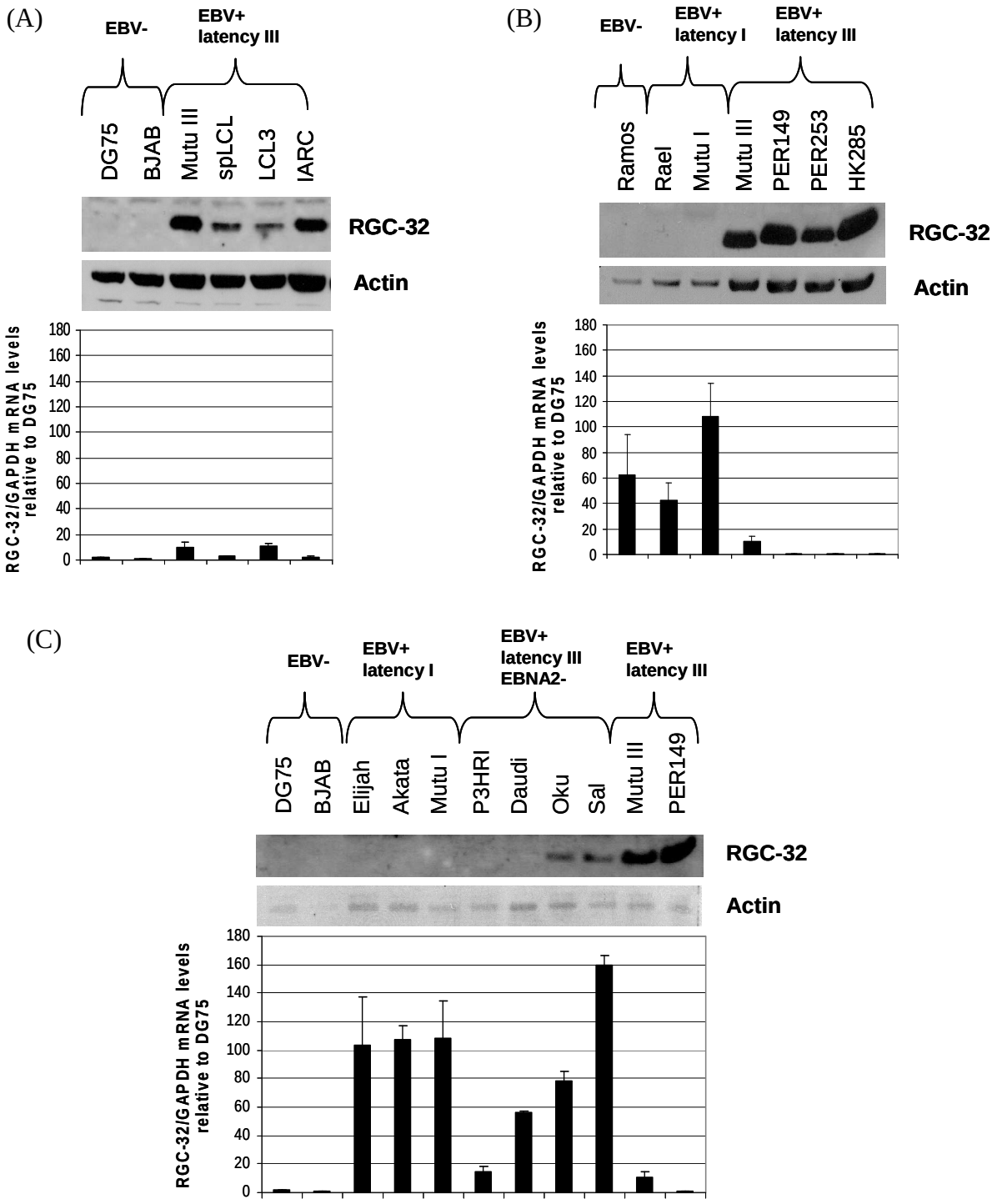

Figure 62 - (A+B+C) Proteins of different cell lines were separated in a 10% NuPAGE Novex Bis-Tris gel in MES running buffer (Invitrogen). Proteins were detected using anti-RGC-32 serum (1:750, final bleed) and anti-actin antibody (1:5000, Sigma). Bands were visualised with ECL. Real-time PCR analysis of respective cDNA is shown below each Western blot and was carried out in duplicate and normalised to GAPDH expression. The graph shows the mean of 3 independent experiments +/- standard deviation.

Significantly, despite no obvious effect on RGC-32 mRNA compared to EBV-negative cells, RGC-32 protein is generally expressed when EBNA 3C is present suggesting that EBNA 3C may play a role in regulating its expression in latency III cell lines. However, reanalysis of the BJAB cell lines overexpressing EBNA 3C where RGC-32 mRNA is upregulated confirmed our earlier results that RGC-32 protein is not expressed in these cells. It is therefore possible that RGC-32 protein expression is also inhibited in EBV-negative cells, but that our results in BJAB cells uncovered an effect of EBNA 3C on RGC-32 gene expression that may be masked by rapid degradation of RGC-32 mRNA in LCLs.

6.8 Investigations into the potential translational inhibition of RGC-32 expression

In the first set of experiments we investigated whether translation of RGC-32 mRNA was prevented by a block to nuclear export. Cellular fractionation was carried out to obtain total nuclear and cytoplasmic RNA samples for analysis from a number of different cell lines using protocols kindly provided by Katherine LB Borden (Topisirovic et al., 2002; Topisirovic et al., 2009). Western blot analysis for nuclear (SPT16) and cytoplasmic (actin) proteins in samples taken from fractions prior to RNA extraction confirmed generally efficient fractionation although some cytoplasmic contamination was detected in nuclear samples from HK285 and Mutu III cells (Figure 63A). Cytoplasmic fractions were however free from nuclear contamination. Real-time PCR analysis for RGC-32 and a control for translated and exported mRNA, GAPDH, detected both messages in both the nucleus and cytoplasm (Figure 63B). In all cell lines examined GAPDH mRNA was present at increased levels in the cytoplasm compared to the nucleus. Although RGC-32 mRNA was present in the nucleus, RGC-32 mRNA was detectable in the cytoplasm. It is therefore unlikely that a block to nuclear export prevents RGC-32 expression. Nonetheless, it is apparent that RGC-32 mRNA is exported less efficiently or to a lesser degree than GAPDH mRNA. It is therefore possible that specific mechanisms exist to prevent RGC-32 mRNA translation in the cytoplasm.

Interestingly, another family of small CDK activators (**R**apid **IN**ducer of **G**2/M progression in **O**ocytes) RINGO have been described that are also subject to regulation

(A)

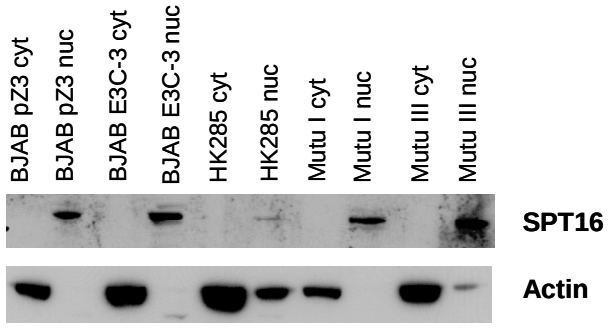

(B)

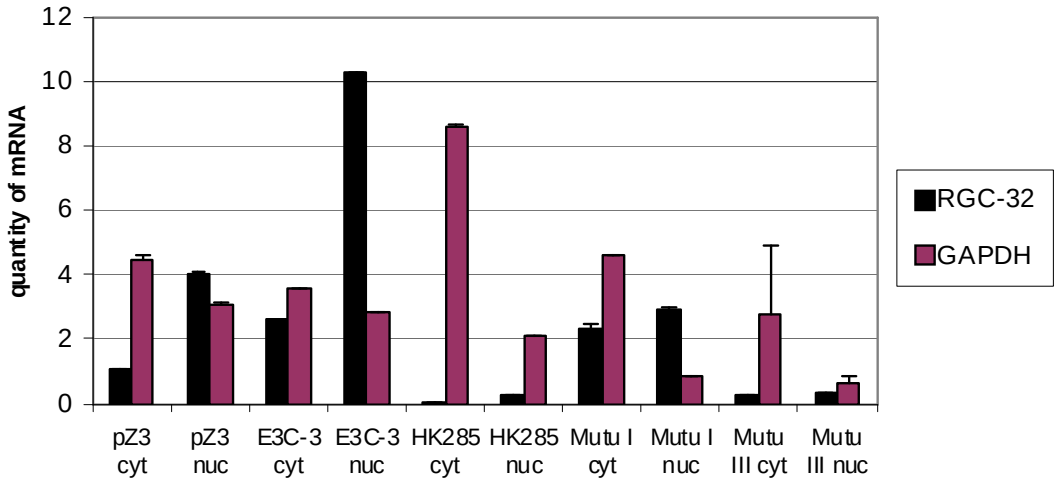

Figure 63 – Cellular fractionation. **(A)** Protein lysates of cytoplasmic (cyt) and nuclear (nuc) fractions of BJAB cell lines pZ3 and E3C-3, the LCL HK285 and the Burkitt's lymphoma cell lines Mutu I (group I) and Mutu III (group III) were separated in a 4-12% NuPAGE Novex Bis-Tris gel in MOPS running buffer (Invitrogen). Proteins were detected using anti-SPT16 antibody (1:500, Santa Cruz) or anti-actin antibody (1:5000, Sigma). Bands were visualised with ECL. **(B)** QPCR analysis of cytoplasmic (cyt) and nuclear (nuc) fractions of BJAB cell lines pZ3 and E3C-3, the LCL HK285 and the Burkitt's lymphoma cell lines Mutu I (group I) and Mutu III (group III). The graph shows the mean of duplicates +/- standard deviation of RGC-32 mRNA levels and GAPDH mRNA levels.

at the level of translation. The RINGO/Speedy family encompasses *Xenopus* RINGO (XRINGO/Speedy), human RINGO/Speedy A (spy1, RINGO 3), RINGO/Speedy B (RINGO 4), RINGO/Speedy C (RINGO 2), RINGO/Speedy D (RINGO 5) and RINGO/Speedy E (RINGO 1) (Cheng et al., 2005; Dinarina et al., 2005). *Xenopus* RINGO/Speedy was shown to share 40% identity with human RINGO/Spy1. RINGO has shown similar features to RGC-32 in binding and activating CDK1 (Badea et al., 2002; Ferby et al., 1999), (reviewed in (Gastwirt et al., 2007)). However, no homologies exist between RGC-32 and the RINGO protein family at the amino acid level (Porter et al., 2002). RINGO protein expression in *Xenopus* oocytes is undetectable since binding of the RNA-binding protein Pumilio-2 (PUM2) to specific sequences in the 3'UTR represses translation (Padmanabhan and Richter, 2006). Pumilio-2 is a translational repressor that plays an important role in anterior-posterior patterning and germ cell development in *Drosophila* (Asaoka-Taguchi et al., 1999; Murata and Wharton, 1995; Parisi and Lin, 1999; Wharton et al., 1998). Due to the similarities in function between the RINGO family and RGC-32, the 3'UTR of RGC-32 was examined for Pumilio-2 binding sites. Human Pumilio-2 was shown to interact with DAZL (**D**eleted in **AZ**oospermia-**L**ike proteins) which is known to interact with mRNAs leading to recruitment of the translation initiation factors (Moore et al., 2003). Pumilio-2 may therefore inhibit initiation factor recruitment. Pumilio-2 binds human PUM2 binding element 1 (hPBE1) which contains the sequence UNUUANNUGUA or the human PUM2 binding element 2 (hPBE2) which contains the sequence UAUANNUAGU (Fox et al., 2005). However, the authors suggest that the length of the random nucleotide sequence in the middle of each binding element can vary (Fox et al., 2005). The left part of the sequence UNUUA or UAUA is termed Box A and the right part UGUA or UAGU is termed Box B.

A perfect match for the Pumilio-2 binding site hPBE2 (Box A: pink, Box B turquoise) and three hPBE1 sites were found in the 3'UTR of the RGC-32 mRNA (Box A: red, Box B: green) (Figure 64). However, the spacing between the Box A and Box B of the hPBE1 sites is relatively large (10-23 nucleotides) compared to previously reported Pumilio-2 binding sites which only showed 1-2 bases between Box A and Box B and may therefore not be identified as hPBE1 sites (Fox et al., 2005). However, the Pumilio-2 binding site on the RINGO mRNA shows spacing of 16 nucleotides between the Box

GUGGCGAGGGCGGUGCCUGGGGGCAGGGGCCUCCUCGGAGGGCGGCGGGGACAGACCCG
UCGCCCCGGCUCCGCAGCCCCGCCCCGGCCCCGCCUCCGCUCCGGCCGCCGAAGGCUAU
AAGAUCUAGGAACCCGAGCCGGUGGUAGGGCGGGCGCGGACCGUGCUGGGAGCGGCGCG
GCUGGAGCGCAGCGCCGAAGGGACUGGCAGGGCUGAAGUGUGCGGGACAGCAAGCCCCC
GAAUAGCCCCGGCUGCCACCUCGCAGGACCCAAGGCCACGCGCGCCGGGCCCAGCUGAG
CCGCCUC**AUG**AAGCCGCCCGCGGCGCAGGGCAGCCCCGCGGCCGCCGCGGCCGCAGCCC
CGGCCCUGGACUCGGCGGCCGCGGAGGACCUGUCGGACGCGCUGUGCGAGUUUGACGCG
GUGCUGGCCGACUUCGCGUCGCCCUUCCACGAGCGCCACUUCCACUACGAGGAGCACCU
GGAGCGCAUGAAGCGGCGCAGCAGCGCCAGUGUCAGCGACAGCAGCGGCUUCAGCGACU
CGGAGAGUGCAGAUUCACUUUAUAGGAACAGCUUCAGCUUCAGUGAUGAAAAACUGAAU
UCUCCAACAGACUCUACCCCAGCUCUUCUCUCUGCCACUGUCACUCCUCAGAAAGCUAA
AUUAGGAGACACAAAAGAGCUAGAAGCCUUCAUUGCUGAUCUUGACAAAACUUUAGCAA
GUAUG**UGA**AACAAGAAGUUCUGGGUCCUUUCAUCAUAAGGGAGAAGCUUCAGAAAGUUC
CGAGGACCUGCUAAAAUCAGCUACUAGAAUCUGCUGCCAGAGGGGACAAAGACGUGCAC
UCAACCUUCUACCAGGCCACUCUCAGGCUCACCUUAAAAUCAGCCCUUGAUCCCAUUUC
UGGGCAAUUUAGACAGUGAAACUGACUUUGUUUACCUGCUUGCAGCA**UAUUAGAACAGA**
CGAUCCAUGCUAAUAUUGUAUUUUC**UCUUAAAACAUAGCUUUCC**UGUAAUUUAAAGUGC
UUUUAUGAAAAUAUUUGUAAUUAAU**UAUAUAUAGU**UGGAAAUAGCAGUAAGCUUUCCCA
UUAUAAUAUAUUUUUGUAUACAAAUAAAAUUUGAACUGAAGUCUGCAAAAAAAAAAAAA
AAAAA

Figure 64 – Sequence of RGC-32 mRNA (accession number NM_014059 on www.ncbi.nlm.nih.gov)
Red-coloured letters represent the coding region for protein translation starting with the start codon **AUG** highlighted in yellow and the stop codon **UGA** highlighted in yellow. The sequence following the stop codon represents the 3'UTR (untranslated region). The Box A sequence **UNUUA** highlighted in red is followed by the Box B sequence UGUA highlighted in green which together represent human Pumilio binding elements 1 (hPBE1). The Box A sequence **UAUA** highlighted in pink is followed by the Box B sequence **UAGU** highlighted in turquoise which together represent human Pumilio binding elements 2 (hPBE2).

A and Box B of the hPBE1 indicating that a hPBE1 site containing large spacing between the Box elements is still recognised by Pumilio-2 (Padmanabhan and Richter, 2006). Further investigations are needed to verify whether Pumilio-2 actually binds the hPBE1 and 2 sites in the RGC-32 mRNA sequence and regulates its translation.

6.9 Discussion

RGC-32 mRNA was found to be downregulated when the transcription factor RUNX1 was downregulated in rat periovulatory cells (Jo and Curry, 2006). RUNX1c mRNA and protein expression is high in Burkitt's lymphoma group I cell lines and latency III-expressing cell lines lacking EBNA 2 expression relative to latency III-expressing cell lines and LCLs, where RUNX1c is downregulated by the presence of RUNX3. Investigations were therefore carried out to determine whether RGC-32 mRNA expression correlated with RUNX1c expression in a panel of EBV-negative and EBV-positive cell lines. Interestingly, RGC-32 mRNA showed a very similar profile to RUNX1c mRNA indicating that RUNX1 may regulate RGC-32 expression in B cells.

To follow up these observations, reporter assays were carried out to determine whether RUNX1c was able to activate a 1.4 kb fragment of the RGC-32 promoter. A 2.2-fold upregulation was detected in the EBV-negative cell line DG75 demonstrating a role for RUNX1 in controlling RGC-32 expression in human B cells. Mutation of the predicted RUNX-binding site in the promoter construct did not result in abrogation of the RGC-32 promoter activation. An additional RUNX-binding site which was predicted further upstream of the originally examined promoter sequences appeared to be non-functional since no increase in RGC-32 promoter activation was detected. We showed that RUNX3 can also upregulate RGC-32 promoter activation but real-time PCR results do not show a correlation between RGC-32 mRNA levels and RUNX3 expression indicating that the effects of these proteins may be context-dependent. However, RGC-32 and RUNX3 protein are co-expressed in LCLs and in a group III Burkitt's lymphoma cell line which may indicate a correlation of protein expression regulation.

The most surprising aspect of this series of experiments came from the first demonstration of endogenous RGC-32 protein expression in B cells. An examination of a panel of cell lines revealed that RGC-32 protein was consistently expressed in LCLs

and in a group III Burkitt's lymphoma cell line and some EBNA 2-deleted group III Burkitt's lymphoma cell lines. These results therefore raise the question of why RGC-32 mRNA expression is high in Burkitt's lymphoma group I cell lines, but no protein can be detected and why RGC-32 protein is not detectable in BJAB cells stably expressing 3C despite increased RNA expression. One possibility is that the export of mRNA from the nucleus is inhibited. Cellular fractionation was carried out to investigate whether the cytoplasmic RNA fraction contained any RGC-32 mRNA or whether a block in RNA export resulted in accumulation of mRNA in the nucleus. Real-time PCR analysis revealed that a proportion of RGC-32 mRNA is present in the cytoplasm so would be available for translation. Due to functional similarities between RINGO proteins and RGC-32 in CDK1 activation and the fact that the translation of *Xenopus* RINGO is repressed by binding of the translational repressor PUM-2 to the 3'UTR of RINGO, the 3'UTR of RGC-32 was examined for PUM-2 binding sites. Interestingly, a perfect match for the Pumilio-2 binding site hPBE2 was found. These results indicate that a similar mechanism may prevent RGC-32 translation in a cell type dependent manner.

Initiation of mRNA translation is often controlled by regulation of the interaction between the eukaryotic initiation factors eIF4E, eIF4G and eIF4A and 5'-cap of the mRNA (Gebauer and Hentze, 2004). The Poly(A)-binding protein (PABP) was also shown to play a role in translation initiation since depletion of PABP from a cell-free extract prevents initiation of mRNA translation (Kahvejian et al., 2005). The 3'-poly(A) tail is bound by DAZL and PABP which were shown to interact in *Xenopus* (Figure 65A) (Collier et al., 2005; Voeltz et al., 2001). PABP in turn interacts with eIF4G and circularizes the translating mRNA (Imataka et al., 1998).

The inhibition of RINGO mRNA translation by PUM2 was suggested to occur via interaction with DAZL (Moore et al., 2003). Therefore, PUM2 may interfere with the interactions between the 5'cap and eukaryotic translation initiation factor 4E (eIF4E), eIF4G or PABP inhibiting the circularisation and therefore translation of the mRNA (Figure 65B), (Menon et al., 2004; Padmanabhan and Richter, 2006). It was suggested that PUM2 inhibition is released during oocyte maturation when it dissociates from RINGO mRNA

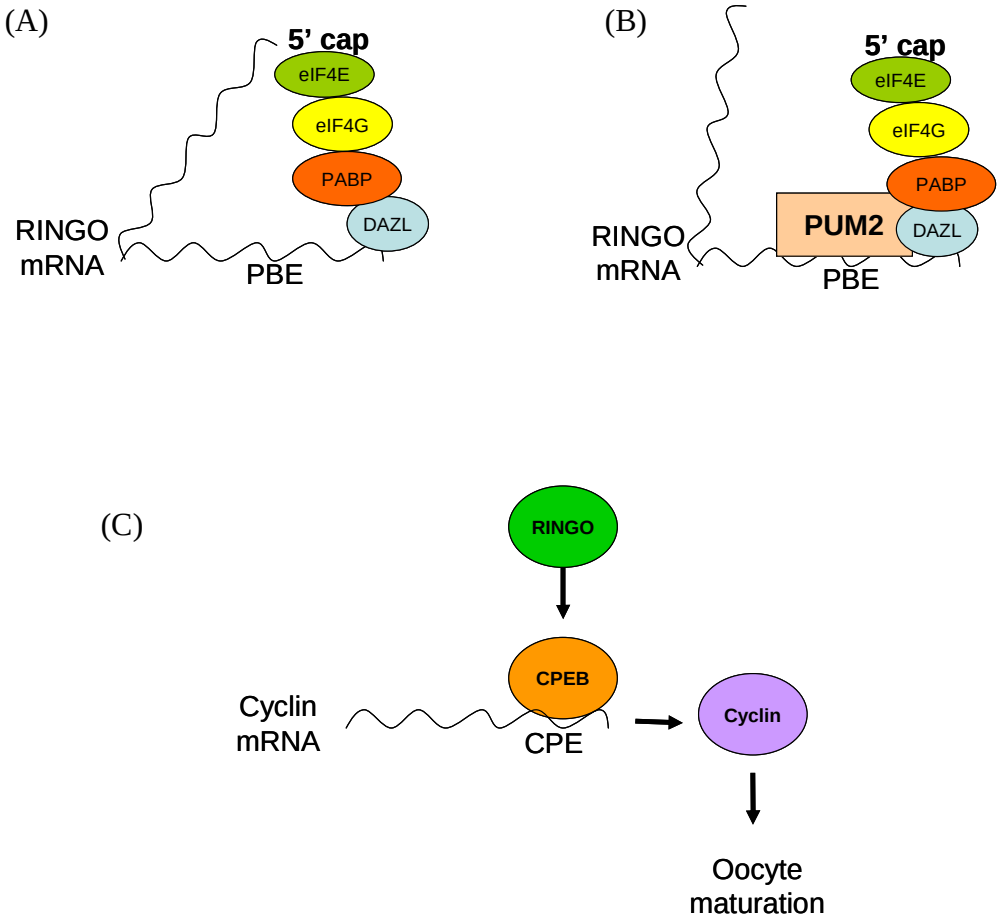

Figure 65 – Potential mechanism of Pumilio-2 inhibition and RINGO activation. **(A)** DAZL and PABP interact with the mRNA and initiation factors that interact with the 5'cap of the mRNA. Circularisation is necessary for mRNA translation **(B)** Pumilio-2 is known to bind a Pumilio-binding element (PBE) located in the 3'UTR of RINGO mRNA. Pumilio-2 is thought to inhibit the circularisation of the mRNA by binding the mRNA and DAZL. **(C)** RINGO protein can activate CBEP, which binds to the CPE promoting polyadenylation of the cyclin mRNA, which is followed by translation. Cyclin expression can then activate its CDK binding partner and induce oocyte maturation.

(Padmanabhan and Richter, 2006). DAZL and ePAB remained associated with RINGO mRNA to promote its translation (Padmanabhan and Richter, 2006).

Cyclin B mRNA translation was shown to be regulated by RINGO expression via activation of the cytoplasmic polyadenylation element binding protein (CPEB) in *Xenopus* oocytes (Figure 65C). CPEB binds to the 3'UTR-residing cytoplasmic polyadenylation element (CPE) which mediates polyadenylation together with other factors which trigger translation of the mRNA (Hake and Richter, 1994; Paris et al., 1991; Sheets et al., 1994). It may be that RGC-32 translation is inhibited by Pumilio-2 in a similar manner to RINGO. It is possible that RGC-32 may be involved in CPEB activation supporting translation of target genes involved in cell cycle progression.

7 Discussion

EBV has been causally linked to numerous types of cancer e.g. Burkitt's lymphoma, nasopharyngeal carcinoma, post-transplant lymphoproliferative disease, AIDS-associated lymphomas as well as Hodgkin's lymphomas. The virus infects and immortalises human B cells through mechanisms that are still not fully understood.

One of the EBV proteins essential for immortalisation, EBNA 3C, has been shown to disrupt many cell cycle checkpoints including the G2/M checkpoint (Krauer et al., 2004b; Parker et al., 2000). Previous studies have suggested that this may be mediated by the ability of EBNA 3C to interact and downregulate chk2 which is activated upon DNA damage leading to cell cycle arrest via CDK1 inactivation (Choudhuri et al., 2007; Krauer et al., 2004b). The inactive form of CDK1, tyrosine-15 phosphorylated CDK1 was also shown to accumulate at reduced levels during G2 arrest in EBNA 3C-expressing cells (Krauer et al., 2004b). It is not known whether EBNA 3C accomplishes this in a direct or indirect manner (Krauer et al., 2004b).

To identify new downstream targets of EBNA 3C, a microarray study was previously carried out in the lab. Interestingly, the response gene to complement 32 (RGC-32) was found to be upregulated by 6.6-fold in an EBV-negative BJAB cell line stably expressing EBNA 3C compared to an EBNA 3C-negative BJAB cell line. The role of RGC-32 as a CDK1 activator led us to investigate whether RGC-32 played a role in mediating the effects of EBNA 3C on the G2/M checkpoint. We confirmed that BJAB cells with upregulated RGC-32 mRNA showed disrupted checkpoint regulation.

In support of a role for RGC-32 overexpression in checkpoint deregulation, previous studies in the lab confirmed that stable expression of RGC-32 alone could lead to partial G2/M disruption in B cell lines. Therefore, increased RGC-32 expression could be partially responsible for G2/M checkpoint disruption by EBNA 3C. However, this observation could not be repeated in transient systems. This may be due to the fact that a transfection efficiency of only 30% could be achieved and this proportion of cells may not be sufficient enough to display a significant phenotypic change in FACS analysis. Further, concentrations of up to 800 nM etoposide did not fully arrest the cells

suggesting that a higher concentration was needed to enable proper visualisation of G2/M checkpoint disruption. Transiently transfected DG75 cells were harvested 48 hours after transfection and were exposed to etoposide after only 24 hours. This relatively short overexpression of RGC-32 may not be efficient enough to produce a similar phenotype seen in BJAB and DG75 cells stably overexpressing RGC-32.

It is important to note that no endogenous RGC-32 protein could be detected in BJAB cell lines stably overexpressing EBNA 3C showing elevated levels of RGC-32 mRNA expression whereas stably expressed RGC-32 protein could be detected in BJAB and DG75 cells. This could not be resolved by new antibody generation or by antibody purification. Unfortunately, we cannot conclude whether cell cycle checkpoint disruption observed in BJAB cells stably expressing EBNA 3C is due to RGC-32 expression or whether it may be caused by a different pathway induced by EBNA 3C.

It is also possible that RGC-32 activates CDK1 in a similar manner to RINGO by using small levels of protein expression which were undetectable by the antibody. It may be that the RGC-32 protein has a relatively fast turnover. However, when we investigated whether RGC-32 protein was actively degraded by the proteasome in BJAB cell lines, we found that treatment with the proteasome inhibitor MG132 did not result in increased RGC-32 expression. However, no positive control was used in this experiment and we cannot rule out the fact that the experiment may not have worked.

We confirmed the role of RGC-32 as a CDK1 activator *in vitro*, but could not show the same result in EBNA 3C-expressing BJAB cells, in BJAB and DG75 cells overexpressing RGC-32 or transiently overexpressing DG75 cells. Surprisingly, decreasing CDK1 activity was found in asynchronous BJAB and DG75 cells stably overexpressing RGC-32 in cyclin B1 or CDK1 immunoprecipitations. It is possible that the differences in CDK1 activity are due to using asynchronous cells where only a small proportion of cells are going through mitosis where CDK1 is active. Comparison of this relatively small amount of CDK1 activity may therefore not be sufficient enough to detect the effects of RGC-32 on CDK1 activity *in vivo*. To further examine the effects of RGC-32 on CDK1 activation, the experiment could be repeated in nocodazole-arrested or elutriated cells to obtain mitotic cells.

Interestingly, work published during the course of the study showed that RGC-32 expression correlated with RUNX1 expression (Jo and Curry, 2006). Jo and Curry showed that RUNX1 gene silencing decreased RGC-32 mRNA levels in cultured granulosa cells obtained from rat periovulatory follicles identifying RUNX1 as a regulator of RGC-32 (Jo and Curry, 2006). This group further found several putative RUNX-binding sites in the RGC-32 gene and ChIP assays revealed that RUNX1 binds to the RGC-32 promoter *in vivo* (Park et al., 2008). Because of differential expression of RUNX1 and RUNX3 in EBV latency, we examined RGC-32 expression and identified RGC-32 mRNA levels that correlated with RUNX1 expression (Table 9). Surprisingly however, RGC-32 protein was only detected in cells expressing the EBV latency III pattern where RUNX1 expression is low.

	RGC-32 mRNA	**RGC-32 protein**	**RUNX1 protein**	**RUNX3 protein**
EBV-negative	Variable/low	none	Variable/low	Variable/high
BL group I	high	none	high	low
BL group III and LCLs	low	high	low	high

Table 9 – Overview of RGC-32, RUNX1 and RUNX3 expression in cell lines with different EBV latency.

7.1 Why is RGC-32 protein not expressed in EBV-negative and Burkitt's lymphoma group I cell lines?

Since EBV-negative and Burkitt's lymphoma group I cell lines show high levels of RGC-32 mRNA but no protein, the nuclear export or translation of RGC-32 mRNA may be inhibited in these cells. We showed that a proportion of RGC-32 mRNA is present in the cytoplasm and is therefore available for translation. Interestingly, the RGC-32 mRNA contains numerous PUM2-binding elements. PUM2 is known to inhibit translation by binding to the 3'UTR of XRINGO mRNAs and some genes involved in cell cycle regulation e.g. Mos and cyclin B1 (Figure 66) (Padmanabhan and Richter, 2006).

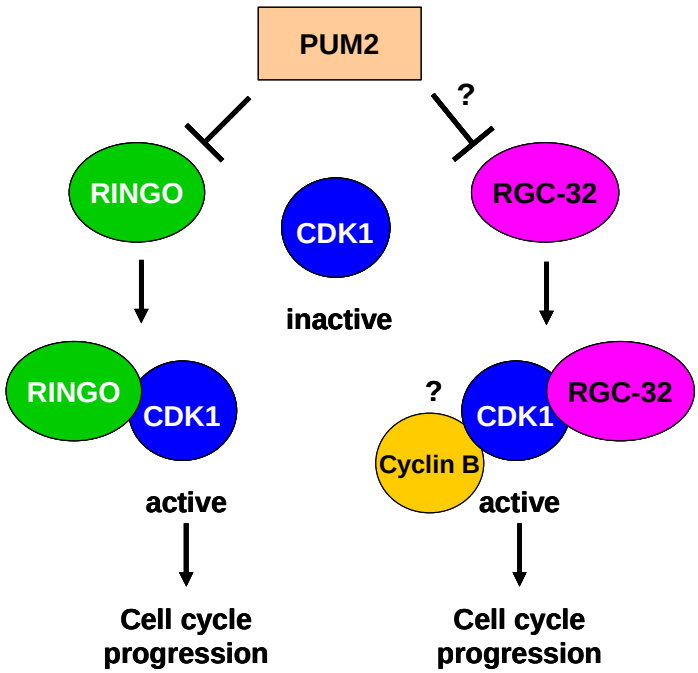

Figure 66 – Pumilio-2 (PUM2) inhibits RINGO and possibly RGC-32 translation. RINGO can bind and activate CDK1 in the absence of its cyclin and induce cell cycle progression. RGC-32 was also shown to bind and activate CDK1, however, it is not known whether RGC-32 binds CDK1 in the presence or absence of cyclin B to induce cell cycle progression.

RINGO/Speedy mRNA was originally discovered in *Xenopus* oocytes by 2 independent groups. Lenormand *et al*. designated the novel RNA Speedy since it induces release of G2-arrested oocytes into meiosis (meiotic maturation) independently of progesterone stimulation (Lenormand et al., 1999). Simultaneously, Ferby *et al*. found the same RNA which they designated RINGO (**R**apid **IN**ducer of **G**2/M progression in **O**ocytes) (Ferby et al., 1999).

PUM2 antibody injection in *Xenopus* oocytes was shown to lead to endogenous XRINGO protein detection and Mos and cyclin B1 synthesis (Padmanabhan and Richter, 2006). Therefore, RGC-32 mRNA translation may be inhibited like the cell cycle regulators XRINGO, cyclin B1 and Mos resulting in accumulation of mRNA (Figure 66).

Although cellular fractionation assays suggested that RGC-32 is being exported from the nucleus into the cytoplasm, we do not know whether any RGC-32 mRNA is being translated in Burkitt's lymphoma group I cell lines. Evidence to support low-level RGC-32 protein expression in EBNA 3C-expressing BJAB cells comes from the observation that silencing of RGC-32 gene expression had an effect on the cell cycle. Reduction of RGC-32 expression results in accumulation of cells in G0/G1 confirming that RGC-32 expression may play an important role in G1/S progression. Therefore, small amounts of RGC-32 protein may also be translated in Burkitt's lymphoma group I cell lines.

To identify whether translation of RGC-32 mRNA is inhibited in EBV-negative and Burkitt's lymphoma group I cell lines, polysome gradient analysis could be carried out to determine whether RGC-32 mRNA associates with ribosomes or whether this step is inhibited. Further, the role of translation inhibition by PUM2 will be investigated to determine whether RGC-32 mRNA is in fact bound and its translation inhibited by PUM2 using RNA band shift experiments. Another possibility is to overexpress RGC-32 3'UTR sequences in cells to determine whether this results in relieve of potential translational repression or PUM2. It would also be interesting to examine the PUM2 expression in a cell panel with different EBV latencies to determine whether differential PUM2 expression controls RGC-32 expression.

7.2 What is the role of RUNX in regulating RGC-32 expression?

Luciferase assays revealed that RUNX1c was able to increase RGC-32 promoter activity (Figure 67) but that RUNX1c does not activate the RGC-32 promoter via the predicted RUNX-binding site. Although RGC-32 mRNA translation may be inhibited by PUM2 in group I Burkitt's lymphoma (latency I), RGC-32 may still be upregulated by RUNX1c.

Therefore, this RUNX1c-mediated RGC-32 upregulation may not result in RGC-32 expression in EBV-transformed Burkitt's lymphoma group I cell lines but may play a crucial role in other tumour cell lines.

Silencing of RUNX3 expression led to upregulation of RUNX1c mRNA and RGC-32 mRNA and protein confirming a role for RUNX1c in upregulating RGC-32. However, RUNX1c protein expression could not be detected in LCLs with silenced RUNX3 expression, although it is noteworthy that the original publication of RUNX3 knockdown only displayed RUNX1 mRNA indicating that the RUNX1c protein expression may remain below detection limits (Spender et al., 2005a).

Additional studies are needed to identify the mechanism for RUNX-induced RGC-32 upregulation. ChIP analysis of a broad range of cell lines using an anti-RUNX1 or anti-RUNX3 antibody could show whether the RUNX proteins associate with the RGC-32 promoter and which RUNX-binding sites may be used. However, no appropriate anti-RUNX1c antibody is commercially available for ChIP analysis. The only anti-RUNX1 antibody available which detects the RUNX1c isoform does not immunoprecipitate the protein.

7.3 What is the role of EBNA 3C in regulating RGC-32 expression?

Luciferase assays revealed a low level increase of RGC-32 promoter activity with increasing amounts of EBNA 3C expression in DG75 cells. However, this observation could not be confirmed in BJAB or Raji cell lines. Moreover, ChIP analysis demonstrated that EBNA 3C-expressing BJAB cell lines do not show increased

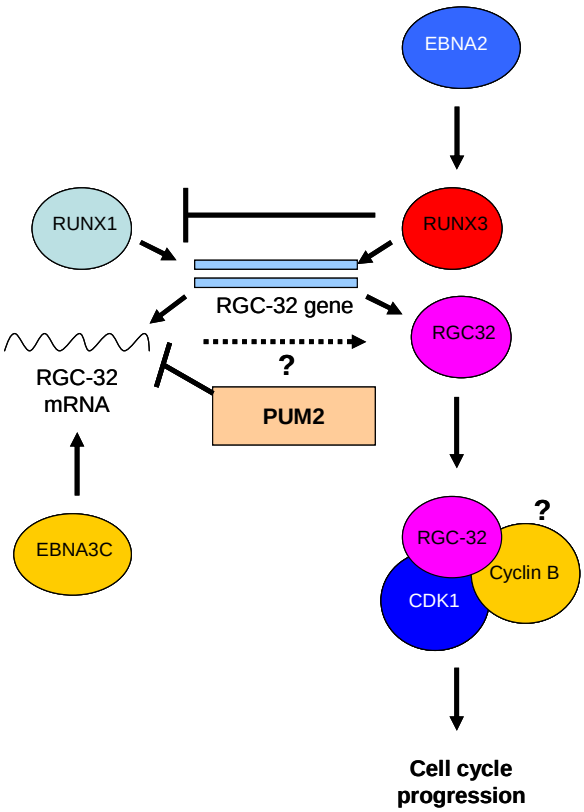

Figure 67 -.EBNA 2 was shown to induce RUNX3 expression. RUNX3 can inhibit RUNX1 expression. Both RUNX1 and RUNX3 can induce RGC-32 gene transcription but RGC-32 translation may be inhibited by PUM2 when RUNX1 is expressed. EBNA 3C stabilises RGC-32 mRNA as a result of translation inhibition or in order to synthesise more RGC-32 protein. In B cell lines where RUNX3 is expressed, RGC-32 protein was detected. RGC-32 protein can bind and activate CDK1. It is not known whether the CDK1 activation occurs in the presence or absence of cyclin B. Activation of CDK1 leads to cell cycle progression.

polymerase II association at the RCG-32 promoter suggesting that the RGC-32 upregulation by EBNA 3C does not occur by induction of RGC-32 gene transcription either directly or indirectly.

Further investigations of the RGC-32 upregulation by EBNA 3C suggested that there is a dramatic increase in the RGC-32 mRNA half life in the EBNA 3C-positive BJAB cell lines E3C-3 and E3C-7 compared to EBNA 3C-negative control cells. Since EBNA 3C is not known to bind to RNA directly, it is likely that message stabilisation by EBNA 3C results from effects on the components of a pathway that normally promotes or prevents RGC-32 mRNA degradation. Although the microarray study did not identify any RNA stabilisation or translation inhibition factors in EBNA 3C-expressing cells, it may be possible that BJAB cells in general express these factors, e.g. Pumilio-2, and repress translation of RGC-32 mRNA in the presence or absence of EBNA 3C. The same phenomenon may be observed in Burkitt's lymphoma group I cell lines.

Interestingly, Raji cells which display a deletion of the EBNA 3C gene do not express detectable RGC-32 protein but RGC-32 mRNA is not accumulated further suggesting that EBNA 3C is involved in upregulation of RGC-32. In addition, since RGC-32 protein could not be detected in EBV type 2 cell lines P3HR1 and Jijoye, our initial studies suggested that type 1 EBNA 3C may be required for RGC-32 upregulation.

Two EBV types, EBV-1 and EBV-2 have been described. A major difference between the two EBV types is found in the EBNA 2 gene with only 64% of the gene and 53% of the amino acid sequence conserved between types (Adldinger et al., 1985). Variation in the EBNA 3 genes was also subsequently discovered (Rowe et al., 1989; Sample et al., 1990). EBV type 2 infection only rarely occurs in Western Europe and USA but is common in Africa and New Guinea (Rowe et al., 1989; Young et al., 1987; Zimber et al., 1986).

Interestingly, the RGC-32 protein was expressed at detectable levels in EBNA 2-deleted Burkitt's lymphoma cell lines Oku and Sal although their RGC-32 mRNA expression resembled the phenotype observed for group I Burkitt's lymphoma cell lines. However, the same observation could not be made for the EBNA 2-deleted Burkitt's lymphoma

cell line Daudi. It is therefore possible that Daudi cells contain changes in the EBNA 3C gene or protein.

In addition, an obvious difference between the cell lines Oku, Sal and Daudi is their time of extraction. The Daudi cell line has been established in 1968 whereas the cell lines Oku and Sal have been established in 1999 (Habeshaw et al., 1999; Klein et al., 1968). The differences in RGC-32 protein expression might therefore be due to the fact that Daudi has been passaged many times which might have resulted in the change of phenotype which has not occurred for the cell lines Oku and Sal which are relatively new cell lines. It could also be possible that the mechanism by which EBV immortalises cells has slightly changed with time and allowed RGC-32 protein expression. Further experiments examining EBNA 2-deleted cell lines are needed to verify this observation.

It would be interesting to examine another panel of cell lines including cells which only differ in EBNA 3C and/or EBNA 2 expression to further investigate the correlation between RGC-32, RUNX, EBNA2 and EBNA 3C expression, for example, Martin Allday's virus constructs with deleted EBNA 3C or EBNA 3A in different BL cells (Young et al., 2008). However, RGC-32 may also be inhibited in those cell lines.

Although ChIP analysis showed that EBNA 3C expression in BJAB cell lines does not result in activation of RGC-32 transcription, it is possible that EBNA 3C may target the RGC-32 promoter via the other two predicted RBP-J kappa sites in cell lines expressing detectable RGC-32 protein. Therefore, ChIP analysis using the anti-EBNA 3C antibody could be repeated in LCLs and Burkitt's lymphoma group III cell lines to confirm this.

7.4 What is the mechanism of CDK1 activation by RGC-32?

A novel protein family, RINGO/Speedy, has been shown to be functionally similar to RGC-32 and can induce cell cycle progression although protein expression could not be detected in *Xenopus* during oogenesis and early embryogenesis, (reviewed in (Gastwirt et al., 2007)).

Like the RINGO family, RGC-32 was found to be able to bind and increase CDK1 activity *in vitro* (Badea et al., 2002). Kinase assays using recombinant RGC-32 protein could confirm this result. However, Saigusa *et al.* reported that RGC-32 was not able to

interact with CDK1 *in vivo* (Saigusa et al., 2007). This suggestion was made after they immunoprecipitated FLAG-RGC-32 in HEK 293-T cells with an anti-FLAG antibody and failed to see cyclin B1 as a co-immunoprecipitate. However, the conclusion of Saigusa *et al.* implies that RGC-32 binds to the CDK1/cyclinB1 complex instead of competing with cyclin B1 for CDK1, neither of which has been shown to date. Since RGC-32 is also phosphorylated by CDK1 like cyclin B1, it might be able to replace cyclin B1 in the cyclin B1/CDK1 complex as observed for RINGO family members (Badea et al., 2002), (reviewed in (Gastwirt et al., 2007)). XRINGO can bind cyclin B and CDK1 individually but not the CDK1/cyclin B complex further confirming that the RINGO family can activate CDK1 in the absence of cyclin B (Ferby et al., 1999). Immunoprecipitation assays using an anti-cyclin B1 antibody may therefore not immunoprecipitate RGC-32 and it can therefore not be concluded that RGC-32 does not bind CDK1. To further investigate the function of RGC-32, kinase assays could be carried out to examine whether RGC-32 can activate CDK1 in the absence of cyclin B1. Immunoprecipitation assays could also be used to determine whether RGC-32 can bind CDK1 and cyclin B1 individually or whether it associates with the complex.

Interestingly, RINGO family members were shown to override the effects of inhibitory CDK1 phosphorylation and that Myt1 expression, which catalyses the inhibitory phosphorylation of CDKs, cannot reduce RINGO/CDK1 activity to the same extent as cyclin B/CDK1 (Karaiskou et al., 2001). RINGO/CDK1 activity could not be reduced due to less inhibitory CDK1 phosphorylation by Myt1 (Karaiskou et al., 2001). RGC-32 may also able to overcome the inhibitory CDK1 phosphorylation since RGC-32-overexpressing BJAB cells showed that a proportion of cells continue cell growth despite DNA damage and Tyr-15 phosphorylation of CDK1. Therefore, the mechanism of CDK1 activation by RGC-32 remains to be fully elucidated.

Additionally, XRINGO has been shown to induce CDK1 activation independent of Thr-161 phosphorylation *in vitro* and *in vivo* and is required for progesterone-induced oocyte maturation (Ferby et al., 1999; Karaiskou et al., 2001). RINGO was further shown to bind and activate CDK2 in the absence of its cyclin and independent of Thr-160 phosphorylation in mammalian cells where RINGO protein is detectable (Karaiskou et al., 2001; Porter et al., 2002). Therefore, it would be interesting to determine whether

the CDK-activating kinase CAK is needed to mediate RGC-32-induced CDK1 activation. Transfection assays using a FLAG-tagged vector expressing the T161A mutant of CDK1 compared to wild-type CDK1 could be carried out. CDK1 immunoprecipitates could then be used in kinase assays to examine whether RGC-32 is still able to activate CDK1 when Thr-161 is mutated.

Interestingly, RGC-32 is unable to enhance CDK1 activity in the presence of $p27^{KIP1}$ (Badea et al., 2002). In contrast, RINGO-activated CDK1 cannot be inhibited by expression of another CDK inhibitor, p21, which was shown to inhibit progesterone induced CDK1 activation in oocytes (Barnes et al., 2003; Karaiskou et al., 2001; Lenormand et al., 1999; Porter et al., 2002). These observations highlight different modes of action of these two CDK1 activators.

7.5 What is the role of RGC-32 expression in LCLs?

RGC-32 protein was only detected in Burkitt's lymphoma group III cells and LCLs indicating that RGC-32 may play an important role in cell proliferation in these cell lines. Interestingly, preliminary experiments carried out by Andrea Gunnell showed that stable expression of RGC-32 siRNA in the LCL IB4 leads to cell death indicating that RGC-32 is essential for cell proliferation in LCLs (our unpublished data).

In support of a tumour promoting role for RGC-32, the expression of the novel CDK1 activator RGC-32 is deregulated in numerous tumours e.g. ovarian, colon, breast and prostate cancers and therefore appears to be involved in tumour development (Donninger et al., 2004; Fosbrink et al., 2005; Kang et al., 2003). Furthermore, inducible overexpression of testis-specific protein Y (TSPY) in HeLa cells has been reported to upregulate RGC-32 and to accelerate progression through G2/M (Oram et al., 2006). Interestingly, TSPY has been shown to be upregulated in gonadoblastoma, testicular germ-cell tumours, prostate and liver cancers and in melanomas (Gallagher et al., 2005; Lau, 1999; Lau et al., 2003; Yin et al., 2005). Its effects on cellular proliferation are further supported by the observation that RGC-32 is upregulated during tissue regeneration and remodelling (Blaxall et al., 2003; Lim et al., 2002; Strom et al., 2005). Due to the suggested role of RGC-32 as a CDK1 activator, the protein may play an important role in tumour development. Further, RGC-32 protein may also be

expressed during early stages of EBV infection but is subsequently downregulated in some cell lines, e.g. Burkitt's lymphoma group I cell lines.

7.6 RGC-32 – Oncogene or tumour suppressor?

Despite its role in cell proliferation, RGC-32 has also been described as a potential tumour suppressor gene which was shown to be deleted in malignant gliomas. RGC-32 was shown to suppress growth when re-introduced into 19 glioma cell lines. Overexpression of RGC-32 in HeLa cells also affected cell cycle progression by delaying the G2/M transition (Saigusa et al., 2007). It is therefore possible that the biological effects of RGC-32 may differ between cell and tumour types.

P53 has also been implicated in the regulation of RGC-32 expression. Both, p53 null U-373 MG cells and mutation of the p53 gene in primary astrocytomas resulted in a decrease of RGC-32 mRNA expression (Saigusa et al., 2007). Expression of p53 in p53 null U-373 MG cells showed induction of RGC-32 mRNA via p53 binding to a regulatory element in the RGC-32 gene (Saigusa et al., 2007).

P53 is known to become activated upon DNA damage, therefore, it may be possible that RGC-32 expression is repressed or activated by p53 (Figure 67). The turnover of normal p53 protein occurs rapidly and can only be detected in cell lines with mutated p53 (Lane and Benchimol, 1990). It does not appear however that the presence of wild-type versus mutant p53 in the cell panel we examined correlates with RGC-32 mRNA or protein expression since Ramos, Raji and P3HRI cells display mutated p53 and BJAB, Akata, Jijoye and LCLs e.g. IB4 show wild-type p53 (Farrell et al., 1991).

In summary, these studies have identified another potential mechanism by which EBV can override cell cycle control. Cell lines expressing EBNA 3C have shown upregulated RGC-32 mRNA expression which could potentially lead to increased CDK1 activity. RGC-32 is most likely essential for cell survival in LCLs and its expression may be induced by RUNX1c in B cells. Further investigations into transcription control of RGC-32 will provide vital information of how and why RGC-32 is expressed differentially in EBV latency. Considering the identified functions of RGC-32, it is possible that RGC-32 upregulation is vital for EBV-induced tumourigenesis and may be a target for tumour therapies.

8 Appendices

8.1 Cell lines

8.1.1 EBV-negative cell lines

Cell line	EBV status	Description	Reference
HeLa	Negative	Human cervical carcinoma from a 31-year old woman transformed by HPV-8.	(Scherer et al., 1953)
BJAB	Negative	African lymphoma originally classed as BL but lacks c-myc translocation.	(Menezes et al., 1975)
BJAB pZ	Negative	BJAB cells stably transfected with pZipNEOSV(X) empty vector.	(Wang et al., 1990a)
BJAB E3C	Negative	BJAB cells stably transfected with pZipNEOSV(X) expressing EBNA 3C.	(Wang et al., 1990a)
DG75	Negative	BL from the pleural effusion of a 10-year-old boy with Burkitt's lymphoma.	(Ben-Bassat et al., 1977).
Ramos	Negative	American-type BL of a 3-year-old boy.	(Klein et al., 1975).
AK31	Negative	An EBV-negative subclone of Akata.	(Jenkins et al., 2000)

8.1.2 Group I Burkitt's Lymphoma cell lines

Cell line	EBV status	Description	Reference
Rael	Type-1	African BL	(Klein et al., 1972)
Elijah	Type-1	BL	
Akata	Type-1	Japanese BL with t(8;14) translocation	(Takada et al., 1991)
Mutu I clone 179	Type-1	African BL derived from a 7-year-old black male.	(Gregory et al., 1990)

8.1.3 Group III Burkitt's Lymphoma cell lines

Cell line	EBV status	Description	Reference
Raji	Type-1	African BL with t(8;14) translocation. Virus has deletion of part of EBNA 3C gene.	(Pulvertaft, 1964)
Raji 13.6 Raji 13.6.4	Type-1	Raji cells stably transfected with the empty vector pSV2Hyg.	(Allday et al., 1993)
Raji 11.2.1 Raji 11.2.5 Raji 11.5.8	Type-1	Raji cells stably transfected with the pSV2E3/4 plasmid containing the EBNA 3C gene.	(Allday et al., 1993)
Mutu III clone 48	Type-1	African BL derived from a 7-year-old black male. Mutu BL drifted in culture to express a latency III pattern.	(Gregory et al., 1990)
Jijoye	Type-2	BL	(Pulvertaft, 1964)
P3HR1	Type-2	BL with deletion of EBNA 2 gene and part of LP gene.	(Henle and Henle, 1966)
Daudi	Type-1	BL from 16-year old African boy with deletion of EBNA 2 gene.	(Klein et al., 1968)
Oku-BL	Type-1	East African BL with deletion of EBNA 2 gene.	(Habeshaw et al., 1999; Kelly et al., 2002b)
Sal-BL	Type-1	East African BL with deletion of EBNA 2 gene.	(Habeshaw et al., 1999; Kelly et al., 2002b)

8.1.4 Lymphoblastoid cell lines

Cell line	EBV status	Description	Reference
spLCL	Type-1	spontaneous lymphoblastic cell line	
LCL3	Type-1	B cells transformed with EBV strain B95.8.	(Sinclair et al., 1994)
IARC 171	Type-1	B cells from the EBV-negative tumour tissue of an 8-year-old Caucasian boy with Burkitt's lymphoma (same patient as BL41) were infected with EBV.	(Lenoir et al., 1985)
IB4	Type-1	Umbilical cord B-lymphocytes infected with EBV strain B95-8.	(King et al., 1980)
PER149	Type-1	B cells were transformed with an EBNA 3B knockout virus (on a B95.8 background). This cell line was originally called PER142.	Gift from Heather Long
PER253	Type-1	B cells transformed with EBV strain B95.8.	Gift from Heather Long
HK285	Type-1	Hong Kong buffy coat donor B cells and is transformed with EBV strain CKL.	Gift from Heather Long

8.2 Plasmids

Plasmid	Information	Generated by / company
pSG5	Expression vector	Stratagene
pSG5 2A	The entire EBNA 2 open reading frame of EBV strain W91 under the control of the SV40 early promoter in the vector pSG5	(Tsang et al., 1991). Gift from M. Rowe
pSG5 3C	pSG5 EBNA 3C contained a deletion in the repeat region of EBNA 3C (aa 571 to 610). The 1.5 kb BglII fragment of pSG5 EBNA 3C was replaced with the corresponding 1.6kb BglII fragment from EBNA 3C-pZip-neoSV to repair the deletion.	(Radkov et al., 1997; West et al., 2004). Repaired by H. Webb
pRL-CMV	CMV immediate-early enhancer/promoter region, which provides strong, constitutive expression of *Renilla* luciferase	Promega
pFLAG	pFLAG-CMV-2 expression vector with FLAG sequence at position 928-951.	Sigma
pFLAG RGC-32	RGC-32 was amplified from BJAB E3C-4 (Wang et al., 1990a) cDNA using the RGC-32 primer set and cloned into pFLAG-CMV-2 as an Xba1/BamH1 fragment.	Created by Helen Webb
FRT	pcDNA5/FRT	Invitrogen
FRT pFLAG RGC-32	FLAG-RGC-32 was cut out of the pFLAG-RGC-32 plasmid as a Sac1/Sma1 fragment and the Sac1 overhang was blunt ended using mung bean nuclease and the fragment cloned into pcDNA5/FRT cut with EcoRV.	Created by Helen Webb
pBK-CMV-RUNX1c	The pBK vector expressing the RUNX1 isoform 1c under control of the CMV promoter.	Gift from Paul Farrell
RGC-32 pLuc (pGL2)	A 1.2 kb fragment (approximately –1150 to +62 relative to predicted transcription start site) of the RGC32 promoter was amplified from genomic DNA and cloned into pGL2-Basic cut with HindIII/Kpn1.	Created by Helen Webb
RGC-32pLuc (pGL3)	The RGC-32 promoter fragment was cut with HindIII/Kpn1 out of RGC-32pLuc (pGL2) and cloned into a pGL3-Basic vector.	Created by S. Schlick
RGC-32pLuc mut (pGL3)	Contains mutated RUNX1-binding site in the RGC-32pLuc plasmid. The mutated promoter sequence was cut with HindIII/NheI/KpnI and inserted into the pGL3 basic vector expressing firefly luciferase.	Created by S. Schlick
pCp-1425-GL2	Contains the SauIIIA fragment of the C promoter (EBV nucleotides 9911 to 11340) in the pGL2 basic vector expressing firefly luciferase.	Created by F. Nitsche
pmaxGFP	Vector expressing fluorescent GFP.	Amaxa
pET RGC-32	RGC-32 was cut out of pFLAG-RGC-32 as a Sal I/BamHI fragment and cloned into pET16b (Sigma) digested with Xho I/ BamHI.	Sigma and created by Helen Webb
pCEP4	Expression vector	Invitrogen

pCEP4 RUNX1c	Expresses the B cell isoform of RUNX1, RUNX1c.	Gift from P. Farrell (Spender et al., 2005a)
pCEP4 RUNX3	Expresses RUNX3.	Gift from P. Farrell (Spender et al., 2005a)

8.3 Oligonucleotides

Gene	Sequence
GAPDH QPCR primer set MW 84 (forward primer) MW 85 (reverse primer)	 TCA AGA TCA TCA GCA ATG CC CAT GAG TCC TTC CAC GAT ACC
RGC-32 QPCR primer set MW 86 (forward primer) MW 87 (reverse primer)	TTA TAG GAA CAG CTT CAG CTT C CTG AGG AGT GAC AGT GGC AG
RUNX1C QPCR 1st exon primer set MW 349 (forward primer) MW 350 (reverse primer)	 AAC CAC AGA ACC ACA AGT TGG TTG CAT TCA GTG TGA TTC GTC
RGC-32 for RUNX1 site-directed mutagenesis MW 351 (forward primer) MW 352 (reverse primer)	 CTA CAT TTA ATT AGC CGT CTG CTT TGA GAG GCG AGA GGC GCC TCT CGC CTC TCA AAG CAG ACG GCT AAT TAA ATG TAG
RUNX3 QPCR primer set MW 353 (forward primer) MW 354 (reverse primer)	 ATT GCT CTT CCT ACC CCA TCC CCC CGT GCT TCC TAC ATC AGT GTG TTT

8.4 Antibodies

Antibody	Host	Dilution	Information	Reference/ company
Anti pFLAG	mouse	1:500	monoclonal	Sigma
Anti pFLAG purified (M2)	mouse	1:200	monoclonal	Sigma
Anti RGC-32	rabbit	1:500 to 1:1000	polyclonal	Eurogentec
Anti EBNA 3C (A10)	mouse	1:300	monoclonal	(Maunders et al., 1994)
Anti EBNA 2 (PE2)	mouse	1:300	monoclonal	(Young et al., 1989)
M. Stacey serum	human	1:200	polyclonal	Gift from M. Rowe.
Cyclin B1	rabbit	1:2000	polyclonal	Santa Cruz
Cyclin B1	mouse	1:2000	monoclonal	Santa Cruz
pCDK1	rabbit	1:1000		Santa Cruz
CDK1	mouse	1:1000	monoclonal	Santa Cruz
CDK1	mouse	1:1000	monoclonal	(Zymed) Invitrogen
RUNX 1	rabbit	1:40	polyclonal	Calbiochem
RUNX3	rabbit	1:500	polyclonal	Calbiochem
Anti actin	rabbit	1:5000	polyclonal	Sigma
Anti BrdU (IgG2a)	mouse	1:1.5	polyclonal	Millipore
Anti IgG2a	mouse	1:15		Becton-Dickinson
Rabbit-anti-mouse	rabbit	1:20	FITC-conjugated	Dako

8.5 HRP-conjugated substances

Substance	Dilution	Reference/ company
Goat-anti-rabbit ab	1:3000	Cell Signaling Technology
Rabbit-anti-mouse ab	1:1000	Dako
Protein A	1:1000	Amersham

8.6 Hygromycin kill curve for IB4 cells

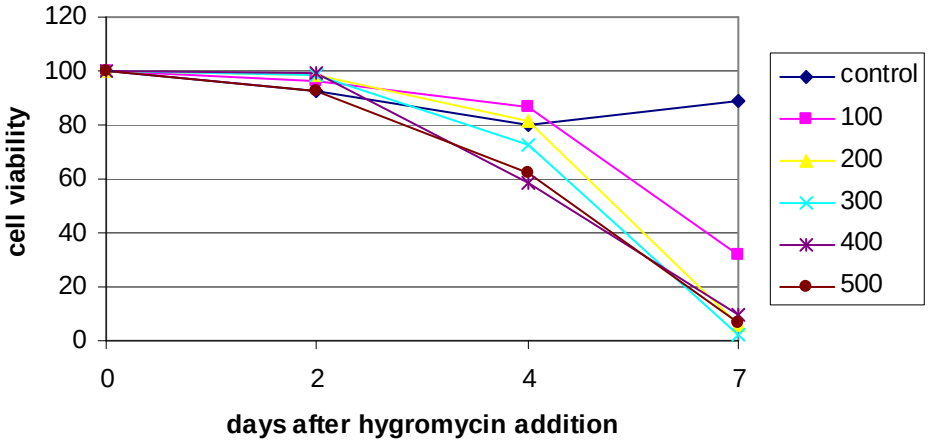

Figure 68 – IB4 cells were set up at $5x10^5$ cells/ml and different concentrations of hygromycin were added (100, 200, 300, 400 or 500 µg/ml). Samples were taken 2, 4 and 7 days after addition of hygromycin. Cells were spun down and resuspended in PBS. Cells were stained with trypan blue to visualise dead cells and counted. The graph represents the viability of cells after treatment with different concentrations of hygromycin against time.

8.7 Sequencing result for RGCpLuc mut (RUNX1) vs. RGCpLuc (wt)

```
CLUSTAL 2.0.11 multiple sequence alignment

Runx1           GAACATTTCTCTATCGATAGGTACCGACAAGCATATCCCTAGGCCACCCAGAGTAGACAA 60
wt              --------------CGGGAGGTACCGACAAGCATATCCCTAGGCCACCCAGAGTAGACAA 46
                              **  ******************************************

Runx1           GAGAGGAGGACTATTCATATGATTAGTGGTCATTAACATATACTCCTTTGTGAGGTGTAT 120
wt              GAGAGGAGGACTATTCATATGATTAGTGGTCATTAACATATACTCCTTTGTGAGGTGTAT 106
                ************************************************************

Runx1           GTTTCAATGTTTTGCTCATTTTTAATTTTTACCAGGTTGTCTATTTGTGATTACTTTGTA 180
wt              GTTTCAATGTTTTGCTCATTTTTAATTTTTACCAGGTTGTCTATTTGTGATTACTTTGTA 166
                ************************************************************

Runx1           GATGGGTCTTTCTATATTCTGAAAACAAATCCTGGCTGGGTGCGGTGGCTCACGCCTGTA 240
wt              GATGGGTCTTTCTATATTCTGAAAACAAATCCTGGCTGGGTGCGGTGGCTCACGCCTGTA 226
                ************************************************************

Runx1           ATCCCAGCACTTTGGGAGGCTGAGGTGGGCAGATCACCTGAGGTCGGGAGTTCGAGACCA 300
wt              ATCCCAGCACTTTGGGAGGCTGAGGTGGGCAGATCACCTGAGGTCGGGAGTTCGAGACCA 286
                ************************************************************

Runx1           GCCTGGCCAACATGGACAAACCCCGTCTCTGCTAAAAATACAAAAACTAGCTGGGAGTGG 360
wt              GCCTGGCCAACATGGACAAACCCCGTCTCTGCTAAAAATACAAAAACTAGCTGGGAGTGG 346
                ************************************************************

Runx1           AGGCTGAATGTTTCACTCCGTTACATGTTAATTGCTCTACATTTAATTAGCCGTCTGCTT 420
wt              AGGCTGAATGTTTCACTCCGTTACATGTTAATTGCTCTACATTTAATTAGCCGTCTGTGG 406
                ************************************************************

Runx1           TGAGAGGCGAGAGGCTAGCGCCTAGCTCAGCGCACAGTCCAGGGCGTTCGCCCCCGCAGG 480
wt              TGAGAGGCGAGAGGCTAGCGCCTAGCTCAGCGCACAGTCCAGGGCGTTCGCCCCCGCAGG 466
                ************************************************************

Runx1           CCGCGGGGCAGGGTGGCTCGTTACTCCGTGGACACTGCAAGGCGCCCTGTTCGCGCTGCG 540
wt              CCGCGGGGCAGGGTGGCTCGTTACTCCGTGGACACTGCAAGGCGCCCTGTTCGCGCTGCG 526
                ************************************************************

Runx1           TCGACGCAGTAGTTTCTTCCCATAATAAACCCCTTCTAGATAAAGTCAGGCTGGCGGGAG 600
wt              TCGACGCAGTAGTTTCTTCCCATAATAAACCCCTTCTAGATAAAGTCAGGCTGGCGGGAG 586
                ************************************************************

Runx1           CGCCCTGGACCGTAGTTCAGGCCCCCGCGCTCCGCGGTGGGAACAGTTCAGGACTCCCCC 660
wt              CGCCCTGGACCGTAGTTCAGGCCCCCGCGCTCCGCGGTGGGAACAGTTCAGGACTCCCCC 646
                ************************************************************

Runx1           AACTCCTGCCCCTCTCGCCCCGACCCTCTCCACTCCGCCCGCCCACCATCTCGGAAGTCC 720
wt              AACTCCTGCCCCTCTCGCCCCGACCCTCTCCACTCCGCCCGCCCACCATCTCGGAAGTCC 706
                ************************************************************

Runx1           CCTTGGGACAATGCGTAGGGGACCTCCGCGTCCCCGACACCCGACTGGGACACGGCCGCG 780
wt              CCTTGGGACAATGCGTAGGGGACCTCCGCGTCCCCGACACCCGACTGGGACACGGCCGCG 766
                ************************************************************

Runx1           GGCTCCTTCGTCCCTCACCGCCAGCCAGGGAGGCTCTGCATGCCCACGTCCACTTCACAG 840
wt              GGCTCCTTCGTCCCTCACCGCCAGCCAGGGAGGCTCTGCATGCCCACGTCCACTTCACAG 826
                ************************************************************

Runx1           CCGAGGAAGCTGCGGCTCGCGGAGGTGCCTGGCACGCGGCGGGAAGCAGCAGAGCTCGCG 900
wt              CCGAGGAAGCTGCGGCTCGCGGAGGTGCCTGGCACGCGGCGGGAAGCAGCAGAGCTCGCG 886
                ************************************************************

Runx1           CCTAGCAGTCAGCTCTGGTGACGCCGAGGACA--------------------------- 932
wt              CCCAGCAGTCAGCTCTGGTGACGCCGAGGACACCGCGTGGGCCGGGTTGTCAGGGCGCGG 946
                ** ****************************
```

9 References

Adams, A. and Lindahl, T. (1975) Epstein-Barr virus genomes with properties of circular DNA molecules in carrier cells. Proc Natl Acad Sci U S A 72(4), 1477-81.

Adldinger, H.K., Delius, H., Freese, U.K., Clarke, J. and Bornkamm, G.W. (1985) A putative transforming gene of Jijoye virus differs from that of Epstein-Barr virus prototypes. Virology 141(2), 221-34.

Aleem, E., Kiyokawa, H. and Kaldis, P. (2005) Cdc2-cyclin E complexes regulate the G1/S phase transition. Nat Cell Biol 7(8), 831-6.

Alfieri, C., Tanner, J., Carpentier, L., Perpete, C., Savoie, A., Paradis, K., Delage, G. and Joncas, J. (1996) Epstein-Barr virus transmission from a blood donor to an organ transplant recipient with recovery of the same virus strain from the recipient's blood and oropharynx, Blood, pp. 812-7. Vol. 87.

Allday, M.J., Crawford, D.H. and Griffin, B.E. (1988) Prediction and demonstration of a novel Epstein-Barr virus nuclear antigen. Nucleic Acids Res 16(10), 4353-67.

Allday, M.J., Crawford, D.H. and Thomas, J.A. (1993) Epstein-Barr virus (EBV) nuclear antigen 6 induces expression of the EBV latent membrane protein and an activated phenotype in Raji cells. J Gen Virol 74 (Pt 3), 361-9.

Allday, M.J. and Farrell, P.J. (1994) Epstein-Barr virus nuclear antigen EBNA3C/6 expression maintains the level of latent membrane protein 1 in G1-arrested cells. J Virol 68(6), 3491-8.

Allday, M.J., Inman, G.J., Crawford, D.H. and Farrell, P.J. (1995a) DNA damage in human B cells can induce apoptosis, proceeding from G1/S when p53 is transactivation competent and G2/M when it is transactivation defective. Embo J 14(20), 4994-5005.

Allday, M.J., Sinclair, A., Parker, G., Crawford, D.H. and Farrell, P.J. (1995b) Epstein-Barr virus efficiently immortalizes human B cells without neutralizing the function of p53. Embo J 14(7), 1382-91.

Altmeyer, A., Simmons, R.C., Krajewski, S., Reed, J.C., Bornkamm, G.W. and Chen-Kiang, S. (1997) Reversal of EBV immortalization precedes apoptosis in IL-6-induced human B cell terminal differentiation. Immunity 7(5), 667-77.

Amann, J.M., Nip, J., Strom, D.K., Lutterbach, B., Harada, H., Lenny, N., Downing, J.R., Meyers, S. and Hiebert, S.W. (2001) ETO, a target of t(8;21) in acute leukemia, makes distinct contacts with multiple histone deacetylases and binds mSin3A through its oligomerization domain. Mol Cell Biol 21(19), 6470-83.

Ambinder, R.F., Shah, W.A., Rawlins, D.R., Hayward, G.S. and Hayward, S.D. (1990) Definition of the sequence requirements for binding of the EBNA-1 protein to its palindromic target sites in Epstein-Barr virus DNA. J Virol 64(5), 2369-79.

Anant, S., Henderson, J.O., Mukhopadhyay, D., Navaratnam, N., Kennedy, S., Min, J. and Davidson, N.O. (2001) Novel role for RNA-binding protein CUGBP2 in mammalian RNA editing. CUGBP2 modulates C to U editing of apolipoprotein B mRNA by interacting with apobec-1 and ACF, the apobec-1 complementation factor. J Biol Chem 276(50), 47338-51.

Anderton, E., Yee, J., Smith, P., Crook, T., White, R.E. and Allday, M.J. (2008) Two Epstein-Barr virus (EBV) oncoproteins cooperate to repress expression of the

proapoptotic tumour-suppressor Bim: clues to the pathogenesis of Burkitt's lymphoma. Oncogene 27(4), 421-33.
Appella, E. and Anderson, C.W. (2001) Post-translational modifications and activation of p53 by genotoxic stresses. Eur J Biochem 268(10), 2764-72.
Aronson, B.D., Fisher, A.L., Blechman, K., Caudy, M. and Gergen, J.P. (1997) Groucho-dependent and -independent repression activities of Runt domain proteins. Mol Cell Biol 17(9), 5581-7.
Asaoka-Taguchi, M., Yamada, M., Nakamura, A., Hanyu, K. and Kobayashi, S. (1999) Maternal Pumilio acts together with Nanos in germline development in Drosophila embryos. Nat Cell Biol 1(7), 431-7.
Atherton-Fessler, S., Parker, L.L., Geahlen, R.L. and Piwnica-Worms, H. (1993) Mechanisms of p34cdc2 regulation. Mol Cell Biol 13(3), 1675-85.
Babcock, G.J., Decker, L.L., Freeman, R.B. and Thorley-Lawson, D.A. (1999) Epstein-barr virus-infected resting memory B cells, not proliferating lymphoblasts, accumulate in the peripheral blood of immunosuppressed patients. J Exp Med 190(4), 567-76.
Babcock, G.J., Decker, L.L., Volk, M. and Thorley-Lawson, D.A. (1998) EBV persistence in memory B cells in vivo. Immunity 9(3), 395-404.
Babcock, G.J., Hochberg, D. and Thorley-Lawson, A.D. (2000) The expression pattern of Epstein-Barr virus latent genes in vivo is dependent upon the differentiation stage of the infected B cell, Immunity, pp. 497-506. Vol. 13.
Babcock, G.J. and Thorley-Lawson, D.A. (2000) Tonsillar memory B cells, latently infected with Epstein-Barr virus, express the restricted pattern of latent genes previously found only in Epstein-Barr virus-associated tumors. Proc Natl Acad Sci U S A 97(22), 12250-5.
Badea, T., Niculescu, F., Soane, L., Fosbrink, M., Sorana, H., Rus, V., Shin, M.L. and Rus, H. (2002) RGC-32 increases p34CDC2 kinase activity and entry of aortic smooth muscle cells into S-phase. J Biol Chem 277(1), 502-8.
Badea, T.C., Niculescu, F.I., Soane, L., Shin, M.L. and Rus, H. (1998) Molecular cloning and characterization of RGC-32, a novel gene induced by complement activation in oligodendrocytes. J Biol Chem 273(41), 26977-81.
Bajaj, B.G., Murakami, M., Cai, Q., Verma, S.C., Lan, K. and Robertson, E.S. (2008) Epstein Barr Virus Nuclear Antigen 3C interacts with and enhances the stability of the c-Myc oncoprotein. J Virol.
Bark-Jones, S.J., Webb, H.M. and West, M.J. (2006) EBV EBNA 2 stimulates CDK9-dependent transcription and RNA polymerase II phosphorylation on serine 5. Oncogene 25(12), 1775-85.
Barnes, E.A., Porter, L.A., Lenormand, J.L., Dellinger, R.W. and Donoghue, D.J. (2003) Human Spy1 promotes survival of mammalian cells following DNA damage. Cancer Res 63(13), 3701-7.
Bartek, J. and Lukas, J. (2001) Pathways governing G1/S transition and their response to DNA damage. FEBS Lett 490(3), 117-22.
Barth, H., Hoffmann, I. and Kinzel, V. (1996) Radiation with 1 Gy prevents the activation of the mitotic inducers mitosis-promoting factor (MPF) and cdc25-C in HeLa cells. Cancer Res 56(10), 2268-72.
Bell, A., Skinner, J., Kirby, H. and Rickinson, A. (1998) Characterisation of regulatory sequences at the Epstein-Barr virus BamHI W promoter. Virology 252(1), 149-61.
Ben-Bassat, H., Goldblum, N., Mitrani, S., Goldblum, T., Yoffey, J.M., Cohen, M.M., Bentwich, Z., Ramot, B., Klein, E. and Klein, G. (1977) Establishment in

continuous culture of a new type of lymphocyte from a "Burkitt like" malignant lymphoma (line D.G.-75). Int J Cancer 19(1), 27-33.
Bernardin, F., Yang, Y., Cleaves, R., Zahurak, M., Cheng, L., Civin, C.I. and Friedman, A.D. (2002) TEL-AML1, expressed from t(12;21) in human acute lymphocytic leukemia, induces acute leukemia in mice. Cancer Res 62(14), 3904-8.
Bhatia, K., Huppi, K., Spangler, G., Siwarski, D., Iyer, R. and Magrath, I. (1993) Point mutations in the c-Myc transactivation domain are common in Burkitt's lymphoma and mouse plasmacytomas, Nat Genet, pp. 56-61. Vol. 5.
Blagosklonny, M.V. and Pardee, A.B. (2002) The restriction point of the cell cycle. Cell Cycle 1(2), 103-10.
Blaxall, B.C., Tschannen-Moran, B.M., Milano, C.A. and Koch, W.J. (2003) Differential gene expression and genomic patient stratification following left ventricular assist device support. J Am Coll Cardiol 41(7), 1096-106.
Bode, A.M. and Dong, Z. (2004) Post-translational modification of p53 in tumorigenesis. Nat Rev Cancer 4(10), 793-805.
Bodescot, M. and Perricaudet, M. (1986) Epstein-Barr virus mRNAs produced by alternative splicing. Nucleic Acids Research 14(17), 7103-14.
Borestrom, C., Zetterberg, H., Liff, K. and Rymo, L. (2003) Functional interaction of nuclear factor Y and Sp1 is required for activation of the Epstein-Barr virus C promoter. Journal of Virology 77(2), 821-829.
Borgne, A., Ostvold, A.C., Flament, S. and Meijer, L. (1999) Intra-M phase-promoting factor phosphorylation of cyclin B at the prophase/metaphase transition. J Biol Chem 274(17), 11977-86.
Brehm, A., Miska, E.A., McCance, D.J., Reid, J.L., Bannister, A.J. and Kouzarides, T. (1998) Retinoblastoma protein recruits histone deacetylase to repress transcription. Nature 391(6667), 597-601.
Brink, A.A., ten Berge, R.L., van den Brule, A.J., Willemze, R., Chott, A. and Meijer, C.J. (2000a) Epstein-Barr virus is present in neoplastic cytotoxic T cells in extranodal, and predominantly in B cells in nodal T non-Hodgkin lymphomas. J Pathol 191(4), 400-6.
Brink, A.A., ten Berge, R.L., van den Brule, A.J., Willemze, R., Chott, A. and Meijer, C.J. (2000b) Epstein-Barr virus is present in neoplastic cytotoxic T cells in extranodal, and predominantly in B cells in nodal T non-Hodgkin lymphomas, J Pathol, pp. 400-6. Vol. 191.
Bristow, C.A. and Shore, P. (2003) Transcriptional regulation of the human MIP-1alpha promoter by RUNX1 and MOZ. Nucleic Acids Res 31(11), 2735-44.
Britos-Bray, M. and Friedman, A.D. (1997) Core binding factor cannot synergistically activate the myeloperoxidase proximal enhancer in immature myeloid cells without c-Myb. Mol Cell Biol 17(9), 5127-35.
Brizuela, L., Draetta, G. and Beach, D. (1989) Activation of human CDC2 protein as a histone H1 kinase is associated with complex formation with the p62 subunit. Proc Natl Acad Sci U S A 86(12), 4362-6.
Burgess, A., Buck, M., Krauer, K. and Sculley, T. (2006) Nuclear localization of the Epstein-Barr virus EBNA3B protein, J Gen Virol, pp. 789-93. Vol. 87.
Calender, A., Billaud, M., Aubry, J.P., Banchereau, J., Vuillaume, M. and Lenoir, G.M. (1987) Epstein-Barr virus (EBV) induces expression of B-cell activation markers on in vitro infection of EBV-negative B-lymphoma cells. Proc Natl Acad Sci U S A 84(22), 8060-4.

Callan, M.F., Steven, N., Krausa, P., Wilson, J.D., Moss, P.A., Gillespie, G.M., Bell, J.I., Rickinson, A.B. and McMichael, A.J. (1996) Large clonal expansions of CD8+ T cells in acute infectious mononucleosis. Nat Med 2(8), 906-11.

Callan, M.F., Tan, L., Annels, N., Ogg, G.S., Wilson, J.D., O'Callaghan, C.A., Steven, N., McMichael, A.J. and Rickinson, A.B. (1998) Direct visualization of antigen-specific CD8+ T cells during the primary immune response to Epstein-Barr virus In vivo. J Exp Med 187(9), 1395-402.

Capoulade, C., Bressac-de Paillerets, B., Lefrere, I., Ronsin, M., Feunteun, J., Tursz, T. and Wiels, J. (1998) Overexpression of MDM2, due to enhanced translation, results in inactivation of wild-type p53 in Burkitt's lymphoma cells. Oncogene 16(12), 1603-10.

Cen, H., Breinig, M.C., Atchison, R.W., Ho, M. and McKnight, J.L. (1991) Epstein-Barr virus transmission via the donor organs in solid organ transplantation: polymerase chain reaction and restriction fragment length polymorphism analysis of IR2, IR3, and IR4, J Virol, pp. 976-80. Vol. 65.

Cesarman, E., Dalla-Favera, R., Bentley, D. and Groudine, M. (1987) Mutations in the first exon are associated with altered transcription of c-myc in Burkitt lymphoma, Science, pp. 1272-5. Vol. 238.

Chakraborty, S., Sinha, K.K., Senyuk, V. and Nucifora, G. (2003) SUV39H1 interacts with AML1 and abrogates AML1 transactivity. AML1 is methylated in vivo. Oncogene 22(34), 5229-37.

Charroux, B., Pellizzoni, L., Perkinson, R.A., Shevchenko, A., Mann, M. and Dreyfuss, G. (1999) Gemin3: A novel DEAD box protein that interacts with SMN, the spinal muscular atrophy gene product, and is a component of gems. J Cell Biol 147(6), 1181-94.

Chaturvedi, P., Eng, W.K., Zhu, Y., Mattern, M.R., Mishra, R., Hurle, M.R., Zhang, X., Annan, R.S., Lu, Q., Faucette, L.F., Scott, G.F., Li, X., Carr, S.A., Johnson, R.K., Winkler, J.D. and Zhou, B.B. (1999) Mammalian Chk2 is a downstream effector of the ATM-dependent DNA damage checkpoint pathway. Oncogene 18(28), 4047-54.

Chehab, N.H., Malikzay, A., Appel, M. and Halazonetis, T.D. (2000) Chk2/hCds1 functions as a DNA damage checkpoint in G(1) by stabilizing p53. Genes Dev 14(3), 278-88.

Chen, A., Divisconte, M., Jiang, X., Quink, C. and Wang, F. (2005) Epstein-Barr virus with the latent infection nuclear antigen 3B completely deleted is still competent for B-cell growth transformation in vitro, J Virol, pp. 4506-9. Vol. 79.

Chen, A., Zhao, B., Kieff, E., Aster, J.C. and Wang, F. (2006) EBNA-3B- and EBNA-3C-regulated cellular genes in Epstein-Barr virus-immortalized lymphoblastoid cell lines. J Virol 80(20), 10139-50.

Chen, J., Marechal, V. and Levine, A.J. (1993) Mapping of the p53 and mdm-2 interaction domains. Mol Cell Biol 13(7), 4107-14.

Cheng, A., Xiong, W., Ferrell, J.E., Jr. and Solomon, M.J. (2005) Identification and comparative analysis of multiple mammalian Speedy/Ringo proteins. Cell Cycle 4(1), 155-65.

Chinnadurai, G. (2002) CtBP, an unconventional transcriptional corepressor in development and oncogenesis. Mol Cell 9(2), 213-24.

Chittenden, T., Lupton, S. and Levine, A.J. (1989) Functional limits of oriP, the Epstein-Barr virus plasmid origin of replication. J Virol 63(7), 3016-25.

Choudhuri, T., Verma, S.C., Lan, K., Murakami, M. and Robertson, E.S. (2007) The ATM/ATR signaling effector Chk2 is targeted by Epstein-Barr virus nuclear antigen 3C to release the G2/M cell cycle block. J Virol 81(12), 6718-30.

Cohen, J.I. and Kieff, E. (1991) An Epstein-Barr virus nuclear protein 2 domain essential for transformation is a direct transcriptional activator. J Virol 65(11), 5880-5.

Cohen, J.I., Wang, F., Mannick, J. and Kieff, E. (1989) Epstein-Barr virus nuclear protein 2 is a key determinant of lymphocyte transformation. Proc Natl Acad Sci U S A 86(23), 9558-62.

Collier, B., Gorgoni, B., Loveridge, C., Cooke, H.J. and Gray, N.K. (2005) The DAZL family proteins are PABP-binding proteins that regulate translation in germ cells. Embo J 24(14), 2656-66.

Cooper, A., Johannsen, E., Maruo, S., Cahir-McFarland, E., Illanes, D., Davidson, D. and Kieff, E. (2003) EBNA3A association with RBP-Jkappa down-regulates c-myc and Epstein-Barr virus-transformed lymphoblast growth. J Virol 77(2), 999-1010.

Cotter, M.A., 2nd and Robertson, E.S. (2000) Modulation of histone acetyltransferase activity through interaction of epstein-barr nuclear antigen 3C with prothymosin alpha. Mol Cell Biol 20(15), 5722-35.

Crawford, D.H. (2001) Biology and disease associations of Epstein-Barr virus. Philos Trans R Soc Lond B Biol Sci 356(1408), 461-73.

Crawford, D.H. and Ando, I. (1986) EB virus induction is associated with B-cell maturation. Immunology 59(3), 405-9.

Daga, A., Tighe, J.E. and Calabi, F. (1992) Leukaemia/Drosophila homology. Nature 356(6369), 484.

D'Alonzo, R.C., Selvamurugan, N., Karsenty, G. and Partridge, N.C. (2002) Physical interaction of the activator protein-1 factors c-Fos and c-Jun with Cbfa1 for collagenase-3 promoter activation. J Biol Chem 277(1), 816-22.

Dang, C.V., O'Donnell, K.A., Zeller, K.I., Nguyen, T., Osthus, R.C. and Li, F. (2006) The c-Myc target gene network. Semin Cancer Biol 16(4), 253-64.

Davenport, M.G. and Pagano, J.S. (1999) Expression of EBNA-1 mRNA is regulated by cell cycle during Epstein-Barr virus type I latency. J Virol 73(4), 3154-61.

De Matteo, E., Baron, A.V., Chabay, P., Porta, J., Dragosky, M. and Preciado, M.V. (2003) Comparison of Epstein-Barr virus presence in Hodgkin lymphoma in pediatric versus adult Argentine patients. Arch Pathol Lab Med 127(10), 1325-9.

Dinarina, A., Perez, L.H., Davila, A., Schwab, M., Hunt, T. and Nebreda, A.R. (2005) Characterization of a new family of cyclin-dependent kinase activators. Biochem J 386(Pt 2), 349-55.

Donninger, H., Bonome, T., Radonovich, M., Pise-Masison, C.A., Brady, J., Shih, J.H., Barrett, J.C. and Birrer, M.J. (2004) Whole genome expression profiling of advance stage papillary serous ovarian cancer reveals activated pathways. Oncogene 23(49), 8065-77.

Duffy, J.B. and Gergen, J.P. (1991) The Drosophila segmentation gene runt acts as a position-specific numerator element necessary for the uniform expression of the sex-determining gene Sex-lethal. Genes Dev 5(12A), 2176-87.

Duffy, J.B., Kania, M.A. and Gergen, J.P. (1991) Expression and function of the Drosophila gene runt in early stages of neural development. Development 113(4), 1223-30.

Dunaief, J.L., Strober, B.E., Guha, S., Khavari, P.A., Alin, K., Luban, J., Begemann, M., Crabtree, G.R. and Goff, S.P. (1994) The retinoblastoma protein and BRG1 form a complex and cooperate to induce cell cycle arrest. Cell 79(1), 119-30.

Durst, K.L., Lutterbach, B., Kummalue, T., Friedman, A.D. and Hiebert, S.W. (2003) The inv(16) fusion protein associates with corepressors via a smooth muscle myosin heavy-chain domain. Mol Cell Biol 23(2), 607-19.

Dyson, N. (1998) The regulation of E2F by pRB-family proteins. Genes Dev 12(15), 2245-62.

Ehlin-Henriksson, B., Mowafi, F., Klein, G. and Nilsson, A. (2006) Epstein-Barr virus infection negatively impacts the CXCR4-dependent migration of tonsillar B cells. Immunology 117(3), 379-85.

Ekholm, S.V. and Reed, S.I. (2000) Regulation of G(1) cyclin-dependent kinases in the mammalian cell cycle. Curr Opin Cell Biol 12(6), 676-84.

el-Deiry, W.S., Tokino, T., Velculescu, V.E., Levy, D.B., Parsons, R., Trent, J.M., Lin, D., Mercer, W.E., Kinzler, K.W. and Vogelstein, B. (1993) WAF1, a potential mediator of p53 tumor suppression. Cell 75(4), 817-25.

Endicott, J.A., Nurse, P. and Johnson, L.N. (1994) Mutational analysis supports a structural model for the cell cycle protein kinase p34. Protein Eng 7(2), 243-53.

Enoch, T., Peter, M., Nurse, P. and Nigg, E.A. (1991) p34cdc2 acts as a lamin kinase in fission yeast. J Cell Biol 112(5), 797-807.

Epstein, M.A., Achong, B.G. and Barr, Y.M. (1964) Virus Particles in Cultured Lymphoblasts from Burkitt's Lymphoma. Lancet 1, 702-3.

Erickson, P., Gao, J., Chang, K.S., Look, T., Whisenant, E., Raimondi, S., Lasher, R., Trujillo, J., Rowley, J. and Drabkin, H. (1992) Identification of breakpoints in t(8;21) acute myelogenous leukemia and isolation of a fusion transcript, AML1/ETO, with similarity to Drosophila segmentation gene, runt. Blood 80(7), 1825-31.

Evans, T., Rosenthal, E.T., Youngblom, J., Distel, D. and Hunt, T. (1983) Cyclin: a protein specified by maternal mRNA in sea urchin eggs that is destroyed at each cleavage division. Cell 33(2), 389-96.

Fahraeus, R., Fu, H.L., Ernberg, I., Finke, J., Rowe, M., Klein, G., Falk, K., Nilsson, E., Yadav, M., Busson, P. and et al. (1988) Expression of Epstein-Barr virus-encoded proteins in nasopharyngeal carcinoma. Int J Cancer 42(3), 329-38.

Fahraeus, R., Jansson, A., Ricksten, A., Sjoblom, A. and Rymo, L. (1990) Epstein-Barr virus-encoded nuclear antigen 2 activates the viral latent membrane protein promoter by modulating the activity of a negative regulatory element. Proc Natl Acad Sci U S A 87(19), 7390-4.

Fainaru, O., Woolf, E., Lotem, J., Yarmus, M., Brenner, O., Goldenberg, D., Negreanu, V., Bernstein, Y., Levanon, D., Jung, S. and Groner, Y. (2004) Runx3 regulates mouse TGF-beta-mediated dendritic cell function and its absence results in airway inflammation. Embo J 23(4), 969-79.

Falck, J., Mailand, N., Syljuasen, R.G., Bartek, J. and Lukas, J. (2001) The ATM-Chk2-Cdc25A checkpoint pathway guards against radioresistant DNA synthesis. Nature 410(6830), 842-7.

Farrell, P.J., Allan, G.J., Shanahan, F., Vousden, K.H. and Crook, T. (1991) p53 is frequently mutated in Burkitt's lymphoma cell lines. Embo J 10(10), 2879-87.

Fenrick, R., Amann, J.M., Lutterbach, B., Wang, L., Westendorf, J.J., Downing, J.R. and Hiebert, S.W. (1999) Both TEL and AML-1 contribute repression domains to the t(12;21) fusion protein. Mol Cell Biol 19(10), 6566-74.

Ferby, I., Blazquez, M., Palmer, A., Eritja, R. and Nebreda, A.R. (1999) A novel p34(cdc2)-binding and activating protein that is necessary and sufficient to trigger G(2)/M progression in Xenopus oocytes. Genes Dev 13(16), 2177-89.

Ferme, C., Eghbali, H., Meerwaldt, J.H., Rieux, C., Bosq, J., Berger, F., Girinsky, T., Brice, P., van't Veer, M.B., Walewski, J.A., Lederlin, P., Tirelli, U., Carde, P., Van den Neste, E., Gyan, E., Monconduit, M., Divine, M., Raemaekers, J.M., Salles, G., Noordijk, E.M., Creemers, G.J., Gabarre, J., Hagenbeek, A., Reman, O., Blanc, M., Thomas, J., Vie, B., Kluin-Nelemans, J.C., Viseu, F., Baars, J.W., Poortmans, P., Lugtenburg, P.J., Carrie, C., Jaubert, J. and Henry-Amar, M. (2007) Chemotherapy plus involved-field radiation in early-stage Hodgkin's disease. N Engl J Med 357(19), 1916-27.

Fingeroth, J.D., Diamond, M.E., Sage, D.R., Hayman, J. and Yates, J.L. (1999) CD21-Dependent infection of an epithelial cell line, 293, by Epstein-Barr virus. J Virol 73(3), 2115-25.

Fisher, R.P. and Morgan, D.O. (1994) A novel cyclin associates with MO15/CDK7 to form the CDK-activating kinase. Cell 78(4), 713-24.

Flavell, K.J. and Murray, P.G. (2000) Hodgkin's disease and the Epstein-Barr virus, Mol Pathol, pp. 262-9. Vol. 53.

Fosbrink, M., Cudrici, C., Niculescu, F., Badea, T.C., David, S., Shamsuddin, A., Shin, M.L. and Rus, H. (2005) Overexpression of RGC-32 in colon cancer and other tumors. Exp Mol Pathol 78(2), 116-22.

Fox, M., Urano, J. and Reijo Pera, R.A. (2005) Identification and characterization of RNA sequences to which human PUMILIO-2 (PUM2) and deleted in Azoospermia-like (DAZL) bind. Genomics 85(1), 92-105.

Fuentes-Panana, E.M., Peng, R., Brewer, G., Tan, J. and Ling, P.D. (2000) Regulation of the Epstein-Barr virus C promoter by AUF1 and the cyclic AMP/protein kinase A signaling pathway. J Virol 74(17), 8166-75.

Fujita, T., Azuma, Y., Fukuyama, R., Hattori, Y., Yoshida, C., Koida, M., Ogita, K. and Komori, T. (2004) Runx2 induces osteoblast and chondrocyte differentiation and enhances their migration by coupling with PI3K-Akt signaling. J Cell Biol 166(1), 85-95.

Gaidano, G., Ballerini, P., Gong, J.Z., Inghirami, G., Neri, A., Newcomb, E.W., Magrath, I.T., Knowles, D.M. and Dalla-Favera, R. (1991) p53 mutations in human lymphoid malignancies: association with Burkitt lymphoma and chronic lymphocytic leukemia. Proc Natl Acad Sci U S A 88(12), 5413-7.

Gallagher, W.M., Bergin, O.E., Rafferty, M., Kelly, Z.D., Nolan, I.M., Fox, E.J., Culhane, A.C., McArdle, L., Fraga, M.F., Hughes, L., Currid, C.A., O'Mahony, F., Byrne, A., Murphy, A.A., Moss, C., McDonnell, S., Stallings, R.L., Plumb, J.A., Esteller, M., Brown, R., Dervan, P.A. and Easty, D.J. (2005) Multiple markers for melanoma progression regulated by DNA methylation: insights from transcriptomic studies. Carcinogenesis 26(11), 1856-67.

Gallant, P. and Nigg, E.A. (1992) Cyclin B2 undergoes cell cycle-dependent nuclear translocation and, when expressed as a non-destructible mutant, causes mitotic arrest in HeLa cells. J Cell Biol 117(1), 213-24.

Gallant, P. and Nigg, E.A. (1994) Identification of a novel vertebrate cyclin: cyclin B3 shares properties with both A- and B-type cyclins. Embo J 13(3), 595-605.

Gartel, A.L., Ye, X., Goufman, E., Shianov, P., Hay, N., Najmabadi, F. and Tyner, A.L. (2001) Myc represses the p21(WAF1/CIP1) promoter and interacts with Sp1/Sp3. Proc Natl Acad Sci U S A 98(8), 4510-5.

Gastwirt, R.F., McAndrew, C.W. and Donoghue, D.J. (2007) Speedy/RINGO regulation of CDKs in cell cycle, checkpoint activation and apoptosis. Cell Cycle 6(10), 1188-93.

Gebauer, F. and Hentze, M.W. (2004) Molecular mechanisms of translational control. Nat Rev Mol Cell Biol 5(10), 827-35.

Gerber, P., Walsh, J.H., Rosenblum, E.N. and Purcell, R.H. (1969) Association of EB-virus infection with the post-perfusion syndrome, Lancet, pp. 593-5. Vol. 1.

Gergen, J.P. and Wieschaus, E. (1986) Dosage requirements for runt in the segmentation of Drosophila embryos. Cell 45(2), 289-99.

Gillian, A.L. and Svaren, J. (2004) The Ddx20/DP103 dead box protein represses transcriptional activation by Egr2/Krox-20. J Biol Chem 279(10), 9056-63.

Girard, F., Strausfeld, U., Cavadore, J.C., Russell, P., Fernandez, A. and Lamb, N.J. (1992) cdc25 is a nuclear protein expressed constitutively throughout the cell cycle in nontransformed mammalian cells. J Cell Biol 118(4), 785-94.

Glaser, S.L., Clarke, C.A., Gulley, M.L., Craig, F.E., DiGiuseppe, J.A., Dorfman, R.F., Mann, R.B. and Ambinder, R.F. (2003) Population-based patterns of human immunodeficiency virus-related Hodgkin lymphoma in the Greater San Francisco Bay Area, 1988-1998, Cancer, pp. 300-9. Vol. 98.

Glaser, S.L., Lin, R.J., Stewart, S.L., Ambinder, R.F., Jarrett, R.F., Brousset, P., Pallesen, G., Gulley, M.L., Khan, G., O'Grady, J., Hummel, M., Preciado, M.V., Knecht, H., Chan, J.K. and Claviez, A. (1997) Epstein-Barr virus-associated Hodgkin's disease: epidemiologic characteristics in international data, Int J Cancer, pp. 375-82. Vol. 70.

Golub, T.R., Barker, G.F., Bohlander, S.K., Hiebert, S.W., Ward, D.C., Bray-Ward, P., Morgan, E., Raimondi, S.C., Rowley, J.D. and Gilliland, D.G. (1995) Fusion of the TEL gene on 12p13 to the AML1 gene on 21q22 in acute lymphoblastic leukemia. Proc Natl Acad Sci U S A 92(11), 4917-21.

Gould, K.L. and Nurse, P. (1989) Tyrosine phosphorylation of the fission yeast cdc2+ protein kinase regulates entry into mitosis. Nature 342(6245), 39-45.

Gregory, C.D., Rowe, M. and Rickinson, A.B. (1990) Different Epstein-Barr virus-B cell interactions in phenotypically distinct clones of a Burkitt's lymphoma cell line. J Gen Virol 71 (Pt 7), 1481-95.

Gregory, C.D., Tursz, T., Edwards, C.F., Tetaud, C., Talbot, M., Caillou, B., Rickinson, A.B. and Lipinski, M. (1987) Identification of a subset of normal B cells with a Burkitt's lymphoma (BL)-like phenotype. J Immunol 139(1), 313-8.

Grossman, S., Johannsen, E., Tong, X. and Yalamanchili, R. (1994a) The Epstein-Barr virus nuclear antigen 2 transactivation is directed to response elements by the J kappa recombination signal binding protein. Proceedings of the National Academy of Sciences of the United States of America 91, 7568-72.

Grossman, S.R., Johannsen, E., Tong, X., Yalamanchili, R. and Kieff, E. (1994b) The Epstein-Barr virus nuclear antigen 2 transactivator is directed to response elements by the J kappa recombination signal binding protein. Proc Natl Acad Sci U S A 91(16), 7568-72.

Grundhoff, A.T., Kremmer, E., Tureci, O., Glieden, A., Gindorf, C., Atz, J., Mueller-Lantzsch, N., Schubach, W.H. and Grasser, F.A. (1999) Characterization of DP103, a novel DEAD box protein that binds to the Epstein-Barr virus nuclear proteins EBNA2 and EBNA3C. J Biol Chem 274(27), 19136-44.

Guo, W.H., Weng, L.Q., Ito, K., Chen, L.F., Nakanishi, H., Tatematsu, M. and Ito, Y. (2002) Inhibition of growth of mouse gastric cancer cells by Runx3, a novel tumor suppressor. Oncogene 21(54), 8351-5.

Habeshaw, G., Yao, Q.Y., Bell, A.I., Morton, D. and Rickinson, A.B. (1999) Epstein-barr virus nuclear antigen 1 sequences in endemic and sporadic Burkitt's lymphoma reflect virus strains prevalent in different geographic areas. J Virol 73(2), 965-75.

Hagting, A., Jackman, M., Simpson, K. and Pines, J. (1999) Translocation of cyclin B1 to the nucleus at prophase requires a phosphorylation-dependent nuclear import signal. Curr Biol 9(13), 680-9.

Hagting, A., Karlsson, C., Clute, P., Jackman, M. and Pines, J. (1998) MPF localization is controlled by nuclear export. Embo J 17(14), 4127-38.

Hake, L.E. and Richter, J.D. (1994) CPEB is a specificity factor that mediates cytoplasmic polyadenylation during Xenopus oocyte maturation. Cell 79(4), 617-27.

Halaban, R. (2005) Rb/E2F: a two-edged sword in the melanocytic system. Cancer Metastasis Rev 24(2), 339-56.

Hammerschmidt, W. and Sugden, B. (1989) Genetic analysis of immortalizing functions of Epstein-Barr virus in human B lymphocytes. Nature 340(6232), 393-7.

Hanahan, D. and Weinberg, R.A. (2000) The hallmarks of cancer. Cell 100(1), 57-70.

Hanai, J., Chen, L.F., Kanno, T., Ohtani-Fujita, N., Kim, W.Y., Guo, W.H., Imamura, T., Ishidou, Y., Fukuchi, M., Shi, M.J., Stavnezer, J., Kawabata, M., Miyazono, K. and Ito, Y. (1999) Interaction and functional cooperation of PEBP2/CBF with Smads. Synergistic induction of the immunoglobulin germline Calpha promoter. J Biol Chem 274(44), 31577-82.

Haque, T., Thomas, J.A., Falk, K.I., Parratt, R., Hunt, B.J., Yacoub, M. and Crawford, D.H. (1996) Transmission of donor Epstein-Barr virus (EBV) in transplanted organs causes lymphoproliferative disease in EBV-seronegative recipients, J Gen Virol, pp. 1169-72. Vol. 77 (Pt 6).

Harada, S. and Kieff, E. (1997) Epstein-Barr virus nuclear protein LP stimulates EBNA-2 acidic domain-mediated transcriptional activation. J Virol 71(9), 6611-8.

Harbour, J.W., Luo, R.X., Dei Santi, A., Postigo, A.A. and Dean, D.C. (1999) Cdk phosphorylation triggers sequential intramolecular interactions that progressively block Rb functions as cells move through G1. Cell 98(6), 859-69.

Haritos, A.A., Goodall, G.J. and Horecker, B.L. (1984) Prothymosin alpha: isolation and properties of the major immunoreactive form of thymosin alpha 1 in rat thymus. Proc Natl Acad Sci U S A 81(4), 1008-11.

Hatfull, G., Bankier, A.T., Barrell, B.G. and Farrell, P.J. (1988) Sequence analysis of Raji Epstein-Barr virus DNA. Virology 164(2), 334-40.

Heald, R., McLoughlin, M. and McKeon, F. (1993) Human wee1 maintains mitotic timing by protecting the nucleus from cytoplasmically activated Cdc2 kinase. Cell 74(3), 463-74.

Henke, C.E., Kurland, L.T. and Elveback, L.R. (1973) Infectious mononucleosis in Rochester, Minnesota, 1950 through 1969, Am J Epidemiol, pp. 483-90. Vol. 98.

Henkel, T., Ling, P.D., Hayward, S.D. and Peterson, M.G. (1994) Mediation of Epstein-Barr virus EBNA2 transactivation by recombination signal-binding protein J kappa. Science 265(5168), 92-5.

Henle, G. and Henle, W. (1966) Studies on cell lines derived from Burkitt's lymphoma. Trans N Y Acad Sci 29(1), 71-9.

Henle, G., Henle, W., Clifford, P., Diehl, V., Kafuko, G.W., Kirya, B.G., Klein, G., Morrow, R.H., Munube, G.M., Pike, P., Tukei, P.M. and Ziegler, J.L. (1969)

Antibodies to Epstein-Barr virus in Burkitt's lymphoma and control groups. J Natl Cancer Inst 43(5), 1147-57.

Herbst, H., Dallenbach, F., Hummel, M., Niedobitek, G., Pileri, S., Muller-Lantzsch, N. and Stein, H. (1991) Epstein-Barr virus latent membrane protein expression in Hodgkin and Reed-Sternberg cells. Proc Natl Acad Sci U S A 88(11), 4766-70.

Herzinger, T., Funk, J.O., Hillmer, K., Eick, D., Wolf, D.A. and Kind, P. (1995) Ultraviolet B irradiation-induced G2 cell cycle arrest in human keratinocytes by inhibitory phosphorylation of the cdc2 cell cycle kinase. Oncogene 11(10), 2151-6.

Hess, J., Porte, D., Munz, C. and Angel, P. (2001) AP-1 and Cbfa/runt physically interact and regulate parathyroid hormone-dependent MMP13 expression in osteoblasts through a new osteoblast-specific element 2/AP-1 composite element. J Biol Chem 276(23), 20029-38.

Hickabottom, M., Parker, G.A., Freemont, P., Crook, T. and Allday, M.J. (2002) Two nonconsensus sites in the Epstein-Barr virus oncoprotein EBNA3A cooperate to bind the co-repressor carboxyl-terminal-binding protein (CtBP), 47197-204 pp. J Biol Chem, 277.

Hochberg, D., Middeldorp, J.M., Catalina, M., Sullivan, J.L., Luzuriaga, K. and Thorley-Lawson, D.A. (2004) Demonstration of the Burkitt's lymphoma Epstein-Barr virus phenotype in dividing latently infected memory cells in vivo. Proc Natl Acad Sci U S A 101(1), 239-44.

Hochegger, H., Dejsuphong, D., Sonoda, E., Saberi, A., Rajendra, E., Kirk, J., Hunt, T. and Takeda, S. (2007) An essential role for Cdk1 in S phase control is revealed via chemical genetics in vertebrate cells. J Cell Biol 178(2), 257-68.

Hochegger, H., Klotzbucher, A., Kirk, J., Howell, M., le Guellec, K., Fletcher, K., Duncan, T., Sohail, M. and Hunt, T. (2001) New B-type cyclin synthesis is required between meiosis I and II during Xenopus oocyte maturation. Development 128(19), 3795-807.

Hoffmann, I., Clarke, P.R., Marcote, M.J., Karsenti, E. and Draetta, G. (1993) Phosphorylation and activation of human cdc25-C by cdc2--cyclin B and its involvement in the self-amplification of MPF at mitosis. Embo J 12(1), 53-63.

Holmes, R.D. and Sokol, R.J. (2002) Epstein-Barr virus and post-transplant lymphoproliferative disease, Pediatr Transplant, pp. 456-64. Vol. 6.

Hurley, E.A. and Thorley-Lawson, D.A. (1988) B cell activation and the establishment of Epstein-Barr virus latency. J Exp Med 168(6), 2059-75.

Ichikawa, M., Asai, T., Saito, T., Seo, S., Yamazaki, I., Yamagata, T., Mitani, K., Chiba, S., Ogawa, S., Kurokawa, M. and Hirai, H. (2004) AML-1 is required for megakaryocytic maturation and lymphocytic differentiation, but not for maintenance of hematopoietic stem cells in adult hematopoiesis. Nat Med 10(3), 299-304.

Imai, Y., Kurokawa, M., Tanaka, K., Friedman, A.D., Ogawa, S., Mitani, K., Yazaki, Y. and Hirai, H. (1998) TLE, the human homolog of groucho, interacts with AML1 and acts as a repressor of AML1-induced transactivation. Biochem Biophys Res Commun 252(3), 582-9.

Imataka, H., Gradi, A. and Sonenberg, N. (1998) A newly identified N-terminal amino acid sequence of human eIF4G binds poly(A)-binding protein and functions in poly(A)-dependent translation. Embo J 17(24), 7480-9.

Inman, G.J. and Farrell, P.J. (1995) Epstein-Barr virus EBNA-LP and transcription regulation properties of pRB, p107 and p53 in transfection assays. J Gen Virol 76 (Pt 9), 2141-9.

Inoue, K., Ozaki, S., Shiga, T., Ito, K., Masuda, T., Okado, N., Iseda, T., Kawaguchi, S., Ogawa, M., Bae, S.C., Yamashita, N., Itohara, S., Kudo, N. and Ito, Y. (2002) Runx3 controls the axonal projection of proprioceptive dorsal root ganglion neurons. Nat Neurosci 5(10), 946-54.

Ito, S., Gotoh, E., Ozawa, S. and Yanagi, K. (2002) Epstein-Barr virus nuclear antigen-1 is highly colocalized with interphase chromatin and its newly replicated regions in particular, J Gen Virol, pp. 2377-83. Vol. 83.

Ito, S. and Yanagi, K. (2003) Epstein-Barr virus (EBV) nuclear antigen 1 colocalizes with cellular replication foci in the absence of EBV plasmids, Journal of Virology, pp. 3824-3831. Vol. 77.

Izumi, T. and Maller, J.L. (1991) Phosphorylation of Xenopus cyclins B1 and B2 is not required for cell cycle transitions. Mol Cell Biol 11(8), 3860-7.

Javed, A., Guo, B., Hiebert, S., Choi, J.Y., Green, J., Zhao, S.C., Osborne, M.A., Stifani, S., Stein, J.L., Lian, J.B., van Wijnen, A.J. and Stein, G.S. (2000) Groucho/TLE/R-esp proteins associate with the nuclear matrix and repress RUNX (CBF(alpha)/AML/PEBP2(alpha)) dependent activation of tissue-specific gene transcription. J Cell Sci 113 (Pt 12), 2221-31.

Jenkins, P.J., Binne, U.K. and Farrell, P.J. (2000) Histone acetylation and reactivation of Epstein-Barr virus from latency. J Virol 74(2), 710-20.

Jimenez-Ramirez, C., Brooks, A.J., Forshell, L.P., Yakimchuk, K., Zhao, B., Fulgham, T.Z. and Sample, C.E. (2006) Epstein-Barr virus EBNA-3C is targeted to and regulates expression from the bidirectional LMP-1/2B promoter. J Virol 80(22), 11200-8.

Jin, Z.H., Kurosu, T., Yamaguchi, M., Arai, A. and Miura, O. (2005) Hematopoietic cytokines enhance Chk1-dependent G2/M checkpoint activation by etoposide through the Akt/GSK3 pathway to inhibit apoptosis. Oncogene 24(12), 1973-81.

Jo, M. and Curry, T.E., Jr. (2006) Luteinizing hormone-induced RUNX1 regulates the expression of genes in granulosa cells of rat periovulatory follicles. Mol Endocrinol 20(9), 2156-72.

Johannsen, E., Koh, E., Mosialos, G., Tong, X., Kieff, E. and Grossman, S.R. (1995a) Epstein-Barr virus nuclear protein 2 transactivation of the latent membrane protein 1 promoter is mediated by J kappa and PU.1. J Virol 69(1), 253-62.

Johannsen, E., Koh, E., Mosialos, G., Tong, X., Kieff, E. and Grossman, S.R. (1995b) Epstein-Barr-Virus Nuclear-Protein 2 Transactivation of the Latent Membrane-Protein-1 Promoter Is Mediated by J-Kappa and Pu1. Journal of Virology 69(1), 253-262.

Johannsen, E., Miller, C.L., Grossman, S.R. and Kieff, E. (1996) EBNA-2 and EBNA-3C extensively and mutually exclusively associate with RBPJ kappa in Epstein-Barr virus-transformed B lymphocytes. Journal of Virology 70(6), 4179-4183.

Johnson, D.G. and Walker, C.L. (1999) Cyclins and cell cycle checkpoints. Annu Rev Pharmacol Toxicol 39, 295-312.

Joseph, A.M., Babcock, G.J. and Thorley-Lawson, D.A. (2000) EBV persistence involves strict selection of latently infected B cells. J Immunol 165(6), 2975-81.

Kahvejian, A., Svitkin, Y.V., Sukarieh, R., M'Boutchou, M.N. and Sonenberg, N. (2005) Mammalian poly(A)-binding protein is a eukaryotic translation initiation factor, which acts via multiple mechanisms. Genes Dev 19(1), 104-13.

Kaiser, C., Laux, G., Eick, D., Jochner, N., Bornkamm, G.W. and Kempkes, B. (1999) The proto-oncogene c-myc is a direct target gene of Epstein-Barr virus nuclear antigen 2. J Virol 73(5), 4481-4.

Kaldis, P. and Aleem, E. (2005) Cell cycle sibling rivalry: Cdc2 vs. Cdk2. Cell Cycle 4(11), 1491-4.

Kamijo, T., Zindy, F., Roussel, M.F., Quelle, D.E., Downing, J.R., Ashmun, R.A., Grosveld, G. and Sherr, C.J. (1997) Tumor suppression at the mouse INK4a locus mediated by the alternative reading frame product p19ARF. Cell 91(5), 649-59.

Kang, Y., Siegel, P.M., Shu, W., Drobnjak, M., Kakonen, S.M., Cordon-Cardo, C., Guise, T.A. and Massague, J. (2003) A multigenic program mediating breast cancer metastasis to bone. Cancer Cell 3(6), 537-49.

Kania, M.A., Bonner, A.S., Duffy, J.B. and Gergen, J.P. (1990) The Drosophila segmentation gene runt encodes a novel nuclear regulatory protein that is also expressed in the developing nervous system. Genes Dev 4(10), 1701-13.

Karaiskou, A., Perez, L.H., Ferby, I., Ozon, R., Jessus, C. and Nebreda, A.R. (2001) Differential regulation of Cdc2 and Cdk2 by RINGO and cyclins. J Biol Chem 276(38), 36028-34.

Kashuba, E., Mattsson, K., Klein, G. and Szekely, L. (2003a) p14ARF induces the relocation of HDM2 and p53 to extranucleolar sites that are targeted by PML bodies and proteasomes. Mol Cancer 2, 18.

Kashuba, E., Mattsson, K., Pokrovskaja, K., Kiss, C., Protopopova, M., Ehlin-Henriksson, B., Klein, G. and Szekely, L. (2003b) EBV-encoded EBNA-5 associates with P14ARF in extranucleolar inclusions and prolongs the survival of P14ARF-expressing cells. Int J Cancer 105(5), 644-53.

Kato, K., Yokoyama, A., Tohya, Y., Akashi, H., Nishiyama, Y. and Kawaguchi, Y. (2003a) Identification of protein kinases responsible for phosphorylation of Epstein-Barr virus nuclear antigen leader protein at serine-35, which regulates its coactivator function. J Gen Virol 84(Pt 12), 3381-92.

Kato, N., Tamura, G., Fukase, M., Shibuya, H. and Motoyama, T. (2003b) Hypermethylation of the RUNX3 gene promoter in testicular yolk sac tumor of infants. Am J Pathol 163(2), 387-91.

Kaul, R., Murakami, M., Choudhuri, T. and Robertson, E.S. (2007) Epstein-Barr virus latent nuclear antigens can induce metastasis in a nude mouse model. J Virol 81(19), 10352-61.

Kaye, K.M., Izumi, K.M. and Kieff, E. (1993) Epstein-Barr virus latent membrane protein 1 is essential for B-lymphocyte growth transformation. Proc Natl Acad Sci U S A 90(19), 9150-4.

Kelly, G., Bell, A. and Rickinson, A. (2002a) Epstein-Barr virus-associated Burkitt lymphomagenesis selects for downregulation of the nuclear antigen EBNA2, Nat Med, pp. 1098-104. Vol. 8.

Kelly, G., Bell, A. and Rickinson, A. (2002b) Epstein-Barr virus-associated Burkitt lymphomagenesis selects for downregulation of the nuclear antigen EBNA2. Nat Med 8(10), 1098-104.

Kelly, G.L., Milner, A.E., Baldwin, G.S., Bell, A.I. and Rickinson, A.B. (2006) Three restricted forms of Epstein-Barr virus latency counteracting apoptosis in c-myc-expressing Burkitt lymphoma cells. Proc Natl Acad Sci U S A 103(40), 14935-40.

Kelly, G.L., Milner, A.E., Tierney, R.J., Croom-Carter, D.S., Altmann, M., Hammerschmidt, W., Bell, A.I. and Rickinson, A.B. (2005) Epstein-Barr virus nuclear antigen 2 (EBNA2) gene deletion is consistently linked with EBNA3A, -3B, and -3C expression in Burkitt's lymphoma cells and with increased resistance to apoptosis, J Virol, pp. 10709-17. Vol. 79.

Kempkes, B., Pich, D., Zeidler, R., Sugden, B. and Hammerschmidt, W. (1995a) Immortalization of human B lymphocytes by a plasmid containing 71 kilobase pairs of Epstein-Barr virus DNA, J Virol, pp. 231-8. Vol. 69.

Kempkes, B., Spitkovsky, D., Jansen-Durr, P., Ellwart, J.W., Kremmer, E., Delecluse, H.J., Rottenberger, C., Bornkamm, G.W. and Hammerschmidt, W. (1995b) B-cell proliferation and induction of early G1-regulating proteins by Epstein-Barr virus mutants conditional for EBNA2. Embo J 14(1), 88-96.

Kharbanda, S., Saleem, A., Datta, R., Yuan, Z.M., Weichselbaum, R. and Kufe, D. (1994) Ionizing radiation induces rapid tyrosine phosphorylation of p34cdc2. Cancer Res 54(6), 1412-4.

Kieff, E. and Rickinson, A. (2001) Fields Virology. In: P. Howley (Ed), 4th edition ed., pp. 2511-2574. Lippincott Williams & Wilkins Publishers, Philadelphia.

Kim, W.Y., Sieweke, M., Ogawa, E., Wee, H.J., Englmeier, U., Graf, T. and Ito, Y. (1999) Mutual activation of Ets-1 and AML1 DNA binding by direct interaction of their autoinhibitory domains. Embo J 18(6), 1609-20.

King, W., Thomas-Powell, A.L., Raab-Traub, N., Hawke, M. and Kieff, E. (1980) Epstein-Barr virus RNA. V. Viral RNA in a restringently infected, growth-transformed cell line. J Virol 36(2), 506-18.

Kitabayashi, I., Yokoyama, A., Shimizu, K. and Ohki, M. (1998) Interaction and functional cooperation of the leukemia-associated factors AML1 and p300 in myeloid cell differentiation. Embo J 17(11), 2994-3004.

Kitay, M.K. and Rowe, D.T. (1996) Cell cycle stage-specific phosphorylation of the Epstein-Barr virus immortalization protein EBNA-LP. J Virol 70(11), 7885-93.

Klein, E., Klein, G., Nadkarni, J.S., Nadkarni, J.J., Wigzell, H. and Clifford, P. (1968) Surface IgM-kappa specificity on a Burkitt lymphoma cell in vivo and in derived culture lines. Cancer Res 28(7), 1300-10.

Klein, G., Dombos, L. and Gothoskar, B. (1972) Sensitivity of Epstein-Barr virus (EBV) producer and non-producer human lymphoblastoid cell lines to superinfection with EB-virus. Int J Cancer 10(1), 44-57.

Klein, G., Giovanella, B., Westman, A., Stehlin, J.S. and Mumford, D. (1975) An EBV-genome-negative cell line established from an American Burkitt lymphoma; receptor characteristics. EBV infectibility and permanent conversion into EBV-positive sublines by in vitro infection. Intervirology 5(6), 319-34.

Klein, G., Lindahl, T., Jondal, M., Leibold, W., Menezes, J., Nilsson, K. and Sundstrom, C. (1974) Continuous lymphoid cell lines with characteristics of B cells (bone-marrow-derived), lacking the Epstein-Barr virus genome and derived from three human lymphomas. Proc Natl Acad Sci U S A 71(8), 3283-6.

Knight, J.S., Lan, K., Subramanian, C. and Robertson, E.S. (2003a) Epstein-Barr virus nuclear antigen 3C recruits histone deacetylase activity and associates with the corepressors mSin3A and NCoR in human B-cell lines. Journal of Virology 77(7), 4261-4272.

Knight, J.S., Lan, K., Subramanian, C. and Robertson, E.S. (2003b) Epstein-Barr virus nuclear antigen 3C recruits histone deacetylase activity and associates with the corepressors mSin3A and NCoR in human B-cell lines. J Virol 77(7), 4261-72.

Knight, J.S. and Robertson, E.S. (2004) Epstein-Barr virus nuclear antigen 3C regulates cyclin A/p27 complexes and enhances cyclin A-dependent kinase activity. J Virol 78(4), 1981-91.

Knight, J.S., Sharma, N., Kalman, D.E. and Robertson, E.S. (2004) A cyclin-binding motif within the amino-terminal homology domain of EBNA3C binds cyclin A

and modulates cyclin A-dependent kinase activity in Epstein-Barr virus-infected cells. J Virol 78(23), 12857-67.

Knight, J.S., Sharma, N. and Robertson, E.S. (2005a) Epstein-Barr virus latent antigen 3C can mediate the degradation of the retinoblastoma protein through an SCF cellular ubiquitin ligase. Proc Natl Acad Sci U S A 102(51), 18562-6.

Knight, J.S., Sharma, N. and Robertson, E.S. (2005b) SCFSkp2 complex targeted by Epstein-Barr virus essential nuclear antigen. Mol Cell Biol 25(5), 1749-63.

Koh, J., Enders, G.H., Dynlacht, B.D. and Harlow, E. (1995) Tumour-derived p16 alleles encoding proteins defective in cell-cycle inhibition. Nature 375(6531), 506-10.

Komori, T., Yagi, H., Nomura, S., Yamaguchi, A., Sasaki, K., Deguchi, K., Shimizu, Y., Bronson, R.T., Gao, Y.H., Inada, M., Sato, M., Okamoto, R., Kitamura, Y., Yoshiki, S. and Kishimoto, T. (1997) Targeted disruption of Cbfa1 results in a complete lack of bone formation owing to maturational arrest of osteoblasts. Cell 89(5), 755-64.

Krauer, K., Buck, M., Flanagan, J., Belzer, D. and Sculley, T. (2004a) Identification of the nuclear localization signals within the Epstein-Barr virus EBNA-6 protein. Journal of General Virology 85, 165-172.

Krauer, K.G., Burgess, A., Buck, M., Flanagan, J., Sculley, T.B. and Gabrielli, B. (2004b) The EBNA-3 gene family proteins disrupt the G2/M checkpoint. Oncogene 23(7), 1342-53.

Krauer, K.G., Burgess, A., Buck, M., Flanagan, J., Sculley, T.B. and Gabrielli, B. (2004c) The EBNA-3 gene family proteins disrupt the G2/M checkpoint, Oncogene, pp. 1342-53. Vol. 23.

Krek, W. and Nigg, E.A. (1991) Differential phosphorylation of vertebrate p34cdc2 kinase at the G1/S and G2/M transitions of the cell cycle: identification of major phosphorylation sites. Embo J 10(2), 305-16.

Kubbutat, M.H., Jones, S.N. and Vousden, K.H. (1997) Regulation of p53 stability by Mdm2. Nature 387(6630), 299-303.

Kumagai, A. and Dunphy, W.G. (1991) The cdc25 protein controls tyrosine dephosphorylation of the cdc2 protein in a cell-free system. Cell 64(5), 903-14.

Kumagai, A. and Dunphy, W.G. (1996) Purification and molecular cloning of Plx1, a Cdc25-regulatory kinase from Xenopus egg extracts. Science 273(5280), 1377-80.

Lacaud, G., Gore, L., Kennedy, M., Kouskoff, V., Kingsley, P., Hogan, C., Carlsson, L., Speck, N., Palis, J. and Keller, G. (2002) Runx1 is essential for hematopoietic commitment at the hemangioblast stage of development in vitro. Blood 100(2), 458-66.

Lacombe, M.L., Milon, L., Munier, A., Mehus, J.G. and Lambeth, D.O. (2000) The human Nm23/nucleoside diphosphate kinases. J Bioenerg Biomembr 32(3), 247-58.

Laherty, C.D., Yang, W.M., Sun, J.M., Davie, J.R., Seto, E. and Eisenman, R.N. (1997) Histone deacetylases associated with the mSin3 corepressor mediate mad transcriptional repression. Cell 89(3), 349-56.

Landschulz, W.H., Johnson, P.F. and McKnight, S.L. (1988) The Leucine Zipper - a Hypothetical Structure Common to a New Class of DNA-Binding Proteins. Science 240(4860), 1759-1764.

Lane, D.P. and Benchimol, S. (1990) p53: oncogene or anti-oncogene? Genes Dev 4(1), 1-8.

Lane, D.P. and Crawford, L.V. (1979) T antigen is bound to a host protein in SV40-transformed cells. Nature 278(5701), 261-3.

Lau, Y.F. (1999) Gonadoblastoma, testicular and prostate cancers, and the TSPY gene. Am J Hum Genet 64(4), 921-7.

Lau, Y.F., Lau, H.W. and Komuves, L.G. (2003) Expression pattern of a gonadoblastoma candidate gene suggests a role of the Y chromosome in prostate cancer. Cytogenet Genome Res 101(3-4), 250-60.

Le Roux, A., Kerdiles, B., Walls, D., Dedieu, J.F. and Perricaudet, M. (1994) The Epstein-Barr virus determined nuclear antigens EBNA-3A, -3B, and -3C repress EBNA-2-mediated transactivation of the viral terminal protein 1 gene promoter. Virology 205(2), 596-602.

Lechner, M.S., Mack, D.H., Finicle, A.B., Crook, T., Vousden, K.H. and Laimins, L.A. (1992) Human papillomavirus E6 proteins bind p53 in vivo and abrogate p53-mediated repression of transcription. Embo J 11(8), 3045-52.

Lee, M.A., Diamond, M.E. and Yates, J.L. (1999) Genetic evidence that EBNA-1 is needed for efficient, stable latent infection by Epstein-Barr virus. J Virol 73(4), 2974-82.

Lee, S., Sakakibara, S., Maruo, S., Zhao, B., Calderwood, M.A., Holthaus, A.M., Lai, C.Y., Takada, K., Kieff, E. and Johannsen, E. (2009) Epstein-Barr virus nuclear protein 3C domains necessary for lymphoblastoid cell growth: interaction with RBP-Jkappa regulates TCL1. J Virol 83(23), 12368-77.

Lenny, N., Meyers, S. and Hiebert, S.W. (1995) Functional domains of the t(8;21) fusion protein, AML-1/ETO. Oncogene 11(9), 1761-9.

Lenoir, G.M., Vuillaume, M. and Bonnardel, C. (1985) The use of lymphomatous and lymphoblastoid cell lines in the study of Burkitt's lymphoma. IARC Sci Publ(60), 309-18.

Lenormand, J.L., Dellinger, R.W., Knudsen, K.E., Subramani, S. and Donoghue, D.J. (1999) Speedy: a novel cell cycle regulator of the G2/M transition. Embo J 18(7), 1869-77.

Levanon, D., Bettoun, D., Harris-Cerruti, C., Woolf, E., Negreanu, V., Eilam, R., Bernstein, Y., Goldenberg, D., Xiao, C., Fliegauf, M., Kremer, E., Otto, F., Brenner, O., Lev-Tov, A. and Groner, Y. (2002) The Runx3 transcription factor regulates development and survival of TrkC dorsal root ganglia neurons. Embo J 21(13), 3454-63.

Levanon, D., Goldstein, R.E., Bernstein, Y., Tang, H., Goldenberg, D., Stifani, S., Paroush, Z. and Groner, Y. (1998) Transcriptional repression by AML1 and LEF-1 is mediated by the TLE/Groucho corepressors. Proc Natl Acad Sci U S A 95(20), 11590-5.

Levitskaya, J., Coram, M., Levitsky, V., Imreh, S., Steigerwald-Mullen, P.M., Klein, G., Kurilla, M.G. and Masucci, M.G. (1995) Inhibition of antigen processing by the internal repeat region of the Epstein-Barr virus nuclear antigen-1, Nature, pp. 685-8. Vol. 375.

Levitskaya, J., Sharipo, A., Leonchiks, A., Ciechanover, A. and Masucci, M.G. (1997) Inhibition of ubiquitin/proteasome-dependent protein degradation by the Gly-Ala repeat domain of the Epstein-Barr virus nuclear antigen 1, Proc Natl Acad Sci U S A, pp. 12616-21. Vol. 94.

Li, F., Luo, Z., Huang, W., Lu, Q., Wilcox, C.S., Jose, P.A. and Chen, S. (2007) Response gene to complement 32, a novel regulator for transforming growth factor-beta-induced smooth muscle differentiation of neural crest cells. J Biol Chem 282(14), 10133-7.

Li, J., Meyer, A.N. and Donoghue, D.J. (1995) Requirement for phosphorylation of cyclin B1 for Xenopus oocyte maturation. Mol Biol Cell 6(9), 1111-24.

Li, J., Meyer, A.N. and Donoghue, D.J. (1997) Nuclear localization of cyclin B1 mediates its biological activity and is regulated by phosphorylation. Proc Natl Acad Sci U S A 94(2), 502-7.

Li, Q.L., Ito, K., Sakakura, C., Fukamachi, H., Inoue, K., Chi, X.Z., Lee, K.Y., Nomura, S., Lee, C.W., Han, S.B., Kim, H.M., Kim, W.J., Yamamoto, H., Yamashita, N., Yano, T., Ikeda, T., Itohara, S., Inazawa, J., Abe, T., Hagiwara, A., Yamagishi, H., Ooe, A., Kaneda, A., Sugimura, T., Ushijima, T., Bae, S.C. and Ito, Y. (2002) Causal relationship between the loss of RUNX3 expression and gastric cancer. Cell 109(1), 113-24.

Li, X., Huang, M., Zheng, H., Wang, Y., Ren, F., Shang, Y., Zhai, Y., Irwin, D.M., Shi, Y., Chen, D. and Chang, Z. (2008) CHIP promotes Runx2 degradation and negatively regulates osteoblast differentiation. J Cell Biol 181(6), 959-72.

Libermann, T.A., Pan, Z., Akbarali, Y., Hetherington, C.J., Boltax, J., Yergeau, D.A. and Zhang, D.E. (1999) AML1 (CBFalpha2) cooperates with B cell-specific activating protein (BSAP/PAX5) in activation of the B cell-specific BLK gene promoter. J Biol Chem 274(35), 24671-6.

Lim, H.W., Lee, J.E., Shin, S.J., Lee, Y.E., Oh, S.H., Park, J.Y., Seong, J.K. and Park, J.S. (2002) Identification of differentially expressed mRNA during pancreas regeneration of rat by mRNA differential display. Biochem Biophys Res Commun 299(5), 806-12.

Lin, Y.C. and Stavnezer, J. (1992) Regulation of transcription of the germ-line Ig alpha constant region gene by an ATF element and by novel transforming growth factor-beta 1-responsive elements. J Immunol 149(9), 2914-25.

Lindahl, T., Adams, A., Bjursell, G., Bornkamm, G.W., Kaschka-Dierich, C. and Jehn, U. (1976) Covalently closed circular duplex DNA of Epstein-Barr virus in a human lymphoid cell line. J Mol Biol 102(3), 511-30.

Lindstrom, M.S., Klangby, U. and Wiman, K.G. (2001) p14ARF homozygous deletion or MDM2 overexpression in Burkitt lymphoma lines carrying wild type p53. Oncogene 20(17), 2171-7.

Lindstrom, M.S. and Wiman, K.G. (2002) Role of genetic and epigenetic changes in Burkitt lymphoma. Semin Cancer Biol 12(5), 381-7.

Linzer, D.I. and Levine, A.J. (1979) Characterization of a 54K dalton cellular SV40 tumor antigen present in SV40-transformed cells and uninfected embryonal carcinoma cells. Cell 17(1), 43-52.

Look, A.T. (1997) Oncogenic transcription factors in the human acute leukemias. Science 278(5340), 1059-64.

Lu, J., Maruyama, M., Satake, M., Bae, S.C., Ogawa, E., Kagoshima, H., Shigesada, K. and Ito, Y. (1995) Subcellular localization of the alpha and beta subunits of the acute myeloid leukemia-linked transcription factor PEBP2/CBF. Mol Cell Biol 15(3), 1651-61.

Lukas, J., Parry, D., Aagaard, L., Mann, D.J., Bartkova, J., Strauss, M., Peters, G. and Bartek, J. (1995) Retinoblastoma-protein-dependent cell-cycle inhibition by the tumour suppressor p16. Nature 375(6531), 503-6.

Lundgren, K., Walworth, N., Booher, R., Dembski, M., Kirschner, M. and Beach, D. (1991) mik1 and wee1 cooperate in the inhibitory tyrosine phosphorylation of cdc2. Cell 64(6), 1111-22.

Lutterbach, B., Westendorf, J.J., Linggi, B., Isaac, S., Seto, E. and Hiebert, S.W. (2000) A mechanism of repression by acute myeloid leukemia-1, the target of multiple chromosomal translocations in acute leukemia. J Biol Chem 275(1), 651-6.

Lutterbach, B., Westendorf, J.J., Linggi, B., Patten, A., Moniwa, M., Davie, J.R., Huynh, K.D., Bardwell, V.J., Lavinsky, R.M., Rosenfeld, M.G., Glass, C., Seto, E. and Hiebert, S.W. (1998) ETO, a target of t(8;21) in acute leukemia, interacts with the N-CoR and mSin3 corepressors. Mol Cell Biol 18(12), 7176-84.

Ma, Q., Jones, D., Borghesani, P.R., Segal, R.A., Nagasawa, T., Kishimoto, T., Bronson, R.T. and Springer, T.A. (1998) Impaired B-lymphopoiesis, myelopoiesis, and derailed cerebellar neuron migration in CXCR4- and SDF-1-deficient mice. Proc Natl Acad Sci U S A 95(16), 9448-53.

MacMahon, E.M., Glass, J.D., Hayward, S.D., Mann, R.B., Becker, P.S., Charache, P., McArthur, J.C. and Ambinder, R.F. (1991) Epstein-Barr virus in AIDS-related primary central nervous system lymphoma, Lancet, pp. 969-73. Vol. 338.

Magnaghi-Jaulin, L., Groisman, R., Naguibneva, I., Robin, P., Lorain, S., Le Villain, J.P., Troalen, F., Trouche, D. and Harel-Bellan, A. (1998) Retinoblastoma protein represses transcription by recruiting a histone deacetylase. Nature 391(6667), 601-5.

Magrath, I. (1990a) The pathogenesis of Burkitt's lymphoma. Adv Cancer Res 55, 133-270.

Magrath, I. (1990b) The pathogenesis of Burkitt's lymphoma, Adv Cancer Res, pp. 133-270. Vol. 55.

Maity, A., McKenna, W.G. and Muschel, R.J. (1995) Evidence for post-transcriptional regulation of cyclin B1 mRNA in the cell cycle and following irradiation in HeLa cells. Embo J 14(3), 603-9.

Mannick, J.B., Cohen, J.I., Birkenbach, M., Marchini, A. and Kieff, E. (1991) The Epstein-Barr virus nuclear protein encoded by the leader of the EBNA RNAs is important in B-lymphocyte transformation. J Virol 65(12), 6826-37.

Mao, S., Frank, R.C., Zhang, J., Miyazaki, Y. and Nimer, S.D. (1999) Functional and physical interactions between AML1 proteins and an ETS protein, MEF: implications for the pathogenesis of t(8;21)-positive leukemias. Mol Cell Biol 19(5), 3635-44.

Marechal, V., Dehee, A., Chikhi-Brachet, R., Piolot, T., Coppey-Moisan, M. and Nicolas, J.C. (1999) Mapping EBNA-1 domains involved in binding to metaphase chromosomes, J Virol, pp. 4385-92. Vol. 73.

Marshall, D. and Sample, C. (1995) Epstein-Barr virus nuclear antigen 3C is a transcriptional regulator. J Virol 69(6), 3624-30.

Maruo, S., Johannsen, E., Illanes, D., Cooper, A. and Kieff, E. (2003) Epstein-Barr Virus nuclear protein EBNA3A is critical for maintaining lymphoblastoid cell line growth. J Virol 77(19), 10437-47.

Maruo, S., Wu, Y., Ito, T., Kanda, T., Kieff, E.D. and Takada, K. (2009) Epstein-Barr virus nuclear protein EBNA3C residues critical for maintaining lymphoblastoid cell growth. Proc Natl Acad Sci U S A 106(11), 4419-24.

Maruo, S., Yang, L. and Takada, K. (2001) Roles of Epstein-Barr virus glycoproteins gp350 and gp25 in the infection of human epithelial cells. J Gen Virol 82(Pt 10), 2373-83.

Masai, H., Matsui, E., You, Z., Ishimi, Y., Tamai, K. and Arai, K. (2000) Human Cdc7-related kinase complex. In vitro phosphorylation of MCM by concerted actions of Cdks and Cdc7 and that of a criticial threonine residue of Cdc7 bY Cdks. J Biol Chem 275(37), 29042-52.

Matsuoka, S., Huang, M. and Elledge, S.J. (1998) Linkage of ATM to cell cycle regulation by the Chk2 protein kinase. Science 282(5395), 1893-7.

Maunders, M.J., Petti, L. and Rowe, M. (1994) Precipitation of the Epstein-Barr-Virus Protein Ebna-2 by an Ebna-3c-Specific Monoclonal-Antibody. Journal of General Virology 75, 769-778.

Mayer, M.M. (1972) Mechanism of cytolysis by complement. Proc Natl Acad Sci U S A 69(10), 2954-8.

McGowan, C.H. and Russell, P. (1993) Human Wee1 kinase inhibits cell division by phosphorylating p34cdc2 exclusively on Tyr15. Embo J 12(1), 75-85.

Medema, R.H., Herrera, R.E., Lam, F. and Weinberg, R.A. (1995) Growth suppression by p16ink4 requires functional retinoblastoma protein. Proc Natl Acad Sci U S A 92(14), 6289-93.

Meijer, L., Arion, D., Golsteyn, R., Pines, J., Brizuela, L., Hunt, T. and Beach, D. (1989) Cyclin is a component of the sea urchin egg M-phase specific histone H1 kinase. Embo J 8(8), 2275-82.

Melnikova, I.N., Crute, B.E., Wang, S. and Speck, N.A. (1993) Sequence specificity of the core-binding factor. J Virol 67(4), 2408-11.

Menezes, J., Leibold, W., Klein, G. and Clements, G. (1975) Establishment and characterization of an Epstein-Barr virus (EBC)-negative lymphoblastoid B cell line (BJA-B) from an exceptional, EBV-genome-negative African Burkitt's lymphoma. Biomedicine 22(4), 276-84.

Menon, K.P., Sanyal, S., Habara, Y., Sanchez, R., Wharton, R.P., Ramaswami, M. and Zinn, K. (2004) The translational repressor Pumilio regulates presynaptic morphology and controls postsynaptic accumulation of translation factor eIF-4E. Neuron 44(4), 663-76.

Meyers, S., Downing, J.R. and Hiebert, S.W. (1993) Identification of AML-1 and the (8;21) translocation protein (AML-1/ETO) as sequence-specific DNA-binding proteins: the runt homology domain is required for DNA binding and protein-protein interactions. Mol Cell Biol 13(10), 6336-45.

Meyers, S., Lenny, N. and Hiebert, S.W. (1995) The t(8;21) fusion protein interferes with AML-1B-dependent transcriptional activation. Mol Cell Biol 15(4), 1974-82.

Michael, D. and Oren, M. (2003) The p53-Mdm2 module and the ubiquitin system. Semin Cancer Biol 13(1), 49-58.

Mileo, A.M., Piombino, E., Severino, A., Tritarelli, A., Paggi, M.G. and Lombardi, D. (2006) Multiple interference of the human papillomavirus-16 E7 oncoprotein with the functional role of the metastasis suppressor Nm23-H1 protein. J Bioenerg Biomembr 38(3-4), 215-25.

Miller, G., Robinson, J., Heston, L. and Lipman, M. (1974) Differences between laboratory strains of Epstein-Barr virus based on immortalization, abortive infection, and interference. Proc Natl Acad Sci U S A 71(10), 4006-10.

Mittnacht, S. (1998) Control of pRB phosphorylation. Curr Opin Genet Dev 8(1), 21-7.

Miyashita, E.M., Yang, B., Babcock, G.J. and Thorley-Lawson, D.A. (1997) Identification of the site of Epstein-Barr virus persistence in vivo as a resting B cell. J Virol 71(7), 4882-91.

Miyoshi, H., Shimizu, K., Kozu, T., Maseki, N., Kaneko, Y. and Ohki, M. (1991) t(8;21) breakpoints on chromosome 21 in acute myeloid leukemia are clustered within a limited region of a single gene, AML1. Proc Natl Acad Sci U S A 88(23), 10431-4.

Moore, F.L., Jaruzelska, J., Fox, M.S., Urano, J., Firpo, M.T., Turek, P.J., Dorfman, D.M. and Pera, R.A. (2003) Human Pumilio-2 is expressed in embryonic stem cells and germ cells and interacts with DAZ (Deleted in AZoospermia) and DAZ-like proteins. Proc Natl Acad Sci U S A 100(2), 538-43.

Moore, J.D., Yang, J., Truant, R. and Kornbluth, S. (1999) Nuclear import of Cdk/cyclin complexes: identification of distinct mechanisms for import of Cdk2/cyclin E and Cdc2/cyclin B1. J Cell Biol 144(2), 213-24.

Morgan, D.O. (1995) Principles of CDK regulation. Nature 374(6518), 131-4.

Morgan, D.O. (1997) Cyclin-dependent kinases: engines, clocks, and microprocessors. Annu Rev Cell Dev Biol 13, 261-91.

Mueller, P.R., Coleman, T.R., Kumagai, A. and Dunphy, W.G. (1995) Myt1: a membrane-associated inhibitory kinase that phosphorylates Cdc2 on both threonine-14 and tyrosine-15. Science 270(5233), 86-90.

Mukhopadhyay, D., Houchen, C.W., Kennedy, S., Dieckgraefe, B.K. and Anant, S. (2003) Coupled mRNA stabilization and translational silencing of cyclooxygenase-2 by a novel RNA binding protein, CUGBP2. Mol Cell 11(1), 113-26.

Murakami, M., Kaul, R., Kumar, P. and Robertson, E.S. (2009) Nucleoside diphosphate kinase/Nm23 and Epstein-Barr virus. Mol Cell Biochem 329(1-2), 131-9.

Murakami, M., Lan, K., Subramanian, C. and Robertson, E.S. (2005) Epstein-Barr virus nuclear antigen 1 interacts with Nm23-H1 in lymphoblastoid cell lines and inhibits its ability to suppress cell migration. J Virol 79(3), 1559-68.

Murata, Y. and Wharton, R.P. (1995) Binding of pumilio to maternal hunchback mRNA is required for posterior patterning in Drosophila embryos. Cell 80(5), 747-56.

Murray, P.G. and Young, L.S. (2001) The Epstein-Barr virus (EBV) genome (online). ©2001 Cambridge University Press. Available from http://www-ermm.cbcu.cam.ac.uk/01003854a.pdf (accessed on 30 July 2006).

Nakayama, T., Fujisawa, R., Izawa, D., Hieshima, K., Takada, K. and Yoshie, O. (2002) Human B cells immortalized with Epstein-Barr virus upregulate CCR6 and CCR10 and downregulate CXCR4 and CXCR5. J Virol 76(6), 3072-7.

Nalesnik, M.A. (1998) Clinical and pathological features of post-transplant lymphoproliferative disorders (PTLD), Springer Semin Immunopathol, pp. 325-42. Vol. 20.

Niculescu, F., Badea, T. and Rus, H. (1999) Sublytic C5b-9 induces proliferation of human aortic smooth muscle cells: role of mitogen activated protein kinase and phosphatidylinositol 3-kinase. Atherosclerosis 142(1), 47-56.

Niculescu, F., Rus, H., van Biesen, T. and Shin, M.L. (1997) Activation of Ras and mitogen-activated protein kinase pathway by terminal complement complexes is G protein dependent. J Immunol 158(9), 4405-12.

Nie, Y., Waite, J., Brewer, F., Sunshine, M.J., Littman, D.R. and Zou, Y.R. (2004) The role of CXCR4 in maintaining peripheral B cell compartments and humoral immunity. J Exp Med 200(9), 1145-56.

Niederman, J.C., McCollum, R.W., Henle, G. and Henle, W. (1968) Infectious mononucleosis. Clinical manifestations in relation to EB virus antibodies, Jama, pp. 205-9. Vol. 203.

Niederman, J.C., Miller, G., Pearson, H.A., Pagano, J.S. and Dowaliby, J.M. (1976) Infectious mononucleosis. Epstein-Barr-virus shedding in saliva and the oropharynx, N Engl J Med, pp. 1355-9. Vol. 294.

Nigg, E.A. (1995) Cyclin-dependent protein kinases: key regulators of the eukaryotic cell cycle. Bioessays 17(6), 471-80.

Nilsson, I. and Hoffmann, I. (2000) Cell cycle regulation by the Cdc25 phosphatase family. Prog Cell Cycle Res 4, 107-14.

Nitsche, F., Bell, A. and Rickinson, A. (1997) Epstein-Barr virus leader protein enhances EBNA-2-mediated transactivation of latent membrane protein 1 expression: a role for the W1W2 repeat domain. J Virol 71(9), 6619-28.

Nonkwelo, C., Ruf, I.K. and Sample, J. (1997) The Epstein-Barr virus EBNA-1 promoter Qp requires an initiator-like element. J Virol 71(1), 354-61.

Nonkwelo, C., Skinner, J., Bell, A., Rickinson, A. and Sample, J. (1996a) Transcription start sites downstream of the Epstein-Barr virus (EBV) Fp promoter in early-passage Burkitt lymphoma cells define a fourth promoter for expression of the EBV EBNA-1 protein. J Virol 70(1), 623-7.

Nonkwelo, C., Skinner, J., Bell, A., Rickinson, A. and Sample, J. (1996b) Transcription start sites downstream of the Epstein-Barr virus (EBV) Fp promoter in early-passage Burkitt lymphoma cells define a fourth promoter for expression of the EBV EBNA-1 protein, J Virol, pp. 623-7. Vol. 70.

Obaya, A.J. and Sedivy, J.M. (2002) Regulation of cyclin-Cdk activity in mammalian cells. Cell Mol Life Sci 59(1), 126-42.

O'Connor, P.M., Ferris, D.K., Hoffmann, I., Jackman, J., Draetta, G. and Kohn, K.W. (1994) Role of the cdc25C phosphatase in G2 arrest induced by nitrogen mustard. Proc Natl Acad Sci U S A 91(20), 9480-4.

Ogawa, E., Inuzuka, M., Maruyama, M., Satake, M., Naito-Fujimoto, M., Ito, Y. and Shigesada, K. (1993a) Molecular cloning and characterization of PEBP2 beta, the heterodimeric partner of a novel Drosophila runt-related DNA binding protein PEBP2 alpha. Virology 194(1), 314-31.

Ogawa, E., Maruyama, M., Kagoshima, H., Inuzuka, M., Lu, J., Satake, M., Shigesada, K. and Ito, Y. (1993b) PEBP2/PEA2 represents a family of transcription factors homologous to the products of the Drosophila runt gene and the human AML1 gene. Proc Natl Acad Sci U S A 90(14), 6859-63.

Okuda, T., van Deursen, J., Hiebert, S.W., Grosveld, G. and Downing, J.R. (1996) AML1, the target of multiple chromosomal translocations in human leukemia, is essential for normal fetal liver hematopoiesis. Cell 84(2), 321-30.

O'Nions, J. and Allday, M.J. (2003) Epstein-Barr virus can inhibit genotoxin-induced G1 arrest downstream of p53 by preventing the inactivation of CDK2. Oncogene 22(46), 7181-91.

O'Nions, J. and Allday, M.J. (2004) Deregulation of the cell cycle by the Epstein-Barr virus. Adv Cancer Res 92, 119-86.

Oram, S.W., Liu, X.X., Lee, T.L., Chan, W.Y. and Lau, Y.F. (2006) TSPY potentiates cell proliferation and tumorigenesis by promoting cell cycle progression in HeLa and NIH3T3 cells. BMC Cancer 6, 154.

Oswald, F., Winkler, M., Cao, Y., Astrahantseff, K., Bourteele, S., Knochel, W. and Borggrefe, T. (2005) RBP-Jkappa/SHARP recruits CtIP/CtBP corepressors to silence Notch target genes. Mol Cell Biol 25(23), 10379-90.

Padmanabhan, K. and Richter, J.D. (2006) Regulated Pumilio-2 binding controls RINGO/Spy mRNA translation and CPEB activation. Genes Dev 20(2), 199-209.

Pajic, A., Staege, M.S., Dudziak, D., Schuhmacher, M., Spitkovsky, D., Eissner, G., Brielmeier, M., Polack, A. and Bornkamm, G.W. (2001) Antagonistic effects of c-myc and Epstein-Barr virus latent genes on the phenotype of human B cells, Int J Cancer, pp. 810-6. Vol. 93.

Pallesen, G., Hamilton-Dutoit, S.J., Rowe, M. and Young, L.S. (1991) Expression of Epstein-Barr virus latent gene products in tumour cells of Hodgkin's disease. Lancet 337(8737), 320-2.

Paris, J., Swenson, K., Piwnica-Worms, H. and Richter, J.D. (1991) Maturation-specific polyadenylation: in vitro activation by p34cdc2 and phosphorylation of a 58-kD CPE-binding protein. Genes Dev 5(9), 1697-708.

Parisi, M. and Lin, H. (1999) The Drosophila pumilio gene encodes two functional protein isoforms that play multiple roles in germline development, gonadogenesis, oogenesis and embryogenesis. Genetics 153(1), 235-50.

Park, E.S., Choi, S., Muse, K.N., Curry, T.E., Jr. and Jo, M. (2008) Response Gene to Complement 32 Expression Is Induced by the Luteinizing Hormone (LH) Surge and Regulated by LH-Induced Mediators in the Rodent Ovary. Endocrinology 149(6), 3025-36.

Parker, G.A., Crook, T., Bain, M., Sara, E.A., Farrell, P.J. and Allday, M.J. (1996) Epstein-Barr virus nuclear antigen (EBNA)3C is an immortalizing oncoprotein with similar properties to adenovirus E1A and papillomavirus E7. Oncogene 13(12), 2541-9.

Parker, G.A., Touitou, R. and Allday, M.J. (2000) Epstein-Barr virus EBNA3C can disrupt multiple cell cycle checkpoints and induce nuclear division divorced from cytokinesis. Oncogene 19(5), 700-9.

Parker, L.L. and Piwnica-Worms, H. (1992) Inactivation of the p34cdc2-cyclin B complex by the human WEE1 tyrosine kinase. Science 257(5078), 1955-7.

Pathmanathan, R., Prasad, U., Sadler, R., Flynn, K. and Raab-Traub, N. (1995) Clonal proliferations of cells infected with Epstein-Barr virus in preinvasive lesions related to nasopharyngeal carcinoma, N Engl J Med, pp. 693-8. Vol. 333.

Pelletier, N., Champagne, N., Stifani, S. and Yang, X.J. (2002) MOZ and MORF histone acetyltransferases interact with the Runt-domain transcription factor Runx2. Oncogene 21(17), 2729-40.

Peter, M. and Herskowitz, I. (1994) Joining the complex: cyclin-dependent kinase inhibitory proteins and the cell cycle. Cell 79(2), 181-4.

Peter, M., Nakagawa, J., Doree, M., Labbe, J.C. and Nigg, E.A. (1990) In vitro disassembly of the nuclear lamina and M phase-specific phosphorylation of lamins by cdc2 kinase. Cell 61(4), 591-602.

Petrovick, M.S., Hiebert, S.W., Friedman, A.D., Hetherington, C.J., Tenen, D.G. and Zhang, D.E. (1998) Multiple functional domains of AML1: PU.1 and C/EBPalpha synergize with different regions of AML1. Mol Cell Biol 18(7), 3915-25.

Petti, L., Sample, C. and Kieff, E. (1990a) Subnuclear localization and phosphorylation of Epstein-Barr virus latent infection nuclear proteins. Virology 176(2), 563-74.

Petti, L., Sample, C. and Kieff, E. (1990b) Subnuclear localization and phosphorylation of Epstein-Barr virus latent infection nuclear proteins, Virology, pp. 563-74. Vol. 176.

Petti, L., Sample, J., Wang, F. and Kieff, E. (1988) A fifth Epstein-Barr virus nuclear protein (EBNA3C) is expressed in latently infected growth-transformed lymphocytes. J Virol 62(4), 1330-8.

Philips, A.V., Timchenko, L.T. and Cooper, T.A. (1998) Disruption of splicing regulated by a CUG-binding protein in myotonic dystrophy. Science 280(5364), 737-41.

Piaggio, G., Farina, A., Perrotti, D., Manni, I., Fuschi, P., Sacchi, A. and Gaetano, C. (1995) Structure and growth-dependent regulation of the human cyclin B1 promoter. Exp Cell Res 216(2), 396-402.

Pines, J. (1995) Cyclins and cyclin-dependent kinases: a biochemical view. Biochem J 308 (Pt 3), 697-711.

Pines, J. and Hunter, T. (1989) Isolation of a human cyclin cDNA: evidence for cyclin mRNA and protein regulation in the cell cycle and for interaction with p34cdc2. Cell 58(5), 833-46.

Pines, J. and Hunter, T. (1991) Human cyclins A and B1 are differentially located in the cell and undergo cell cycle-dependent nuclear transport. J Cell Biol 115(1), 1-17.

Pines, J. and Hunter, T. (1994) The differential localization of human cyclins A and B is due to a cytoplasmic retention signal in cyclin B. Embo J 13(16), 3772-81.

Polack, A., Hortnagel, K., Pajic, A., Christoph, B., Baier, B., Falk, M., Mautner, J., Geltinger, C., Bornkamm, G.W. and Kempkes, B. (1996) c-myc activation renders proliferation of Epstein-Barr virus (EBV)-transformed cells independent of EBV nuclear antigen 2 and latent membrane protein 1. Proc Natl Acad Sci U S A 93(19), 10411-6.

Polyak, K., Lee, M.H., Erdjument-Bromage, H., Koff, A., Roberts, J.M., Tempst, P. and Massague, J. (1994) Cloning of p27Kip1, a cyclin-dependent kinase inhibitor and a potential mediator of extracellular antimitogenic signals. Cell 78(1), 59-66.

Ponthier, J.L., Schluepen, C., Chen, W., Lersch, R.A., Gee, S.L., Hou, V.C., Lo, A.J., Short, S.A., Chasis, J.A., Winkelmann, J.C. and Conboy, J.G. (2006) Fox-2 splicing factor binds to a conserved intron motif to promote inclusion of protein 4.1R alternative exon 16. J Biol Chem 281(18), 12468-74.

Pope, J.H., Horne, M.K. and Scott, W. (1968a) Transformation of foetal human keukocytes in vitro by filtrates of a human leukaemic cell line containing herpes-like virus, Int J Cancer, pp. 857-66. Vol. 3.

Pope, J.H., Horne, M.K. and Scott, W. (1968b) Transformation of foetal human leukocytes in vitro by filtrates of a human leukaemic cell line containing herpes-like virus. Int J Cancer 3(6), 857-66.

Porter, L.A., Dellinger, R.W., Tynan, J.A., Barnes, E.A., Kong, M., Lenormand, J.L. and Donoghue, D.J. (2002) Human Speedy: a novel cell cycle regulator that enhances proliferation through activation of Cdk2. J Cell Biol 157(3), 357-66.

Puccetti, E., Obradovic, D., Beissert, T., Bianchini, A., Washburn, B., Chiaradonna, F., Boehrer, S., Hoelzer, D., Ottmann, O.G., Pelicci, P.G., Nervi, C. and Ruthardt, M. (2002) AML-associated translocation products block vitamin D(3)-induced differentiation by sequestering the vitamin D(3) receptor. Cancer Res 62(23), 7050-8.

Puglielli, M.T., Woisetschlaeger, M. and Speck, S.H. (1996) oriP is essential for EBNA gene promoter activity in Epstein-Barr virus-immortalized lymphoblastoid cell lines. J Virol 70(9), 5758-68.

Pulvertaft, J.V. (1964) Cytology of Burkitt's Tumour (African Lymphoma). Lancet 1, 238-40.

Quelle, D.E., Zindy, F., Ashmun, R.A. and Sherr, C.J. (1995) Alternative reading frames of the INK4a tumor suppressor gene encode two unrelated proteins capable of inducing cell cycle arrest. Cell 83(6), 993-1000.

Raab-Traub, N. and Flynn, K. (1986) The structure of the termini of the Epstein-Barr virus as a marker of clonal cellular proliferation, Cell, pp. 883-9. Vol. 47.

Radkov, S.A., Bain, M., Farrell, P.J., West, M., Rowe, M. and Allday, M.J. (1997) Epstein-Barr virus EBNA3C represses Cp, the major promoter for EBNA expression, but has no effect on the promoter of the cell gene CD21. J Virol 71(11), 8552-62.

Radkov, S.A., Touitou, R., Brehm, A., Rowe, M., West, M., Kouzarides, T. and Allday, M.J. (1999) Epstein-Barr virus nuclear antigen 3C interacts with histone deacetylase to repress transcription. J Virol 73(7), 5688-97.

Rawlins, D.R., Milman, G., Hayward, S.D. and Hayward, G.S. (1985) Sequence-specific DNA binding of the Epstein-Barr virus nuclear antigen (EBNA-1) to clustered sites in the plasmid maintenance region. Cell 42(3), 859-68.

Reed-Inderbitzin, E., Moreno-Miralles, I., Vanden-Eynden, S.K., Xie, J., Lutterbach, B., Durst-Goodwin, K.L., Luce, K.S., Irvin, B.J., Cleary, M.L., Brandt, S.J. and Hiebert, S.W. (2006) RUNX1 associates with histone deacetylases and SUV39H1 to repress transcription. Oncogene 25(42), 5777-86.

Reedman, B.M. and Klein, G. (1973) Cellular localization of an Epstein-Barr virus (EBV)-associated complement-fixing antigen in producer and non-producer lymphoblastoid cell lines. Int J Cancer 11(3), 499-520.

Reisman, D. and Sugden, B. (1986) trans activation of an Epstein-Barr viral transcriptional enhancer by the Epstein-Barr viral nuclear antigen 1, Mol Cell Biol, pp. 3838-46. Vol. 6.

Resnitzky, D., Hengst, L. and Reed, S.I. (1995) Cyclin A-associated kinase activity is rate limiting for entrance into S phase and is negatively regulated in G1 by p27Kip1. Mol Cell Biol 15(8), 4347-52.

Robertson, E.S., Grossman, S., Johannsen, E., Miller, C., Lin, J., Tomkinson, B. and Kieff, E. (1995) Epstein-Barr virus nuclear protein 3C modulates transcription through interaction with the sequence-specific DNA-binding protein J kappa. J Virol 69(5), 3108-16.

Robertson, E.S., Lin, J. and Kieff, E. (1996) The amino-terminal domains of Epstein-Barr virus nuclear proteins 3A, 3B, and 3C interact with RBPJ kappa. Journal of Virology 70(5), 3068-3074.

Romana, S.P., Mauchauffe, M., Le Coniat, M., Chumakov, I., Le Paslier, D., Berger, R. and Bernard, O.A. (1995a) The t(12;21) of acute lymphoblastic leukemia results in a tel-AML1 gene fusion. Blood 85(12), 3662-70.

Romana, S.P., Poirel, H., Leconiat, M., Flexor, M.A., Mauchauffe, M., Jonveaux, P., Macintyre, E.A., Berger, R. and Bernard, O.A. (1995b) High frequency of t(12;21) in childhood B-lineage acute lymphoblastic leukemia. Blood 86(11), 4263-9.

Rowe, M., Rowe, D.T., Gregory, C.D., Young, L.S., Farrell, P.J., Rupani, H. and Rickinson, A.B. (1987) Differences in B cell growth phenotype reflect novel patterns of Epstein-Barr virus latent gene expression in Burkitt's lymphoma cells. Embo J 6(9), 2743-51.

Rowe, M., Young, L.S., Cadwallader, K., Petti, L., Kieff, E. and Rickinson, A.B. (1989) Distinction between Epstein-Barr virus type A (EBNA 2A) and type B (EBNA 2B) isolates extends to the EBNA 3 family of nuclear proteins. J Virol 63(3), 1031-9.

Rus, H.G., Niculescu, F. and Shin, M.L. (1996) Sublytic complement attack induces cell cycle in oligodendrocytes. J Immunol 156(12), 4892-900.

Russell, P. and Nurse, P. (1986) cdc25+ functions as an inducer in the mitotic control of fission yeast. Cell 45(1), 145-53.

Ryan, K.M., Phillips, A.C. and Vousden, K.H. (2001) Regulation and function of the p53 tumor suppressor protein. Curr Opin Cell Biol 13(3), 332-7.

Saha, A., Murakami, M., Kumar, P., Bajaj, B., Sims, K. and Robertson, E.S. (2009) Epstein-Barr virus nuclear antigen 3C augments Mdm2-mediated p53 ubiquitination and degradation by deubiquitinating Mdm2. J Virol 83(9), 4652-69.

Saigusa, K., Imoto, I., Tanikawa, C., Aoyagi, M., Ohno, K., Nakamura, Y. and Inazawa, J. (2007) RGC32, a novel p53-inducible gene, is located on centrosomes during mitosis and results in G2/M arrest. Oncogene 26(8), 1110-21.

Sample, J., Henson, E.B. and Sample, C. (1992) The Epstein-Barr virus nuclear protein 1 promoter active in type I latency is autoregulated, J Virol, pp. 4654-61. Vol. 66.

Sample, J., Young, L., Martin, B., Chatman, T., Kieff, E. and Rickinson, A. (1990) Epstein-Barr virus types 1 and 2 differ in their EBNA-3A, EBNA-3B, and EBNA-3C genes. J Virol 64(9), 4084-92.

Sanchez, Y., Wong, C., Thoma, R.S., Richman, R., Wu, Z., Piwnica-Worms, H. and Elledge, S.J. (1997) Conservation of the Chk1 checkpoint pathway in mammals: linkage of DNA damage to Cdk regulation through Cdc25. Science 277(5331), 1497-501.

Santoni-Rugiu, E., Falck, J., Mailand, N., Bartek, J. and Lukas, J. (2000) Involvement of Myc activity in a G(1)/S-promoting mechanism parallel to the pRb/E2F pathway. Mol Cell Biol 20(10), 3497-509.

Schaefer, B.C., Strominger, J.L. and Speck, S.H. (1995a) Redefining the Epstein-Barr virus-encoded nuclear antigen EBNA-1 gene promoter and transcription initiation site in group I Burkitt lymphoma cell lines. Proc Natl Acad Sci U S A 92(23), 10565-9.

Schaefer, B.C., Strominger, J.L. and Speck, S.H. (1995b) Redefining the Epstein-Barr virus-encoded nuclear antigen EBNA-1 gene promoter and transcription initiation site in group I Burkitt lymphoma cell lines, Proc Natl Acad Sci U S A, pp. 10565-9. Vol. 92.

Schavolt, K.L. and Pietenpol, J.A. (2007) p53 and Delta Np63 alpha differentially bind and regulate target genes involved in cell cycle arrest, DNA repair and apoptosis. Oncogene 26(42), 6125-32.

Scherer, W.F., Syverton, J.T. and Gey, G.O. (1953) Studies on the propagation in vitro of poliomyelitis viruses. IV. Viral multiplication in a stable strain of human malignant epithelial cells (strain HeLa) derived from an epidermoid carcinoma of the cervix. J Exp Med 97(5), 695-710.

Schroeder, T.M., Kahler, R.A., Li, X. and Westendorf, J.J. (2004) Histone deacetylase 3 interacts with runx2 to repress the osteocalcin promoter and regulate osteoblast differentiation. J Biol Chem 279(40), 41998-2007.

Schwarzmann, F., Jager, M., Prang, N. and Wolf, H. (1998) The control of lytic replication of Epstein-Barr virus in B lymphocytes (Review). Int J Mol Med 1(1), 137-42.

Sculley, T.B., Buck, M., Gabrielli, B., Parsons, P.G. and Krauer, K.G. (2002) A histone deacetylase inhibitor, azelaic bishydroxamic acid, shows cytotoxicity on Epstein-Barr virus transformed B-cell lines: a potential therapy for posttransplant lymphoproliferative disease. Transplantation 73(2), 271-9.

Shapiro, R., Fett, J.W., Strydom, D.J. and Vallee, B.L. (1986) Isolation and characterization of a human colon carcinoma-secreted enzyme with pancreatic ribonuclease-like activity. Biochemistry 25(23), 7255-64.

Sheets, M.D., Fox, C.A., Hunt, T., Vande Woude, G. and Wickens, M. (1994) The 3'-untranslated regions of c-mos and cyclin mRNAs stimulate translation by regulating cytoplasmic polyadenylation. Genes Dev 8(8), 926-38.

Sherr, C.J. and Roberts, J.M. (1995) Inhibitors of mammalian G1 cyclin-dependent kinases. Genes Dev 9(10), 1149-63.

Sherr, C.J. and Roberts, J.M. (1999) CDK inhibitors: positive and negative regulators of G1-phase progression. Genes Dev 13(12), 1501-12.

Sherr, C.J. and Weber, J.D. (2000) The ARF/p53 pathway. Curr Opin Genet Dev 10(1), 94-9.

Shi, M.J. and Stavnezer, J. (1998) CBF alpha3 (AML2) is induced by TGF-beta1 to bind and activate the mouse germline Ig alpha promoter. J Immunol 161(12), 6751-60.

Shi, Y., Sawada, J., Sui, G., Affar el, B., Whetstine, J.R., Lan, F., Ogawa, H., Luke, M.P. and Nakatani, Y. (2003) Coordinated histone modifications mediated by a CtBP co-repressor complex. Nature 422(6933), 735-8.

Shiloh, Y. (2003) ATM: ready, set, go. Cell Cycle 2(2), 116-7.

Silins, S.L. and Sculley, T.B. (1994) Modulation of vimentin, the CD40 activation antigen and Burkitt's lymphoma antigen (CD77) by the Epstein-Barr virus nuclear antigen EBNA-4, Virology, pp. 16-24. Vol. 202.

Silins, S.L. and Sculley, T.B. (1995) Burkitt's lymphoma cells are resistant to programmed cell death in the presence of the Epstein-Barr virus latent antigen EBNA-4, Int J Cancer, pp. 65-72. Vol. 60.

Silins, S.L., Sherritt, M.A., Silleri, J.M., Cross, S.M., Elliott, S.L., Bharadwaj, M., Le, T.T., Morrison, L.E., Khanna, R., Moss, D.J., Suhrbier, A. and Misko, I.S. (2001) Asymptomatic primary Epstein-Barr virus infection occurs in the absence of blood T-cell repertoire perturbations despite high levels of systemic viral load. Blood 98(13), 3739-44.

Sinclair, A.J., Palmero, I., Peters, G. and Farrell, P.J. (1994) EBNA-2 and EBNA-LP cooperate to cause G0 to G1 transition during immortalization of resting human B lymphocytes by Epstein-Barr virus. Embo J 13(14), 3321-8.

Solomon, M.J., Lee, T. and Kirschner, M.W. (1992) Role of phosphorylation in p34cdc2 activation: identification of an activating kinase. Mol Biol Cell 3(1), 13-27.

Spender, L.C., Cornish, G.H., Rowland, B., Kempkes, B. and Farrell, P.J. (2001) Direct and indirect regulation of cytokine and cell cycle proteins by EBNA-2 during Epstein-Barr virus infection. J Virol 75(8), 3537-46.

Spender, L.C., Cornish, G.H., Sullivan, A. and Farrell, P.J. (2002a) Expression of transcription factor AML-2 (RUNX3, CBF(alpha)-3) is induced by Epstein-Barr virus EBNA-2 and correlates with the B-cell activation phenotype, J Virol, pp. 4919-27. Vol. 76.

Spender, L.C., Cornish, G.H., Sullivan, A. and Farrell, P.J. (2002b) Expression of transcription factor AML-2 (RUNX3, CBF(alpha)-3) is induced by Epstein-Barr virus EBNA-2 and correlates with the B-cell activation phenotype. J Virol 76(10), 4919-27.

Spender, L.C., Whiteman, H.J., Karstegl, C.E. and Farrell, P.J. (2005a) Transcriptional cross-regulation of RUNX1 by RUNX3 in human B cells. Oncogene 24(11), 1873-81.

Spender, L.C., Whiteman, H.J., Karstegl, C.E. and Farrell, P.J. (2005b) Transcriptional cross-regulation of RUNX1 by RUNX3 in human B cells, Oncogene, pp. 1873-81. Vol. 24.

Steeg, P.S., Bevilacqua, G., Kopper, L., Thorgeirsson, U.P., Talmadge, J.E., Liotta, L.A. and Sobel, M.E. (1988) Evidence for a novel gene associated with low tumor metastatic potential. J Natl Cancer Inst 80(3), 200-4.

Steegenga, W.T., van Laar, T., Riteco, N., Mandarino, A., Shvarts, A., van der Eb, A.J. and Jochemsen, A.G. (1996) Adenovirus E1A proteins inhibit activation of transcription by p53. Mol Cell Biol 16(5), 2101-9.

Strobeck, M.W., Knudsen, K.E., Fribourg, A.F., DeCristofaro, M.F., Weissman, B.E., Imbalzano, A.N. and Knudsen, E.S. (2000) BRG-1 is required for RB-mediated cell cycle arrest. Proc Natl Acad Sci U S A 97(14), 7748-53.

Strober, B.E., Dunaief, J.L., Guha and Goff, S.P. (1996) Functional interactions between the hBRM/hBRG1 transcriptional activators and the pRB family of proteins. Mol Cell Biol 16(4), 1576-83.

Strom, C.C., Aplin, M., Ploug, T., Christoffersen, T.E., Langfort, J., Viese, M., Galbo, H., Haunso, S. and Sheikh, S.P. (2005) Expression profiling reveals differences in metabolic gene expression between exercise-induced cardiac effects and maladaptive cardiac hypertrophy. Febs J 272(11), 2684-95.

Subramaniam, D., Natarajan, G., Ramalingam, S., Ramachandran, I., May, R., Queimado, L., Houchen, C.W. and Anant, S. (2008) Translation inhibition during cell cycle arrest and apoptosis: Mcl-1 is a novel target for RNA binding protein CUGBP2. Am J Physiol Gastrointest Liver Physiol 294(4), G1025-32.

Subramanian, C. and Robertson, E.S. (2002) The metastatic suppressor Nm23-H1 interacts with EBNA3C at sequences located between the glutamine- and proline-rich domains and can cooperate in activation of transcription. Journal of Virology 76(17), 8702-8709.

Sugden, B. and Warren, N. (1989) A promoter of Epstein-Barr virus that can function during latent infection can be transactivated by EBNA-1, a viral protein required for viral DNA replication during latent infection, J Virol, pp. 2644-9. Vol. 63.

Sung, N.S., Kenney, S., Gutsch, D. and Pagano, J.S. (1991) EBNA-2 transactivates a lymphoid-specific enhancer in the BamHI C promoter of Epstein-Barr virus. J Virol 65(5), 2164-9.

Sung, N.S., Wilson, J., Davenport, M., Sista, N.D. and Pagano, J.S. (1994) Reciprocal regulation of the Epstein-Barr virus BamHI-F promoter by EBNA-1 and an E2F transcription factor, Mol Cell Biol, pp. 7144-52. Vol. 14.

Takada, K., Horinouchi, K., Ono, Y., Aya, T., Osato, T., Takahashi, M. and Hayasaka, S. (1991) An Epstein-Barr virus-producer line Akata: establishment of the cell line and analysis of viral DNA. Virus Genes 5(2), 147-56.

Tassan, J.P., Jaquenoud, M., Fry, A.M., Frutiger, S., Hughes, G.J. and Nigg, E.A. (1995) In vitro assembly of a functional human CDK7-cyclin H complex requires MAT1, a novel 36 kDa RING finger protein. Embo J 14(22), 5608-17.

Tee, Y.T., Chen, G.D., Lin, L.Y., Ko, J.L. and Wang, P.H. (2006) Nm23-H1: a metastasis-associated gene. Taiwan J Obstet Gynecol 45(2), 107-13.

Thorley-Lawson, D.A. (2001) Epstein-Barr virus: exploiting the immune system. Nat Rev Immunol 1(1), 75-82.

Thorley-Lawson, D.A. and Gross, A. (2004) Persistence of the Epstein-Barr virus and the origins of associated lymphomas. N Engl J Med 350(13), 1328-37.

Tierney, R.J., Steven, N., Young, L.S. and Rickinson, A.B. (1994) Epstein-Barr virus latency in blood mononuclear cells: analysis of viral gene transcription during primary infection and in the carrier state, J Virol, pp. 7374-85. Vol. 68.

Tomkinson, B., Robertson, E. and Kieff, E. (1993a) Epstein-Barr virus nuclear proteins EBNA-3A and EBNA-3C are essential for B-lymphocyte growth transformation. J Virol 67(4), 2014-25.

Tomkinson, B., Robertson, E. and Kieff, E. (1993b) Epstein-Barr virus nuclear proteins EBNA-3A and EBNA-3C are essential for B-lymphocyte growth transformation, J Virol, pp. 2014-25. Vol. 67.

Tong, X., Drapkin, R., Reinberg, D. and Kieff, E. (1995a) The 62- and 80-kDa subunits of transcription factor IIH mediate the interaction with Epstein-Barr virus nuclear protein 2. Proc Natl Acad Sci U S A 92(8), 3259-63.

Tong, X., Wang, F., Thut, C.J. and Kieff, E. (1995b) The Epstein-Barr virus nuclear protein 2 acidic domain can interact with TFIIB, TAF40, and RPA70 but not with TATA-binding protein. J Virol 69(1), 585-8.

Topisirovic, I., Capili, A.D. and Borden, K.L. (2002) Gamma interferon and cadmium treatments modulate eukaryotic initiation factor 4E-dependent mRNA transport of cyclin D1 in a PML-dependent manner. Mol Cell Biol 22(17), 6183-98.

Topisirovic, I., Gutierrez, G.J., Chen, M., Appella, E., Borden, K.L. and Ronai, Z.A. (2009) Control of p53 multimerization by Ubc13 is JNK-regulated. Proc Natl Acad Sci U S A 106(31), 12676-81.

Touitou, R., Hickabottom, M., Parker, G., Crook, T. and Allday, M.J. (2001) Physical and functional interactions between the corepressor CtBP and the Epstein-Barr virus nuclear antigen EBNA3C. J Virol 75(16), 7749-55.

Toyoshima, F., Moriguchi, T., Wada, A., Fukuda, M. and Nishida, E. (1998) Nuclear export of cyclin B1 and its possible role in the DNA damage-induced G2 checkpoint. Embo J 17(10), 2728-35.

Tsang, S.F., Wang, F., Izumi, K.M. and Kieff, E. (1991) Delineation of the cis-acting element mediating EBNA-2 transactivation of latent infection membrane protein expression. J Virol 65(12), 6765-71.

Uccini, S., Monardo, F., Stoppacciaro, A., Gradilone, A., Agliano, A.M., Faggioni, A., Manzari, V., Vago, L., Costanzi, G., Ruco, L.P. and et al. (1990) High frequency of Epstein-Barr virus genome detection in Hodgkin's disease of HIV-positive patients, Int J Cancer, pp. 581-5. Vol. 46.

van Wijnen, A.J., Stein, G.S., Gergen, J.P., Groner, Y., Hiebert, S.W., Ito, Y., Liu, P., Neil, J.C., Ohki, M. and Speck, N. (2004) Nomenclature for Runt-related (RUNX) proteins. Oncogene 23(24), 4209-10.

Voeltz, G.K., Ongkasuwan, J., Standart, N. and Steitz, J.A. (2001) A novel embryonic poly(A) binding protein, ePAB, regulates mRNA deadenylation in Xenopus egg extracts. Genes Dev 15(6), 774-88.

Vousden, K.H. (2002) Activation of the p53 tumor suppressor protein. Biochim Biophys Acta 1602(1), 47-59.

Vousden, K.H. and Lu, X. (2002) Live or let die: the cell's response to p53. Nat Rev Cancer 2(8), 594-604.

Wada, M., Yazumi, S., Takaishi, S., Hasegawa, K., Sawada, M., Tanaka, H., Ida, H., Sakakura, C., Ito, K., Ito, Y. and Chiba, T. (2004) Frequent loss of RUNX3 gene expression in human bile duct and pancreatic cancer cell lines. Oncogene 23(13), 2401-7.

Wade, M. and Allday, M.J. (2000) Epstein-Barr virus suppresses a G(2)/M checkpoint activated by genotoxins. Mol Cell Biol 20(4), 1344-60.

Walls, D. and Perricaudet, M. (1991) Novel downstream elements upregulate transcription initiated from an Epstein-Barr virus latent promoter. Embo J 10(1), 143-51.

Waltzer, L., Perricaudet, M., Sergeant, A. and Manet, E. (1996) Epstein-Barr virus EBNA3A and EBNA3C proteins both repress RBP- J kappa-EBNA2-activated transcription by inhibiting the binding of RBP-J kappa to DNA. Journal of Virology 70(9), 5909-5915.

Wang, D., Liebowitz, D. and Kieff, E. (1985) An EBV membrane protein expressed in immortalized lymphocytes transforms established rodent cells. Cell 43(3 Pt 2), 831-40.

Wang, D., Liebowitz, D., Wang, F., Gregory, C., Rickinson, A., Larson, R., Springer, T. and Kieff, E. (1988) Epstein-Barr virus latent infection membrane protein alters the human B-lymphocyte phenotype: deletion of the amino terminus abolishes activity. J Virol 62(11), 4173-84.

Wang, F., Gregory, C., Sample, C., Rowe, M., Liebowitz, D., Murray, R., Rickinson, A. and Kieff, E. (1990a) Epstein-Barr virus latent membrane protein (LMP1) and nuclear proteins 2 and 3C are effectors of phenotypic changes in B lymphocytes: EBNA-2 and LMP1 cooperatively induce CD23. J Virol 64(5), 2309-18.

Wang, F., Gregory, C., Sample, C., Rowe, M., Liebowitz, D., Murray, R., Rickinson, A. and Kieff, E. (1990b) Epstein-Barr-Virus Latent Membrane-Protein (Lmp1) and Nuclear Protein-2 and Protein-3c Are Effectors of Phenotypic Changes in Lymphocytes-B - Ebna-2 and Lmp1 Cooperatively Induced Cd23. Journal of Virology 64(5), 2309-2318.

Wang, J., Hoshino, T., Redner, R.L., Kajigaya, S. and Liu, J.M. (1998) ETO, fusion partner in t(8;21) acute myeloid leukemia, represses transcription by interaction with the human N-CoR/mSin3/HDAC1 complex. Proc Natl Acad Sci U S A 95(18), 10860-5.

Wang, L., Grossman, S.R. and Kieff, E. (2000) Epstein-Barr virus nuclear protein 2 interacts with p300, CBP, and PCAF histone acetyltransferases in activation of the LMP1 promoter. Proc Natl Acad Sci U S A 97(1), 430-5.

Wang, L. and Hiebert, S.W. (2001) TEL contacts multiple co-repressors and specifically associates with histone deacetylase-3. Oncogene 20(28), 3716-25.

Wang, Q., Stacy, T., Binder, M., Marin-Padilla, M., Sharpe, A.H. and Speck, N.A. (1996a) Disruption of the Cbfa2 gene causes necrosis and hemorrhaging in the central nervous system and blocks definitive hematopoiesis. Proc Natl Acad Sci U S A 93(8), 3444-9.

Wang, Q., Stacy, T., Miller, J.D., Lewis, A.F., Gu, T.L., Huang, X., Bushweller, J.H., Bories, J.C., Alt, F.W., Ryan, G., Liu, P.P., Wynshaw-Boris, A., Binder, M., Marin-Padilla, M., Sharpe, A.H. and Speck, N.A. (1996b) The CBFbeta subunit is essential for CBFalpha2 (AML1) function in vivo. Cell 87(4), 697-708.

Wang, S., Wang, Q., Crute, B.E., Melnikova, I.N., Keller, S.R. and Speck, N.A. (1993) Cloning and characterization of subunits of the T-cell receptor and murine leukemia virus enhancer core-binding factor. Mol Cell Biol 13(6), 3324-39.

Ward, G.E. and Kirschner, M.W. (1990) Identification of cell cycle-regulated phosphorylation sites on nuclear lamin C. Cell 61(4), 561-77.

Weiss, L.M., Movahed, L.A., Warnke, R.A. and Sklar, J. (1989) Detection of Epstein-Barr viral genomes in Reed-Sternberg cells of Hodgkin's disease, N Engl J Med, pp. 502-6. Vol. 320.

West, M.J. (2006) Structure and function of the Epstein-Barr virus transcription factor, EBNA 3C. Curr Protein Pept Sci 7(2), 123-36.

West, M.J., Webb, H.M., Sinclair, A.J. and Woolfson, D.N. (2004) Biophysical and mutational analysis of the putative bZIP domain of Epstein-Barr virus EBNA 3C. J Virol 78(17), 9431-45.

Westendorf, J.J., Yamamoto, C.M., Lenny, N., Downing, J.R., Selsted, M.E. and Hiebert, S.W. (1998) The t(8;21) fusion product, AML-1-ETO, associates with C/EBP-alpha, inhibits C/EBP-alpha-dependent transcription, and blocks granulocytic differentiation. Mol Cell Biol 18(1), 322-33.

Westendorf, J.J., Zaidi, S.K., Cascino, J.E., Kahler, R., van Wijnen, A.J., Lian, J.B., Yoshida, M., Stein, G.S. and Li, X. (2002) Runx2 (Cbfa1, AML-3) interacts with histone deacetylase 6 and represses the p21(CIP1/WAF1) promoter. Mol Cell Biol 22(22), 7982-92.

Wharton, R.P., Sonoda, J., Lee, T., Patterson, M. and Murata, Y. (1998) The Pumilio RNA-binding domain is also a translational regulator. Mol Cell 1(6), 863-72.

Whiteman, H.J. and Farrell, P.J. (2006) RUNX expression and function in human B cells. Crit Rev Eukaryot Gene Expr 16(1), 31-44.

Williams, H., Macsween, K., McAulay, K., Higgins, C., Harrison, N., Swerdlow, A., Britton, K. and Crawford, D. (2004) Analysis of immune activation and clinical events in acute infectious mononucleosis. J Infect Dis 190(1), 63-71.

Woisetschlaeger, M., Yandava, C.N., Furmanski, L.A., Strominger, J.L. and Speck, S.H. (1990) Promoter Switching in Epstein-Barr-Virus During the Initial- Stages of Infection of Lymphocytes-B. Proceedings of the National Academy of Sciences of the United States of America 87(5), 1725-1729.

Wu, D.Y., Kalpana, G.V., Goff, S.P. and Schubach, W.H. (1996) Epstein-Barr virus nuclear protein 2 (EBNA2) binds to a component of the human SNF-SWI complex, hSNF5/Ini1. J Virol 70(9), 6020-8.

Wu, D.Y., Krumm, A. and Schubach, W.H. (2000) Promoter-specific targeting of human SWI-SNF complex by Epstein-Barr virus nuclear protein 2. J Virol 74(19), 8893-903.

Xiao, W.H. and Liu, W.W. (2004) Hemizygous deletion and hypermethylation of RUNX3 gene in hepatocellular carcinoma. World J Gastroenterol 10(3), 376-80.

Yalamanchili, R., Tong, X., Grossman, S., Johannsen, E., G, M. and Kieff, E. (1994) Genetic and biochemical evidence that EBNA2 interaction with a 63-kDa cellular GTG-binding protein is essential for B lymphocyte growth transformation in EBV. Virology 204(2), 634-41.

Yamashiro, T., Wang, X.P., Li, Z., Oya, S., Aberg, T., Fukunaga, T., Kamioka, H., Speck, N.A., Takano-Yamamoto, T. and Thesleff, I. (2004) Possible roles of Runx1 and Sox9 in incipient intramembranous ossification. J Bone Miner Res 19(10), 1671-7.

Yan, X., Mouillet, J.F., Ou, Q. and Sadovsky, Y. (2003) A novel domain within the DEAD-box protein DP103 is essential for transcriptional repression and helicase activity. Mol Cell Biol 23(1), 414-23.

Yang, J., Bardes, E.S., Moore, J.D., Brennan, J., Powers, M.A. and Kornbluth, S. (1998) Control of cyclin B1 localization through regulated binding of the nuclear export factor CRM1. Genes Dev 12(14), 2131-43.

Yang, J., Song, H., Walsh, S., Bardes, E.S. and Kornbluth, S. (2001a) Combinatorial control of cyclin B1 nuclear trafficking through phosphorylation at multiple sites. J Biol Chem 276(5), 3604-9.

Yang, W., Shen, J., Wu, M., Arsura, M., FitzGerald, M., Suldan, Z., Kim, D.W., Hofmann, C.S., Pianetti, S., Romieu-Mourez, R., Freedman, L.P. and Sonenshein, G.E. (2001b) Repression of transcription of the p27(Kip1) cyclin-dependent kinase inhibitor gene by c-Myc. Oncogene 20(14), 1688-702.

Yasukawa, M., Hasegawa, A., Sakai, I., Ohminami, H., Arai, J., Kaneko, S., Yakushijin, Y., Maeyama, K., Nakashima, H., Arakaki, R. and Fujita, S. (1999) Down-

regulation of CXCR4 by human herpesvirus 6 (HHV-6) and HHV-7. J Immunol 162(9), 5417-22.

Yates, J.L., Warren, N. and Sugden, B. (1985) Stable replication of plasmids derived from Epstein-Barr virus in various mammalian cells. Nature 313(6005), 812-5.

Yi, F., Saha, A., Murakami, M., Kumar, P., Knight, J.S., Cai, Q., Choudhuri, T. and Robertson, E.S. (2009) Epstein-Barr virus nuclear antigen 3C targets p53 and modulates its transcriptional and apoptotic activities. Virology 388(2), 236-47.

Yin, Y., Manoury, B. and Fahraeus, R. (2003) Self-inhibition of synthesis and antigen presentation by Epstein-Barr virus-encoded EBNA1. Science 301(5638), 1371-4.

Yin, Y.H., Li, Y.Y., Qiao, H., Wang, H.C., Yang, X.A., Zhang, H.G., Pang, X.W., Zhang, Y. and Chen, W.F. (2005) TSPY is a cancer testis antigen expressed in human hepatocellular carcinoma. Br J Cancer 93(4), 458-63.

Yoshida, C.A., Yamamoto, H., Fujita, T., Furuichi, T., Ito, K., Inoue, K., Yamana, K., Zanma, A., Takada, K., Ito, Y. and Komori, T. (2004) Runx2 and Runx3 are essential for chondrocyte maturation, and Runx2 regulates limb growth through induction of Indian hedgehog. Genes Dev 18(8), 952-63.

Young, L., Alfieri, C., Hennessy, K., Evans, H., Ohara, C., Anderson, K.C., Ritz, J., Shapiro, R.S., Rickinson, A., Kieff, E. and Cohen, J.I. (1989) Expression of Epstein-Barr Virus Transformation Associated Genes in Tissues of Patients with Ebv Lymphoproliferative Disease. New England Journal of Medicine 321(16), 1080-1085.

Young, L.S., Dawson, C.W., Clark, D., Rupani, H., Busson, P., Tursz, T., Johnson, A. and Rickinson, A.B. (1988) Epstein-Barr virus gene expression in nasopharyngeal carcinoma. J Gen Virol 69 (Pt 5), 1051-65.

Young, L.S., Yao, Q.Y., Rooney, C.M., Sculley, T.B., Moss, D.J., Rupani, H., Laux, G., Bornkamm, G.W. and Rickinson, A.B. (1987) New type B isolates of Epstein-Barr virus from Burkitt's lymphoma and from normal individuals in endemic areas. J Gen Virol 68 (Pt 11), 2853-62.

Young, P., Anderton, E., Paschos, K., White, R. and Allday, M.J. (2008) Epstein-Barr virus nuclear antigen (EBNA) 3A induces the expression of and interacts with a subset of chaperones and co-chaperones. J Gen Virol 89(Pt 4), 866-77.

Zetterberg, H., Borestrom, C., Nilsson, T. and Rymo, L. (2004) Multiple EBNA1-binding sites within oriPI are required for EBNA1-dependent transactivation of the Epstein-Barr virus C promoter, Int J Oncol, pp. 693-6. Vol. 25.

Zhang, D.E., Hetherington, C.J., Meyers, S., Rhoades, K.L., Larson, C.J., Chen, H.M., Hiebert, S.W. and Tenen, D.G. (1996) CCAAT enhancer-binding protein (C/EBP) and AML1 (CBF alpha2) synergistically activate the macrophage colony-stimulating factor receptor promoter. Mol Cell Biol 16(3), 1231-40.

Zhang, H.S., Gavin, M., Dahiya, A., Postigo, A.A., Ma, D., Luo, R.X., Harbour, J.W. and Dean, D.C. (2000a) Exit from G1 and S phase of the cell cycle is regulated by repressor complexes containing HDAC-Rb-hSWI/SNF and Rb-hSWI/SNF. Cell 101(1), 79-89.

Zhang, Y., Xiong, Y. and Yarbrough, W.G. (1998) ARF promotes MDM2 degradation and stabilizes p53: ARF-INK4a locus deletion impairs both the Rb and p53 tumor suppression pathways. Cell 92(6), 725-34.

Zhang, Y.W., Yasui, N., Ito, K., Huang, G., Fujii, M., Hanai, J., Nogami, H., Ochi, T., Miyazono, K. and Ito, Y. (2000b) A RUNX2/PEBP2alpha A/CBFA1 mutation displaying impaired transactivation and Smad interaction in cleidocranial dysplasia. Proc Natl Acad Sci U S A 97(19), 10549-54.

Zhao, B., Marshall, D.R. and Sample, C.E. (1996) A conserved domain of the Epstein-Barr virus nuclear antigens 3A and 3C binds to a discrete domain of J kappa. Journal of Virology 70(7), 4228-4236.

Zhao, B. and Sample, C.E. (2000) Epstein-barr virus nuclear antigen 3C activates the latent membrane protein 1 promoter in the presence of Epstein-Barr virus nuclear antigen 2 through sequences encompassing an spi-1/Spi-B binding site. J Virol 74(11), 5151-60.

Zimber, U., Adldinger, H.K., Lenoir, G.M., Vuillaume, M., Knebel-Doeberitz, M.V., Laux, G., Desgranges, C., Wittmann, P., Freese, U.K., Schneider, U. and et al. (1986) Geographical prevalence of two types of Epstein-Barr virus. Virology 154(1), 56-66.

Zimber-Strobl, U. and Strobl, L.J. (2001) EBNA2 and Notch signalling in Epstein-Barr virus mediated immortalization of B lymphocytes. Semin Cancer Biol 11(6), 423-34.

Zimber-Strobl, U., Strobl, L.J., Meitinger, C., Hinrichs, R., Sakai, T., Furukawa, T., Honjo, T. and Bornkamm, G.W. (1994) Epstein-Barr virus nuclear antigen 2 exerts its transactivating function through interaction with recombination signal binding protein RBP-J kappa, the homologue of Drosophila Suppressor of Hairless. Embo J 13(20), 4973-82.